Development of Carbohydrate-based Diblock Polymers for Nucleic Acid Delivery

Antons Sizovs

Dissertation submitted to the faculty of the Virginia Polytechnic Institute and State University in partial fulfillment of the requirements for the degree of

Doctor of Philosophy

In

Chemistry

Theresa M. Reineke

Paul R. Carlier

Harry W. Gibson

Louis A. Madsen

Judy S. Riffle

05/04/2012

Blacksburg, VA

Keywords: Gene Delivery, RAFT, Polytrehalose, Polyglucose, Nanoparticle

Development of Carbohydrate-based Diblock Polymers for Nucleic Acid Delivery

Antons Sizovs

Development of Carbohydrate-based Diblock Polymers for Nucleic Acid Delivery

Antons Sizovs

ABSTRACT

The delivery of nucleic acids remains the major obstacle for nucleic acid-based therapies such as gene therapy and gene silencing therapies based on RNA interference. In this dissertation we have developed and studied nucleic acid delivery vehicles based on cationic diblock glycopolymers that contain glucosamine and trehalosamine.

Practical procedures were developed to synthesize 2-methacrylamido-2-deoxy glucose and 6-methacrylamido-6-deoxy trehalose starting with commercially available carbohydrates and utilizing trimethylsilyl protecting group chemistry. These monomers were polymerized via reversible addition-fragmentation chain transfer (RAFT) polymerization to yield glycopolymers with the desired lengths and low polydispersity indexes. Glycopolymers were chain-extended with aminoethylmethacrylamide to produce cationic diblock copolymers.

The ability of cationic diblock copolymers to bind nucleic acids was demonstrated with gel electrophoresis and heparin exclusion assays. Complexes of the synthesized polymers with nucleic acids were studied with dynamic light scattering to reveal nanoparticles of 100-250 nm that were stable in the presence of serum proteins. Quartz crystal microbalance experiments showed that serum proteins adsorb on polytrehalose coated gold surfaces and it was suggested that these interactions may help mask the polytrehalose coated nanoparticles from potential actions of the immune system.

Polytrehalose was also shown to suppress water crystallization similarly to trehalose by lowering the energies associated with the water/ice phase transition. The property was utilized to freeze-dry siRNA containing polyplexes which could be re-dissolved in water after lyophilization to yield nanoparticles.

The polyplexes formulated with cationic diblock copolymers were shown to efficiently enter cervical cancer cells (HeLa cell line) and glioblastoma cells (U-87 cell line) and to deliver their nucleic acid cargo. Polyglucose-containing polymers were efficient mediators of exogenous gene expression in HeLa cells, and polytrehalose-containing polymers were effective in promoting the target gene down-regulation via RNA interference by delivered siRNA.

ACKNOWLEDGEMENTS

I would like to first thank my advisor prof. Theresa M. Reineke for having me as a member of her research team. It has not always been easy, but I have learnt a lot from you Dr. Reineke and I am especially thankful for teaching me the importance of communicating research to the public. I would also like to thank my committee members profs. Paul Carlier, Harry Gibson, Louis Madsen and Judy Riffle – you were always helpful with your support and suggestions. Special thanks to you Dr. Carlier for becoming my co-advisor and allowing me to participate in your group meetings – I have enjoyed them a lot. Dr. Madsen, you are the main reason I have a clear understanding about how NMR works – thank you for that! I would also like to thank my committee members at the University of Cincinnati profs. George Stan and David Smithrud for their advices in the very beginning of my graduate career. I will always be grateful to Dr. Mehdi Ashraf-Khorassani for the tremendous amount of help with LC-MS. Many thanks to all of my lab mates. Thank you Dr. Karina Kizjakina for being a wonderful friend and colleague, for your support and for all the scientific discussions we had. Thank you Lian, Dan, Nilesh, Giovanna, Adam and Kevin for the fruitful collaborations (Dan and Gio special thanks for the collaboration in the field of practical jokes). I will never forget all the guidance, mentorship and the good times we had with my older lab mates: thank you Josh, Patrick and Vijay. Good luck to younger members of the group; with such smart and dedicated people like Swapnil and Sneha the science in the Reineke lab will always be first-rate!

Many thanks go to Dr. Einars Loza for the invaluable experience in synthesis and philosophy of science that I have received in his lab during my college years. I would

never become a chemist if not for immeasurable teaching talent and selfless dedication of Mariana Teze – thank you very much. I want to also thank all of my friends, and especially Mana Tamami, who always knew the right words of support in the most stressful moments of my graduate life. Finally, I thank my whole family for always believing in me and supporting me every minute of my life.

Contents

List of Figures

Chapter 1. Introduction

The completion of the human genome project in 2003[1] and the discovery of RNA interference[2] have stimulated interest in nucleic acid (NA) based therapies. Advances in the research tools available for analysis of the genome have helped to link myriad of genes to certain diseases and this information is available through multiple online databases.[3]

The idea of gene therapy is not new and has been around for at least 40 years.[4] This idea evolved into a field of research because of the great potential that it holds. Gene therapy addresses a disease on the very basic – genome level, and thus in principle can cure genetic disorders and hereditary diseases.[5] Despite the fact that gene therapy is still far from reaching its full potential, some success has been achieved.[6,7]

Currently there are multiple gene therapies in various phases of clinical trials.[8] The majority of these trials use viral vectors for delivery of genetic material due to the innate ability of viruses to infect cells, an ability that has evolved over millions of years of evolution. Not surprisingly the first successful gene therapy clinical trials aimed at curing severe combined immunodeficiency disease (SCID) used viral vectors.[9,10] Unfortunately there has been a drawback – two out of ten patients have developed leukemia-like symptoms, possibly due to activation of an oncogene by the retroviral delivery vector.[11] Additionally, viruses have other limitations such as immunogenicity[12]

and high cost of production. These limitations have prompted the development of non-viral delivery vehicles for gene therapy.

The delivery of genetic material has been called "the Achilles heel of gene therapy"[13]. It also has been a major obstacle in another type of NA-based therapy that is based on gene silencing by RNA interference (RNAi) mechanism.[2,14] This type of therapeutic approach requires delivery of small interfering RNA (siRNA).[15] From the delivery point of view the siRNA-based therapy has one less barrier than gene therapy: the gene silencing takes place in the cytoplasm and is accomplished by the RNA-induced silencing complex (RISC);[16] thus nuclear localization and nuclear delivery are not required.

The number of research papers dealing with development of non-viral nucleic acid delivery agents and approaches is growing fast since the beginning of the 1990s.[17-19] One of the general approaches to delivery of both DNA and RNA is based on the use of polymers.[20-22] A special niche among the polymeric NA delivery agents is occupied by carbohydrate-based agents.[23] Great advantage of these agents comes from the availability of small molecule carbohydrates and carbohydrate polymers, their non-toxic nature, hydrophilicity, and the presence of multiple sites for functionalization. Literature on carbohydrate based NA delivery agents is reviewed in Chapter 2 of this dissertation.

In the Reineke lab a step-growth approach was traditionally used for synthesis of polyglycoamidoamines (PGAAs) – the AABB type carbohydrate-based polymers.[24-28] Among these polymers the trehalose-based (Tr) series demonstrated a special property: the nanoparticles formed between Tr-polymers and plasmid DNA (pDNA) were significantly more colloidally stable in biological media containing serum proteins than

other PGAAs.[27] This property along with remarkable cryoprotective and lyoprotective properties of trehalose led to the idea which became a core of the research investigated in this dissertation.

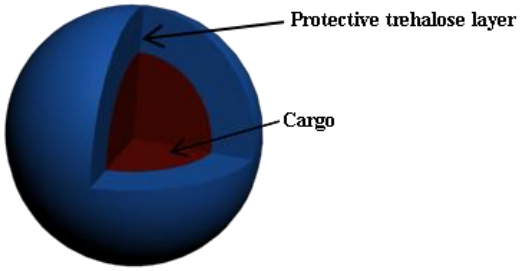

It was rationalized that coating the polyplexes with multiple trehalose residues would create a high local concentration of this carbohydrate and colloidal stability and would potentially allow freeze-drying of the polyplexes – a highly desirable property which would allow long-term storage of the polyplexes.

Diblock polymers consisting of a block grafted with trehalose and a cationic block grafted with ethyleneamine units were developed. The rationale behind the design, synthesis, physical and biological evaluations is discussed in Chapter 3.

Trehalose monomer synthesis was challenging, but it was finally optimized to contain only one column chromatography. The trehalose monomer was polymerized using reversible addition-fragmentation chain transfer (RAFT) polymerization[29] to yield homopolymer and cationic diblock polymers with low polydispersities.

Polytrehalose-based polymers and their complexes with siRNA (termed ‘polyplexes’) were studied with various physical characterization techniques to reveal some interesting properties, including the ability to protect particles during lyophilization.

Moreover, these polyplexes were shown to efficiently enter U-87 glioblastoma cells and cause the downregulation of the target gene.

The initial stages of the trehalose project were problematic and glucosamine was used as a model compound to replace trehalose. This model study evolved into a stand-alone project and successful preparation of the cationic diclock polymers and their evaluation as pDNA delivery agents in HeLa cells is described in Chapter 4.

Within the glucosamine project a simple and high yielding procedure was developed for preparation of 2-methacrylamido-2-deoxyglucose (MAG) starting with commercially available glucosamine hydrochloride. The ease of preparation of this monomer has added to the potential of polyMAG as a polymer for coating the nanoparticles in biomedical applications.

Finally, in Chapter 5 of this thesis future research directions are suggested, including some general ideas, specific experiments and the potential problems that must be addressed in order for the polyMAG and polytrehalose glycopolymers to become clinically relevant materials.

1.1. References

1 *Genome.gov | National Human Genome Research Institute (NHGRI) - Homepage*, 1/1/2012).

2 Fire, A., Xu, S. Q., Montgomery, M. K., Kostas, S. A., Driver, S. E. & Mello, C. C. Potent and specific genetic interference by double-stranded RNA in Caenorhabditis elegans. *Nature* **391**, 806-811 (1998).

3 Tiffin, N., Andrade-Navarro, M. A. & Perez-Iratxeta, C. Linking genes to diseases: it's all in the data. *Genome Med.* **1**, 77 (2009).

4 Friedmann, T. & Roblin, R. Gene therapy for human genetic disease? *Science* **175**, 949 (1972).

5 Sheridan, C. Gene therapy finds its niche. *Nat. Biotechnol.* **29**, 121-128 (2011).
6 Herzog, R., Cao, O. & Srivastava, A. Two decades of clinical gene therapy-success is finally mounting. *Discov. Med.* **9**, 105 (2010).
7 Kohn, D. B. & Candotti, F. Gene therapy fulfilling its promise. *N. Engl. J. Med.* **360**, 518-521 (2009).
8 *Gene Therapy Trials Worldwide*, <http://www.wiley.com/legacy/wileychi/genmed/clinical/> (Accessed 1/1/2012).
9 Cavazzana-Calvo, M., Hacein-Bey, S., de Saint Basile, G., Gross, F., Yvon, E., Nusbaum, P., Selz, F., Hue, C., Certain, S. & Casanova, J. L. Gene therapy of human severe combined immunodeficiency (SCID)-X1 disease. *Science* **288**, 669-672 (2000).
10 Aiuti, A., Slavin, S., Aker, M., Ficara, F., Deola, S., Mortellaro, A., Morecki, S., Andolfi, G., Tabucchi, A. & Carlucci, F. Correction of ADA-SCID by stem cell gene therapy combined with nonmyeloablative conditioning. *Science* **296**, 2410-2413 (2002).
11 Hacein-Bey-Abina, S., Von Kalle, C., Schmidt, M., McCormack, M., Wulffraat, N., Leboulch, P., Lim, A., Osborne, C., Pawliuk, R. & Morillon, E. LMO2-associated clonal T cell proliferation in two patients after gene therapy for SCID-X1. *Science* **302**, 415-419 (2003).
12 Tripathy, S. K., Black, H. B., Goldwasser, E. & Leiden, J. M. Immune responses to transgene–encoded proteins limit the stability of gene expression after injection of replication–defective adenovirus vectors. *Nat. Med.* **2**, 545-550 (1996).
13 Somia, N., Wang, L. & Gage, F. Gene therapy: promises, problems and prospects in *Genes and resistance to disease.* 147 pp. (Springer Verlag, 2000).
14 Hannon, G. J. RNA interference. *Nature* **418**, 244-251 (2002).
15 Elbashir, S. M., Harborth, J., Lendeckel, W., Yalcin, A., Weber, K. & Tuschl, T. Duplexes of 21-nucleotide RNAs mediate RNA interference in cultured mammalian cells. *Nature* **411**, 494-498 (2001).
16 Bartel, D. P. MicroRNAs: genomics, biogenesis, mechanism, and function. *Cell* **116**, 281-297 (2004).
17 Al-Dosari, M. S. & Gao, X. Nonviral gene delivery: principle, limitations, and recent progress. *The AAPS journal* **11**, 671-681 (2009).
18 Pathak, A., Patnaik, S. & Gupta, K. C. Recent trends in non-viral vector-mediated gene delivery. *Biotechnol. J.* **4**, 1559-1572 (2009).
19 Midoux, P., Pichon, C., Yaouanc, J. J. & Jaffrès, P. A. Chemical vectors for gene delivery: a current review on polymers, peptides and lipids containing histidine or imidazole as nucleic acids carriers. *Br. J. Pharmacol.* **157**, 166-178 (2009).
20 Mintzer, M. A. & Simanek, E. E. Nonviral vectors for gene delivery. *Chem. Rev.* **109**, 259-302 (2008).
21 Green, J. J., Langer, R. & Anderson, D. G. A combinatorial polymer library approach yields insight into nonviral gene delivery. *Acc. Chem. Res.* **41**, 749-759 (2008).
22 Whitehead, K. A., Langer, R. & Anderson, D. G. Knocking down barriers: advances in siRNA delivery. *Nat. Rev. Drug Discov.* **8**, 129-138 (2009).

23 Sizovs, A., McLendon, P., Srinivasachari, S. & Reineke, T. Carbohydrate Polymers for Nonviral Nucleic Acid Delivery. *Top. Curr. Chem.* **296**, 131-190 (2010).
24 Liu, Y., Wenning, L., Lynch, M. & Reineke, T. M. New poly (d-glucaramidoamine) s induce DNA nanoparticle formation and efficient gene delivery into mammalian cells. *J. Am. Chem. Soc.* **126**, 7422-7423 (2004).
25 Liu, Y. & Reineke, T. M. Hydroxyl stereochemistry and amine number within poly (glycoamidoamine) s affect intracellular DNA delivery. *J. Am. Chem. Soc.* **127**, 3004-3015 (2005).
26 Liu, Y. & Reineke, T. M. Poly (glycoamidoamine) s for gene delivery: stability of polyplexes and efficacy with cardiomyoblast cells. *Bioconj. Chem.* **17**, 101-108 (2006).
27 Srinivasachari, S., Liu, Y., Zhang, G., Prevette, L. & Reineke, T. M. Trehalose click polymers inhibit nanoparticle aggregation and promote pDNA delivery in serum. *J. Am. Chem. Soc.* **128**, 8176-8184 (2006).
28 Liu, Y. & Reineke, T. M. Poly (glycoamidoamine) s for gene delivery. Structural effects on cellular internalization, buffering capacity, and gene expression. *Bioconj. Chem.* **18**, 19-30 (2007).
29 Moad, G., Rizzardo, E. & Thang, S. H. Living radical polymerization by the RAFT process. *Aust. J. Chem.* **58**, 379-410 (2005).

Chapter 2. Carbohydrate Containing Transfection Agents*

* Chapter adapted from: Sizovs, A., McLendon, P.M., Srinivasachari, S., Reineke, T.M. Top. Curr. Chem. *296*, 131–190 (2010).

Abstract

Carbohydrates have been investigated and developed as delivery vehicles for shuttling nucleic acids into cells. In this review, we present the state of the art in carbohydrate-based polymeric vehicles for nucleic acid delivery, with a focus on recent successes in preclinical models, both *in vitro* and *in vivo*. Polymeric scaffolds based on the natural polysaccharides chitosan, hyaluronan, pullulan, dextran, and schizophyllan each have unique properties and potential for modification, and these results are discussed with a focus on facile synthetic routes and favorable performance in biological systems. Many of these carbohydrates have been used to develop alternative types of biomaterials for nucleic acid delivery to typical polyplexes, and these novel materials are discussed. Also presented are polymeric vehicles that incorporate copolymerized carbohydrates into polymer backbones based on polyethylenimine and polylysine and their effect on transfection and biocompatibility. Unique scaffolds, such as clusters and polymers based on cyclodextrin(CD), are also discussed, with a focus on recent successes *in vivo* and in the clinic. These results are presented with an emphasis on the role of carbohydrate and charge on transfection. Use of carbohydrates as molecular recognition ligands for cell-type specific delivery is also briefly reviewed. We contend that

carbohydrates have contributed significantly to progressing the field of *non-viral* DNA delivery, and these new discoveries are impactful for developing new vehicles and materials for treatment of human disease.

Abbreviations

APC	antigen-presenting cell
apoB	apolipoprotein B
ASF	asialofetuin
ASGP	asialoglycoprotein receptor
AS-ODN	antisense oligonucleotide
CD	cyclodextrin
CDI	1,1´-carbonyldiimidazole
CDP	cyclodextrin-containing polycations
CPP	cell penetrating peptide
DCC	N,N'-Dicyclohexylcarbodiimide
DDMC	2-Diethyl-aminoethyl–Dextran–Methyl Methacrylate Graft Copolymer
DEAE	2-diethyl-aminoethyl
DMEM	dulbecco's Modified Eagle Medium
EDC	1-ethyl-3-(3-dimethyl amino)propyl carbodiimide
EtiBr	ethidium bromide
HA	hyaluronic acid
IL	interleukin
N4C3	tripropylenetetraamine
NHS	N-hydroxysuccinimide
NPC	non-parenchymal
PAMAM	polyamidoamine
PBS	phosphate buffered saline
PC	parenchymal
PDGF	platelet-derived growth factor
PEG	poly(ethylene glycol)
PEI	polyethylenimine
PGP	PEGylated glycopeptide
PLGA	poly(lactide-co-glycolide)
PLL	poly-L-lysine
PO-DNA	phosphodiester-DNA
poly(A)	polyadenine
poly(C)	polycytosine
poly(dA)	polydeoxyadenine
poly(dT)	polydeoxythymine
PS-DNA	phosphorothioate-DNA
PVP	poly(vinylpyrrolidone)
R8	octaarginine
RGD	arginine-glycine-aspartic acid
SMC	smooth muscle cell
SPG	schizophyllan
TNF	tumor necrosis factor

2.1. Introduction

Nucleic acids have broad potential for use in human therapeutics. The completion of the Human Genome Project has brought the promise of nucleic acid-based drugs to treat myriad acquired and inherited human diseases, including HIV, cancer, cystic fibrosis, rheumatoid arthritis, asthma, cardiovascular disease, and neurodegenerative disorders.[1-3] As nucleic acids are large, charged molecules and susceptible to enzymatic degradation, a delivery vehicle is required to condense the polynucleotide into a compact structure which protects it from degradation and facilitates its cellular internalization. Past and present delivery vehicle technology has been centered about the genetically-engineered virus as a means of nucleic acid delivery. Viral vectors have demonstrated successful gene transfer *in vivo* due to their innate cellular internalization and gene transduction capabilities, and many viral vectors have progressed into the clinic.[4,5] However, the widespread applicability of viral vehicles is tempered by the potential to elicit unpredictable immune responses and their relative difficultly of manufacture.[6,7] The potential clinical pitfalls of viral-based nucleic acid delivery have spurred a broad research focus devoted to developing nonviral delivery systems that allows similar gene transduction capacities but have reduced potential for toxicity.

Synthetic materials for nucleic acid condensation can offer marked improvement over viral delivery. Materials can be designed for high nucleic acid loading capacity, cell-specific targeting through chemical conjugation of molecular recognition elements, and biocompatibility, and are better suited to scale up for mass production.These materials are typically cationic, and may contain primary, secondary, and tertiary amines that can be protonated at physiological pH, which is necessary for electrostatic binding with the

negatively-charged phosphate groups on the DNA backbone. This cooperative binding event and polycation charge neutralization facilitates compaction of the polymer nucleic acid complexes into small colloidal nanoparticles (termed polyplexes).[8,9] Structures such as branched and linear polyethylenimine (PEI),[9-11] poly-L-lysine (PLL),[12-14] spermine,[15,16] and polyamidoamine (PAMAM)[5,17-19] can bind nucleic acids quite well and have been developed for DNA delivery with varied success. A fine, detailed review of nonviral delivery has been published recently.[20] However, these charge-dense polycations have demonstrated toxicity;[4,8,21] thus, design of a nontoxic analog is key to development of a suitable vehicle for human therapy.

Using carbohydrates in nucleic acid delivery is an obvious choice for improving toxicity. Carbohydrates are naturally-available unique scaffolds that have been exploited by synthetic chemists for materials design. Unique structural features, such as the presence of an anomeric carbon, multiple hydroxyl groups, cyclic ring structures, and chirality are advantageous for designing biomacromolecules.[22-25] In addition, carbohydrates are readily available, renewable resources, inexpensive materials for introducing hydrophilicity and biocompatibility into polymeric systems. These facets have led to their use in developing novel sustainable materials for biomedical applications.[26,27]

Glycopolymers have broadened the scope of nucleic acid delivery research, as many novel saccharide-based materials have been developed and analyzed for favorable nucleic acid delivery and toxicity profiles. This review provides critical perspective on the progress and favorable results of carbohydrate-based vehicles in nucleic acid delivery. We have focused on glycopolymeric delivery systems, including those derived from pure

carbohydrates (chitosan, hyaluronan, pullulan, schizophyllan, dextran, and cyclodextrin) as well as carbohydrate comonomers incorporated into a polymer backbone. Carbohydrates have also been used as molecular recognition elements for targeting receptor-mediated endocytosis and have been conjugated as pendent groups for recognition by cell-surface lectins. Polymers incorporating carbohydrate-mediated targeting will be discussed; however, a full review of their use in targeting is beyond the scope of this review.

2.2. Natural Polysaccharides as Nucleic Acid Delivery Scaffolds

Polysaccharides are complex carbohydrates possessing high structural diversity. They are composed of several monosaccharide units joined together through glycosidic bonds. Typically, polysaccharides are isolated from a natural source, prepared via ring-opening polymerization of anhydro sugars or synthesized by enzymatic polymerization, which provides stereo-control, even at high molecular weight.[28] The natural polysaccharides, such as dextran,[29] schizophyllan,[30] chitosan,[31] hyaluronan,[32] and pullulan[33] have all been studied as nucleic acid carriers, and the following section highlights significant recent findings with these polysaccharides.

2.2.1. Dextran

Dextrans are biodegradable homopolymers of glucose with predominantly α-(1→6) linkages with some branching via α-(1→3) linkage which vary depending on the source of dextran. They are synthesized from sucrose by the action of bacteria, such as

Streptococcus mutans or *Leuconostoc mesenteroides*. The first report of polycation-mediated DNA complexation was published in 1965 on 2-diethylaminoethyl (DEAE)–dextran, synthesized from diethyleaminoethyl chloride and dextran.[34] This study was an important milestone in this area, because it was the first published example of a nonviral polysaccharide nucleic acid carrier. These vehicles continue to be investigated. The cationic nature of DEAE–dextran enables it to effectively complex with a variety of nucleic acids, types and sizes.[29]

About three decades after these first studies, Mack and coworkers[35] used DEAE-dextran to transfect primary cultured human macrophages. Macrophages play a pivotal role in regulating immune response and gene expression and, hence, transfection experiments performed in this study were both interesting and challenging, as macrophages are difficult to transfect. Reproducible luciferase expression was observed with DEAE-dextran, as opposed to with liposome delivery or electroporation. The addition of 100 or 400 μM concentrations of chloroquine also was not seen to enhance gene expression, suggesting that DEAE-dextran particles were not sequestered in endosomes. However, the presence of serum in the transfection medium reduced transgene expression by 60%.

Onishi *et al.*[36] grafted DEAE-dextran with methyl methacrylate (DDMC), with the hypothesis that methyl methacrylate graft chains could protect the complex from degradation by dextranases present in the cytoplasm, resulting in increased transfection efficiency and decreased cytotoxicity. Transfection experiments were completed in primary human embryonal kidney (HEK293) cells in serum-containing media. The results showed a 5-fold increase in transgene expression with DDMC polyplexes

compared with DEAE-dextran polyplexes, supporting the authors' hypothesis. In addition, the cytotoxicity was shown to be reduced by DDMC grafting during these experiments.

Cationic dextrans (40 kDa) were synthesized by Azzam *et al.* through conjugation with a variety of oligoamines, including spermine and spermidine.[37,38] An ethidium bromide exclusion assay (qualitative assay for binding affinity) revealed that the dextran-spermine conjugates bound DNA more strongly than other oligoamine derivatives. Transfection efficiency experiments in NIH3T3 and HEK293 cells showed high gene expression in serum-free media, similar to the positive controls Transfast and DOTAP/Chol (1/1), and much enhanced from calcium phosphate (**Figure 2.1**). The most efficacious vehicles were 6-8 kDa in molecular weight, with a spermine content of 2 μmol/mg and 25-30% branching. Unfortunately, a reduction in gene expression was noted with a similar experiment in serum-containing media. To improve the transfection in serum, Hosseinkhani *et al.*[39] synthesized a poly(ethylene glycol) (PEG)-containing dextran-spermine conjugate (G7TA141) and three dextran-based spermine conjugates (G7TA103, G7TA107, and G7TA141). When NIH3T3 cells were transfected with these PEGylated vectors in NIH3T3 cells in serum-containing media, they showed higher luciferase expression than their nonPEGylated counterparts, with maximum gene expression

observed at a polycation:DNA weight ratio of 5:1. Intramuscular injection of

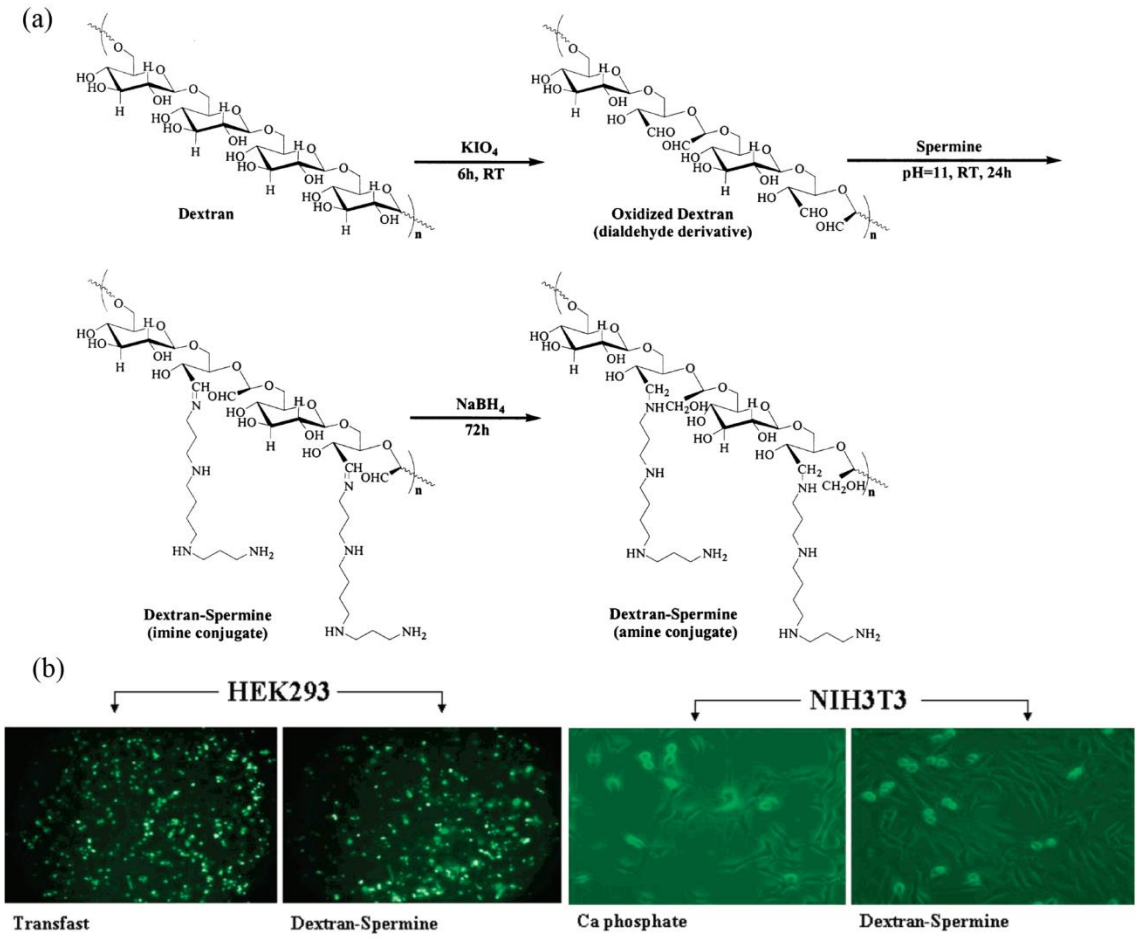

Figure 2.1 A. Synthesis of dextran-spermine conjugates. **B.** Fluorescence micrographs of dextranspermine compared to common transfection reagents in HEK293 and NIH3T3 cells. Adapted from[38] with permission. © 2002 American Chemical Society

PEGylated G7TA141 in mice at a 5:1 weight ratio (polyplexes formulated at a pDNA concentration of 50 μg/mouse) revealed a higher level of transgene (β-galactosidase) expression in mouse muscle than naked pDNA or pDNA complex with the non-

PEGylated analog. Gene expression in the liver was monitored for mice dosed with complexes prepared with dextran-spermine conjugates modified with different levels of PEG conjugation. The results indicated the highest level of β-galactosidase expression in the liver resulted from the 5% PEGylated complexes noted 2 days post-injection. These results demonstrated that delivery in serum-containing media can be improved through PEGylation strategies and elicit favorable results in animal models.

Further *in vivo* studies with dextran-spermine conjugates have been explored recently by Eliyahu et al.[40,41] The efficacy of local and systemic delivery in mice was assessed through intramuscular (i.m.) and intranasal (i.n.) injections, respectively. Efficacy, measured by X-gal expression in paraffin-sectioned tissue, was observed primarily in lung tissue (bronchial epithelial cells, pneumocytes, and alveoli), fibrocytes in the skeletal muscle, and hepatocytes. X-gal expression was higher in each organ when pDNA was delivered by the cationic dextran compared to pDNA only. In comparison, lipoplex (DOTAP/cholesterol lipoplexes) injections resulted in expression only at the site of injection, with distant sites such as liver not being transfected, an observation that did not change with increased lipoplex dosing. Upon histopathological assessment of toxicity, mild inflammation and necrosis were observed in the skeletal muscle, but no toxic effects were seen locally in the lung or liver tissue when pDNA was delivered by dextrans. Systemic toxicity was also low, as injections of polyplex or free polymer showed little effect to organ weight, white blood cell and platelet counts, and serum transaminase levels.[41] PEGylation of spermine-dextran conjugates and decrease in spermine content resulted in lower transgene expression. Systemic transfection of PEGylated dextrans was not dose dependent, since increasing the dose from 6 μg DNA to

40 μg DNA did not increase transgene expression. This series of initial studies demonstrate the promise of DEAE-dextran as a nonviral delivery vehicle; it remains a promising delivery platform.

Additional recent work has focused on developing dextrans into functional hydrogels for effective delivery of nucleic acids. Singh *et al.* developed hydrogels containing crosslinked dextran vinyl sulfone and tetra-functional PEG thiols encapsulating siRNA/pDNA-loaded microparticles and dendritic cell chemoattractants for the dual delivery of chemokines and nucleic acids.[42] The chemoattractants were encapsulated in degradable microspheres composed of poly(lactide-co-glycolide) (PLGA); the siRNA was also encapsulated in PLGA and functionalized with PEI before addition of pDNA. Hydrogels were crosslinked *in situ* via Michael-type addition reactions, and the dextran vinyl sulfone and PEG components were mixed to form hydrogels, and the stoichiometry of the components was varied to control the crosslinking density, which can impact the release rate of the microparticles. These materials were nontoxic in multiple cell lines *in vitro* and exhibited slow release of chemokine with 30% dextran/10% PEG hydrogels. These hydrogels released 70% of encapsulated chemokine after 72 hours, indicating that sustained drug release is possible. In primary antigen-presenting cells (APCs), chemokine-induced dendritic cell migration was observed, as well as siRNA-induced knockdown of IL-3. These promising results show that dextran can be used in functional material design for sustained release of drugs and nucleic acids.

Other promising work describing DNA delivery with dextrans has been published recently from the Fréchet laboratory.[43] Acetal-derivatized dextran was solvent

evaporated to form dextran nanoparticles which are cleavable under acidic pH.[44] Exploiting the reducing chain ends present on the carbohydrate particles, the authors used alkoxyamine-terminated poly(arginine), commonly referred to as a cell penetrating peptide (CPP), for its purported ability to transiently penetrate cell membranes, to introduce CPP onto the dextran particles through formation of oxime linkages. Using CPP-derivatized dextran particles (containing 20% poly(β-amino ester) polymer) encapsulating a pDNA encoding luciferase, they attained a 60-fold increase in luciferase expression in HeLa cells compared to unmodified particles.[43] These results demonstrate the broad applicability and the future use of dextran in nucleic acid delivery.

2.2.2. Schizophyllan

Schizophyllans (SPGs) are naturally-occurring water soluble polysaccharides that are produced by the fungus *Schizophyllan commune*. SPG belongs to the family of β-(1→3) glucans, and it has one branch through β-(1→6)-D-glucosyl linkage per three glucose units (**Figure 2.2**). The safety of these materials has been well demonstrated, as they have been used as adjuvants for over two decades in drug formulations and routinely used in the treatment of gynecological cancer.[45,46]

In water, SPG exists as a thermodynamically stable triple-helix (**Figure 2.2**) held together by hydrogen bonds. Under special conditions these hydrogen bonds can be broken; for further discussion, it is important to know that, in DMSO, schizophyllan dissociates and exists as a single randomly coiled chain, but it will re-associate into triple helices upon dilution with water.

The Sakurai lab has reported that SPG can form complexes with polycytosine (poly(C)) and polyadenine (poly(A)).[47] Shortly thereafter, they reported that polydeoxyadenine (poly(dA)) and polydeoxythymine (poly(dT)) can form such

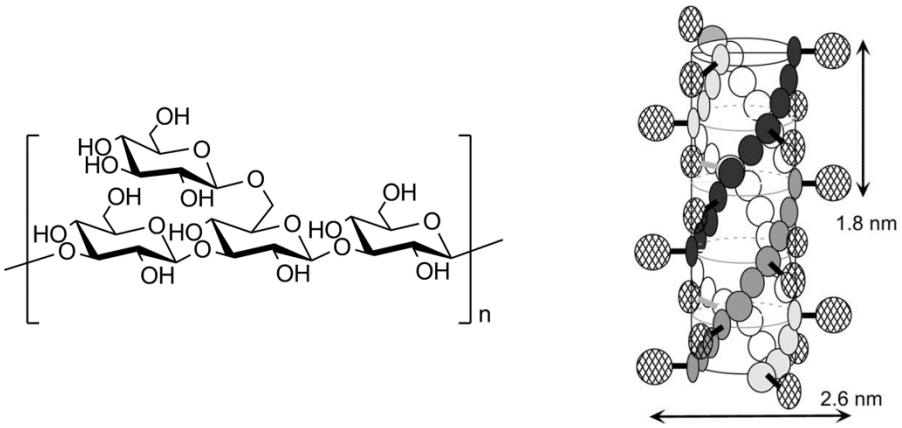

Figure 2.2. Structure of schizophyllan repeat unit and a schematic representation of the triple helix formed in aqueous solution. Figure adapted with permission from [55] . © 2003 Elsevier.

complexes with SPG as well.[48] It was also noted that none of these homopolynucleotides form supramolecular structures on their own and, instead, exist in solutions as single chains, thus not self-assembling via hydrogen bond formation. This seems to be a necessary requirement, as other homopolynucleotides (e.g., polyuracil) which form intermolecular and/or intramolecular bonds in solution do not form complexes with SPG. The structure of SPG-polynucleotide complexes is not yet completely clear. Sakurai proposed,[48] based on circular dichroism studies, that the SPG-polynucleotide complex is a hetero-triplex similar to the original SPG-triplex, with one of the schizophyllan chains

being replaced by one homopolynucleotide chain.[48] Additionally, the complex will form only with single-stranded SPG. Both of these statements were recently challenged,[49] as it was shown that SPG-poly(C) complex can be formed with triplex-SPGs that have been previously denatured and renatured, and these complexes have identical melting temperatures to ones that are formed with a single-stranded SPGs. This newer approach allows one to prepare SPG-polynucleotide polyplexes in more physiologically relevant conditions—since no use of DMSO is required—but complex stoichiometry will likely be different.

Since schizophyllan can form complexes only with single stranded *homo*polynucleotides, this polynucleotide fragment must be incorporated into DNA/RNA that is used for delivery. Nonetheless, it was demonstrated that such polynucleotides can be efficiently complexed with SPG and be protected from degradation by nucleases within the complex,[50] as well as acting as an antisense inhibitor of a complementary mRNA in cell-free media.[51] It was concluded that, in order to retain its silencing function, the single stranded antisense oligonucleotide (AS-ODN) must have higher affinity toward target mRNA than SPG. This effect was confirmed by Koumoto *et al*., who demonstrated that the presence of the ss-homopolynucleotide complementary to the one complexed inside SPG·DNA and SPG·RNA polyplex is sufficient to induce release of the cargo.[52]

For the complexation of double-stranded DNA, a more elaborate polynucleotide morphology has been designed via the introduction of homopolynucleotide sequences on the ends for SPG binding .[53] Poly(dA) 80-mer was introduced at both ends of DNA, forming loops which provide protection from degradation by endonucleases, an approach adopted from viruses.

It is also possible to avoid incorporation of homopolynucleotide by using ternary complexes between polynucleotide, SPG, and polycation. It was recently demonstrated that such ternary complexes can be prepared with PEI and cationic cellulose (quaternized nitrogen is a charged functional group in cationic cellulose).[54] However, this kind of approach is a step away from the non-cationic nature of schizophyllan-based delivery systems and will not be discussed here.

Soon after the discovery of the ability of SPG to complex homopolynucleotides, it was demonstrated that schizophyllan complexes with poly(A) or poly(C) will dissociate at pH 4-6.[55] This property is important as SPG polyplexes could potentially release their polynucleotide cargo in the acidic pH environment of endosomes and/or lysosomes. Since these polyplexes possess a net negative charge and lack targeting groups, however, they are inefficient in terms of cellular internalization.

In initial attempts to improve SPG as a nucleic acid delivery vehicle, lactose and mannose were incorporated in schizophyllan by chemical modifications of branching glucose units.[50,56] The chemical modification is chemoselective to the branched glucose units on the main polymer backbone, such that the polymer backbone remains intact. Oxidation by periodate ion requires hydroxyl groups to be vicinal, and that is why the oxidation of schizophyllan main chain is avoided. Aldehydes formed in this step are good handles to be used in further modifications, which, as we shall see further, mostly involve reductive amination. Furthermore, these modifications do not interfere with the ability of SPG to form triple-helices and polyplexes. Mannose- and lactose-modified SPGs were demonstrated to protect homopolynucleotides poly(C) and poly(dA) from degradation, and these targeted polyplexes were able to bind to corresponding lectins. It is not clear if

similar protection and recognition by receptors can be achieved in the case of AS-ODNs, since data for such experiments was not presented, but *in vitro* studies demonstrated that lactose-functionalized SPG deliver antisense oligonucleotide to HepG2 cells. Phosphorothioate AS-ODN that would suppress mRNA of *c-myb*, a proto oncogene that causes cancer when overexpressed, was used. The antisense effect was 10% higher for SPG-mediated delivery and 40% higher for lactose-SPG-mediated delivery compared to naked AS-ODN at 30 μg/mL; it was 10% and 45% higher, respectively, at 60 μg/mL. The delivery efficiency was decreased for lactose-SPG-mediated delivery, but not for SPG-mediated delivery in the presence of galactose; however, a large concentration of galactose—20 mM—was used to demonstrate the specificity.

An analogous strategy was used for grafting SPG with folic acid (FA) and, as in the previously-described study, SPG-FA was used for the delivery of phosphorothioate AS-ODN that would suppress *c-myb*.[46] This time it was noted that after grafting the weight-averaged molecular weight of SPG was decreased from 150 to 90 kDa. The degree of grafting was estimated to be 9% and grafted folic acid could be recognized by folate binding proteins. *In vitro* experiments showed that SPG-FA complexes can efficiently deliver AS-ODN to KB cells, causing 45% decrease in cell viability, and that delivery efficiency is dependent on the concentration of free folic acid in the media. Importantly, it was demonstrated that scrambled AS-ODN delivered by the same SPG-FA vehicle does not suppress cell growth, proving that cell growth suppression is mediated by the antisense ODN and not a nonspecific effect of the delivery vehicle.

Following initial work on SPGs, Matsumoto *et al.*,[50] in an attempt to improve cellular internalization, modified SPGs with octaarginine (R8), spermine, arginine-

glycine-aspartic acid tripeptide (RGD), or single amino acids (Arg and Ser). The SPG modification was done using the route described above and was in a 0.5-24.7 mol% range. Antisense delivery experiments were conducted in A375 melanoma cells and the HL-60 leukemia cell line. A 60% decrease in cell growth was observed with AS-ODN complexes formed with R8-SPG, and a 56% decrease in cell growth was revealed with RGD-SPG complexes at a concentration of 12.5 μg/mL in A375 cells. It should be noted that the antisense activity was minimal while using the positive control, Lipofectamine™, or SPGs modified with spermine, arginine, or serine. When the same experiment was performed using the sense sequence (S-*c-myb*), Lipofectamine™ and spermine-modified SPGs were highly cytotoxic compared to naked S-*c-myb*, but the rest of modified SPG-systems showed the level of toxicity similar to naked S-*c-myb*. An analogous trend was observed when the experiments were performed in HL-60 cells. Thus, the authors demonstrated that octaarginine- or RGD-modified SPGs elicited a more potent antisense effect (likely derived from increased internalization) than Lipofectamine™ and negligible toxicity comparable to unmodified SPG thereby providing a new insight into schizophyllans as nucleic acid carriers. It is important to note here that, although schizophyllan was modified with cationic (at physiological pH) functionalities, the N/P ratio used for polyplex formulation was less than 1. The polyplex ζ-potential was not reported, but the authors expect it to be negative based on the N/P ratio and stress that modified SPG is principally different and advantageous compared to polycationic polynucleotide carriers.

Work on the modification of SPG and delivery of AS-ODN to A375 cells was continued with introduction of amino-modified PEG (5 kDa) through previously-

described reductive amination.[57] The degree of modification used in this study was 10.1%. The PEGylation strategy was suggested in order to promote fusion of polyplexes with the cell membrane—as opposed to endocytic cellular internalization; this approach is very unusual, because PEG is typically used to shield vehicle charge, preventing aggregation in serum and nonspecific associations. Cell culture studies show that inhibition of endocytosis leads to a decreased antisense effect, which suggests internalization occurs through an endocytic route, rather than by vesicle fusion. Using nigericin, a chemical inhibitor that blocks transport from endosomes to lysosomes, the antisense-mediated decrease in cell growth was preserved for PEG-SPG/AS-ODN but nearly completely abrogated for RGD-SPG/AS-ODN. The authors suggest that this result confirms endosomal escape of PEG-SPA/AS-ODNs prior to transport to the lysosome. Instead, this result could be indicative that the incorporation of PEG on the delivery vehicle affects the internalization route. These polyplexes may also enter the cell through an alternative pathway which does not traffic to lysosomes, in which case nigericin would have no effect. This is evidenced with the RGD-modified polyplex, for which nigericin-sensitive trafficking appears to be essential for efficient function. More studies are needed to elucidate the effect of PEG on polyplex trafficking.

PEG modification of SPG was attempted together with galactose modification as well.[58] Galactose-terminated PEGs of different lengths were introduced into SPG by reductive amination. *In vitro* studies conducted in serum-containing medium with HepG2 cells demonstrated that, among tested PEG lengths (0.2, 0.6, 2, and 6 kDa) used for SPG modification, the longest one (6 kDa) was the most efficient in reducing cell growth through delivery of AS-ODN. This 10 mol% Gal-PEG-modified SPG delivery vehicle

was more efficient in reducing cell growth than 8.7 mol% galactose-modified SPG (Gal8.7-SPG), naked AS-ODN, and SPGs modified by glucose-terminated PEGs. Importantly, there was no difference in the antisense effect in A375 cells (which do not express galactose receptors) when SPGs modified by glucose- and galactose-terminated PEG-SPGs were compared. However, both of these delivery vectors caused a significant (up to 65%) decrease in cell viability; this toxicity is potentially problematic for systemic delivery applications. In addition, this work demonstrates the propensity for internalization of complexes made with galactose-modified PEG-SPGs by cells other than hepatocytes.

Mizu and coworkers[51] utilized the same SPG modification strategy with spermine, R8, RGD, or cholesterol to deliver unmethylated, CpG motif-containing single stranded oligo DNA with $(dA)_{40}$ tail at the 3′ end into murine macrophage-like cells (J774.A1) to enhance cytokine secretion. Consistent with the study described above, the degree of functionalization was kept low: 0.5 mol% and 6.9 mol% in the cases of R8 and cholesterol, respectively. CpG DNA has been shown to be an effective adjuvant in various vaccines to treat numerous diseases.[59] Previous studies have shown that complexation of phophorothioate AS-ODNs with modified SPGs reduces their non-specific interactions with proteins and increases their cellular uptake. In this study, the secretion of three different cytokines (IL-6, IL-12, and TNF-α) was assessed. A 5–10 fold increase in cytokine secretion was observed for the modified SPG complexed with CpG DNA over naked CpG DNA. The SPGs modified with octaarginine were found to have the highest efficacy, followed by RGD- and cholesterol-modified SPGs. However, only

20–40% enhancement in cytokine secretion was found when CpG DNA complexed with unmodified SPG was used.

This work with antigen-presenting cells was continued using phosphodiester (PO)-DNA instead of phosphorothioate (PS)-DNA to avoid "unexpected biological responses".[60] For many antisense oligonucleotides, the phosphodiester bond is replaced by phosphorothioate, which reduces nuclease susceptibility, presumably by introducing chirality.[61] *In vitro* experiments with mice primary spleen cells revealeded an interleukin (IL) expression trend similar to those described by Mizu *et al*,[51]—R8-modified SPG elicited the highest expression of IL-6 and IL-12 at both 25 μg/mL and 50 μg/mL DNA concentrations, while spermine-modified SPG yielded a slightly lower response. When PO-DNA was used, 4-6 fold higher DNA concentrations were needed to induce IL secretion comparable to PS-DNA, a finding attributed to lower PO-DNA stability toward nuclease degradation. While further development of SPG vehicles for PO-DNA delivery is needed, the ability to deliver DNA to primary cells by SPG vehicles is a substantial achievement. Follow-up *in vivo* experiments in mice showed a significant increase in IL-12 secretion when SPG was used for delivery, as compared to naked DNA. Unfortunately it was not mentioned whether PS-DNA or PO-DNA was used, but the ability to deliver DNA *in vivo* was demonstrated.

SPG modifications to create cationic vehicles by grafting amines (ethanolamine, spermine, spermidine and tripropylenetetraamine (N4C3)) onto the SPG backbone have also been attempted. [45] *In vitro* experiments in COS-1 cells revealed that, among amines used for SPG grafting, N4C3-modified SPG was the most efficient in transfection, a result related to its high amine density. Thus 34 kDa SPG containing 41 mol% grafting

with N4C3 was 5 fold more efficient in transfection (at N/P 10) than PEI (25 kDa); however, it was also the most toxic vehicle – 40% more toxic than PEI. Toxicity followed the same trend as the transfection efficiency, suggesting that the more charge-dense polymers were also the most toxic. The molecular weight of glucan has a role as well, and 80 kDa SPG was the most efficient (among 12, 34, 80 and 150 kDa tested), while 12 and 150 kDa were the least efficient. To reduce toxicity, PEG was introduced via amide linkage with succinimide-activated, carbonyl-terminated PEG. Both 2 and 5 kDa PEG-SPG derivatives showed 100% cell viability, but transfection efficiency was also reduced, becoming similar to PEI. Finally, it was demonstrated that SPG vectors have long-term transfection, with detectable cellular plasmid DNA over 30 days post-transfection. This sustained DNA residence was speculated to be the result of *slow* non-enzymatic hydrolysis of the SPG backbone.

Studies utilizing SPG as a nucleic acid carrier have been performed over the last decade and highlight the potential applicability of SPG for nucleic acid delivery applications. The unique ability to form complexes with polynucleotides via hydrogen bonding—without electrostatic interactions—has great promise, since cytotoxicity mediated by positive charge density can thereby be avoided. Moreover, branched glucose units offer attractive and facile modification sites due to selective modification by oxidation or reductive amination; this leaves the main chain intact, preserving the ability to condense polynucleotides. The SPG backbone cannot be cleaved enzymatically in mammals due to the lack of appropriate enzymes, making schizophyllan a good candidate for slow-release delivery vehicle development. Further research on the efficiency and

versatility of this polymer will reveal the future of schizophyllan as a non-viral nucleic acid carrier.

2.2.3. Hyaluronan

Hyaluronan, also called hyaluronic acid (HA), is a glycosaminoglycan, a major component of the extracellular matrix. It is composed of N-acetyl-D-glucosamine and D-glucuronic acid (**Figure 2.3**).[62] It has been extensively used in biomedical applications due to its biodegradability as well as lubricating, shock-absorbing, and non-immunogenic properties.[63] As can be seen from the structure, hyaluronic acid has several sites for chemical modifications. Functionalization via the carboxyl group is used most often in gene delivery applications, because there is only one carboxyl group per repeat unit (as opposed to multiple hydroxyl groups). Such modification removes the negative charge, which is beneficial for the complexation of negatively-charged polynucleotides. As later

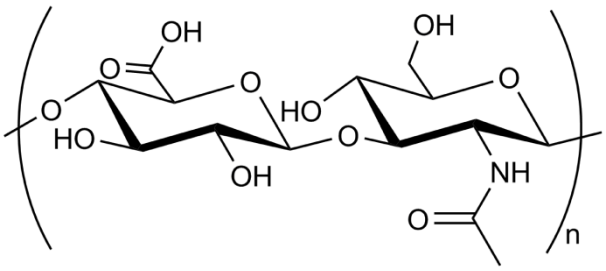

Figure 2.3. Structure of hyaluronan.

discussed in this chapter, the carboxyl group can be activated toward nucleophiles in aqueous solution.

In 2003, Kim and coworkers[63] formulated pDNA encoding platelet-derived growth factor (PDGF) with HA and studied *in vitro* transfection efficiency in COS-1 cells (**Figure 2.4**). In this study, solutions containing various amounts of pDNA were mixed with HA solution, flash-frozen and lyophilized, yielding DNA-HA matrices. These matrices were then placed in a DMF/H_2O solution of adipic dihydrazide and 1-ethyl-3-(3-dimethylamino)propyl carbodiimide (EDC), a conventional water-soluble, carboxyl-activating agent. An HCl solution was subsequently added to lower the pH. By allowing these mixtures to incubate for various amounts of time, DNA-HA matrices with different degrees of crosslinking could be obtained. It should be pointed out here that the DNA is physically entrapped in a pre-formed, mesh-like HA matrix. While relatively uncommon for nucleic acid delivery, this approach is regularly employed for the delivery of small molecule therapeutics.

The pDNA release kinetics from the matrices in the presence of the enzyme hyaluronidase (at concentrations that were aimed to resemble serum conditions) were shown to be dependent on the pDNA loading and the degree of HA crosslinking. It was observed that pDNA release is faster from the matrices with lesser degrees of crosslinking, and it was suggested that matrices with higher extents of crosslinking could be potentially used for slow release applications.

One such application could be delivery of Has2-pDNA, a plasmid that codes for hyaluronan synthase 2.[64] This enzyme facilitates the synthesis of larger HA molecules and can prevent post-surgical peritoneal adhesions. In one study, DNA-HA films were prepared using previously-described chemistry; however, lyophilization was replaced with air-drying under sterile conditions and an isopropanol/H_2O mixture was used instead

of DMF/H_2O. The release kinetics of DNA were similar to that from the HA film described previously, but release did not occur until after 7 days. The reason for this delay was not completely clear; the authors suggest that a possible way to overcome the delay is to use a crosslinked DNA-HA film sandwiched between two non-crosslinked DNA-HA films. Non-crosslinked film would be expected to undergo rapid hydrolysis, thus serving as a source of HA during the initial period.

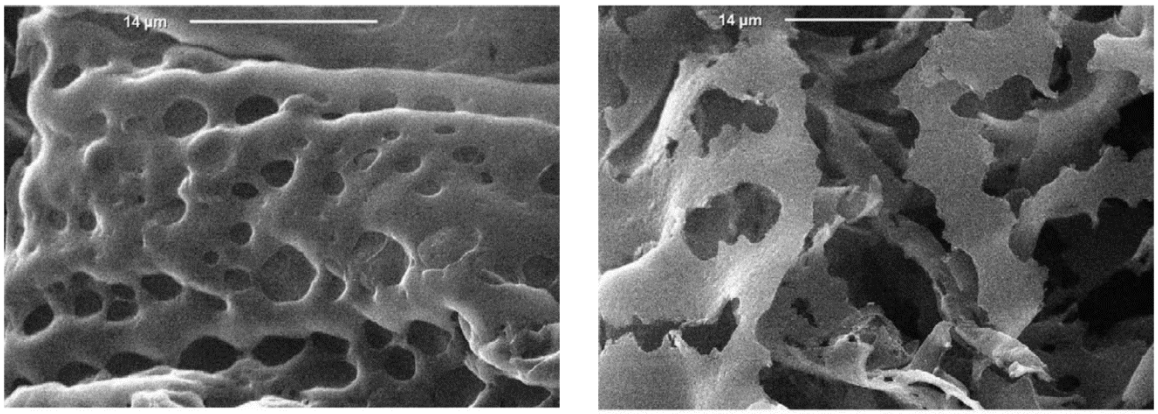

Figure 2.4. SEM images of DNA-HA matrices: (**a**) before and (**b**) after incubation in hyaluronidase solution (10 units/ml) for 7 days. Figure adapted from reference [63] with permission. © 2003 Elsevier

As an extension of the HA film approach, Yun and coworkers[65] synthesized hyaluronan microspheres using the chemistry described above, but the synthesis was completed as an emulsion in one step, yielding 5-20 µm microspheres. These microspheres were found to be biodegradable and released three times more pDNA when incubated with hyaluronidase in PBS (phosphate buffered saline) solution (versus enzyme-free PBS). As in the case of films, DNA release from the microspheres was

dependent on the DNA loading. DNA-HA microspheres were not directly used for transfection; instead, DNA obtained from release experiments was used in transfection of Chinese hamster ovary (CHO) cells using Lipofectamine™. The relative levels of transfection over time had the same trend as DNA release from the DNA-HA microspheres and confirmed that released DNA is bioactive.

The transfection capabilities of the HA microspheres were investigated *in vivo* by injecting the microspheres containing pDNA (encoding β-galactosidase) in rat hind limb muscles.[66] Three weeks post-injection, animals were sacrificed and RT-PCR showed detectable pDNA, indicating that DNA-HA microspheres are suitable for slow DNA release *in vivo*. In addition, the humanized monoclonal antibody that recognizes E- and P-selectin in modified CHO cells and human umbilical vein endothelial cells (HUVECs) was conjugated to HA microspheres. Antibody-conjugated HA microspheres showed very specific binding to cells expressing E- and P-selectin, demonstrating a great potential for development of site-selective HA delivery vectors.[66]

Recently, other approaches and modifications of HA for gene delivery applications have been investigated. Among the most interesting ones are mixed chitosan-hyaluronan based gene delivery systems [67-69] and PEG-HA photocrosslinked hydrogels.[70] HA has also been used to improve the biocompatibility of branched PEI via covalent conjugation.[71]

A more sophisticated system was reported recently in which HA is modified with spermine and a lipophilic amine containing a long hydrocarbon chain. This system was shown to be efficient in siRNA complexation, has a very low critical micelle

concentration (40-140 mg/L, depending on the length of lipophilic amine chain), and forms cationic micelles with 125-555 nm diameter.[72]

2.2.4. Pullulan

Pullulan is a neutral, water-soluble polysaccharide synthesized from starch by the fungus *Aureobasidium pullulans*. It is composed of maltotriose units, in which the three glucose units of the maltotriose are linked via α-(1→4) glycosidic linkages and consecutive maltotriose units are linked by a α-(1→6) glycosidic unit (**Figure 2.5**).[73] The versatility of pullulan has encouraged its usage in a variety of applications, including use as decorative materials in baking, coatings, capsules, and also in soft-chew candies.[73,74] Perhaps the most significant work has been done with pullulan

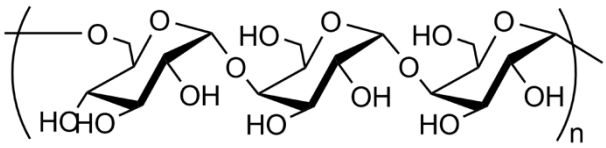

Figure 2.5. Structure of pullulan.

nanoparticles as drug carriers; water-insoluble drug molecules,[75] vitamins,[76] or cholesterol[77] have been encapsulated in the hydrophobic pullulan interior and used in treating a variety of diseases. However, it was not until 2004 that pullulan was used to design biomaterials that could be used to deliver nucleic acid therapeutics.

In 2002 Hosseinkhani *et al*. synthesized and evaluated several pullulan derivatives for gene delivery *in vivo*.[78] This work will not be discussed here in detail, since no *in*

vitro transfection experiments were conducted; however, this study presents an interesting approach to delivery vehicle design. Pullulan was grafted with diethylene triamine pentaacetic acid (using a corresponding anhydride and DMAP (4-(dimethylamino)pyrindine)) and with diethylenetriamine and triethylenetetraamine (using 1,1′-carbonyldiimidazole (CDI)). After purification, pullulan derivative solutions were mixed with pDNA solutions. This was followed by addition of Zn^{2+} ions, which were chelated by delivery vectors to allow tighter DNA encapsulation. These complexes showed enhanced gene expression in liver parenchymal cells which lasted for over 14 days.

In their further studies, the Tabata lab have synthesized pullulans grafted with spermine, using the same approach—CDI-mediated coupling.[79] The procedure requires about 15 equivalents of spermine per hydroxyl group (or 69 equivalents per primary hydroxyl group) of pullulan, but it is a very simple one-step synthesis, yielding pullulan with 12.3% spermine introduction. After the purification, modified pullulan was used for transfection of human bladder cancer T24 cells. This study revealed that pullulan-g-spermine polyplexes enter the cell through clathrin- and caveolae-mediated endocytosis with involvement of sugar-recognition receptors. The transfection efficiency evaluated by reporter gene expression was 10-fold better than Lipofectamine™. Moreover, it is mentioned that, according to the authors' unpublished data, similar enhancement in transfection is observed for Caki-1, ACHN, PC3, LNCaP, HepG2, UMUC-3, EJ and primary isolated rat bone marrow stromal cells.

Their next study investigated the influence of pullulan molecular weight and the amount of spermine grafting on transfection.[80] Among three tested molecular weights

(22.8, 47.3, and 112 kDa), pullulan with an intermediate molecular weight (47.3 kDa) was the most efficient in transfecting HepG2 cells. The optimal amount of grafted spermine for transfection varied for different molecular weight pullulans, and this amount decreased with increasing pullulan molecular weight. However, the optimal molar ratio of polymer to DNA was similar (close to 100) for all three tested molecular weights. Receptor-mediated endocytosis was suggested because transfection inhibition was observed upon pretreatment of cells with asialofetuin, a competitive inhibitor for the asialoglycoprotein receptor on hepatocytes.

Gupta and coworkers have formulated pullulan hydrogel nanoparticles as a pDNA delivery carrier.[33] The *in vitro* delivery efficacy and cytotoxicity of this approach were determined by β-gal expression and MTT assay, respectively, in HEK293 and COS-7 cells. In this study, water-soluble materials such as pDNA could be encapsulated within the hydrophilic core of these hydrogels and thus transported into the cells. The extent of pDNA protection from nuclease degradation was tested using gel electrophoresis. The results indicated that the pullulan nanoparticles were effective in protecting pDNA against DNase degradation. The cell viability in COS-7 and HEK293 cells determined using an MTT assay indicated that pullulan was relatively nontoxic; however, the cell viability decreased to about 80% (COS-7 cells) and 70% (HEK293 cells) with an increase in dosage to about 20 mg/mL. The cellular uptake mechanism of these nanoparticles was studied using SEM and fluorescent staining of cytoskeleton components in primary human fibroblasts (hTERT-bJ1) cells, which revealed that the nanoparticles entered the cells via an endocytic pathway. Following this, transfection was performed in serum-containing media to mimic *in vivo* conditions in both COS-7 and HEK293 cell lines. The

results indicated maximum expression at pullulan concentration 250 μg/mL. However, the transfection decreased with an increase in polymer concentration, which could be related to the cytotoxicity revealed in the MTT assay. The delivery efficacy was cell-type dependent, with COS-7 cells having higher gene expression than HEK293 cells. The pullulan-containing nanoparticles yielded comparable β-galactosidase expression to Lipofectamine™. This was the first study demonstrating the utility of pullulan as a DNA delivery carrier, and these results have been significant in motivating further development of pullulan-based nonviral vectors.

Consequently, San Juan and coworkers chemically cross-linked DEAE-pullulan and synthesized a cationic, 3D pullulan matrix that could be loaded with pDNA (pSEAP) and function as a delivery vehicle (**Figure 2.6**).[81] *In vitro* transfection and cytotoxicity

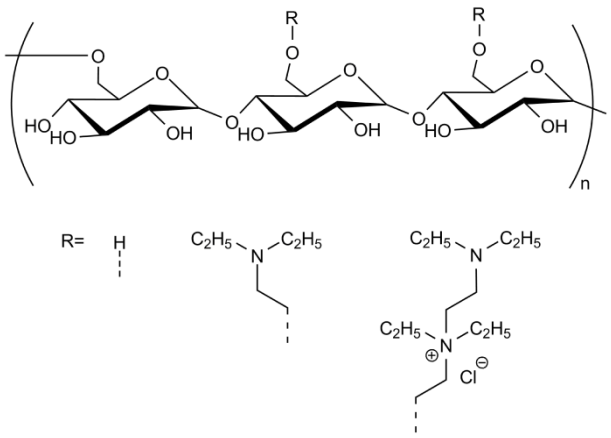

Figure 2.6. Structure of DEAE-pullulan.

experiments were performed in vascular smooth muscle cells (SMCs). In this study, pullulan was first grafted with N,N-diethylamin groups, yielding cationic DEAE-pullulan and then chemically crosslinked using $POCl_3$ to form a 3D matrix in the form of a

hydrogel disc. All the experiments were performed with both cationic DEAE-pullulan and the crosslinked DEAE-pullulan matrix. The extent of DEAE-pullulan/pDNA binding was studied via dye exclusion assay using PicoGreen®. The results indicated that neutral pullulan did not bind pDNA, as no fluorescence quenching was observed. However, fluorescence intensity decreased sharply with DEAE-pullulan, indicating pDNA binding with the cationic molecule (and PicoGreen® exclusion). The cell viability determined via the MTT assay indicated no significant toxicity when the SMCs were treated with either pSEAP/pullulan or pSEAP/DEAE-pullulan. The delivery efficacy in media containing serum was 150-fold higher using DEAE-pullulan than for naked pSEAP or a pSEAP/neutral pullulan mixture. The pSEAP extracted from the DEAE-pullulan matrix was found to be protected from nuclease degradation when compared with neutral pullulan, as indicated by gel electrophoresis. Furthermore, the DEAE-pullulan matrix has been shown to be nontoxic to SMCs, as revealed via MTT assay. Significant delivery efficacy was noted using DEAE-pullulan matrix at 6 days after initial transfection (when compared to pSEAP only). The nontoxicity and biodegradability of these 3D pullulan hydrogels will be useful towards their development as efficient nonviral DNA carriers for implantable devices to facilitate controlled release from surfaces.

The research performed by several groups on pullulans has demonstrated their potential as nucleic acid delivery vehicles. Although most of the pullulan-based delivery systems yielded low toxicity, some modifications of the backbone or introduction of substituents resulted in higher toxicity. Such modifications are unavoidable because the parent structure is incapable of efficient delivery and lacks target specificity.

2.2.5 Chitosan

Chitosan is the most widely studied polymeric vehicle for nucleic acid delivery, and the remainder of this section is devoted to its use and development as a delivery vehicle. Chitosan is a polysaccharide composed of glucosamine and N-acetyl glucosamine units bonded via β(1→4) glycosidic bonds (**Figure 2.7a**). The intense study of chitosan stems from its low cost, low toxicity, biodegradability, and the presence of primary and secondary hydroxyls and primary amines—functional groups that can be readily used for

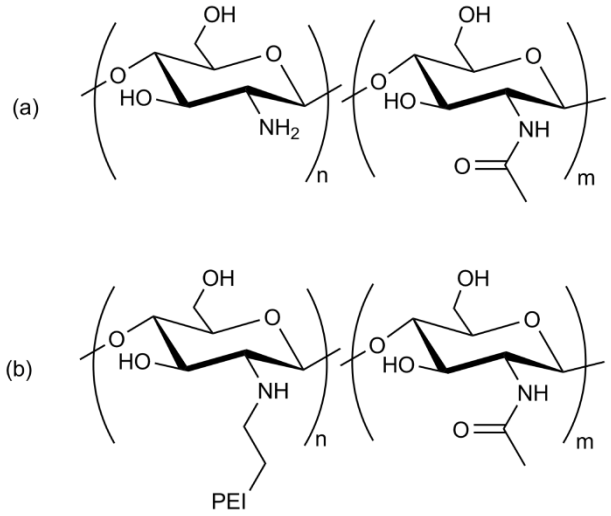

Figure 2.7. A. Structure of chitosans. **B.** Structure of chitosan-graft-PEI.

modifications via a range of well-establish hed reactions. Amino groups in chitosan have a pK_a value of ~6.5, making chitosan positively-charged in neutral and acidic solutions. Chitosan has been found to complex with a variety of polyanions, such as indomethacin,[82] sodium hyaluronate,[83] pectin, and acacia polysaccharides,[84] via electrostatic interactions. This concept has been explored extensively to complex chitosan with therapeutic nucleic acids.[31,85] The first study describing the formation of

chitosan/nucleic acid nanoparticles for gene delivery was reported by Mumper and coworkers in 1995.[86]

Chitosan is produced by basic hydrolysis of chitin.[87-89] Chitin is a natural polysaccharide, found widely in fungi and various arthropods, like spiders, insects and crustaceans (shrimp, crabs, lobsters, etc.). In its native state, chitin is a long polymer (molecular weight of 1-10 MDa), insoluble in water and organic solvents. It is made of N-acetyl-2-amino-2-deoxyglucose units linked via β(1→4) glycosidic bonds. Because chitin is semicrystalline and water-insoluble, its hydrolysis is heterogeneous, possibly leading to the formation of localized blocks of N-acetyl-2-amino-2-deoxyglucose units.[90] The influence of these blocks on polyplex formation and transfection is not well documented. In general, the deacetylation degree of commercially-available chitosan is ~80%, but methods affording complete (100%) deacetylation have been reported.[91] Notably, by fractionating chitosan via semi-preparative SEC, it was possible to reveal heterogeneity in molecular weights. In the case of the low-molecular-weight fractions of chitosan obtained via degradation with nitrous acid, a deacetylation degree dependence on molecular weight has been shown.[92] Methods for characterization of the deacetylation degree and molecular weight of chitosan and their influence on properties directly related to transfection efficiency, such as biodegradability, mucoadhesion, endothelium permeation enhancement and others, have been extensively reviewed, and the authors suggest using chitosan of ~10 kDa with deacetylation degree ≤ 80% for gene delivery applications.[89]

Chitosan is generally considered nontoxic, with the rare reported toxicity explained by Köping-Höggård *et al*. as a result of impurities.[93] In their study conducted with

ultrapure chitosan, transfection efficiency of 293 cells was shown to be dependent on the polyplex stability, which in turn was dependent on the deacetylation degree of chitosan. A deacetylation degree of at least 65% was found to be required to give efficient transfection. Variations in the molecular weight of chitosan within the range of 31-170 kDa, however, were shown to have no significant effect on polyplex stability and transfection results. *In vivo* experiments in mice showed that ultrapure chitosan is less efficient in gene delivery to the lung than PEI, but comparable to lipid-based delivery vehicles.

Kiang *et al.*[94] synthesized chitosans with different deacetylation degrees via acylation of high-deacetylation degree chitosan with acetic anhydride. Cell culture studies with HEK293, HeLa and SW756 cell lines revealed that the transfection efficiency is dependent on both the deacetylation degree and molecular weight, with chitosan of highest deacetylation degree being the most efficient. This was attributed to a greater polyplex stability afforded by the high-deacetylation degree chitosan in serum-containing media. However, for intramuscular injection of polyplexes in mice, high-deacetylation degree chitosan was the least efficient, likely due to slower release of the cargo. This study illustrates the potential differences between *in vitro* and *in vivo* transfection efficiencies.[94]

Similar *in vitro* results were obtained in a study by Huang *et al.*[95] High-deacetylation degree chitosans were also more efficient in protecting DNA from degradation. Transfection of A549 cells with pDNA was more efficient with increasing the deacetylation degree of chitosan. These results showed good correlation between ζ-potential, cellular uptake and transfection efficiency, suggesting that the electrostatic

interactions between the nanoparticle and the cell membrane mediate cellular uptake and lead to gene expression.[95] Similar effects were observed with siRNA gene silencing experiments, as polyplex stability and delivery efficiency was generally higher for high-molecular-weight chitosans with higher deacetylation degrees in H1299 human lung carcinoma cells.[96]

As discussed in the aforementioned studies, deacetylation degree plays a crucial role in transfection, with desirable value being in the range of 65-80%. Polyplexes prepared with chitosans having lower amine density do not protect the cargo from degradation by enzymes and are not stable in serum. The influence of chitosan molecular weight is less well understood. As previously described, variations in chitosan molecular weight within the range of 31-170 kDa did not affect transfection of 293 cells. However, in an earlier study by MacLaughlin and coworkers,[87] it was discovered that a decrease in molecular weight of chitosan, from 540 to 7 kDa caused a concomitant decrease the complex size, from 500 nm to 100 nm. The ability to modify polyplex size can influence the mechanism of endocytosis,[97] which likely affects the intracellular fate of the polyplex. In serum-containing media, pDNA delivered with 540 kDa chitosan leads to higher transgene expression than other molecular weight chitosans. In general, it can be speculated that longer chains of high-molecular-weight chitosan are able to form more stable polyplexes with DNA but are less efficient in releasing the cargo than low-molecular-weight chitosans.

The size of the polyplex depends not only on the chemical structure of chitosan but also on the ratio between chitosan and DNA used for polyplex formulation, the concentrations of polymers, and formulation technique. This is commonly described in

terms of "N/P ratio," the ratio of protonatable polymer amines to phosphate groups in the nucleic acid. Increasing N/P ratios typically lead to formation of polyplexes with more positive surface charge, also known as ζ-potential. High ζ-potential may seem desirable because it should increase interactions with the negatively-charged cell surface and, hence, lead to higher cellular uptake and transfection. However, high charge density usually results in cytotoxicity, likely caused by the disruption of the cellular membrane.[98] It was shown by Erbacher *et al.*[99] that N/P ratios greater than 2 are necessary for formation of polyplexes with chitosan (70 kDa was used in this study) having positive ζ-potential. The optimal N/P ratio is specific to each polymer and is usually based on polyplex stability, polyplex ζ-potential, and the ability of the polymer to protect cargo from degradation.

As previously discussed, the protection of pDNA against degrading enzymes is a critical parameter for a nonviral carrier. Such ability is needed for the polyplex to protect the nucleic acid for an extended period of time in the blood while the polyplex circulates and distributes. Research conducted in 1999 by Richardson and coworkers[100] to study the ability of chitosan to protect against DNase degradation revealed that incubation of polyplexes prepared at N/P ratio of 3/1 in the presence of DNase I (8 U, 1 h incubation) protected pDNA from degradation. Other studies of chitosans as gene delivery vehicles confirm that the N/P ratio has to be at least 3/1 to 5/1 in order to provide a sufficient protective effect against DNases.

Shortly after Mumper and coworkers published their original work with chitosan, Murata *et al*. synthesized quaternary chitosan using MeI in N-methylpyrrolidone (it was also further derivatized by incorporation of galactose).[101,102] Since then, quaternization of

chitosan has become a primary strategy in the development of chitosan nucleic acid delivery systems. Quaternization introduces pH-independent charges into the polymer backbone and increases the charge density. The efficiency of the quaternization approach was elegantly demonstrated by Thanou and coworkers.[103] They investigated the transfection efficiency and cytotoxicity of quaternized chitosan oligomers (< 20 monomer units) in COS-1 and Caco-2 cells. The results demonstrated higher transfection, in both serum-free and serum-containing media, for polyplexes prepared with quaternized chitosan than with unmodified chitosan polyplexes. The increase in transfection was especially significant in COS-1 cells. The efficacy was dependent on the weight ratio of the DNA/chitosan-oligomer polyplexes. The optimal weight ratio for transfection of COS-1 cells in serum-free media was 1/14. MTT assays revealed that the quaternized chitosan remained nontoxic, comparable to unmodified chitosan, in both cell lines.

Kean and coworkers investigated the difference in transfection efficiencies of oligomeric (3-6 kDa) and polymeric (~100 kDa) quaternized chitosans, using monkey kidney fibroblasts (COS-7) and epithelial breast cancer cells (MCF-7).[104] Both oligomeric and polymeric chitosan at optimized degrees of quaternization (44% for oligomeric chitosan, 57% and 93% for polymeric chitosan) transfected MCF-7 cells more efficiently than PEI as measured by luciferase assay. In the case of COS-7 cells, however, only oligomeric chitosan with 44% quaternization showed transfection comparable to, but not exceeding that of, PEI. Importantly, chitosans showing the highest transfection efficiency showed moderate cytotoxicity, with the polymeric chitosan exhibiting higher toxicity than its oligomeric counterpart.

Attempts to improve transfection of chitosan-based vectors by grafting PEI onto a chitosan backbone have been reported. The goal of such efforts is improvement of the buffering capacity and charge density of chitosan while preserving its low inherent cytotoxicity. One of the first attempts to utilize PEI buffering properties in chitosan based gene delivery systems was made by Kim *et al.*[105] PEI was physically added to (not chemically grafted on) chitosan/DNA polyplexes; addition of PEI to water-soluble chitosan/DNA polyplexes increased their transfection efficiency in HeLa, A549 and 293T cells. Furthermore, a synergistic effect between water-soluble chitosan and PEI was demonstrated in the transfection of 293T cells. This approach was also efficient in the case of a targeted delivery system—galactosylated chitosan. Addition of moderate amounts (1-2 μg) of PEI to galactosylated chitosan/DNA polyplexes increased the transfection efficiency in HepG2 cells while retaining receptor-mediated cellular internalization. However, addition of a greater amount of PEI (5 μg) decreased cell specificity, and, in this case, the transfection efficiency of HepG2 cells by galactosylated chitosan/DNA was not different from that of nongalactosylated water-soluble chitosan/DNA polyplexes.

Taking the idea a step further, Wong and coworkers[106] grafted low molecular weight PEI (M_n = 206 Da) on water-soluble chitosan (M_n = 3.4 kDa) via cationic polymerization of aziridine, with chitosan amino groups functioning either as initiators or terminators of polymerization (**Figure 2.7b**). It should be noted that such an approach can lead to formation of free, non-bound oligoethyleneamines. but dialysis performed after polymerization likely removes this side product. The effect of PEI grafting was studied in HeLa, HepG2, and primary hepatocytes. Chitosan-g-PEI complexed pDNA at

an N/P ratio of 2.5, but the maximum transfection efficiency in serum-free media was achieved at N/P=40 for all three tested cell lines. At this N/P ratio, transfection efficiency was similar to PEI (25 kDa) at N/P=10. The cell viability, assessed via the MTT assay, was reported only for free polymers in HeLa cells and revealed, interestingly, that chitosan-g-PEI had a 7-fold higher LD_{50} than PEI. Chitosan-g-PEI transfection was investigated *in vivo* by administration of polyplexes into the common bile duct in rats for liver delivery. Delivery with chitosan-g-PEI at N/P=10 was 141-fold greater than that of naked DNA, 58-fold greater than PEI (25 kDa), and 3-fold greater than unmodified chitosan.

Following their successful tandem use of water soluble chitosan/galactosylated chitosan and PEI for the polyplex formulation, Cho *et al.* chemically grafted PEI onto chitosan.[107,108] The grafting was accomplished by partial oxidation of 100 kDa chitosan with periodate followed by reductive amination using 1.8 kDa PEI (**Figure 2.8**).

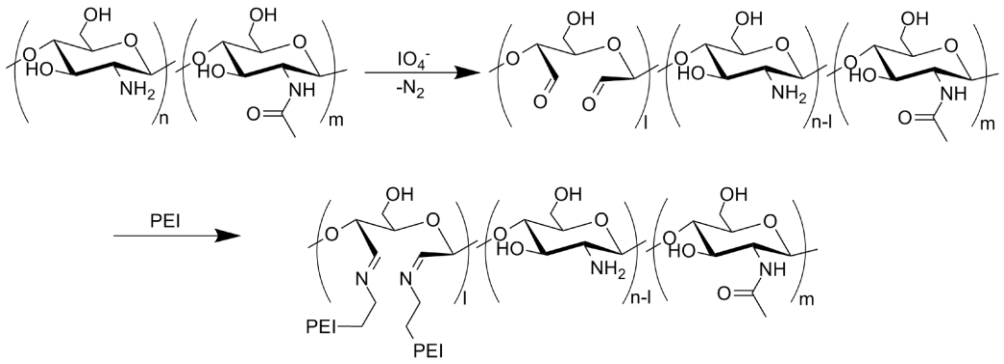

Figure 2.8. Synthesis of chitosan-graft-PEI. Figure reproduced from reference [107] with permission. © 2007 Elsevier.

Periodate is widely used in oxidation of vicinal diols, presumably via a five-membered intermediate. However, as noted by Vold *et al.*, IO_4^- oxidative cleavage of 1,2-aminoalcohols is also known[109] and can be successfully used for oxidative cleavage of the C2-C3 bond within the glucoseamine unit in chitosan.[110] Thus, it is necessary to exercise careful control of reaction conditions to avoid overoxidation and depolymerization of chitosan.

Synthesized chitosan-g-PEI was evaluated by transfection in HeLa, HepG2, and 293T cells. In this case, chitosan-g-PEI was found to complex pDNA stably, with an average polyplex size of 250 nm, and protected pDNA from nuclease degradation. The cytotoxicity of these polymers was much lower than that of PEI (25 kDa) in all three cell lines. Similar to the aforementioned study by Wong *et al.*, the transfection efficiency for this grafted system in serum-free media was higher than unmodified PEI (25 kDa) at N/P=35 (N/P=10 was used in the study by Wong *et al*.). Furthermore, high luciferase expression, similar to that of Lipofectamine™, was noted in 293T cells using chitosan-g-PEI. Interestingly, transgene expression in serum-containing media with chitosan-g-PEI was only slightly decreased in comparison to PEI and Lipofectamine™.

To further explore the potential of chitosan-g-PEI vectors, Jiang *et al.* have synthesized galactosylated chitosan-g-PEI[111] and galactosylated poly(ethylene glycol)-chitosan-g-PEI (Gal-PEG-chitosan-g-PEI),[112] with the latter prepared by linking galactose-terminated PEG carboxylic acid to chitosan-g-PEI via amide bonds. Incorporation of PEG is a standard approach to improve the polyplex colloidal stability and prevent undesirable electrostatic interactions with negatively-charged components of plasma and cellular membranes. This approach was successful in this case as well,

showing that Gal-PEG-chitosan-g-PEI was less efficient in transfection of HepG2 and HeLa cells than chitosan-g-PEI due to reduced electrostatic interactions. But, more importantly, Gal-PEG-chitosan-g-PEI was better in transfecting HepG2 cells than non-targeted PEG-chitosan-g-PEI, whereas in HeLa cells their transfection efficiency was similar. These results show that cell-specific targeting can be achieved for chitosan-g-PEI vectors.

Recently, new ways to graft PEI onto chitosan have emerged. Lu *et al*. have used a maleic acid anhydride reaction with the amino groups of chitosan, followed by the Michael-type addition of PEI.[113] Lou and coworkers used ethylene glycol diglycidyl ether to link PEI with chitosan through hydroxyl and amino groups of chitosan.[114] Wu *et al.* have used alkylation of primary hydroxyl groups of chitosan with chloroacetic acid, followed by purification, activation of carboxyl groups with N,N'-dicyclohexylcarbodiimide (DCC) and N-hydroxysuccinimide (NHS), and subsequent coupling with PEI through amide bond formation.[115] It is not clear how self-coupling of chitosan was avoided in this approach, however.

PEI grafting on chitosan is becoming a popular approach for modification of chitosan for gene delivery applications. In recent years several efforts to develop chitosan-g-PEI delivery vectors have been published. These include incorporation of mannose[116] and folic acid[117] derivatives for targeted delivery and application of chitosan-g-PEI for the delivery of siRNA.[118]

A means by which the buffering capacity of chitosan delivery vehicles can be improved without significantly increasing their cationic character is to graft the chitosan backbone with imidazole. Imidazole contains a protonatable nitrogen having a pK_a of

6.15; thus, imidazole may facilitate endosomal rupture through the proton-sponge mechanism. For this reason, imidazole has been used widely in nucleic acid delivery vectors, and these materials have been discussed elsewhere.[119-121]

Kim *et al.* decorated the chitosan backbone with imidazole groups by coupling of urocanic acid to chitosan through EDC/NHS condensation (**Figure 2.9**).[122] Urocanic acid-modified water-soluble chitosan (50 kDa) was evaluated for transfection efficiency using 293T, HeLa and MCF-7 cells. The modified chitosans were found to bind pDNA and also protected from DNase degradation at charge (N/P) ratios between 5 and 30. The transfection performed in 293T cells yielded greater transgene expression for urocanic acid-modified chitosan than the unmodified analog, and the efficacy also tended to increase with greater extents of grafting, demonstrating the role of imidazole groups for transfection of 293T cells. However, no significant enhancement in gene expression was evident when the same experiment was performed in HeLa and MCF-7 cells, thereby indicating that the transfection is highly cell-type dependent. This delivery vehicle was later also used for *in vivo* studies for aerosol delivery of nucleic acids to the lung, which led to tumor suppression in this model.[123,124]

Thiols are typically incorporated into polymers for gene delivery to take advantage of the reducing environment of the cytoplasm. Thiols can be mildly oxidized to produce disulfide (S-S) bonds for delivery vehicle crosslinking, providing protection

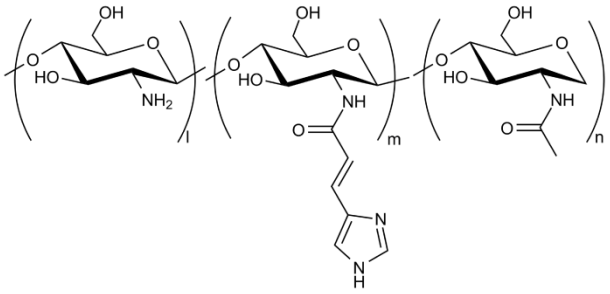

Figure 2.9. Structure of urocanic acid-modified chitosan.

for the cargo from degradative enzymes and preventing premature nucleic acid release. In the cytosol, the S-S bond can be reduced (primarily due to high concentrations of glutathione), causing changes in polyplex organization that result in release of carried nucleic acid. More information on disulfide usage in polymeric gene delivery systems, disulfide bond synthesis, and mechanism of action can be found in a recent review by Bauhuber *et al*.[125]

Thiolated chitosans[126] (**Figure 2.10**) have been used for the development of an oral gene delivery vehicle.[127] The synthesis was accomplished in aqueous media using 2-iminothiolane and low-molecular-weight chitosan. Thiolated chitosan complexed pDNA into 125 nm polyplexes with a positive ζ-potential and was able to protect pDNA in artificial intestinal fluids at multiple physiologically-relevant salt concentrations. These complexes were stable at pH=1.2. Under reducing conditions, thiolated chitosan releases 50% of its pDNA cargo in ~3.5 hours, whereas in non-reducing conditions only ~7% of pDNA is released at this time point. Moderate transfection of Caco2 cells was observed with thiolated chitosan, but it was higher than both controls – naked pDNA and (unmodified) chitosan/pDNA. Based on the stability to artificial intestinal fluids and low

pH, as well as low cytotoxicity, it was concluded that thiolated chitosans are candidates to be further studied as oral gene delivery vectors.

In another study from the same lab,[128] thiolated chitosan (12 kDa) was synthesized by conjugation of chitosan with thioglycolic acid. The thiolated chitosan/DNA nanoparticles were more resistant to DNase degradation at pH 4.0 and 5.0 than naked DNA and complexes formed with unmodified chitosan. MTT assays performed at pH 5.0 in Caco-2 cells indicated that the nanoparticles formed using unmodified chitosan and non-crosslinked thiolated chitosan were nontoxic. Crosslinked chitosan at pH 5.0 and both non-crosslinked and crosslinked thiolated chitosans at pH 4.0, were slightly toxic, with a cell viability 80–90% of untreated cells. The transfection experiments performed in Caco-2 cells revealed that both non-crosslinked and crosslinked thiolated chitosan yielded higher transgene expression levels than their unmodified analog in this cell model. In addition, thiolated chitosan/DNA formulated at pH 4.0 exhibited 5-fold higher efficiency than unmodified chitosan.

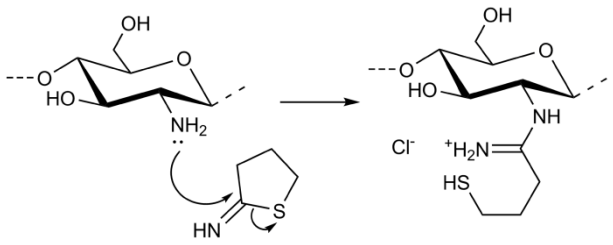

Figure 2.10. Synthesis of thiolated chitosan. Figure reproduced with permission from reference [126]. © 2004 Elsevier.

Chitosan has also been grafted with saccharide-based ligands as molecular recognition elements to promote receptor-mediated endocytosis for cell specific delivery *in vivo*. Extensive research has been completed by various groups in developing chitosan-based delivery vectors conjugated to saccharides for target-specific delivery. The remainder of this section focuses on targeting cell surface lectins with carbohydrates grafted onto a chitosan backbone.

Nearly a decade ago, Murata *et al.*[129] synthesized quaternary chitosan polymers grafted with galactosyl residues along the side chain **(Figure 2.11a)** and utilized them to transfect HepG2 cells (which express the asialoglycoprotein receptor (ASGPr), for which galactose is a ligand) in serum-free media. The β-galactosidase expression observed in HepG2 cells revealed that the gene expression tended to be higher for galactosylated TMC than the non-galactosylated polymer. It was also found that increased amounts of galactose substitution yielded higher transfection efficiency, suggesting a multivalent effect for efficient uptake. Furthermore, the cytotoxic effects of these galactosylated chitosans were similar to that of DEAE-dextran.

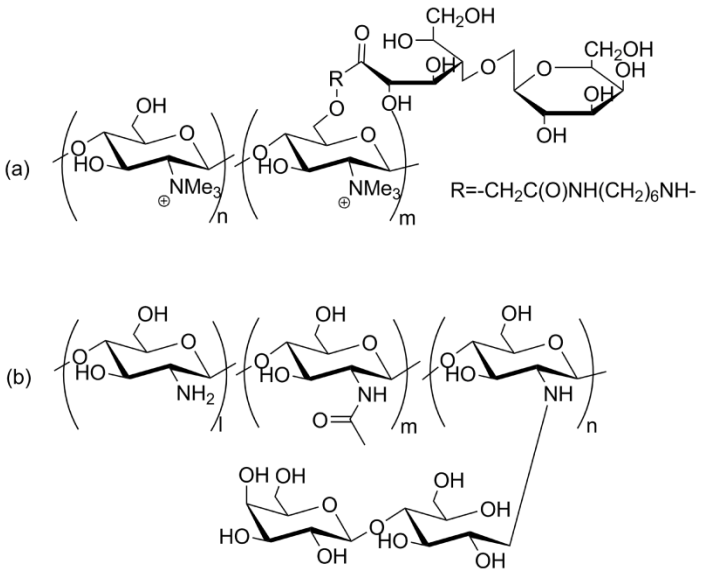

Figure 2. 11. A. Structure of galactosylated chitosan. Figure reproduced from reference [101] with permission. © 1996 Elsevier. **B.** Structure of lactose conjugated chitosan. Figure reproduced from reference[130] with permission. © 2006 American Chemical Society.

In a similar study, Park and coworkers[131] synthesized chitosan-based vectors in which the chitosans were conjugated to lactobionic acid, which contains galactose residues. These structures were then grafted with either dextrans (M_n = 5.9 kDa) (GCD), poly(ethylene glycol) (M_n = 5.0 kDa) (GCP), or poly(vinylpyrrolidone) (GCPVP) to enhance polyplex stability (prevent aggregation). In the first study, galactosyl chitosan (M_n = 4.0 kDa) was conjugated with dextran and examined for delivery efficacy in Chang liver cells (express ASGPr) and HeLa cells (non-ASGPr-expressing). As expected, the dextran conjugation was found to stabilize the polyplexes from aggregation and yielded higher gene expression in Chang liver cells than in HeLa cells. In a related study by the same group, similar results were obtained when galactosyl chitosan (M_n = 7.0 kDa) was conjugated with PEG.[132] Polyplexes formed with this polymer were used to transfect in HeLa, CT-26, and HepG2 cells, and the results were compared to those from the previous study. It was found that these PEGylated analogs had stability comparable to the dextran-mediated vectors and were found to protect pDNA from nuclease degradation. The transfection experiments indicated the vehicle had negligible cytotoxicity and that GCP/pDNA yielded transgene (green fluorescent protein) expression in HepG2 cells, but not in HeLa and CT-26 cells, thereby suggesting that the transfection occurs through ASGPr. In a more recent study by the same group, galactosyl chitosan (10 and 50 kDa)

were grafted with poly(vinylpyrrolidone) (PVP) using radical polymerization[133] and similarly studied as a hepatocyte-targeting vehicle. PVP has been found to have similar properties to PEG; however, the PVP-modified polyplexes were found to have longer retention time in the blood than the PEG-modified systems.

All of the aforementioned studies demonstrate that chitosan-grafted with polycations can be effectively used for hepatocyte-specific delivery applications. In addition, incorporation of flexible hydrophilic groups in the polymer structure provides a steric barrier that prevents aggregation and reduces interactions of the complexes with plasma proteins and phagocytes, thereby increasing the circulation time of these complexes in the plasma and facilitating complexes reaching target cells. However, the syntheses of these grafted systems are slightly more tedious and difficult to manufacture on an industrial scale; in addition, they often result in a highly polydisperse polymer mixture with high batch to batch differences in conjugation efficiency.

Similar results to galactosyl chitosan were seen when lactose-conjugated chitosan (53 kDa) conjugates (lac-chitosan) were synthesized (**Figure 2.11b**) by Hashimoto *et al.*[130] and used to transfect HepG2 cells. In this study, conjugates were prepared for which the amines along the chitosan backbone were either 8% or 33% functionalized with lactose. Both were found to bind and compact pDNA into ~140-nm polyplexes at N/P≥3 (ζ-potential = +43 mV). Unlike polyplexes prepared with nonlactosylated chitosan, these lac-chitosan-containing polyplexes were stable to aggregation and adsorption after 1 h incubation with bovine serum albumin (polyplexes remained ~150 nm in diameter), thereby indicating that the lactose modification on chitosan results in serum stability. The 8% lac-chitosan/pDNA complexes revealed transfection efficiency in

COS-7 cells similar to those made with the unmodified analog, whereas polyplexes formulated with the 33% lac-chitosan/DNA had about 2-fold lower transfection efficiency than unmodified chitosan/DNA complex. However, in HepG2 cells, a 16-fold enhancement in transgene (luciferase) expression was observed when 8% lac-chitosan/DNA was used for transfection, suggesting that receptor-mediated delivery leads to higher gene expression. In both cell lines, Lipofectamine™ showed much higher gene expression when compared to the conjugated and non-conjugated chitosans.

Inspired by earlier work on galactose-conjugated chitosans, Hashimoto and coworkers[134] synthesized mannose-grafted chitosan (53 kDa) conjugates (man-chitosan) to deliver pDNA in mouse peritoneal macrophages that express the mannose receptor. Here, man-chitosan containing either 5% or 21% modification were synthesized, and mixing with pDNA resulted in formation of ~300 nm polyplexes. Both complexes formed with the man-chitosan derivatives were found to exhibit increased transfection in macrophages compared to pDNA/chitosan polyplexes and yielded comparable transfection to man-PEI/DNA polyplexes in macrophages. When a control experiment was performed in COS-7 cells, the transgene expression of pDNA/5% man-chitosan polyplexes was the same as that of pDNA/chitosan; however, the transfection efficiency of pDNA/chitosan was four times higher than pDNA/21% man-chitosan. The cell viability in experiments in macrophages also revealed negligible cytotoxicity of the man-chitosan polyplexes, which contrasted with the toxicity observed for man-PEI/pDNA complexes .

Even though all the above experiments have been promising and shown effective transfection and target-specificity particularly with hepatocytes, most of these *in vitro*

experiments have been performed only in serum-free media. The future of this area depends on performing these experiments in media containing serum, which are a better simulation of *in vivo* conditions. Also, *in vivo* data in this field is minimal and more is needed to advance this area toward the clinic. These extensive studies using chitosan have shown that this polysaccharide is indeed very useful for delivering therapeutic DNA into cells and the structure affords nearly limitless potential for chemical modification. However, their lower transfection efficiencies than other non-viral analogs and viral-vehicles needs to be overcome by chemical and structural modifications. Much further work on this delivery platform is ongoing.

2.3. Carbohydrate Copolymers

Saccharide copolymers are recently emerging biomaterials with high applicability as nucleic acid delivery vehicles. To date, the structures created can generally be categorized as AABB step-growth type polymers consisting of two different monomers, where one monomer facilitates nucleic acid binding and the other (carbohydrate) monomer imparts biocompatibility. Previous results have shown that saccharide groups contribute to reduction of the cytotoxicity of nonviral vehicles. For example, when relatively toxic polymers, such as PEI, are grafted with carbohydrates, the cytotoxicity is decreased (e.g.[135]). For this reason, carbohydrate moieties have been incorporated in the polymer backbone using a variety of synthetic organic reactions, such as polycondensation, cycloaddition, or ring-opening polymerization. The structure of the monomers and synthetic methodologies have been found to influence various parameters,

such as solubility, degree of polymerization, branching, and tacticity of the polymers. Furthermore, as with previously-presented systems, the studies in this section also demonstrate that subtle changes in the chemical and structural characteristics of these polycations have a significant effect on the cellular uptake, gene expression, and cell viability. This section describes novel polymers that have been synthesized with a variety of monosaccharides,[21,136] disaccharides,[137-139] or cyclic oligosaccharides,[140] and their efficacy as *non-viral* nucleic acid delivery vehicles.

2.3.1. Monosaccharide-based Copolymers

The introduction of carbohydrates in polymeric structures could temper the cytotoxicity observed with these vehicles. Two commonly-studied polymeric vectors—poly-L-lysine (PLL), a polypeptide consisting of repeating lysine residues, and polyethylenimine (PEI), composed of repeating ethylenediamine units—have shown the ability to deliver DNA for gene expression at a high level *in vitro* and *in vivo*.[10,13,141] Significant cytotoxicity, likely due to their high charge density and possible membrane-disrupting effects, limits the potential clinical utility of these vehicles. Reduction of the charge density by incorporation of carbohydrates could yield transfection efficiencies greater than those of polysaccharide-based vehicles and afford increased biocompatibility, thus resulting in an improved delivery system. In the first study using this strategy, published by Reineke and coworkers in 2004, esterified glucose was polymerized with diethylenetriamine, triethylenetetramine, tetraethylenepentamine, and pentaethylenehexamine to derive polymers containing 1-4 secondary amines in the

polymer repeat unit.[136] These polymers were able to self-assemble with DNA into polyplexes. When transfected into BHK-21 cells, pDNA complexes containing these polymers showed high levels of transgene expression with considerably lower toxicity than PEI. In fact, the analog with four secondary amines, dubbed D4, showed transgene expression comparable to PEI. A similar study was published after by Guan *et al*. in 2005, using a similar strategy; however, the incorporated charge centers were L-lysines.[142] An acid chloride derivative of galactose was polymerized with oligolysines to develop three polymers with varied amounts of primary amines and spacing between the primary amine and the polymer backbone. These polymers also showed enhanced biocompatibility versus PLL and gene expression was comparable to PLL at low molar concentrations. These polymers did not elicit an immune response when administered to rats via intravenous or subcutaneous injection.[142] These first two studies showed that interrupting the charge density of PEI and PLL is advantageous for achieving low toxicity *in vitro* and *in vivo* without sacrificing delivery efficacy.

These favorable results led Reineke and colleagues to expand their initial study using three different carbohydrates to study the effect that hydroxyl number and stereochemistry, as well as amine stoichiometry, have on biological activity. A library of 16 polycations was developed, containing alternating monosaccharides and amine units along the main polymeric backbone, and were termed poly(glycoamidoamine)s

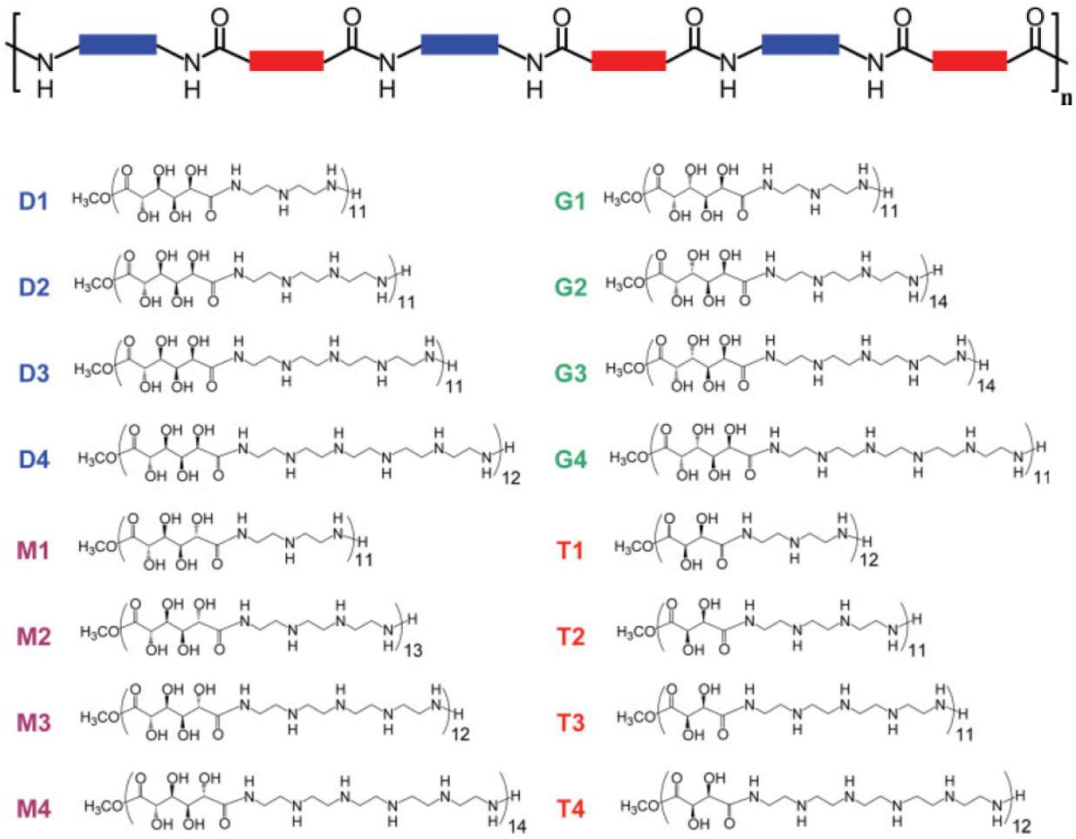

Figure 2.12. Generalized block diagram of PGAA design structure and structures of the 16-polymer library of PGAAs. These polymers allow the direct comparison of changes in amine stoichiometry, as well as hydroxyl number and stereochemistry, on biological properties. Figure adapted from reference [143] with permission. © 2006 John Wiley & Sons, Inc.

(PGAAs), **Figure 2.12** [21,136] These polymers contain one of four different carbohydrate comonomers: a mixture of dimethyl-D-glucarate, methyl-D-glucarate 1,4-lactone, and methyl-D-glucarate 6,3-lactone (D), dimethyl-*meso*-galactarate (G), D-mannaro-1,4:6,3-

dilactone (M), or dimethyl-L-tartrate (T). These comonomers were polymerized with the same series of oligoamine comonomers as the first study (diethylenetriamine (1), triethylenetetramine (2), tetraethylenepentamine (3), or pentaethylenehexamine (4)) via step-growth polymerization to generate a series of polymers (D1 – D4, G1 – G4, M1 – M4, T1 – T4) with degrees of polymerization (*n*) around 11–14. These initial structures were found to bind and compact pDNA into cationic polyplexes, and increasing the amine number generally led to more efficient DNA binding and smaller polyplex size.

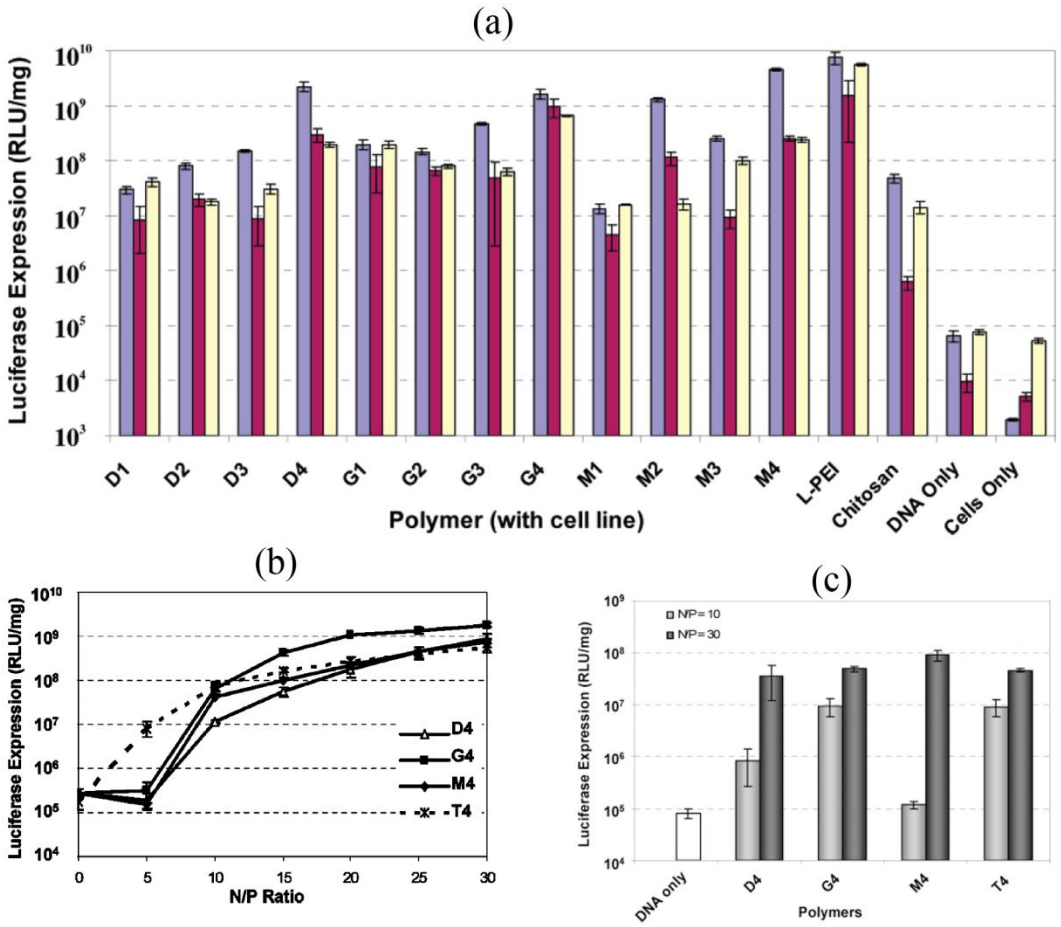

Figure 2.13. Transgene expression efficiency of PGAA polymers in multiple mammalian cell types. (**A**). G, D, and M polyplexes shown high levels of transfection in multiple cell

types. PGAAs with 4 secondary amines/repeat unit in H9c2 cells in (**B**) serum-free and (**C**) serum-containing media. Figures adapted from references [21] and [145] with permission. © 2005 and 2006 American Chemical Society.

This library of cationic glycopolymers was screened for cell viability and transgene expression, and the results were compared to chitosan and PEI to assess the improvements achieved over these vehicles (**Figure 2.13**). To ensure widespread utility, these vehicles were tested in four different cell lines to mimic a wide range of mammalian cell types: BHK-21, HeLa, HepG2, and H9c2(2-1).[21,144,145] High levels of transgene expression were observed in all cell lines; the polymers containing four secondary amines yielded the highest transfection levels (**Figure 2.13**). At the N/P ratio of maximum expression, the luciferase expression efficiency of these vehicles was comparable (within an order of magnitude) to that of PEI and significantly enhanced over chitosan. These results also showed very low toxicity that was comparable to chitosan and significantly lower than PEI. The highest transgene efficiency was observed for G4 and T4, which bind DNA the strongest among the series and were shown to protect pDNA from degradation by nucleases. Further study in cardiomyoblast (H9c2(2-1)) cells revealed that, despite a significant polyplex size increase in salt and serum, high levels of gene expression were also observed, which were related to high levels of polyplex cellular internalization. Using polyplexes containing FITC-labeled pDNA, the cellular internalization of PGAA polyplexes was assessed in serum-free and serum-containing media. The data shows high levels of uptake, with nearly every cell analyzed containing

DNA-associated fluorescence under both conditions. These data illustrate the high efficiency by which PGAA polyplexes can enter cells.

These promising results have led to systematic study on the effects of polymer structure on DNA binding and bioactivity. These further studies probe many aspects of polymer structure to determine the structural elements that lead to efficient delivery. DNA binding of PGAAs occurs through a combination of electrostatics and hydrogen bonding, a direct result of carbohydrate incorporation into the polymer.[146] The close-

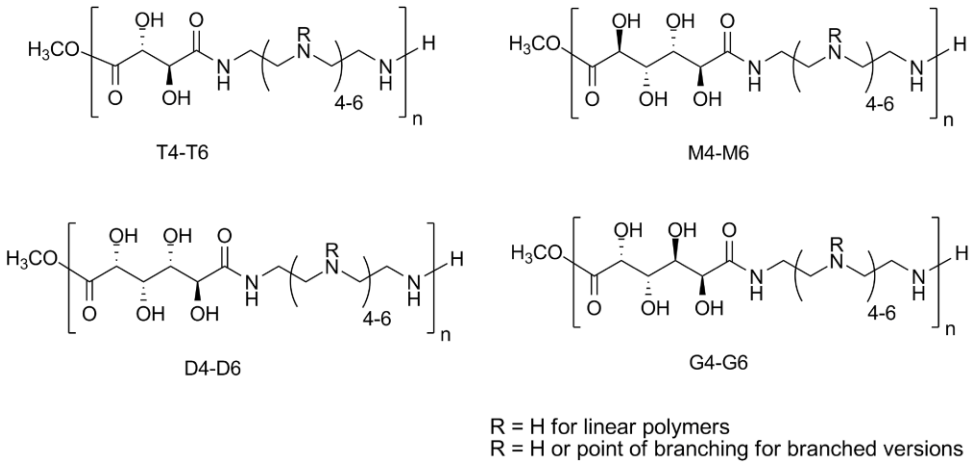

Figure 2.14. Structures of linear PGAAs.

range hydrogen bonding interactions likely afford greater polyplex stability such that the DNA can remain packaged while inside the cell. Using similar techniques as described above, Lee *et al*. investigated the effect of increasing the number of secondary amines in the polymer backbone from four to five and six (**Figure 2.14**), as well as the effect of polymer branching, on delivery efficacy and toxicity.[147] The linear and branched polymers yielded polyplexes of generally larger size than those with four secondary amines, but the galactose and tartrate series with five and six secondary amines did not

significantly swell or aggregate in serum-containing media, suggesting the higher secondary amine numbers prevent increasing size in serum. However, these modifications did not result in much enhancement of cellular uptake, as polyplex internalization was mostly unaffected (in some cases it was lower or a little higher and this depended on the cell type). Similar results were observed for transgene expression, as transfection. However, these modifications did have a significant effect on cell viability, as the linear polymers with five and six secondary amines displayed increased toxicity over the series with four secondary amines in the polymer repeat unit. This study confirmed that four secondary amines in the polymer repeat unit yields the highest internalization and transgene expression, and these analogs are the focus of further structure-bioactivity studies.

Polymer buffering capacity can have a significant effect on the cellular uptake and gene expression in mammalian cells, as polymer charge likely plays a key role in cell surface binding and either escape or trafficking out of the endosomal/lysosomal path. Liu *et al*. used titration experiments to calculate the buffering capacity of the D-glucaroamidoamine (D1-D4) and L-tartaroamidoamine (T1-T4), which allows a direct measure of the percentage of amines that can be protonated during endosome acidification.[96] The results of these experiments allow a direct comparison of polymer buffering capacity with cellular internalization and transgene expression. Two new polymers were created by polymerizing the dimethyl-D-glucarate (this is a mixture with lactone derivatives) or dimethyl-L-tartrate with spermine (yielding DS and TS, respectively) to incorporate butylene groups between neighboring secondary amines, thereby increasing the amine spacing. Interestingly, buffering capacity decreased with

increasing amine number; however, the delivery efficacy and gene expression increased with the increase in amine number. This argues against the proton sponge mechanism of endosomal escape, as this hypothesis states that a higher buffering capacity should promote greater endosomal escape and should lead to increased gene expression. However, when the comparing differences in amine spacing, the polymers containing the spermine groups (DS and TS) yielded a substantial decrease in buffering capacity compared to the original PGAAs with ethylene spacing. This suggests that proximal amines (ethylene spacer) have a lower charged state at pH 7.5 due to electrostatic suppression of protonation from neighboring charged amines. However, when comparing the gene expression results, DS and TS had higher gene expression than their PGAA analoges with two ethylene amines (D2 and T2) but the analogs with four amines (D4 and T4) still remained the most efficient delivery systems. Polymers with increased amine spacers also exhibited much higher toxicity, suggesting the charge spacing and charge density plays a significant role in biocompatibility. Buffering capacity also appears to influence the transfection of polymers having the same amine stoichiometry but different carbohydrates, as D4 possesses lower buffering capacity than T4, resulting in higher transgene expression with T4. Increasing cellular uptake was observed with higher amine number, which suggests higher amine density promotes multivalent interactions with the cell surface proteoglycans, facilitating higher uptake. Indeed, cellular uptake was found to be a major contributing factor to efficient transgene expression. This study proves that ethylene spacers between amines lead to more biocompatible gene expression and reveals a complex role of polymer buffering capacity that does not directly correlate with high delivery efficiency and gene expression.

Recent results in the Reineke lab reveal that the PGAAs are biodegradable under physiological conditions, and that removal of the carbohydrate or the oligoethyleneamine groups leads to a polymer that does not degrade under physiological conditions.[148] This points toward a synergistic effect in the presence of both the carbohydrates and ethyleneamine groups in polymer degradation.

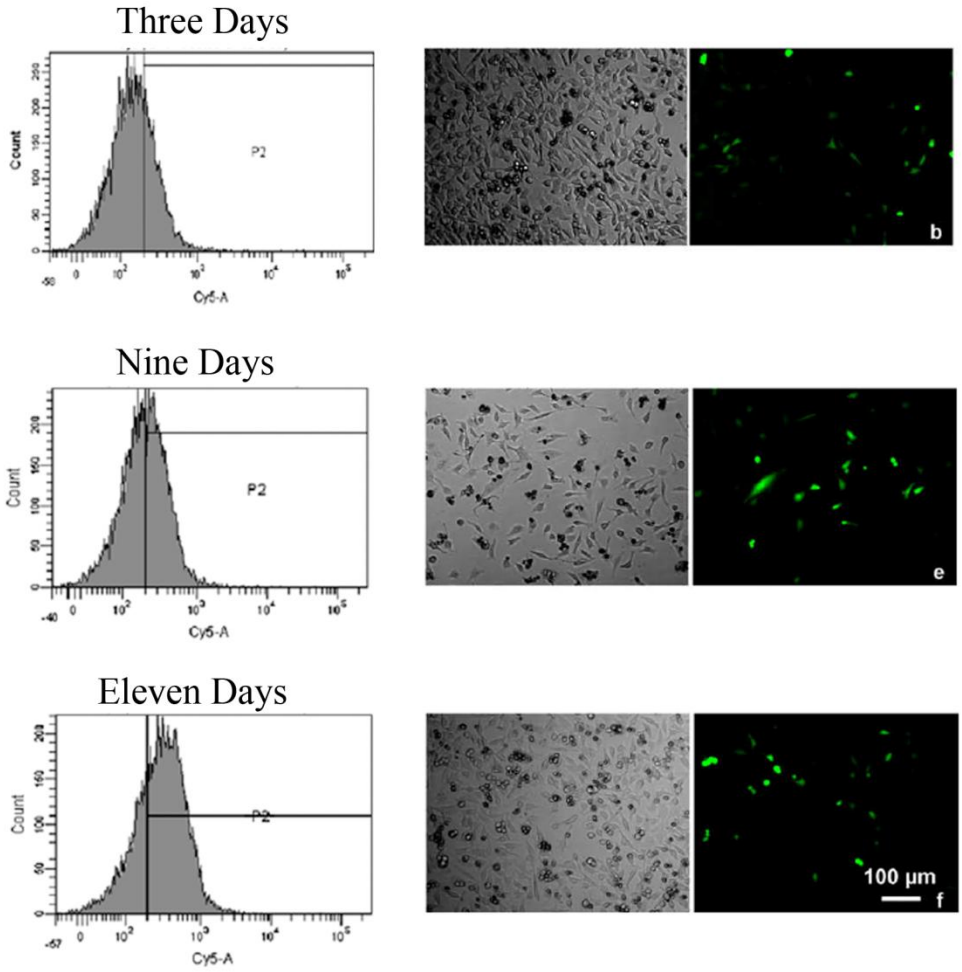

Figure 2.15. Internalization and gene expression of pDNA released from a multilayer assembly. Release of pDNA occurs upon degradation of T4 polyamide. Notable increase in fluorescence intensity over time is observed in the flow histograms. Gene expression (measured by intracellular GFP fluorescence) does not increase at the same rate as DNA uptake. Figure adapted from reference [148] with permission. © 2009 Elsevier.

However, the transgene expression efficiency suffers when non-degradable polymer analogs are used as the delivery vehicles, suggesting that polymer degradation facilitates pDNA release and availability for transcription. This feature can possibly be exploited to develop novel nanodevices for sustained release of nucleic acids. Using dip-coating, the biodegradable polymer T4 and pDNA were deposited in a layer-by-layer assembly on a quartz slide **(Figure 2.15)**.[148] Layer thickness of these devices could be assessed by ellipsometry and monitored by measurement of DNA absorbance. These materials resulted in slow, sustained release of pDNA over time which could be easily delivered into cells for gene expression by another suitable vehicle added separatly. The amount of pDNA that was internalized by cells increased with time, consistent with slow release of pDNA. Interestingly, despite more released DNA at the earlier time points, gene expression remained constant, which is likely a function of the pathway of internalization/trafficking of DNA such that only a portion of the internalized DNA reaches the nucleus. This type of study demonstrates the wide utility of these polymers for sustained release. The favorable bioactivity can be further developed for use as a therapeutic delivery vehicle or in novel scaffolds and nanodevices in biomedical applications.

2.3.2. Disaccharide-containing polymers

Disaccharides can have similar utility to monosaccharides in DNA delivery polymers. Trehalose, a disaccharide composed of two glucose units linked via an α-(1→1) glycosidic bond, has been shown to have cryo- and lyo-protective properties,

attributed to an unusually large hydration sphere.[149] As a function of these properties, trehalose has been shown to prevent aggregation and fusion of proteins and lipids.[150] Logically, incorporation of these features into a polymer backbone could afford similar characteristics to a DNA delivery system and may prevent aggregation of polyplexes in physiological serum concentrations and ionic strengths. In a pioneering study, Reineke and Davis[137] synthesized a series of polymers via condensation polymerization of amine-functionalized D-trehalose monomers with amidine-based comonomers (AP2 and AP3) (**Figure 2.16**). Based on previous studies,[140] six methylene units were used as spacers between the amidine units; however, the distance between the amidine groups and the carbohydrate units was modified to understand the polymer structure-bioactivity relationships. These polymers self-assemble with pDNA into cationic nanostructures around 80 nm in diameter. The delivery efficiency, in terms of transgene

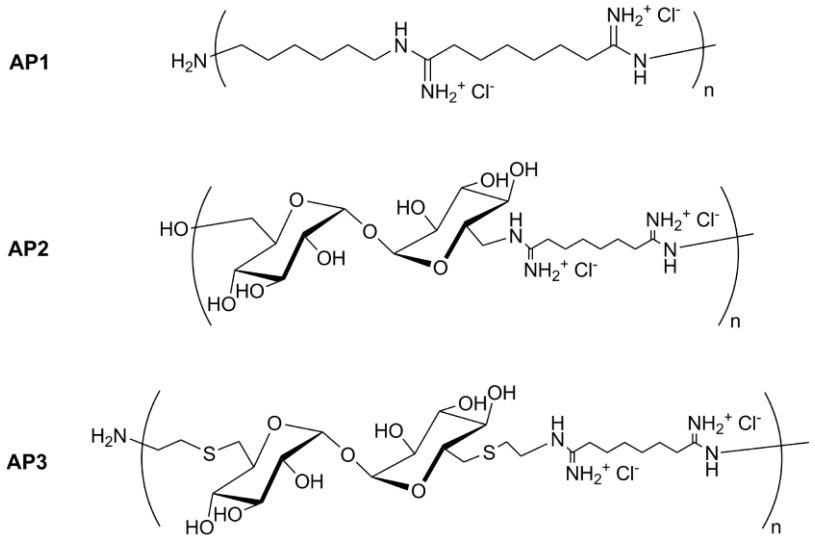

Figure 2.16. Structures of trehalose-containing copolymers. Figure adapted from[151] with permission. © 2003 American Chemical Society.

expression and toxicity, in BHK-21 cells *in vitro* was determined under serum-free conditions to preliminarily assess the bioactivity of these polymers, compared to an analogous structure (AP1) in which the carbohydrate group was replaced with a butylene spacer. Trehalose-based polymers (AP2 and AP3) exhibited improved biocompatibility compared to the non-carbohydrate analog (AP1), which exhibited significant toxicity at low charge (N/P) ratios (including only 20% cell survival at N/P=5). Toxicity appears to be a function of spacer distance between the amidine and the carbohydrate moieties, with AP2 maintaining ~40% lower toxicity than AP3 at charge ratios greater than 10. The transfection experiments in BHK-21 cells indicated that AP3 yielded an order-of-magnitude higher luciferase expression at N/P=5 when compared to AP2. At the same charge ratio, the trehalose containing polymers AP2 and AP3 have 2 and 3 orders-of-magnitude higher luciferase expression, respectively, than AP1. These favorable results confirm the benefit of incorporating trehalose into a polymer structure for gene delivery.

Based on these initial results, new trehalose-based vehicles were developed and their efficacy assessed under physiological conditions, as these previous studies[137] have been performed under serum-free conditions. Previous work has shown that polyplexes can aggregate *in vivo* and are rapidly cleared from the blood stream, such that extended circulation times are not achieved.[8,152] Successful results previously described by Liu *et al.*[21,145] and Reineke and Davis[151] prompted Srinivasachari *et al*. to synthesize a series of trehalose-containing polymers by systematically increasing the amine number (1–4) in the polymer structure, as well as to develop longer polymers to determine if polymer length plays a role in formation of stable complexes with pDNA.[139]

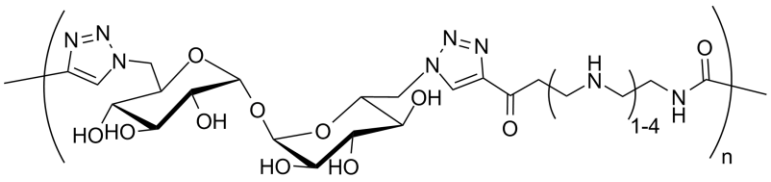

Figure 2.17. Structures of trehalose-containing copolymers.

A series of trehalose-based polymers (Tr1–Tr3) with 1,2,3-triazole linkages were synthesized via the "click reaction" of acetylated-diazido trehalose and a series of dialkyne-oligoethyleneamines (1–3) **(Figure 2.17)**. Gel electrophoresis revealed that the polymers bind pDNA stably at N/P = 2, with TEM revealing the polyplexes to have either spherical or rod-like morphologies with diameters around 50 – 125 nm.. Dynamic light scattering measurements demonstrated an increase in polyplex size upon incubation in serum-free media (Opti-MEM), suggesting swelling or aggregation of the particles. This effect appeared suppressed in serum-containing media; polyplex resistance to size increases improved with increasing amine stoichiometry. Cellular internalization, transgene expression efficiency and cell viability were assessed *in vitro* in HeLa cells under both serum-free and serum-containing experimental conditions.[139,153] When the HeLa cells were transfected with complexes containing FITC-labeled pDNA in Opti-MEM (N/P = 7), the cellular uptake profile showed that Tr1 and Tr3 were the most effective vehicles, transfecting a higher percentage of cells (>99%) than Tr2 or the positive control, jetPEI™. However, in serum-containing media – Dulbecco's Modified Eagle Medium (DMEM), 99% of cells internalized complexes containing Tr3, more than for Tr1 (76%) or Tr2 (35%) and similar to jetPEI™. This could be attributed to the increased stability of Tr3-containing polyplexes from aggregation in the presence of

serum proteins. The transfection efficiency results in serum-free and serum-containing media indicated increased bioactivity of Tr3, which yielded higher transgene (luciferase) levels than Tr1 and Tr3. In serum-free media, luciferase expression from Tr2 was comparable to Tr3, whereas in serum-containing media, Tr3 induced 1 and 2 orders-of-magnitude higher gene expression than Tr1 and Tr2, respectively; these results correlated with the enhanced stability of Tr3 in DMEM. The trehalose-based polymers exhibit low (<20%) toxicity in serum-containing media at N/P=7, markedly lower than control polymer jetPEI™. These results suggest that incorporation of trehalose imparts favorable biological properties. In line with previous polymers, favorable biological activity improves with increasing amine stoichiometry across the polymer series, reaffirming that subtle changes in the polymer structures can measurably influence bioactivity.

To directly test these theories, trehalose-based polymers with four oligoethyleneamine units in the polymer chain were developed. The degree of polymerization of these analogs was varied to assess the influence of polymer length on biological properties.[153] Binding of pDNA and polyplex stability improved as a function of increasing degrees of polymerization in both Opti-MEM and DMEM. The polymers with greater amine stoichiometry have been shown to promote tight DNA binding and favorable polyplex stability due to a combination of electrostatic and hydrogen bonding interactions with the pDNA, with hydrogen bonding likely occurring between secondary amines and/or triazole nitrogens and the guanine/thymine nucleobases **(Figure 2.18)**.[154] In contrast to Tr4, Tr1 did not show evidence of interaction with DNA structure elements, and the interaction appears to be more electrostatic in nature with lower amine stoichiometry. Due to higher amount of secondary amine and triazole groups in the

longer Tr4 polymers, binding cooperativity plays a large role in increasing pDNA binding and stability with the increase in degree of polymerization. Indeed, the increase in both the electrostatic and the hydrogen bonding potential of the polymer increases cooperativity.

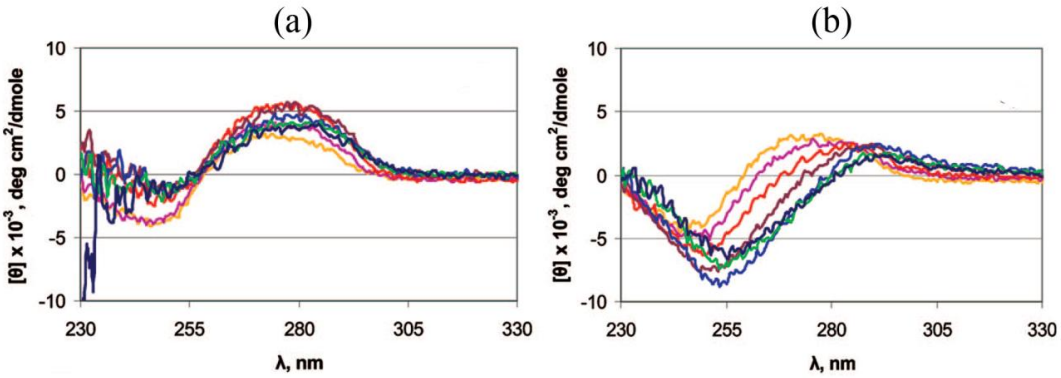

Figure 2.18. Circular dichroism spectra comparing (**a**) Tr1 and (**b**) Tr4. Titration of pDNA with Tr1 results in minimal change in molar ellipticity representative of B-form DNA. Tr4 elicits a shift in ellipticity to a modified B-form, suggesting interaction with DNA base pairs by the polymer. Figure adapted from reference [154] with permission. © 2008 American Chemical Society.

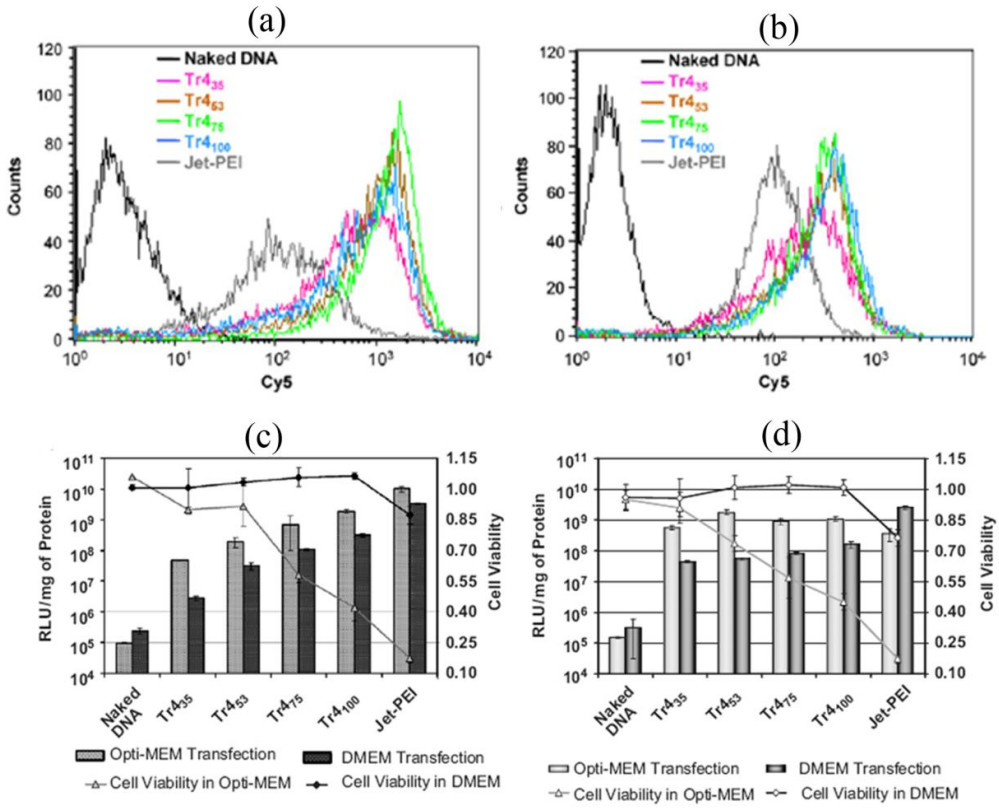

Figure 2.19. Cellular internalization, transgene expression, and relative cell viability of Tr4. Cellular uptake in (a) serum-free and (b) serum-containing media. Transgene expression and cell viability in (c) HeLa and (d) H9c2(2-1) cells. Figure adapted from reference [153] with permission. © 2007 American Chemical Society.

Cytotoxicity was shown to increase with increasing polymer length under serum-free conditions, but the polyplexes were nontoxic in serum in HeLa and H9c2(2-1) cells **(Figure 2.19)**. Cellular internalization under both conditions increased with increasing degree of polymerization, as did transgene expression in serum-free media. However, increasing degree of polymerization did not influence transgene expression in serum, as all analogs had similar transgene expression in serum at N/P=7. Furthermore, all Tr4 analogs were internalized to a higher degree and were less toxic than jetPEI™ in both

serum-free and serum-containing media and, in HeLa cells, higher levels of transgene expression were observed for Tr4. This effect was cell-type dependent, as transgene expression was slightly lower in cardiomyocytes compared to PEI.[153] These results suggest that the stability of these polymers to aggregation in serum-containing media is an important property and may be advantageous in developing these materials towards various *in vivo* applications.

2.3.3. Polycationic Cyclodextrin Polymers

Cyclodextrins (CDs) have been popular in developing supramolecular polycations for DNA delivery. Of particular utility is the ability to selectively modify the primary and secondary hydroxyl groups, which has enabled synthesis of a wide variety of biomaterials.[155-159] In contrast to other carbohydrates, CDs contain a hydrophobic interior cavity which has been shown to form inclusion complexes with hydrophobic molecules. CDs have been extensively used in a variety of biomedical applications, and numerous drug molecules have been included in the interior of CDs and utilized towards target-specific delivery.[160-165] Such applications have used CDs as an adjuvant to complex and increase the bioavailability of hydrophobic drugs, an approach used particularly in delivery of inhaled drugs.[166] This hydrophobic "cup" opens up the potential to conjugate functional groups to a hydrophobic molecule for serum stability or cell-specific targeting, such that the hydrophobic molecule is bound within the CD core, and conjugates a pendant molecule for delivery enhancement. This section will describe some notable DNA delivery scaffolds based on CDs, as well as describe recent work with targeted β-CD polymers in clinical and pre-clinical studies for treatment against cancer.

Star polymeric scaffolds based on α-CD have been developed by Yang *et al*. They were prepared by conjugation of mono-, penta-, nano- and tetradeca-ethyleneamine units to hydroxyl groups on carbon 6 of glucose moieties using 1,1′-carbonyldiimidazole, such that pendant amine-containing arms stretch from the CD.[167] Since difunctional oligoamines were used, large excesses were needed to minimize intra- and inter-molecular crosslinking, the purification required precipitation and size exclusion chromatography. The number of oligoamine arms per CD was calculated using ^{1}H-NMR and it varied from 3.4 to 6.8. Unfortunately no attempt was made to explain how the number of oligoamine arms could exceed 6. M_w, M_n and polydispersity index of synthesized macromolecules were not reported. These star polymers have been found to compact pDNA stably into spherical cationic nanoparticles ranging between 100 – 200 nm at N/P≥8. These polymers show significant, dose-dependent toxicity in HEK293 and COS-7 cells; this toxicity and resulting transgene expression both increased with increasing oligoethyleneamine content. The transgene expression was comparable in both serum-free and serum-containing media, suggesting that serum does not interfere with polyplex structure. Transgene expression profiles were cell type-dependent, with star polymers exhibiting transgene expression similar to PEI in HEK293 cells but significantly less in COS-7 cells.[167] While the transgene expression profiles in serum are encouraging, high toxicity will likely limit the future utility of these materials.

Cryan and coworkers[168] synthesized a series of polycations by modifying the 6-position of each glucose moiety within the CD structure with a variety of functional groups, such as pyridylamino (AP), alkylimidazole (IM), methoxyethylamino (ME), or primary amine (AM). Ethidium bromide (EtiBr) exclusion experiments indicated that the

pDNA binding affinity of these polycationic CDs was wholly dependent on the substituents present in the branching arms. These studies further showed that AP- and AM-modified CDs had higher pDNA binding that ME-CD. These three analogs displayed significantly higher EtiBr exclusion than the IM-CD, a result which could be attributed to increasing hydrophobicity of the IM group. Overall, the N/P ratio required for pDNA binding was quite high (optimal N/P for transfections was 200), necessitating a high concentration of polymer for efficient pDNA compaction. Transgene expression experiments in serum-free conditions revealed high levels of transgene (luciferase) expression compared to uncomplexed pDNA, with AM-substituted CD leading to the highest expression. Addition of chloroquine, used to disrupt endosomal membranes, yielded 10-to 400-fold enhancement in luciferase expression for modified CDs compared to the untreated polymers, suggesting sequestration in endosomal compartments inhibits transfection. In serum, AM-CD showed comparable transgene expression to the cationic lipid, DOTAP. The modified CDs were cytotoxic in a concentration-dependent manner, and were quite toxic at high N/P(the cell viability was around 70% at N/P 200), suggesting limited potential for development as gene delivery agents.

Gonzalez and coworkers synthesized a series of polyamidine-CD polymers via AABB-type condensation of diamino-CD or di(2-aminoethanethio)-CD monomers with difunctionalized-amidine comonomers (six methylene groups between the amidine units). These materials were used to study the effect of spacer length between the charge center and the carbohydrate moiety on pDNA binding and gene expression in BHK-21 and CHO-K1 cells under both serum-free and serum-rich conditions.[169] The polymers had a degree of polymerization around 6 that was determined using gel permeation

chromatography. Binding studies revealed that a longer spacer between the CDs and the charge center was required for pDNA condensation, likely due to steric constraints with shorter linkers. Using the longer spacers, stable nanoparticles of 150–180 nm at N/P=10 were attained. Transfection experiments resulted in similar transgene expression as branched PEI (25 kDa) and slightly higher expression than PLL, SuperFect® and Lipofectamine™ in both cell lines under serum-free conditions. When similar experiments were performed in serum-containing media, a 10% decrease in gene expression was observed for all the polyplexes. The cell viability assay demonstrated that the CD-containing polymers were less toxic than commercial vectors under both conditions.

In a similar study, Hwang *et al.*[140] studied the effect of spacing between the amidine groups on pDNA binding ability and gene expression by systematic modifications to the number of methylene groups (from 4 to 10) in between the amidine units (**Figure 2.20**). The polymers (β-CDPs) contained 4-5 repeat units and compacted pDNA into nanoparticles of 12 –150 nm in diameter.; This study also showed that polymers with 4, 5, and 10 methylene units formed slightly larger particles than the other β-CDPs. The DNase protection ability of these polymers revealed that polymers containing 4, 6, 8 and 10 methylene units protected pDNA against nuclease degradation, while analogs possessing 5 and 7 methylene units offered only partial protection. These results could possibly be due to an effect of odd vs. even methylene spacing on pDNA binding and/or stability. Transfection experiments in BHK-21 cells showed β-CDP6 (6 methylene spacing) yielded higher transgene (luciferase) expression than the other β-

CDPs. In addition, nearly 20% reduction in luciferase gene expression was observed

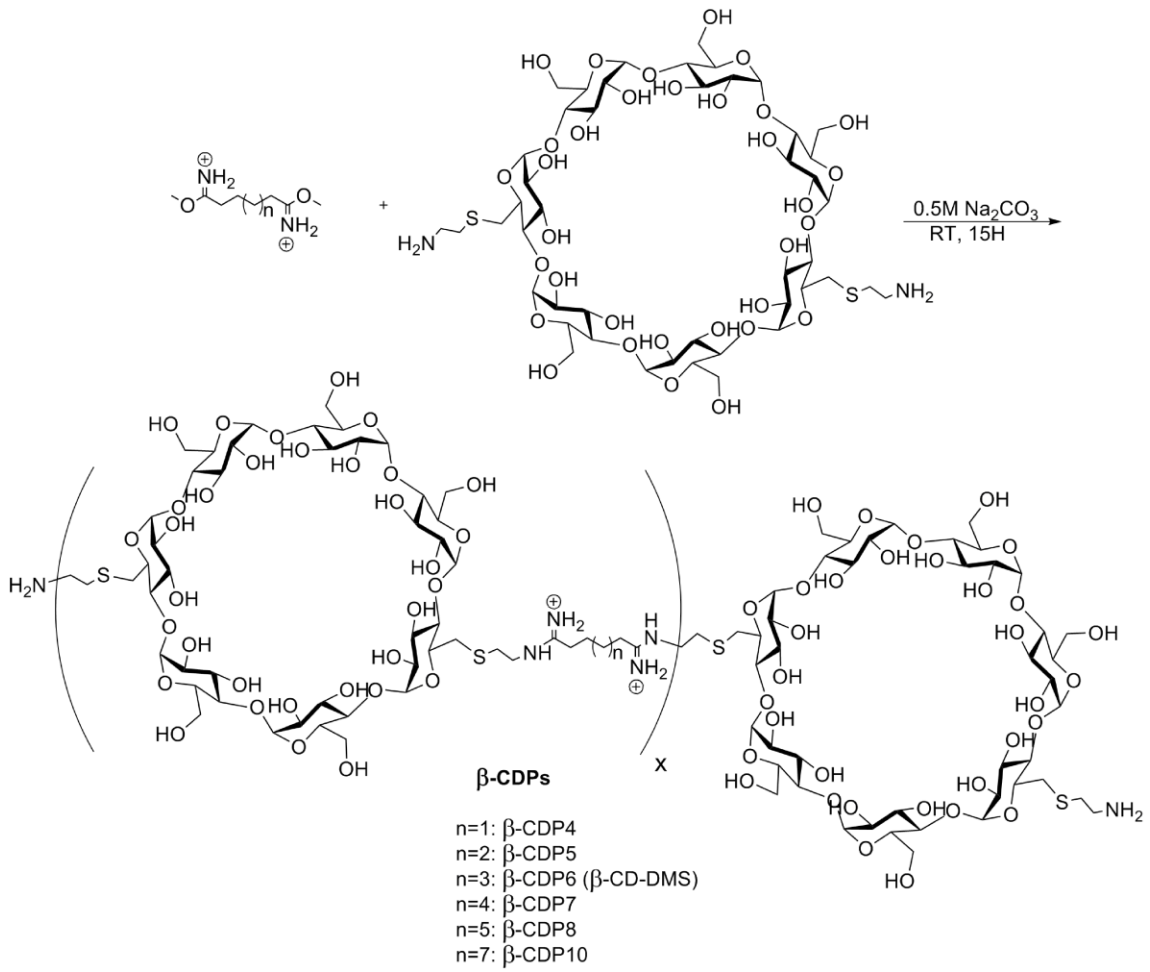

Figure 2.20. Synthesis of β-CD-based polymer. Reproduced from by Hwang *et al.*[140] with permission. © 2001American Chemical Society

when the cells were transfected with β-CDP5 (5 methylene spacing), thereby demonstrating that an optimal spacer length between the amidine units is important for maximal delivery. The cytotoxicity assay at N/P=50 showed that β-CDP8 and β-CDP7 afforded almost 100% cell viability. However, all the other β-CDPs were found to be toxic, which was also evident via MTT assay. Thus, these experiments demonstrate that

an optimal spacing between the amidine units is significant for increased transfection efficiency and decreased cytotoxicity.

Srinivasachari *et al*. designed a novel series of macromolecule vehicles using a β-CD core, where the 6-position of the glucose units has been grafted with pendant oligoethyleneamine groups of specified length (where the secondary amine stoichiometry varied from 0–4).[170] To avoid formation of under-substituted impurities, the core and the branching units were conjugated via a 1,2,3-trizole linkage utilizing the high-yielding 1,3-dipolar cycloaddition, termed the "click reaction." These completely monodisperse β-CD "click clusters" bind and compact pDNA at N/P>2 into spherical nanoparticles with a diameter around 80–130 nm. Structures with 2, 3, or 4 secondary amines in the oligoethyleneamine arms protected pDNA from nuclease degradation when incubated in serum at 37°C for up to 48 h. These macromolecules were able to efficiently deliver Cy5-labeled pDNA into HeLa and H9c2(2-1) cells, and the internalization was comparable to transfection reagents jetPEI™ and SuperFect® with dramatically lower toxicity. Transgene expression in both cell lines increased with increasing secondary amine content, and the analogs with 3 and 4 secondary amines showed (within an order-of-magnitude) transgene expression similar to jetPEI™ and SuperFect®.

These promising initial results on the click cluster vehicles were succeeded by analogous studies to incorporate β-CD into a polymeric scaffold for gene delivery.[171] In this case, the β-CD was di-functionalized with azide groups and polymerized with dialkyne-functionalized oligoethylenamines to derive linear β-CD polymers containing

between 1-4 secondary amines per repeat unit (Cd1-Cd4; **Figure 2.120**). Based upon

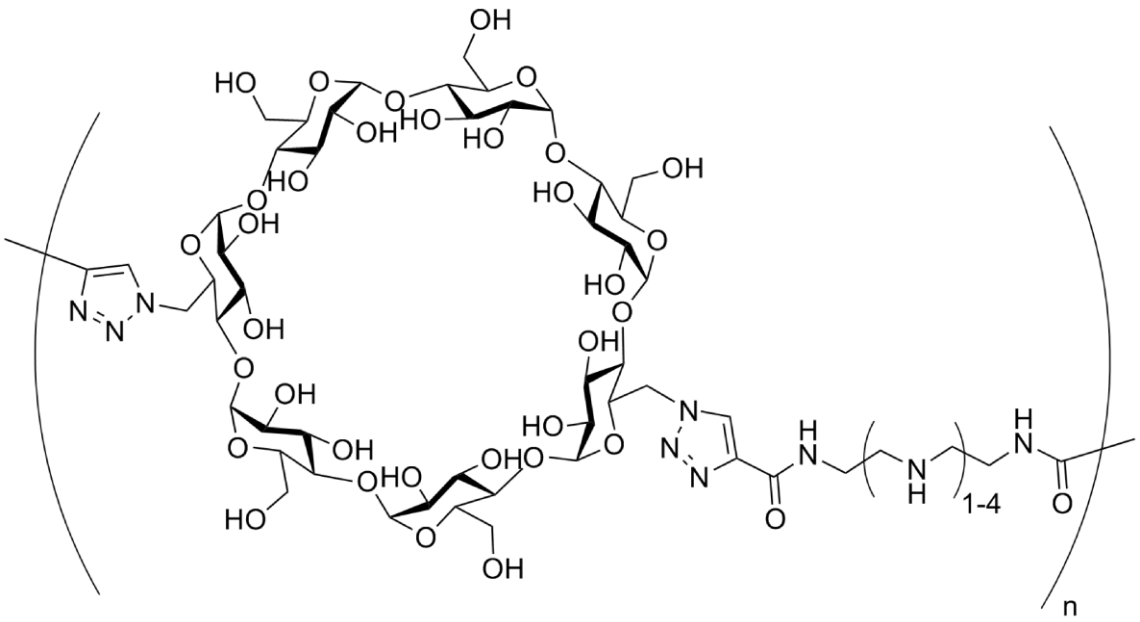

Figure 2.21 Structure of βCD "click" polymers. Figure reproduced from reference [171] with permission. © 2009 American Chemical Society

earlier favorable results with similar systems,[21,139,145,153] several different molecular weights of Cd4 (contains 4 secondary amines in the repeat unit), were synthesized to examine the effect of variation in the polymer length. Incorporation of β-CD into this polymer showed similar DNA binding and polyplex size and cationic surface profiles as were seen previously for the β-CD click clusters. CD-containing polymers showed significant enhancement in cellular uptake over jetPEI™ in HeLa cells, with Cd2, Cd3, and Cd4 internalized significantly better that Cd1. With polymer vehicle Cd4, molecular weight did not appear to significantly affect internalization, as similar high levels of polyplex internalization was observed for all lengths. In general, high levels of transgene expression were observed with these polymers, and the highest expression was observed

with Cd3, slightly higher that Cd4, and both had profiles similar to Jet-PEI. The authors attribute the high delivery of Cd3 to a more flexible, randomly-coiled structure. This assessment is sensible, as lack of polymer rigidity could be important in DNA release, or accessibility of RNA polymerases, depending on how the polymer:DNA polyplex traffics within the cell. Interestingly, despite much more favorable uptake profiles compared to jetPEI™, similar transgene expression was observed. This may be due to differences in trafficking mechanisms and rates, which may lead PEI to the nucleus in a more efficient manner. However, if nuclear delivery is not exclusive, this may afford a unique opportunity to deliver siRNA in high levels to the cytosol, an advantageous result for gene knockdown via RNA interference as a therapeutic strategy.

Oligonucleotide delivery with β-CD for targeted cancer therapeutics has been explored extensively by the group of Mark Davis, and the remainder of this section is focused on the groundbreaking *in vivo* results attained by this laboratory. Previous work in this lab has extensively exploited the hydrophobic interior cavity of β-CD for inclusion of hydrophobic molecules conjugated to targeting groups,[172] and this technology will be discussed in greater detail in the next section. In many of these studies, a β-CD polycation end-capped with imidazole groups was used as the delivery vehicle, and the human transferrin protein was used as a targeting ligand due to upregulation of transferrin receptors on tumor cells (**Figure 2.22**). Pun *et al*. used these targeted β-CD-containing polycations to deliver fluorescently-labeled DNAzymes targeted to the *c-myc* proto-oncogene—to which tumor cells have been shown to require for proliferation—in tumor-

bearing mice.[173]

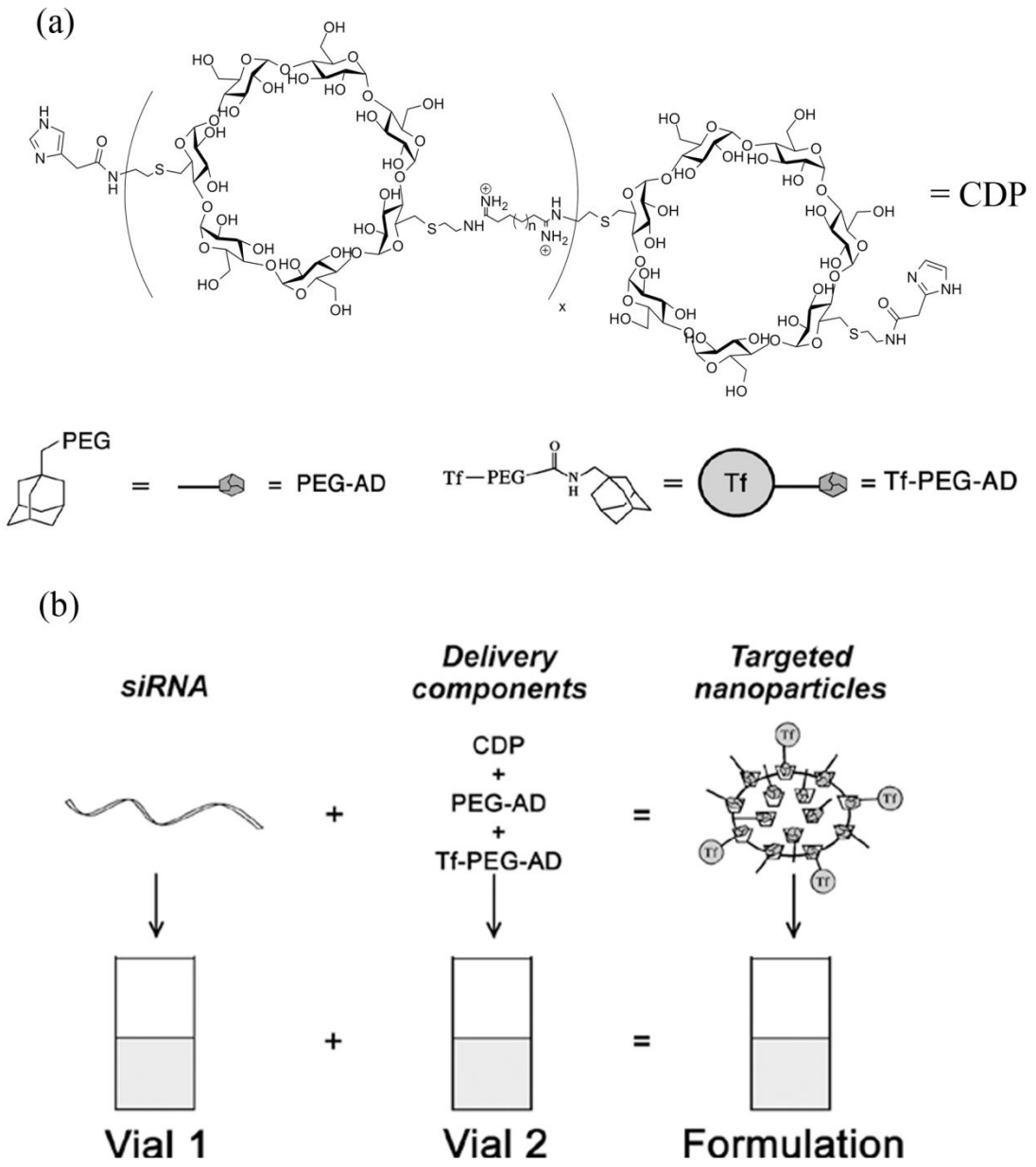

Figure 2.22 (**a**) Structure of β-cyclodextrin-containing polycations (CDP)s and (**b**) formulation of siRNA-containing targeted nanoparticles formed with CDP. Figure adapted from reference [174]. © 2007 National Academy of Sciences, U.S.A.

Using whole-body imaging techniques, Cy3-labeled DNAzymes were seen associating with the actin cytoskeleton. The highest levels of sustained fluorescence were observed when polyplexes were administered via intravenous bolus injection (compared to intraperitoneal injection, for which uptake of particles by tumor tissue was low). Unmodified DNAzyme was observed in cyrosectioned tumor, liver, and kidneys 8 hours post-injection but was not observed after 24 hours, suggesting clearance from the body within this time frame. However, DNAzymes delivered in -CD polyplexes were sustained in the tissues after 24 hours, suggesting that the PEG groups afford prolonged circulation time that allows tumor delivery over extended time.[173] These experiments show that targeted delivery of oligonucleotides can be achieved *in vivo* by β-CD-containing polycations.

In a mouse model of Ewing's sarcoma, Hu-Lieskovan *et al*. used these β-CD-containing vehicles to deliver siRNA against the *EWS-FLI1* gene expressed in this disease model.[175] Ewing's sarcoma (TC71) cells were modified to stably express luciferase and injected into immunocompromised mice to attain a disseminated tumor model, which was verified by bioluminescence imaging and MRI. Mice were dosed twice weekly with transferrin-targeted β-CD polycations complexing siRNA against *EWS-FLI1* (siEFBP2), with treatment beginning the same day as injection of tumor cells. Delivery of naked siEFBP2 and targeted polyplexes containing control (non-*EWS-FLI1*-targeting; siCON1) siRNA did not decrease tumor size compared to control mice, and untargeted siEFBP2 polyplexes showed delayed tumor formation. However, targeted polyplexes containing siEFBP2 reduced tumor growth to 20% of that of control mice, indicating that targeted delivery of siRNA to transferrin-overexpressing tumor cells

prevented the tumorigenicity of injected Ewing's sarcoma cells. Substantial tumor reduction was observed over the time course of the experiment (**Figure 2.23a**). Importantly, these repeated treatments did not lead to increased cytokine levels or induce

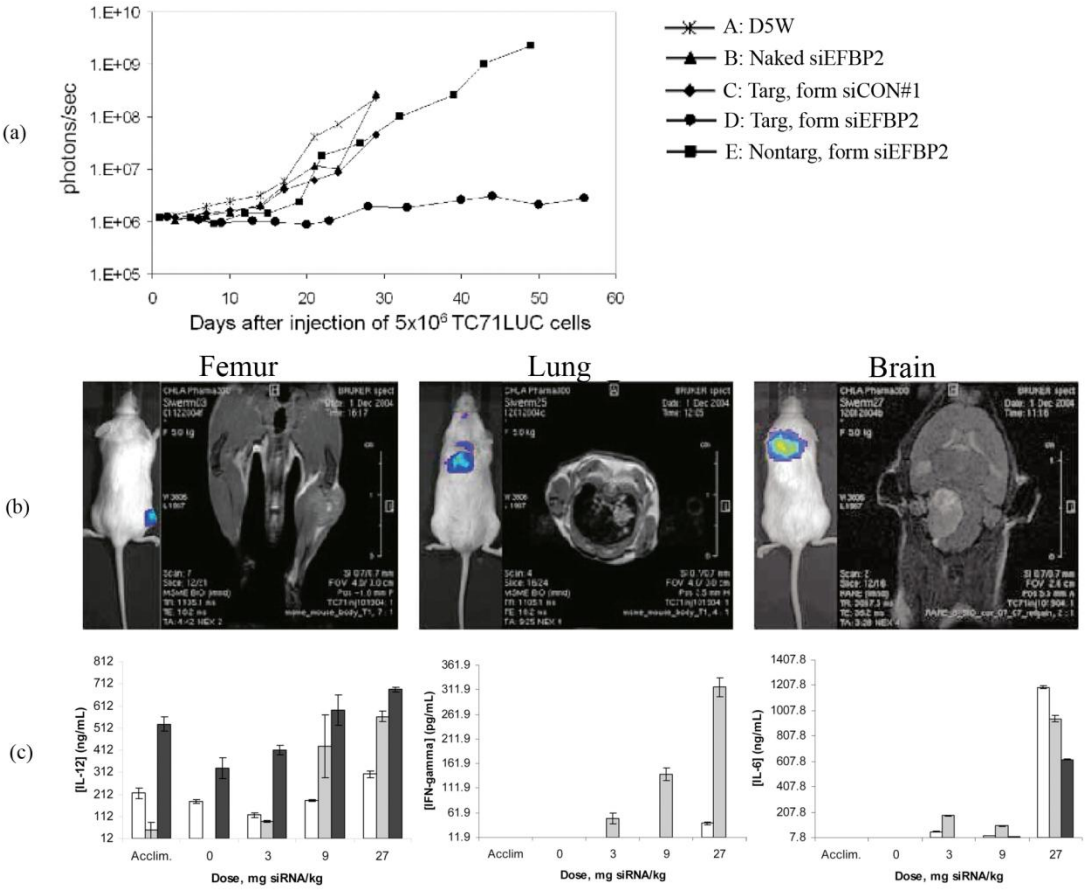

Figure 2.23. *In vivo* performance of targeted cyclodextrin polycations. **(a)** Growth curves for engrafted tumors. The median integrated tumor bioluminescent signal (photons/s) for each treatment group (n = 8-10) is plotted versus time after cell injection (days). **(b)** MRI confirmation of tumor engraftment. **(c)** Dose-dependent effects on cytokine production in non-human primates. Only very high dosage led to significant increases in cytokines. Figures (a) and (b) reproduced from reference [175] with permission. © 2005 American Association for Cancer Research. Figure (c) reproduced from reference [174]. © 2007 National Academy of Sciences, U.S.A

tissue damage, suggesting toxic and immune responses by the animals were minimal. These results show that targeted, systemic delivery of siRNA can treat disseminated cancers with carbohydrate-based *non-viral* gene delivery in a sequence-specific manner.

These promising results have led to further studies *in vivo* to assess gene knockdown efficacy of vehicles targeted to cancer cells. Heidel *et al*. used escalating doses of β-CD-siRNA nanoparticles delivered intravenously in monkeys (**Figure 2.23b**). These are fundamental studies, as determination of dose-dependent tolerance levels is crucial for minimization of drug-induced toxicity and/or other untoward side effects. Escalating doses of 3, 9, and 27 mg/kg (with respect to the siRNA component) were administered 3 days apart, followed by a washout period of 11-12 days prior to a final dosing of 3 mg/kg. Serum chemistry and immune effects were measured 6 hours post-injection. The lower doses of nanoparticle (3 and 9 mg/kg) were well tolerated and did not lead to significant increases in hematological factors (i.e., coagulation factors) or pro-inflammatory cytokines (**Figure 2.23c**). At the highest dose (27 mg/kg), increases in creatinine and blood urea nitrogen were observed, indicative of acute renal toxicity. Coagulation factors were unaffected by the high dosage, but increases in pro-inflammatory cytokines IL-6 and IFN-γ indicative of a helper T-cell response, were observed shortly after injection of high doses of siRNA. Interestingly, increasing levels of TNF-α were not observed, providing convincing evidence that systemic inflammation is not occurring. Unfortunately, longer term measurements of these cytokines were not reported, so it is unclear if these effects are transient or chronic. Exposure of the animals to high dosage of siRNA-containing nanoparticles did not lead to high titer antibody formation, suggesting that repeated doses of nanoparticles over time would be well-

tolerated by the animals and would not lead to ineffective dosing due to an immune (neutralizing antibody) response. Importantly, high levels of nanoparticles were detected in the blood 5 minutes post-injection, verifying circulation of nanoparticles and avoiding rapid clearance from the bloodstream.[174] This elegant study confirms the safety of these nanoparticle siRNA delivery systems and suggests that repeating high dosage treatment could be well tolerated in patients. These promising vehicles have shown that high delivery and treatment efficacy can be attained with *non-viral* nucleic acid delivery, and are among the first carbohydrate-based vehicles to advance to human clinical trials. These preliminary studies have been reviewed recently[176] and provide a bright outlook to the future of the field.

2.4. Targeted Gene Delivery with Carbohydrates

As described earlier, carbohydrates have been used extensively in their native forms and as components of novel polymeric structures to transfer exogenous nucleic acids into cells. In addition, carbohydrates have also been conjugated to polymeric delivery systems as a targeting moieties. While an extensive amount of work has been completed and continues to be published utilizing various carbohydrate structures for targeting, a full review of this area is beyond the scope of this review article. As an example of the promise of this extensive research, we briefly review the use of β-D-galactose and β-D-galactoseamine cell-specific targeting of polyplexes to hepatocytes, which are commonly studied targeting ligands in this research field. Hepatocytes overexpress the asialoglycoprotein receptor (ASGPr), a lectin that specifically recognizes

the β-D-galactose and β-D-galactosamine carbohydrates. Conjugating these sugars as pendant groups on polymeric vehicles has been used extensively to achieve hepatocyte-specific targeting *in vitro* and *in vivo*. The following section briefly describes recently-published work to facilitate hepatocyte-selective delivery of DNA.

Early work by Zanta *et al*. describes galactosylated PEI (lactose was used in a reductive amination with PEI) as a liver-specific delivery system, which maintained tight DNA binding at low N/P ratios.[177] These galactosylated polyplexes were able to transfect NIH 3T3, a non-hepatocyte cell line, indicating incomplete specificity for ASGPr. However, the transgene expression efficiency was less than that observed for unmodified PEI, which can be interpreted as being due to a lack of cell-surface affinity from low levels of ASGPr. By contrast murine (BNL CL.2) and human (HepG2) hepatocytes showed higher transgene expression from galactosylated PEI than unmodified PEI at low N/P. At high N/P, unmodified PEI demonstrated higher transgene expression, which may be artificially high due to increased toxicity. Incubation of cells with a competitive binding inhibitor to ASGPr, asialofetuin (ASF), led to a decrease in transgene expression, signifying receptor-mediated uptake.[177] A later study by Pun and Davis described the development of a hepatocyte-specific DNA delivery system using β-CD-containing polymers. In this approach, galactosamine was installed at the PEG end of galactose-PEG-tetrapeptide-adamantane via amide bond and this macromolecule was used to create a targeted vehicle by taking advantage of the ability of adamantane to form inclusion complexes with the hydrophobic core of β-CD.[172] Specific delivery to HepG2 cells was partially successful, as inhibition of targeted polyplex internalization was inhibited by ASF. However, as before, significant internalization was still observed for targeted

polyplexes inhibited with ASF—this was seen for untargeted polyplexes as well. These studies demonstrate that galactosylation of polymeric vehicles can possibly provide receptor-specific uptake *in vitro*, but non-specific delivery is still observed. In addition, transgene expression is used to assess receptor-specific uptake, but this is a downstream event from receptor-mediated internalization. It was clear from these studies that more work was needed to achieve exclusive delivery to hepatocytes and better research tools were needed to assess receptor-mediated internalization.

Further studies have attempted to optimize the amount of galactose conjugation with the specific delivery efficiency. The mole percentage of galactose on PEI was modified by varying the amount of lactose used in reductive amination reaction, to assess the effect of galactose concentration on transfection.[178] Increasing the mol % galactose up to 31.1% did not affect binding of PEI analogs to DNA. However, polyplex size grew with increasing galactose, and this was accompanied by a decrease in zeta potential, which became nearly neutral at high (31.1%) galactose concentration. Increasing galactose has a favorable effect on cell viability—improvement in biocompatibility was directly proportional to percent galactose, which corresponded to lower membrane-damaging effects as evidenced by LDH release. However, receptor-specific delivery was not achieved, as unmodified PEI showed higher levels of luciferase expression than galactosylated analogs. However, polyplex size and charge clearly played a role in delivery, as larger, more neutral particles showed lower transgene expression than smaller, cationic polyplexes. A similar study by Ren *et al*. observed the effect of increasing the number of galactose molecules from one to three on a dendritic structure.[26] Less trasngene (luciferase) expression was seen in HepG2 cells than in a non-hepatocyte

cell line (BL-6 cells), indicating that hepatocyte specificity is not observed. However, increasing luciferase expression was observed as a function of number of conjugated galactose, as highest luciferase expression was observed for the tri-galactosylated compounds at low concentration. These results suggest that increasing the number of galactose groups may improve targeting based on a multivalent effect.

A potential problem with assessing receptor-mediated delivery may indeed be use of an *in vitro* system. HepG2 cells are hepatocellular carcinoma cells, so receptor expression may be more varied than a typical liver cell, and the rapid growth of malignant cells may help to non-specifically internalize polyplexes. Therefore, Nishikawa *et al*. monitored targeted DNA delivery *in vivo* to determine pharmacokinetic and biodistribution profiles with poly-L-ornithine-based polymers conjugated with galactose.[179] The conjugation was done using 2-imino-2-methoxyethyl-thio-β-D-galactopyranoside. Conjugation of galactose did not impact the polyplex size, so polyplexes formulated with [^{32}P] DNA were injected intravenously into mice. As these materials are not serum-stabilized in any way, rapid clearance of polyplexes occurred, as the half-life was 8.2 minutes or less. However, the majority of radioactivity and luciferase expression was observed in the liver (with respect to other organs monitored—lungs, kidneys, spleen, heart), and the delivery to the liver increased with time. More significantly, when parenchymal (hepatocytes) and non-parenchymal (Kupffer, non-hepatocytes) liver cells were separated by collagenase perfusion, much higher radioactivity and luciferase expression was seen in the parenchymal cells than the non-parenchymal cells, suggesting hepatocyte-specific delivery was preferred over non-specific delivery. Some non-specific delivery was still observed—particularly to the

lungs—but these are generally promising results that suggest that, in an animal model, hepatocyte specificity can be achieved.

The previously-published work in the fields of hepatocyte-targeted nucleic acid delivery and serum stabilization can be combined to develop smart delivery vehicles that contain structural elements for overcoming cellular barriers. In an elegant study, Chen *et al*. described the design and synthesis of PEGylated glycopeptides containing a cysteine-terminated triantennary glycopeptide (**Figure 2.24**), PEGylated peptide, and melittin to form polymers through formation of disulfide bonds under oxidative conditions.[180]

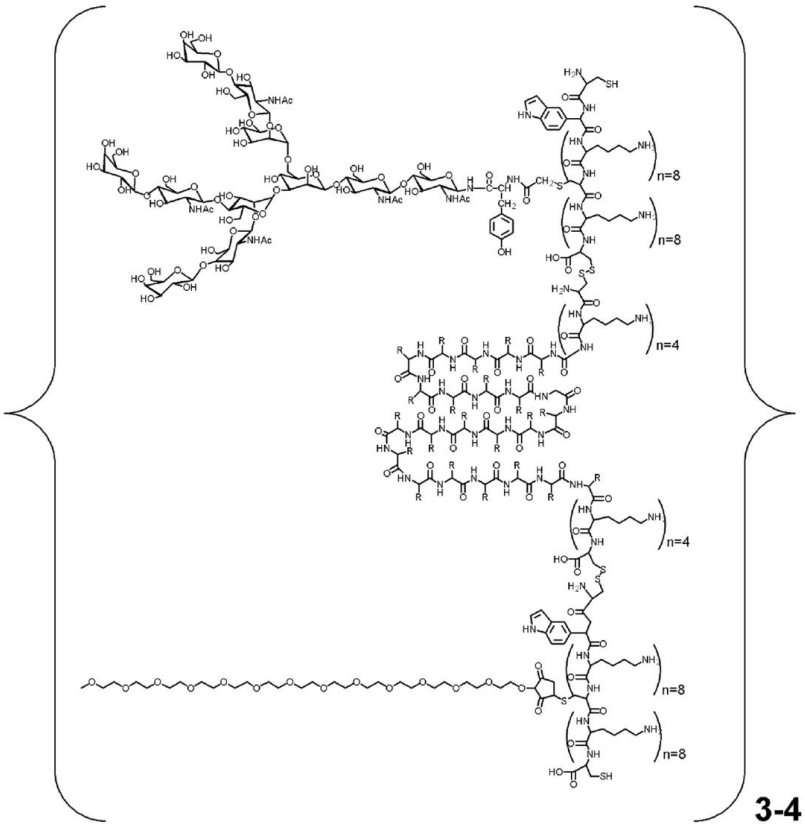

Figure 2.24. Structure of PEGylated glycopeptide. Figure reproduced from reference [180] with permission. © 2007 American Chemical Society

structure	monomer composition[a] (mol %)	measured composition[b] (mol %)	molecular weight (PLL),[c] (PEO)[d]	particle size[e]	zeta potential[f]	$t_{1/2}$[g] hr	PC/NPC[h]
PGP 1	0:90:10	0:91.7:8.3	106 kDa, 50 kDa	221 ± 8	+0.5	1.1	60:40
PGP 2	10:80:10	12.8:82.5:4.7	109 kDa, 51 kDa	210 ± 13	+5	1.2	59:41
PGP 3	20:70:10	24.4:70.3:5.3	99 kDa, 47 kDa	227 ± 11	+6	1.2	65:35
PGP 4	40:50:10	44.8:46.4:8.8	83 kDa, 46 kDa	232 ± 1	+6	1.3	60:40
PGP 5	70:20:10	73.2:19.8:7.0	35 kDa, 21 kDa	295 ± 7	+5	1.1	63:37
PGP 3*[i]	20:70:10	12.6:80.9:6.5	99 kDa, 47 kDa	227 ± 11	+6	1.0	38:62

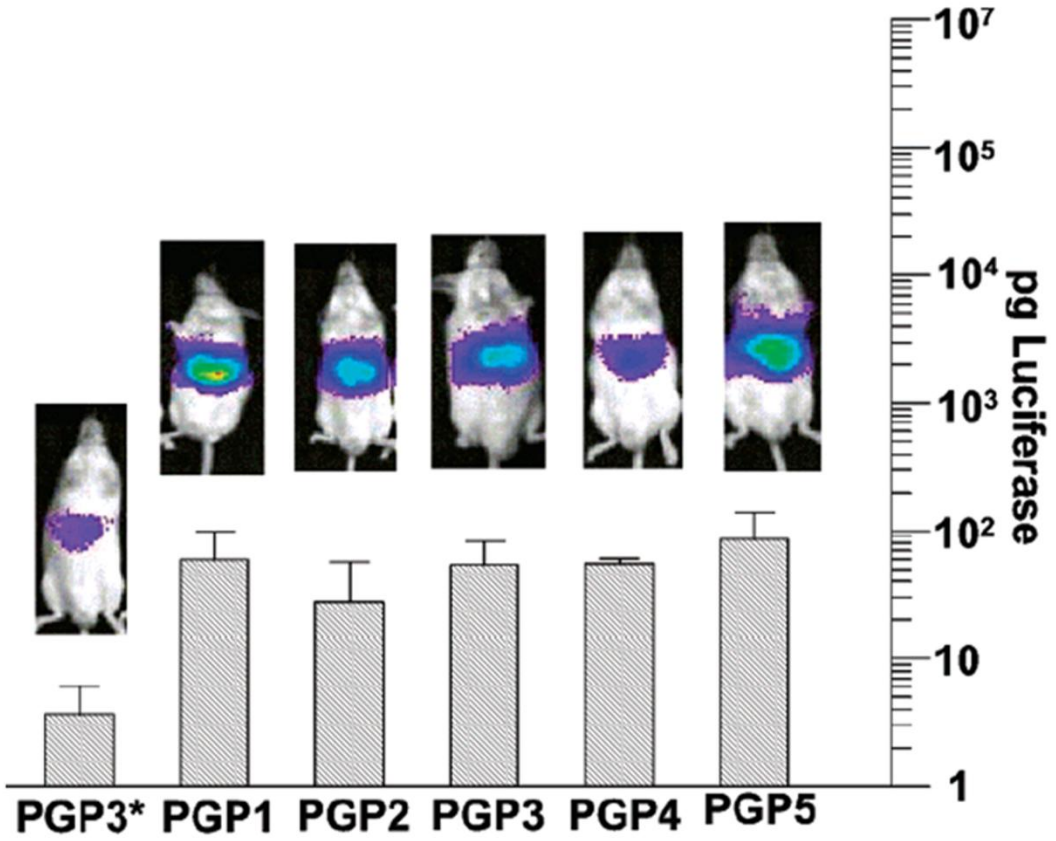

Figure 2.25. Characterization and luciferase expression of PGP DNA condensates *in vivo***.** These results show that luciferase expression is dependent on galactose incorporation but independent of amount of melittin. [a] Represents the input mol ratio of Cys-terminated melittin, PEG- peptide, and glycopeptide. [b] Represents the measured mol ratio of Cys-terminated melittin, PEG-peptide, and glycopeptide for each purified PGP. [c] Values are the calculated MW based on polylysine standards. [d] Values are the calculated MW based on PEG standards. [e] The mean particle size determined at a stoichiometry of 0.3 nmol of PGP per μg of DNA. The value represents the mean diameter (nm) based on unimodal analysis. [f] The zeta potential of PGP DNA condensates at a stoichiometry of 0.3 nmol of PGP per μg of DNA. [g] The metabolic half-life of PGP ^{125}I-DNA in triplicate mice. The results are derived from Figure 6. [h] The PC/NPC ratio of DNA-targeted liver. [i]

Represents a control PGP 3 in which galactose has been removed. Figure adapted from reference [180] with permission. © 2007 American Chemical Society

These polymers have been designed to achieve serum stability and sustained circulation with the PEGylated peptide, specific targeting to hepatocytes with galactosylated peptide, and increased cellular internalization and endosomal disruption with the fusogenic peptide monomer (melittin). Under the reducing conditions of the cell, the disulfide bonds can be reduced to sulfhydryl groups, degrading the polymer and releasing the pDNA. They developed five PEGylated glycopeptides (PGPs) with increasing melittin concentrations from 0% (PGP1) to 73% (PGP5), as well as a control polymer, PGP3*, that did not contain galactose for targeting. The specific delivery of DNA to hepatocytes was monitored in a murine model (**Figure 2.25**). Polyplexes were administered intravenously by injection into the tail vein, which was followed by hydrodynamic stimulation via saline injection 5 minutes later to promote high levels of cellular uptake. Polymeric delivery of DNA was retained in the body twice as long as uncomplexed DNA, having a half-life of one hour. Hepatocyte-specific targeting was assessed by the ratio of DNA in parenchymal vs non-parenchymal liver cells, and the galactosylated polymers led to 50% higher delivery to parenchymal cells than to non-parenchymal cells. A control of non-galactosylated polymer showed 50% higher uptake in non-parenchymal cells vs. parenchymal cells. Luciferase expression was measured 24 hours post-injection, and significantly higher luciferase expression was observed in the galactosylated analogs (**Figure 2.25**). These results suggest that hepatocyte-favored

delivery leading to transgene expression of DNA can be achieved through rational therapeutic design.

Targeted delivery of siRNA has also been achieved using rationally-designed polymeric vehicles using galactose as a hepatocyte-targeting group. Rozema *et al*. describe a polymeric system, dubbed Dynamic PolyConjugates, to attach N-

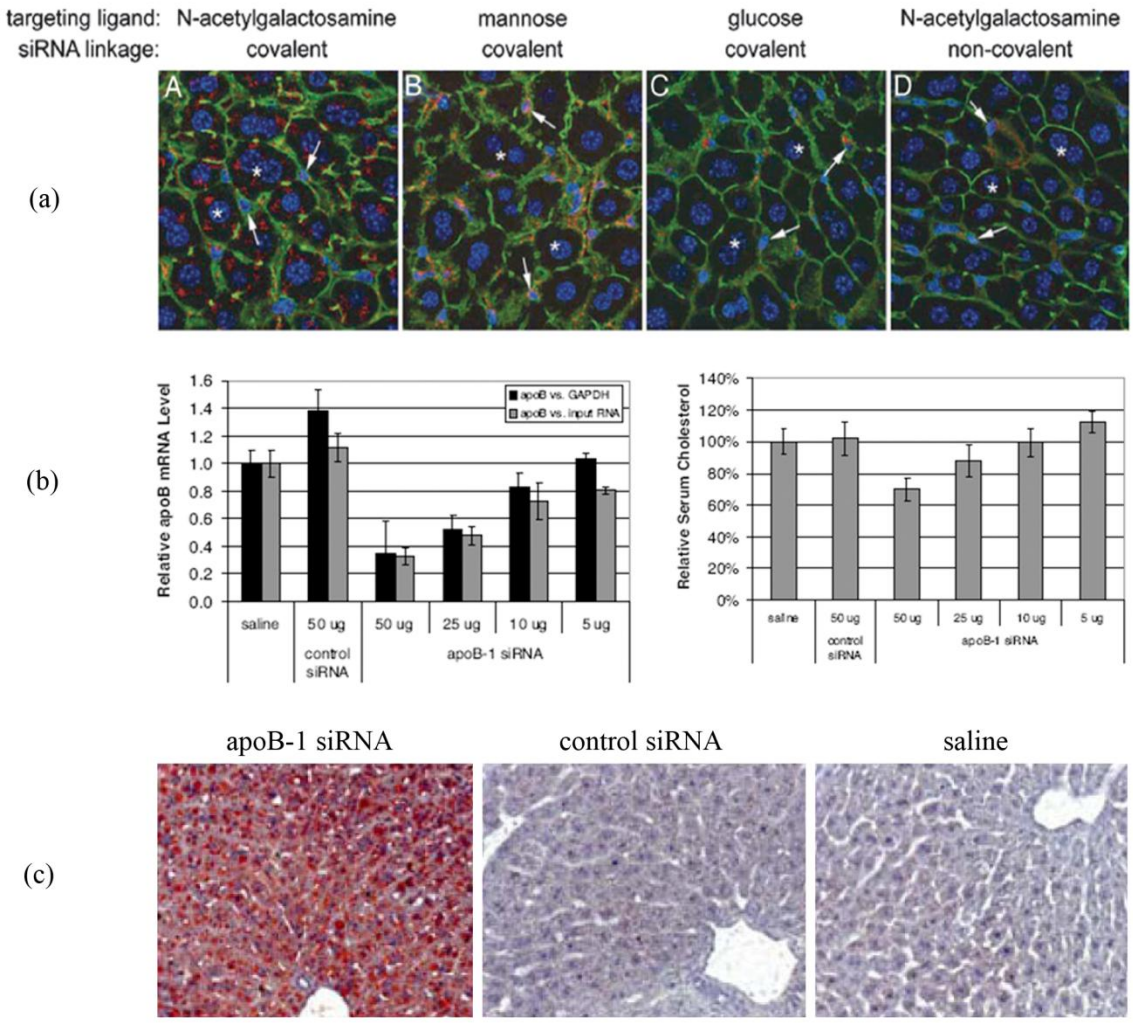

Figure 2.26. Specific delivery of siRNA to hepatocytes with Dynamic PolyConjugates. (**a**) Confocal micrographs indicate specific intracellular delivery of oligonucleotides by targeting hepatocytes with N-acetylgalactosamine, as Cy3-labeled oligonucleotide (red) is seen within mouse hepatocytes, compared to when mannose and glucose are used as targeting moieties and Cy3 oligonucleotides are seen in the pericellular regions. (**b**) RT-

qPCR shows dose-dependent decrease in apoB mRNA, corresponding to (**c**) decreasing serum cholesterol levels. (**d**) Increased hepatic lipid content (stained with OIL RED) relative to control siRNA and saline injections confirm knockdown of apoB-mediated cholesterol transport from the liver. Figure adapted from reference [80]. © 2007 National Academy of Sciences, U.S.A

actetylgalactosamine, PEG, and siRNA to a polymeric backbone for hepatocyte-targeting, charge shielding for serum stability, and gene knockdown, respectively.[80] The PEG was conjugated through an acid-labile maleamate linkage for release of PEG in endosomal compartments that can expose polymer amines for endosome disruption, and the siRNA was attached through a disulfide linkage which is cleaved under the reducing conditions of the cytoplasm. Using an siRNA targeted against the mRNA for apolipoprotein B (apoB), a gene expressed by hepatocytes, they were able to achieve 80% knockdown of apoB in mouse primary hepatocytes compared to 60-70% knockdown for a commerically-available transfection reagent, *Trans*IT-siQuest®. Mice injected intravenously with N-acetylgalactosylated oligonucleotide polyconjugates showed intracellular delivery of Cy3-oligonucleotide to hepatocytes, compared to no intracellular delivery when the targeting group was mannose or glucose (**Figure 2.26a**). Mice injected with apoB siRNA-containing polyconjugates (**Figure 2.26b-c**) showed dose-dependent knockdown of apoB mRNA two-days post-injection, as well as corresponding decreases in serum cholesterol. Hepatic lipid content was visualized by OIL RED staining of tissue sections, and mice treated with apoB siRNA showed increased lipid content corresponding in decreasing cholesterol transport from the tissue by apoB (**Figure 2.26d**). These results confirm the liver-specific delivery of siRNA with polymers conjugated to N-acetylgalactosamine.

The results discussed in this section present a brief sampling of the literature focused on hepatocyte-specific delivery with carbohydrate-based targeting ligands. This section focused on galactose for targeting the ASGPr on hepatocytes, but other carbohydrates have also been studied for cell-specific targeting, including lactose for targeting the airway epithelia and mannose for targeting cells of the immune system.[181-183] While a detailed review of this subfield is beyond the scope of this article, work in this area is ongoing and continues to develop polymeric systems for specific delivery of nucleic acids through lectin-mediated targeting.

References

1 Pickler, R. H. & Munro, C. L. Gene Therapy for Inherited Disorders. *J. Ped. Nursing* **10**, 40 - 47 (1995).

2 Anderson, W. F. Human gene therapy. *Science* **256**, 803-813 (1992).

3 Mulligan, R. C. The basic science of gene therapy. *Science* **260**, 926-932 (1993).

4 Wiethoff, C. M. Barriers to nonviral gene delivery. *J. Pharm. Sci.* **92**, 203-217 (2003).

5 Braun, C. S., Vetro, J. A., Tomalia, D. A., Koe, G. S., Koe, J. G. & Middaugh, C. R. Structure/function relationships of polyamidoamine/DNA dendrimers as gene delivery vehicles. *J. Pharm. Sci.* **94**, 423-436 (2005).

6 Behr, J.-P. Synthetic Gene-Transfer Vectors. *Acc. Chem. Res.* **26**, 274-279 (1993).

7 Luo, D. & Saltzman, W. M. Synthetic DNA delivery systems. *Nat. Biotechnol.* **18**, 33-37 (2000).

8 Davis, M. E. Non-viral gene delivery systems. *Curr. Opin. Biotechnol.* **13**, 128-131 (2002).

9 Kircheis, R. & Wagner, E. Polycation/DNA complex for *in vivo* gene delivery. *Gene Ther. Regul.* **1**, 95 - 114 (2000).

10 Godbey, W. T., Wu, K. K. & Mikos, A. G. Poly(ethylenimine) and its role in gene delivery. *J. Controlled Release* **60**, 149-160 (1999).

11 Godbey, W. T., Wu, K. K. & Mikos, A. G. Size matters: molecular weight affects the efficiency of poly(ethylenimine) as a gene delivery vehicle. *J. Biomed. Mater. Res., Part B* **45**, 268-275 (1999).

12 Mannisto, M., Vanderkerken, S., Toncheva, V., Elomaa, M., Ruponen, M., Schacht, E. & Urtti, A. Structure-activity relationships of poly(L-lysines): effects of pegylation and molecular shape on physicochemical and biological properties in gene delivery. *J. Controlled Release* **83**, 169-182 (2002).

13 Kim, S. W. Polylysine copolymers for gene delivery. *Gene Transfer*, 461 - 471 (2007).

14 Kwoh, D. Y., Coffin, C. C., Lollo, C. P., Jovenal, J., Banaszczyk, M. G., Mullen, P., Phillips, A., Amini, A., Fabrycki, J., Bartholomew, R. M., Brostoff, S. W. & Carlo, D. J. Stabilization of poly-L-lysine/DNA polyplexes for in vivo gene delivery to the liver. *Biochim. Biophys. Acta* **1444**, 171-190 (1999).

15 Smith, D. K. Dendritic supermolecules--towards controllable nanomaterials. *Chem. Commun.*, 34-44 (2006).

16 Eliyahu, H., Siani, S., Azzam, T., Domb, A. J. & Barenholz, Y. Relationships between chemical composition, physical properties and transfection ef.ciency of polysaccharide–spermine conjugates. *Biomaterials* **27**, 1646-1655 (2006).

17 Hong, S., Bielinska, A. U., Mecke, A., Keszler, B., Beals, J. L., Shi, X., Balogh, L., Orr, B. G., Baker, J. R. & BanaszakHoll, M. M. Interaction of Poly(amidoamine) Dendrimers with Supported Lipid Bilayers and Cells: Hole Formation and the Relation to Transport. *Bioconjugate Chem.* **15**, 774-782 (2004).

18 Kraemer, M. Dendritic polyamines: simple access to new materials with defined treelike structures for application in nonviral gene delivery. *ChemBioChem* **5**, 1081 (2004).
19 Svenson, S. & Tomalia, D. A. Dendrimers in biomedical applications-reflections on the field. *Adv. Drug Deliv. Rev.* **57**, 2106-2129 (2005).
20 Mintzer, M. A., and Simanek, E. E. Nonviral Vectors for Gene Delivery. *Chem. Rev.* **109**, 259-303 (2009).
21 Liu, Y. & Reineke, T. M. Hydroxyl Stereochemistry and Amine Number within Poly(glycoamidoamine)s Affect Intracellular DNA Delivery. *J. Am. Chem. Soc.* **127**, 3004-3015 (2005).
22 Velter, I., La Ferla, B. & Nicotra, F. Carbohydrate-Based Molecular Scaffolding. *J. Carb. Chem.* **25**, 97 - 138 (2006).
23 Varma, A. J., Kennedy, J. F. & Galgali, P. Synthetic polymers functionalized by carbohydrates: a review. *Carbohyd. Polym.* **56**, 429 - 445 (2004).
24 Yudovin-Farber, I. & Domb, A. J. Cationic polysaccharides for gene delivery. *Mat. Sci. Eng.* **27**, 595 - 598 (2007).
25 Miyata, T. & Nakamae, k. Polymers with Pendant Saccharides - 'Glycopolymers'. *TRIP* **5**, 198 - 205 (1997).
26 Ren, T., Zhang, G. & Liu, D. Synthesis of Galactosyl Compounds for Targeted Gene Delivery. *Bioorg. Med. Chem.* **9**, 2969 - 2978 (2001).
27 Lundquist, J. J. & Toone, E. J. The Cluster Glycoside Effect. *Chem. Rev.* **102**, 555-578 (2002).
28 Ladmiral, V., Melia, E. & Haddleton, D. M. Synthetic glycopolymers: an overview. *Eur. Polym. J.* **40**, 431 - 449 (2004).
29 Mehvar, R. Dextrans for targeted and sustained delivery of therapeutic and imaging agents. *J. Controlled Release* **69**, 1 - 25 (2000).
30 Sakurai, K., Uezu, K., Numata, M., Hasegawa, T., Li, C., Kanekoc, K. & Shinkai, S. b-1,3-Glucan polysaccharides as novel one-dimensional hosts for DNA/RNA, conjugated polymers and nanoparticles. *Chem. Commun.* **35**, 4383 - 4398 (2005).
31 Borchard, G. Chitosans for gene delivery. *Adv. Drug. Deliv. Rev.* **52**, 145 - 150 (2001).
32 Yun, Y. H., Goetz, D. J., Yellen, P. & Chen, W. Hyaluronan microspheres for sustained gene delivery and site-specific targeting. *Biomaterials* **25**, 147 - 157 (2004).
33 Gupta, M. & Gupta, A. K. Hydrogel pullulan nanoparticles encapsulating pBUDLacZ plasmid as an efficient gene delivery carrier. *J. Controlled Release* **99**, 157 - 166 (2004).
34 Vaheri, A. & Pagano, J. S. Infectious Poliovirus RNA: a Sensitive Method of Assay. *Virology* **27**, 434 - 436 (1965).
35 Mack, K. D., Wei, R., Elbagarri, A., Abbey, N. & McGrath, M. S. A novel method for DEAE-dextran mediated transfection of adherent primary cultured human macrophages. *J. Immunological Methods* **211**, 79 - 86 (1998).
36 Onishi, Y., Eshita, Y., Murashita, A., Mizuno, M. & Yoshida, J. Synthesis and Characterization of 2-Diethyl-aminoethyl–Dextran–Methyl Methacrylate Graft

Copolymer for Nonviral Gene Delivery Vector. *J. Appl. Polym. Sci.* **98**, 9 -14 (2005).

37 Azzam, T., Eliyahu, H., Makocitzki, A. & Domb, A. J. Dextran-Spermine Conjugate: An Efficient Vector for Gene Delivery. *Macromol. Symp.* **195**, 247 - 261 (2003).

38 Azzam, T., Raskin, A., Makovitzki, A., Brem, H., Vierling, P., Lineal, M. & Domb, A. J. Cationic Polysaccharides for Gene Delivery. *Macromolecules* **35**, 9947-9953 (2002).

39 Hosseinkhani, H., Azzam, T., Tabata, Y. & Domb, A. J. Dextran–spermine polycation: an efficient nonviral vector for in vitro and in vivo gene transfection. *Gene Ther.* **11**, 194 - 203 (2004).

40 Eliyahu, H., Joseph, A., Schillemans, J. P., Azzam, T., Domb, A. J. & Barenholz, Y. Characterization and in vivo performance of dextran-spermine polyplexes and DOTAP/cholesterol lipoplexes administered locally and systemically. *Biomaterials* **28**, 2339-2349 (2007).

41 Eliyahu, H., Joseph, A., Azzam, T., Barenholz, Y. & Domb, A. J. Dextran-spermine-based polyplexes--Evaluation of transgene expression and of local and systemic toxicity in mice. *Biomaterials* **27**, 1636-1645 (2006).

42 Singh, A., Suri, S. & Roy, K. In-situ crosslinking hydrogels for combinatorial delivery of chemokines and siRNA-DNA carrying microparticles to dendritic cells. *Biomaterials* **30**, 5187-5200 (2009).

43 Beaudette, T. T., Cohen, J. A., Bachelder, E. M., Broaders, K. E., Cohen, J. L., Engleman, E. G. & Frel□chet, J. M. J. Chemoselective Ligation in the Functionalization of Polysaccharide-Based Particles. *J. Am. Chem. Soc.* **131**, 10360-10361 (2009).

44 Bachelder, E. M., Beaudette, T. T., Broaders, K. E., Dashe, J. & Frel□chet, J. M. J. Acetal-Derivatized Dextran: An Acid-Responsive Biodegradable Material for Therapeutic Applications. *J. Am. Chem. Soc.* **130**, 10494-10495 (2008).

45 Nagasaki, T., Hojo, M., Uno, A., Satoh, T., Koumoto, K., Mizu, M., Sakurai, K. & Shinkai, S. Long-Term Expression with a Cationic Polymer Derived from a Natural Polysaccharide: Schizophyllan. *Bioconjugate Chem.* **15** (2004).

46 Hasegawa, T., Fujisawa, T., Haraguchi, S., Numata, M., Karinaga, R., Kimura, T., Okumura, S., Sakurai, K. & Shinkai, S. Schizophyllan–folate conjugate as a new non-cytotoxic and cancer-targeted antisense carrier. *Bioorg. Med. Chem. Lett.* **15**, 327 - 330 (2005).

47 Sakurai, K. & Shinkai, S. Molecular recognition of adenine, cytosine, and uracil in a single-strand RNA by a natural polysaccharide: schizophyllan. *J. Am. Chem. Soc.* **122**, 4520-4521 (2000).

48 Sakurai, K., Mizu, M. & Shinkai, S. Polysaccharide-polynucleotide complexes.2.Complementary polynucleotide mimic behavior of a natural polysaccharide: schizophyllan in the macromolecular comple with a single strand RNA: poly(C). *Biomacromolecules* **2**, 641-650 (2001).

49 Sletmoen, M., Naess, S. N. & Stokke, B. T. Structure and stability of polynucleotide-(1,3)-[beta]-D-glucan complexes. *Carbohydr. Polym.* **76**, 389-399 (2009).

50 Hasegawa, T., Umeda, M., Matsumoto, T., Numata, M., Mizu, M., Koumoto, K., Sakurai, K. & Shinkai, S. Lactose-appended schizophyllan is a potential candidate as a hepatocyte-targeted antisense carrier. *Chem. Commun.*, 382-383 (2004).

51 Mizu, M., Koumoto, K., Anada, T., Matsumoto, T., Numata, M., Shinkai, S., Nagasaki, T. & Sakurai, K. A polysaccharide carrier for immunostimulatory CpG DNA to enhance cytokine secretion. *J. Am. Chem. Soc.* **126**, 8372 - 8373 (2004).

52 Koumoto, K., Mizu, M., Sakurai, K., Kunitake, T. & Shinkai, S. Polysaccharide/Polynucleotide Complexes. Part 6. *Chem. Biodivers.* **1**, 520-529 (2004).

53 Anada, T., Karinaga, R., Koumoto, K., Mizu, M., Nagasaki, T., Kato, Y., Taira, K., Shinkai, S. & Sakurai, K. Linear double-stranded DNA that mimics an infective tail of virus genome to enhance transfection. *J. Controlled Release* **108**, 529-539 (2005).

54 Takeda, Y., Shimada, N., Kaneko, K., Shinkai, S. & Sakurai, K. Ternary Complex Consisting of DNA, Polycation, and a Natural Polysaccharide of Schizophyllan to Induce Cellular Uptake by Antigen Presenting Cells. *Biomacromolecules* **8**, 1178-1186 (2007).

55 Sakurai, K., Iguchi, R., Mizu, M., Koumoto, K. & Shinkai, S. Polysaccharide-polynucleotide complexes. Part 7. Hydrogen-ion and salt concentration dependence of complexation between schizophyllan and single-stranded homo RNAs. *Bioorg. Chem.* **31**, 216-226 (2003).

56 Hasegawa, T., Fujisawa, T., Numata, M., Matsumoto, T., Umeda, M., Karinaga, R., Mizu, M., Koumoto, K., Kimura, T., Okumura, S., Sakurai, K. & Shinkai, S. Schizophyllans carrying oligosaccharide appendages as potential candidates for cell-targeted antisense carrier. *Org. Biomol. Chem.* **2**, 3091-3098 (2004).

57 Karinaga, R., Koumoto, K., Mizu, M., Anada, T., Shinkai, S. & Sakurai, K. PEG-appended beta-(1-->3)-D-glucan schizophyllan to deliver antisense-oligonucleotides with avoiding lysosomal degradation. *Biomaterials* **26**, 4866-4873 (2005).

58 Karinaga, R., Anada, T., Minari, J., Mizu, M., Koumoto, K., Fukuda, J., Nakazawa, K., Hasegawa, T., Numata, M., Shinkai, S. & Sakurai, K. Galactose-PEG dual conjugation of beta-(1-->3)-D-glucan schizophyllan for antisense oligonucleotides delivery to enhance the cellular uptake. *Biomaterials* **27**, 1626-1635 (2006).

59 Klinman, D. M., Klaschik, S., Sato, T. & Tross, D. CpG oligonucleotides as adjuvants for vaccines targeting infectious diseases. *Adv. Drug Deliv. Rev.* **61**, 248-255 (2009).

60 Shimada, N., Coban, C., Takeda, Y., Mizu, M., Minari, J., Anada, T., Torii, Y., Shinkai, S., Akira, S., Ishii, K. J. & Sakurai, K. A Polysaccharide Carrier to Effectively Deliver Native Phosphodiester CpG DNA to Antigen-Presenting Cells. *Bioconj. Chem.* **18**, 1280-1286 (2007).

61 Dias, N. & Stein, C. A. Antisense Oligonucleotides: Basic Concepts and Mechanisms. *Mol. Cancer Ther.* **1**, 347-355 (2002).

62 Pouyani, T. & Prestwich, G. D. Functionalized Derivatives of Hyaluronic Acid Oligosaccharides: Drug Carriers and Novel Biomaterials. *Bioconjugate Chem.* **5**, 339 - 347 (1994).
63 Kim, A., Checkla, D. M., Dehazya, P. & Chen, W. Characterization of DNA-hyaluronan matrix for sustained gene transfer. *J. Controlled Release* **90**, 81 - 95 (2003).
64 Kim, A. P., Yellen, P., Yun, Y. H., Azeloglu, E. & Chen, W. Delivery of a vector encoding mouse hyaluronan synthase 2 via a crosslinked hyaluronan film. *Biomaterials* **26**, 1585-1593 (2005).
65 Yun, Y. H., Goetz, D. J., Yellen, P. & Chen, W. Hyaluronan microspheres for sustained gene delivery and site-specific targeting. *Biomater.* **25**, 147 - 157 (2004).
66 Yun, Y. H. & Chen, W. Microspheres formulated from native hyaluronan for applications in gene therapy. *Polym. Gene Delivery*, 475-486 (2005).
67 de la Fuente, M., Seijo, B. & Alonso, M. J. Bioadhesive hyaluronan-chitosan nanoparticles can transport genes across the ocular mucosa and transfect ocular tissue. *Gene Ther.* **15**, 668-676 (2008).
68 de la Fuente, M., Seijo, B. & Alonso, M. J. Design of novel polysaccharidic nanostructures for gene delivery. *Nanotech.* **19**, 075105/075101-075105/075109 (2008).
69 Duceppe, N. & Tabrizian, M. Factors influencing the transfection efficiency of ultra low molecular weight chitosan/hyaluronic acid nanoparticles. *Biomaterials* **30**, 2625-2631 (2009).
70 Wieland, J. A., Houchin-Ray, T. L. & Shea, L. D. Non-viral vector delivery from poly(ethylene glycol)-hyaluronic acid hydrogels. *J. Controlled Release* **120**, 233-241 (2007).
71 Saraf, A., Hacker, M. C., Sitharaman, B., Grande-Allen, K. J., Barry, M. A. & Mikos, A. G. Synthesis and Conformational Evaluation of a Novel Gene Delivery Vector for Human Mesenchymal Stem Cells. *Biomacromolecules* **9**, 818-827 (2008).
72 Shen, Y., Li, Q., Tu, J. & Zhu, J. Synthesis and characterization of low molecular weight hyaluronic acid-based cationic micelles for efficient siRNA delivery. *Carbohydr. Polym.* **77**, 95-104 (2009).
73 Bruneel, D. & Schacht, E. End group modification of pullulan. *Polymer* **36**, 169-172 (1995).
74 Kaneo, Y., Tanaka, T., Nakano, T. & Yamaguchi, Y. Evidence for receptor-mediated hepatic uptake of pullulan in rats. *J. Controlled Release* **70**, 365-373 (2001).
75 Nabi, I. R., and Le, P. U. Caveolae/Raft-dependent Endocytosis. *J. Cell Biol.* **161**, 673-677 (2003).
76 Na, K., Lee, E. S. & Bae, Y. H. Self-assembled nanoparticles of hydrophobically-modified polysaccharide bearing vitamin H as a targeted anti-cancer drug delivery system. *Eur. J. Pharm. Biopharm.* **18**, 165-173 (2003).
77 Akiyoshi, K., Kobayashi, S., Shichibe, S., Mix, D., Baudys, M., Kim, S. W. & Sunamoto, J. Self-assembled hydrogel nanoparticle of cholesterol-bearing

pullulan as a carrier of protein drugs: complexation and stabilization of insulin. *J. Controlled Release* **54**, 313-320 (1998).

78 Hosseinkhani, H., Aoyama, T., Ogawa, O. & Tabata, Y. Liver targeting of plasmid DNA by pullulan conjugation based on metal coordination. *J. Controlled Release* **83**, 287-302 (2002).

79 Kanatani, I., Ikai, T., Okazaki, A., Jo, J.-i., Yamamoto, M., Imamura, M., Kanematsu, A., Yamamoto, S., Ito, N., Ogawa, O. & Tabata, Y. Efficient gene transfer by pullulan-spermine occurs through both clathrin- and raft/caveolae-dependent mechanisms. *J. Controlled Release* **116**, 75-82 (2006).

80 Rozema, D. B., Lewis, D. L., Wakefield, D. H., Wong, S. C., Klein, J. J., Roesch, P. L., Bertin, S. L., Reppen, T. W., Chu, Q., Blokhin, A. V., Hagstrom, J. E. & Wolff, J. A. Dynamic PolyConjugates for targeted in vivo delivery of siRNA to hepatocytes. *Proc. Natl. Acad. Sci. USA* **104**, 12982-12987 (2007).

81 San Juan, A., Hlawaty, H., Chaubet, F., Letourneur, D. & Feldman, L. J. Cationized pullulan 3D matrices as new materials for gene transfer. *J. Biomed. Mater. Res. A* **82A**, 354 - 362 (2007).

82 Imai, T., Shiraishi, S., Saito, H. & Otagiri, M. Interaction of indomethacin with low molecular weight chitosan, and improvements of some pharmacuetical properties of indomethacin by low molecular weight chitosans. *Int. J. Pharm.* **67**, 11-20 (1991).

83 Takayama, K., Hirata, M., Machida, Y., Masada, T., Sannan, T. & Nagai, T. Effect of interpolymer complex formation on bioadhesive property and drug release phenomenon of compressed tablet consisting of chitosan and sodium hyaluronate. *Chem. Phar. Bull.* **38**, 1993-1997 (1990).

84 Meshali, M. M. & Gabr, K. E. Effect of interpolymer complex formation of chitosan with pectin or acacia on the release behavior of chlorpromazine HCl. *Int. J. Pharm.* **89**, 177-181 (1993).

85 Mao, H.-Q. Chitosan-DNA nanoparticles as gene carriers: synthesis, characterization and transfection efficiency. *J. Controlled Release* **70**, 399-421 (2001).

86 Mumper, R. J., J, W. J., Claspell, J. M. & Rolland, A. P. Novel polymeric condensing carriers for gene delivery. *Proc. Intl. Sym. Controlled Release Bioact. Mater.* **22**, 178-179 (1995).

87 MacLaughlin, F. C., Mumper, R. J., Wang, J., Tagliaferri, J. M., Gill, I., Hinchcliffe, M. & Rolland, A. P. Chitosan and depolymerized chitosan oligomers as condensing carriers for in vivo plasmid delivery. *J. Controlled Release* **56**, 259 - 272 (1998).

88 Dodane, V. & Vilivalam, V. D. Pharmaceutical Applications of chitosan. *PSIT* **1**, 246 - 253 (1998).

89 Aranaz, I., Mengibar, M., Harris, R., Panos, I., Miralles, B., Acosta, N., Galed, G. & Heras, A. Functional Characterization of Chitin and Chitosan. *Curr. Chem. Biol.* **3**, 203-230 (2009).

90 Aiba, S.-i. Studies on chitosan: 3. Evidence for the presence of random and block copolymer structures in partially N-acetylated chitosans. *Int. J. Biol. Macromol.* **13**, 40-44 (1991).

91 Mima, S., Miya, M., Iwamoto, R. & Yoshikawa, S. Highly deacetylated chitosan and its properties. *J. Appl. Polym. Sci.* **28**, 1909-1917 (1983).
92 Nguyen, S., Hisiger, S., Jolicoeur, M., Winnik, F. M. & Buschmann, M. D. Fractionation and characterization of chitosan by analytical SEC and 1H NMR after semi-preparative SEC. *Carbohydr. Polym.* **75**, 636-645 (2009).
93 M Köping-Höggård, I. T., H Guan, K Edwards, M Nilsson, K M Vårum and P Artursson. Chitosan as a nonviral gene delivery system. Structure–property relationships and characteristics compared with polyethylenimine in vitro and after lung administration in vivo. *Gene Ther.* **8** (2001).
94 Kiang, T., Wen, J., Lim, H. W. & Leong, K. M. The effect of the degree of chitosan deacetylation on the efficiency of gene transfection. *Biomaterials* **25**, 5293 - 5301 (2004).
95 Huang, M., Fong, C.-W., Khor, E. & Lim, L.-Y. Transfection efficiency of chitosan vectors: Effect of polymer molecular weight and degree of deacetylation. *J. Controlled Release* **106**, 391-406 (2005).
96 Liu, X., Howard, K. A., Dong, M., Andersen, M. Ø., Rahbek, U. L., Johnsen, M. G., Hansen, O. C., Besenbacher, F. & Kjems, J. The influence of polymeric properties on chitosan/siRNA nanoparticle formulation and gene silencing. *Biomaterials* **28**, 1280-1288 (2007).
97 Rejman, J., Oberle, V., Zuhorn, I. S. & Hoekstra, D. Size-dependent internalization of particles via the pathways of clathrin- and caveolae-mediated endocytosis. *Biochem. J.* **377**, 159-169 (2004).
98 Choksakulnimitr, S., Masuda, S., Tokuda, H., Takakura, Y. & Hashida, M. In vitro cytotoxicity of macromolecules in different cell culture systems. *J. Controlled Release* **34**, 233-241 (1995).
99 Erbacher, P., Zou, S., Bettinger, T., Steffan, A.-M. & Remy, J.-S. Chitosan-Based Vector/DNA Complexes for Gene Delivery: Biophysical Characteristics and Transfection Ability. *Pharm. Res.* **15**, 1332- 1339 (1998).
100 Richardson, S. C. W., Kolbe, H. V. J. & Duncan, R. Potential of low molecular mass chitosan as a DNA delivery system: biocompatibility, body distribution and ability to complex and protect DNA. *Int. J. Pharm.* **178**, 231- 243 (1999).
101 Murata, J., Ohya, Y. & Ouchi, T. Possibility of application of quaternary chitosan having pendant galactose residues as gene delivery tool. *Carbohydr. Polym.* **29**, 69-74 (1996).
102 Murata, J., Ohya, Y. & Ouchi, T. Design of quaternary chitosan conjugate having antennary galactose residues as a gene delivery tool. *Carbohydr. Polym.* **32**, 105-109 (1997).
103 Thanou, M., Florea, B. I., Geldof, M., Junginger, H. E. & Borchard, G. Quaternized chitosan oligomers as novel gene delivery vectors in epithelial cell lines. *Biomaterials* (2002).
104 Kean, T., Roth, S. & Thanou, M. Trimethylated chitosans as non-viral gene delivery vectors: Cytotoxicity and transfection efficiency. *J. Controlled Release* **103**, 643 - 653 (2005).

105 Kim, T. H., Kim, S. I., Akaike, T. & Cho, C. S. Synergistic effect of poly(ethylenimine) on the transfection efficiency of galactosylated chitosan/DNA complexes. *J. Controlled Release* **105**, 354-366 (2005).
106 Wong, K., Sun, G., Zhang, X., Dai, H., Liu, Y., He, C. & Leong, K. M. PEI-g-chitosan, a Novel Gene Delivery System with Transfection Efficiency Comparable to Polyethylenimine in Vitro and after Liver Administration in Vivo. *Bioconjugate Chem.* **17** (2006).
107 Jiang, H.-L., Kim, Y.-K., Arote, R., Nah, J.-W., Cho, M.-H., Choi, Y.-J., Akaike, T. & Cho, C.-S. Chitosan-graft-polyethylenimine as a gene carrier. *J. Controlled Release* **117**, 273 - 280 (2007).
108 Kim, T.-H., Jiang, H.-L., Jere, D., Park, I.-K., Cho, M.-H., Nah, J.-W., Choi, Y.-J., Akaike, T. & Cho, C.-S. Chemical modification of chitosan as a gene carrier in vitro and in vivo. *Prog. Polym. Sci.* **32**, 726-753 (2007).
109 Nicolet, B. H. & Shinn, L. A. The action of periodic acid on b-amino alcohols. *J. Am. Chem. Soc.* **61**, 1615-1615 (1939).
110 Vold, I. M. N. & Christensen, B. E. Periodate oxidation of chitosans with different chemical compositions. *Carbohydr. Res.* **340**, 679-684 (2005).
111 Jiang, H., Kwon, J., Kim, Y., Kim, E., Arote, R., Jeong, H., Nah, J., Choi, Y., Akaike, T. & Cho, M. Galactosylated chitosan-graft-polyethylenimine as a gene carrier for hepatocyte targeting. *Gene Ther.* **14**, 1389-1398 (2007).
112 Jiang, H.-L., Kwon, J.-T., Kim, E.-M., Kim, Y.-K., Arote, R., Jere, D., Jeong, H.-J., Jang, M.-K., Nah, J.-W., Xu, C.-X., Park, I.-K., Cho, M.-H. & Cho, C.-S. Galactosylated poly(ethylene glycol)-chitosan-graft-polyethylenimine as a gene carrier for hepatocyte-targeting. *J. Controlled Release* **131**, 150-157 (2008).
113 Lu, B., Xu, X.-D., Zhang, X.-Z., Cheng, S.-X. & Zhuo, R.-X. Low Molecular Weight Polyethylenimine Grafted N-Maleated Chitosan for Gene Delivery: Properties and In Vitro Transfection Studies. *Biomacromolecules* **9**, 2594-2600 (2008).
114 Lou, Y.-L., Peng, Y.-S., Chen, B.-H., Wang, L.-F. & Leong, K. W. Poly(ethylene imine)-g-chitosan using EX-810 as a spacer for nonviral gene delivery vectors. *J. Biomed. Mater. Res. A* **88A**, 1058-1068 (2009).
115 Wu, Y., Liu, C., Zhao, X. & Xiang, J. A new biodegradable polymer: PEGylated chitosan-g-PEI possessing a hydroxyl group at the PEG end. *J. Polym. Res.* **15**, 181-185 (2008).
116 Jiang, H.-L., Kim, Y.-K., Arote, R., Jere, D., Quan, J.-S., Yu, J.-H., Choi, Y.-J., Nah, J.-W., Cho, M.-H. & Cho, C.-S. Mannosylated chitosan-graft-polyethylenimine as a gene carrier for Raw 264.7 cell targeting. *Int. J. Pharm.* **375**, 133-139 (2009).
117 Jiang, H.-L., Xu, C.-X., Kim, Y.-K., Arote, R., Jere, D., Lim, H.-T., Cho, M.-H. & Cho, C.-S. The suppression of lung tumorigenesis by aerosol-delivered folate-chitosan-graft-polyethylenimine/Akt1 shRNA complexes through the Akt signaling pathway. *Biomaterials* **30**, 5844-5852 (2009).
118 Jere, D., Jiang, H.-L., Kim, Y.-K., Arote, R., Choi, Y.-J., Yun, C.-H., Cho, M.-H. & Cho, C.-S. Chitosan-graft-polyethylenimine for Akt1 siRNA delivery to lung cancer cells. *Int. J. Pharm.* **378**, 194-200 (2009).

119 Pack, D. W., Putnam, D. & Langer, R. Design of imidazole-containing endosomolytic biopolymers for gene delivery. *Biotechnol. Bioeng.* **67**, 217-223 (2000).
120 Muzzarelli, R. A. A., Mattioli-Belmonte, M., Tietz, C., Biagini, R., Ferioli, G., Brunelli, M. A., Fini, M., Giardino, R., Ilari, P. & Biagini, G. Stimulatory effect on bone formation exerted by a modified chitosan. *Biomaterials* **15**, 1075-1081 (1994).
121 Midoux, P. & Monsigny, M. Efficient Gene Transfer by Histidylated Polylysine/pDNA Complexes. *Bioconj. Chem.* **10**, 406-411 (1999).
122 Kim, T. H., Ihm, J. E., Choi, Y. J., Nah, J. W. & Cho, C. S. Efficient gene delivery by urocanic acid-modified chitosan. *J. Controlled Release* **93**, 389-402 (2003).
123 Jin, H., Kim, T., Hwang, S., Chang, S., Kim, H., Anderson, H., Lee, H., Lee, K., Colburn, N. & Yang, H. Aerosol delivery of urocanic acid–modified chitosan/programmed cell death 4 complex regulated apoptosis, cell cycle, and angiogenesis in lungs of K-ras null mice. *Mol. Cancer Ther.* **5**, 1041 (2006).
124 Jin, H. *et al.* Urocanic acid-modified chitosan-mediated PTEN delivery via aerosol suppressed lung tumorigenesis in K-rasLA1 mice. *Cancer Gene Ther* **15**, 275-283 (2008).
125 Bauhuber, S., Hozsa, C., Breunig, M. & Göpferich, A. Delivery of Nucleic Acids via Disulfide-Based Carrier Systems. *Adv. Mater.* **21**, 3286-3306 (2009).
126 Bernkop-Schnürch, A., Hornof, M. & Guggi, D. Thiolated chitosans. *Eur. J. Pharm. Biopharm.* **57**, 9-17 (2004).
127 Schmitz, T., Bravo-Osuna, I., Vauthier, C., Ponchel, G., Loretz, B. & Bernkop-Schnürch, A. Development and in vitro evaluation of a thiomer-based nanoparticulate gene delivery system. *Biomaterials* **28**, 524-531 (2007).
128 Martien, R., Loretz, B., Thaler, M., Majzoob, S. & Bernkop-Schnurch, A. Chitosan–thioglycolic acid conjugate: An alternative carrier for oral nonviral gene delivery? *J. Biomed. Mater. Res. A*, 1 - 9 (2007).
129 Murata, J.-i., Ohya, Y. & Ouchi, T. Possibility of application of quarternary chitosan having pendant galactose residues as gene delivery tool. *Carbohyd. Polym.* **29**, 69 - 74 (1996).
130 Hashimoto, M., Morimoto, M., Saimoto, H., Shigemasa, Y. & Sato, T. Lactosylated chitosan for DNA delivery into hepatocytes: the effect of lactosylation on the physicochemical properties and intracellular trafficking of pDNA/chitosan complexes. *Bioconj. Chem.* **17**, 309-316 (2006).
131 Park, Y. K., Park, Y. H., Shin, B. A., Choi, E. S., Park, Y. R., Akaike, T. & Cho, C. S. Galactosylated chitosan-graft-dextran as hepatocyte-targeting DNA carrier. *J. Controlled Release* **69**, 97-108 (2000).
132 Park, I. K., Kim, T. H., Park, Y. H., Shin, B. A., Choi, E. S., Chowdhury, E. H., Akaike, T. & Cho, C. S. Galactosylated chitosan-*graft*-poly(ethylene glycol) as hepatocyte-targeting DNA carrier. *J. Controlled Release* **76**, 349-362 (2001).
133 Park, I. K., Ihm, J. E., Park, Y. H., Choi, Y. J., Kim, S. I., Kim, W. J., Akaike, T. & Cho, C. S. Galactosylated chitosan (GC)-graft-poly(vinyl pyrrolidone) (PVP) as hepatocyte-targeting DNA carrier: Preparation and physicochemical

characterization of GC-graft-PVP/DNA complex (1). *J. Controlled Release* **86**, 349-359 (2003).

134 Hashimoto, M., Morimoto, M., Saimoto, H., Shigemasa, Y., Yanagie, H., Eriguchi, M. & Sato, T. Gene transfer by DNA/mannosylated chitosan complexes into mouse peritoneal macrophages. *Biotecnol Lett* **28**, 815 - 821 (2006).

135 Forrest, M. L., Gabrielson, N. & Pack, D. W. Cyclodextrin-polyethylenimine conjugates for targeted in vitro gene delivery. *Biotechnol. Bioeng.* **89**, 416-423 (2005).

136 Liu, Y., Wenning, L., Lynch, M. & Reineke, T. M. New Poly(D-glucaramidoamine)s Induce DNA Nanoparticle Formation and Efficient Gene Delivery into Mammalian Cells. *J. Am. Chem. Soc.* **126**, 7422-7423 (2004).

137 Reineke, T. M. & Davis, M. E. Structural Effects of Carbohydrate-Containing Polycations on Gene Delivery. 1. Carbohydrate Size and Its Distance from Charge Centers. *Bioconjugate Chem.* **14**, 247-254 (2003).

138 Reineke, T. M. & Davis, M. E. Structural Effects of Carbohydrate-Containing Polycations on Gene Delivery. 2. Charge Center Type. *Bioconjugate Chem.* **14**, 255-261 (2003).

139 Srinivasachari, S., Liu, Y., Zhang, G., Prevette, L. & Reineke, T. M. Trehalose Click Polymers Inhibit Nanoparticle Aggregation and Promote pDNA Delivery in Serum. *J. Am. Chem. Soc.* **128**, 8176-8184 (2006).

140 Hwang, S. J., Bellocq, N. C. & Davis, M. E. Effects of Structure of Beta-Cyclodextrin-Containing Polymers on Gene Delivery. *Bioconjugate Chem.* **12**, 280-290 (2001).

141 Boussif, O., Lezoualc'h, F., Zanta, M. A., Mergny, M. D., Scherman, D., Demeneix, B., Behr, J. P. A Versatile Vector for Gene and Oligonuceotide Transfer into Cells in Culture and *in vivo*: Polyethylenimine. *Proc. Natl. Acad. Sci. U. S. A.* **92**, 7297-7301 (1995).

142 Metzke, M., O'Connor, N., Maiti, S., Nelson, E. & Guan, Z. Saccharide–Peptide Hybrid Copolymers as Biomaterials. *Angew. Chem. Int. Ed.* **44**, 6529 - 6533 (2005).

143 Reineke, T. M. Poly(glycoamidoamine)s: Cationic glycopolymers for DNA delivery. *J. Polym. Sci. A.* **44**, 6895-6908 (2006).

144 Liu, Y., Wenning, L., Lynch, M. & Reineke, T. M. Gene delivery with novel poly(L-tartaramidoamine)s. *Pol. Drug Del. Vol. I. Particulate Drug Carriers* **923**, 217-227 (2006).

145 Liu, Y. & Reineke, T. M. Poly(glycoamidoamine)s for Gene Delivery: Stability of Polyplexes and Efficacy with Cardiomyoblast Cells. *Bioconjugate Chem.* **17**, 101-108 (2006).

146 Prevette, L. E., Kodger, T. E., Reineke, T. M. & Lynch, M. L. Deciphering the role of hydrogen bonding in enhancing pDNA-Polycation interactions. *Langmuir* **23**, 9773-9784 (2007).

147 Lee, C.-C., Liu, Y. & Reineke, T. M. General Structure-Activity Relationship for Poly(glycoamidoamine)s: The Effect of Amine Density on Cytotoxicity and DNA Delivery Efficiency. *Bioconj. Chem.* **19**, 428-440 (2008).

148 Taori, V. P., Liu, Y. & Reineke, T. M. DNA delivery in vitro via surface release from multilayer assemblies with poly(glycoamidoamine)s. *Acta Biomaterialia* **5**, 925-933 (2009).
149 Paiva, C. & Panek, A. Biotechnological applications of the disaccharide trehalose. *Biotechnol. Ann. Rev.* **2**, 293 (1996).
150 Lins, R. D., Pereira, C. S. & Hünenberger, P. H. Trehalose-protein interaction in aqueous solution. *Proteins Struct. Funct. Bioinf.* **55**, 177-186 (2004).
151 Reineke, T. M., Davis, M. E. Structural Effects of Carbohydrate-Containing Polycations on Gene Delivery. 1. Carbohydrate Size and Its Distance from Charged Centers. *Bioconjugate Chem.* **14**, 247-254 (2003).
152 Wagner, E. Strategies to improve DNA polyplexes for in vivo gene transfer: Will "artificial viruses" be the answer? *Pharm. Res.* **21**, 8-14 (2004).
153 Srinivasachari, S., Liu, Y., Prevette, L. E. & Reineke, T. M. Effects of trehalose click polymer length on pDNA complex stability and delivery efficacy. *Biomaterials* **28**, 2885-2898 (2007).
154 Prevette, L. E., Lynch, M. L., Kizjakina, K. & Reineke, T. M. Correlation of Amine Number and pDNA Binding Mechanism for Trehalose-Based Polycations. *Langmuir* **24**, 8090-8101 (2008).
155 Ortiz-Mellet, C., Benito, J. M., Garcia Fernandez, J. M., Law, H., Chmurski, K., Defaye, J., O'Sullivan, M. L. & Caro, H. N. Cyclodextrin-scaffolded glyco-clusters. *Chem. Eur. J.* **4**, 2523-2531 (1998).
156 Perez-Balderas, F., Ortega-Munoz, M., Morales-Sanfrutos, J., Hernandez-Mateo, F., Calvo-Flores, F. G., Calvo-Asin, J. A., Isac-Garcia, J. & Santoyo-Gonzalez, F. Multivalent Neoglycoconjugates by Regiospecific Cycloaddition of Alkynes and Azides Using Organic-Soluble Copper Catalysts. *Org. Lett.* **5**, 1951-1954 (2003).
157 Garcia-Lopez, J. J., Hernandez-Mateo, F., Isac-Garcia, J., Kim, J. M., Roy, R., Santoyo-Gonzalez, F. & Vargas-Berenguel, A. Synthesis of Per-Glycosylated **beta**-Cyclodextrins Having Enhanced Lectin Binding Affinity. *J. Org. Chem.* **64**, 522-531 (1999).
158 Gadella, A. & Defaye, J. Selective Halogenation at Primary Postions of Cyclomaltooligosaccharides and a Synthesis of Per-3,6-anhydro Cyclomaltooligosaccharides. *Angew. Chem. Int. Ed.* **30**, 78 - 80 (1991).
159 Andre, S., Kaltner, H., Furuike, T., Nishimura, S.-I. & Gabius, H.-J. Persubstituted Cyclodextrin-Based Glycoclusters as Inhibitors of Protein-Carbohydrate Recognition Using Purified Plant and Mammalian Lectins and Wild-Type and Lectin-Gene-Transfected Tumor Cells as Targets. *Bioconjugate Chem.* **15**, 87-98 (2004).
160 Bellocq, N. C., Pun, S. H., Jensen, G. S. & Davis, M. E. Transferrin-Containing, Cyclodextrin Polymer-Based Particles for Tumor-Targeted Gene Delivery. *Bioconjugate Chem.* **14**, 1122-1132 (2003).
161 Davis, M. E. & Bellocq, N. C. Cyclodextrin-Containing Polymers for Gene Delivery. *J. Inclusion Phenom. Macrocyclic Chem.* **44**, 17 - 22 (2001).
162 Croyle, M. A., Roessler, B. J., Hsu, C.-P., Sun, R. & Amidon, G. L. Beta-Cyclodextrins Enhance Adenoviral-Mediated Gene Delivery to the Intestine. *Pharm. Res.* **15**, 1349-1355 (1998).

163 Boger, J., Corcoran, R. J. & Lehn, J.-M. Cyclodextrin chemistry. Selective modification of all primary hydroxyl groups of alpha- and beta-cyclodextrins. *Helv. Chim. Acta* **61**, 2190-2218 (1978).
164 Mocanu, G., Vizitiu, D. & Carpov, A. Cyclodextrin Polymers. *J. Bioact. Compat. Pol.* **16**, 315-328 (2001).
165 Zhao, Q., Temsamani, J. & Agrawal, S. Use of cyclodextrin and its derivatives as carriers for oligonucleotide delivery. *Antisense Res. Dev.* **5**, 185 - 192 (1995).
166 Salem, L. B., Bosquillon, C., Dailey, L. A., Delattre, L., Martin, G. P., Evrard, B. & Forbes, B. Sparing methylation of [beta]-cyclodextrin mitigates cytotoxicity and permeability induction in respiratory epithelial cell layers in vitro. *J. Controlled Release* **136**, 110-116 (2009).
167 Yang, C., Li, H., Goh, S. H. & Li, J. Cationic star polymers consisting of [alpha]-cyclodextrin core and oligoethylenimine arms as nonviral gene delivery vectors. *Biomaterials* **28**, 3245-3254 (2007).
168 Cryan, S.-A. Cell transfection with polycationic cyclodextrin vectors. *Eur. J. Pharm. Sci.* **21**, 625-633 (2004).
169 Gonzalez, H., Hwang, S. J. & Davis, M. E. New Class of Polymers for the Delivery of Macromolecular Therapeutics. *Bioconjugate Chem.* **10**, 1068-1074 (1999).
170 Srinivasachari, S., Fichter, K. M., and Reineke, T. M. Polycationic β-Cyclodextrin "Click Clusters": Monodisperse and Versatile Scaffolds for Nucleic Acid Delivery. *J. Am. Chem. Soc.* **130**, 4618-4627 (2008).
171 Srinivasachari, S. & Reineke, T. M. Versatile supramolecular pDNA vehicles via "click polymerization" of [beta]-cyclodextrin with oligoethyleneamines. *Biomaterials* **30**, 928-938 (2009).
172 Pun, S. H., and Davis, M. E. Development of a Nonviral Gene Delivery Vehicle for Systemic Application. *Bioconjugate Chem.* **13** (2002).
173 Pun, S. H., Tack, F., Bellocq, N. C., Cheng, J., Grubbs, B. H., Jensen, G. S., Davis, M. E., Brewster, M., Janicot, M., Janssens, B., Floren, W., Bakker, A. Targeted Delivery of RNA-Cleaving DNA Enzyme (DNAzyme) to Tumor Tissue by Transferrin-Modifed, Cyclodextrin-Based Particles. *Cancer Biol. and Ther.* **3**, 641-650 (2004).
174 Heidel, J. D., Yu, Z. P., Liu, J. Y. C., Rele, S. M., Liang, Y. C., Zeidan, R. K., Kornbrust, D. J. & Davis, M. E. Administration in non-human primates of escalating intravenous doses of targeted nanoparticles containing ribonucleotide reductase subunit M2 siRNA. *Proc. Natl. Acad. Sci. USA* **104**, 5715-5721 (2007).
175 Hu-Lieskovan, S., Heidel, J. D., Bartlett, D. W., Davis, M. E., and Triche, T. J. Sequence-Specific Knockdown of EWS-EFI1 by Targeted, Nonviral Delivery of Small Interfering RNA Inhibits Tumor Growth in a Murine Model of Metastatic Ewing's Sarcoma. *Cancer Res.* **65**, 8984-8992 (2005).
176 Davis, M. E. The First Targeted Delivery of siRNA in Humans via a Self-Assembling, Cyclodextrin Polymer-Based Nanoparticle: From Concept to Clinic. *Mol. Pharm.* **6**, 659-668 (2009).

177 Zanta, M.-A., Boussif, O., Adib, A., and Behr, J.-P. In vitro Gene Delivery to Hepatocytes with Galactosylated Polyethylenimine. *Bioconjugate Chem.* **8** (1997).
178 Kunath, K., von Harpe, A., Fischer, D. & Kissel, T. Galactose-PEI-DNA complexes for targeted gene delivery: degree of substitution affects complex size and transfection efficiency. *J. Control. Rel.* **88**, 159-172 (2003).
179 Nishikawa, M., Yamauchi, M., Morimoto, K., Ishida, E., Takakura, Y. & Hashida, M. Hepatocyte-targeted in vivo gene expression by intravenous injection of plasmid DNA complexed with synthetic multi-functional gene delivery system. *Gene Ther.* **7**, 548-555 (2000).
180 Chen, C.-p., Kim, J.-s., Liu, D., Rettig, G. R., McAnuff, M. A., Martin, M. E. & Rice, K. G. Synthetic PEGylated Glycoproteins and Their Utility in Gene Delivery. *Bioconjugate Chem.* **18**, 371-378 (2007).
181 Weiss, S. I., Sieverling, N., Niclasen, M., Maucksch, C., Thünemann, A. F., Möhwald, H., Reinhardt, D., Rosenecker, J. & Rudolph, C. Uronic acids functionalized polyethyleneimine (PEI)-polyethyleneglycol (PEG)-graft-copolymers as novel synthetic gene carriers. *Biomaterials* **27**, 2302-2312 (2006).
182 Diebold, S. S., Kursa, M., Wagner, E., Cotten, M., and Zenke, M. . Mannose Polyethylenimine Conjugates for Targeted DNA Delivery into Dendritic Cells. *J. Biol. Chem.* **274**, 19087-19094 (1999).
183 Grosse, S., Aron, Y., Honore, I., Thevenot, G., Danel, C., Roche, A.-C., Monsigny, M., Fajac, I. Lactosylated Polyethylenimine for Gene Transfer into Airway Epithelial Cells: Role of the Sugar Moiety in Cell Delivery and Intracellular Trafficking of the Complexes. *J. Gene Med.* **2004**, 345-356 (2004).

Chapter 3. Trehalosamine-based Cationic Diblock Polymers for Nucleic Acid Delivery*

*The work described in this chapter is a result of collaborative efforts between the dissertation author, Lian Xue, and Dr. Nilesh Ingle. Flow cytometry experiments were performed by Lian Xue and Dr. Nilesh Ingle; cellular toxicity and gene down-regulation experiments were performed by Lian Xue; confocal microscopy images were acquired by Dr. Nilesh Ingle.

Abstract

When nanoparticles interact with their environment, the nature of that interaction is governed largely by the properties of their outermost/surface layer. While materials like polyethylene glycol are routinely utilized to decrease nonspecific interactions and enhance colloidal stability of macromolecules and nanosystems, drawbacks exist that have prompted researchers to explore alternatives. Here, we exploit the exceptional properties of a common disaccharide, trehalose, which is well known for its unique biological stabilization effects. Trehalose-based polymer ("polytrehalose") has been developed that ensures colloidal stability and can protect inter-polyelectrolyte-based nanoparticles from undesired interactions with each other (e.g., aggregation) in high salt, serum, and even during lyophilization. Moreover, polycation-siRNA nanoparticles ("polyplexes") coated with polytrehalose demonstrate exceptional cellular internalization in glioblastoma cells, without any apparent toxicity, and achieve significant siRNA-induced target gene down-regulation. This ability to mediate target gene down-regulation was maintained after freeze-drying and resuspension of polytrehalose-coated polyplexes.

These findings suggest that polytrehalose has the potential to serve as an important component of therapeutic nanoparticle formulations of nucleic acids and has great promise to be extended as a new coating for other nano-based technologies and macromolecules, in particular, those related to nanomedicine applications.

3.1 Introduction

α,α-D-Trehalose is a unique disaccharide with special properties ideal for use in materials research. This non-reducing disaccharide is very stable to acidic hydrolysis, even at high temperatures[1] and been found to protect cells during oxidative stress[2] and freezing.[3,4] In nature, trehalose is found in numerous plants, animals and fungi that can withstand amazing environmental extremes. Trehalose is a known mediator of autophagy, thus effectively shielding intracellular organelles and biomolecules from aggregation and water crystallization, aiding in cryptobiosis. This has been readily observed in the *Selaginalla lepidophylla* plant, known also as the resurrection plant or Rose of Jericho, which contains about 12% of trehalose by dry mass. Exposure of an apparent lifeless resurrection plant to water leads to a remarkable transformation and restoration of normal metabolism that occurs within several hours.[5] Trehalose is accumulated under stress in a number of animals and insects with cryptobiotic ability; for example, tardigrades (water bears) can undergo almost complete dessication and withstand temperature extremes down to -196 ^{o}C.[6] Yet, when exposed to water, they resume normal biological function and behavior.[7]

This property of trehalose has long been recognized and, consequently, trehalose is widely studied by cryobiologists. This disaccharide has enabled freezing, freeze-drying

and hypothermal storage of various macromolecules, such as proteins, antibodies, DNA, liposomes and DNA/lipid complexes, whole cells, and even organs.[8] While trehalose is not biosynthesized in humans, we have the ability to metabolize this sugar via trehalase, an enzyme that hydrolyzes the glycosidic bond of trehalose producing two glucose molecules. To this end, several groups have exploited this sugar for its special properties. Trehalose has been found to induce autophagy in the brain; its presence has been linked to neuroprotective effects in cases of Huntington, Parkinson, and prion diseases.[9,10] Wada et al. have demonstrated that multivalent trehalose inhibits the aggregation of amyloid β peptide, associated with Alzheimer's disease.[11] Moreover, the presence of trehalose has been shown to enhance plasmid DNA (pDNA) delivery by poly(ethyleneimine) (PEI) to various cell lines.[12] We have also been interested in this disaccharide for a number of years and previously shown that step-growth cationic polymers containing alternating trehalose units in their backbones yield high cellular delivery efficiency of plasmid DNA (pDNA) and promote some stability in polymer/DNA complexes (polyplexes) within serum-containing solutions.[13]

Inspired by these works and the unique properties of trehalose, we rationalized that a block copolymer comprised of densely-placed trehalose units ("polytrehalose") would deter non-specific aggregation/adsorption and confer lyoprotective and cryoprotective properties similar to those of trehalose itself as a surface layer on nanoparticles. In addition, this material may also offer neuroprotective effects during treatment, which parallels our interests in delivering therapeutic siRNA to glioblastomas (brain tumors). Such a polymer could offer incredible properties as a surface layer/coating of nanoparticles, ensuring a high local concentration of this carbohydrate

(Fig. 1). Its polymeric nature would be expected to potentially impart an increase in the local viscosity on the particle surface, thus enhancing vitrification of the surface-bound water and colloidal stability.[14] Indeed, many other polymers have been explored to enhance colloidal stability of macromolecules and nanoparticles, the most common being poly(ethylene glycol) (PEG). While PEG prevents flocculation and non-specific interactions, it does not biodegrade, is prone to oxidation, and PEG-coated particles have been shown to undergo accelerated blood clearance.[15] These limitations have motivated us and others to explore potential alternatives to PEG. To the best of our knowledge, this is the first report to explore a polytrehalose motif for enhancing colloidal stability of self-assembled nanosystems.

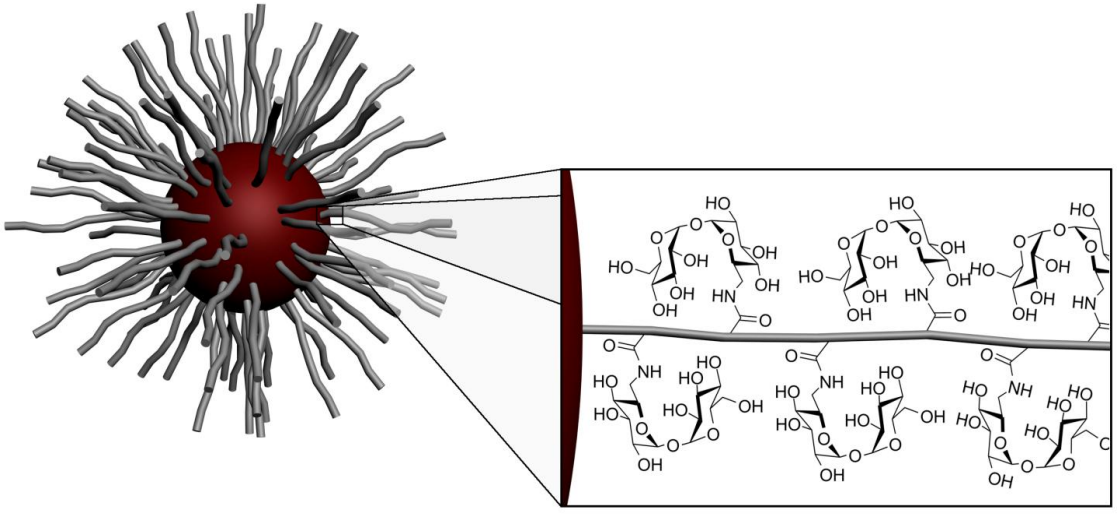

Figure 3.1. Schematic representation of a nanoparticle coated with a polytrehalose polymer.

3.2 Materials and Methods

3.2.1 Material synthesis and evaluation of physical properties

All reagents for synthesis were obtained at highest possible purity from Fisher Scientific Co (Pittsburgh, PA) or Sigma-Aldrich Co (St. Louis, MO) and used as received unless noted otherwise. N-(2-Aminoethyl)methacrylamide was purchased from Polysciences (Warrington, PA). JetPEI was obtained from PolyPlus Transfections (Illkirch, France). Dialysis membranes were obtained from Spectrum Laboratories, Inc. (Rancho Dominguez, CA). Dry methylene chloride, dimethyl formamide, methanol and tetrahydrofuran were obtained using an MBRAUN MB solvent purification system manufactured by M. Braun Inertgas-Systeme GmbH (Garching, Germany), using HPLC grade solvents obtained from Fisher Scientific Co (Pittsburgh, PA).

Thin layer chromatographies (TLC) were done using aluminum-backed silica gel plates (silica gel 60, F_{254}) obtained from Merck (Darmstadt, Germany) and visualized using UV light (254 nm) or staining agents: ninhydrin solution in ethanol for the visualization of amines, *p*-anisaldehyde solution in H_2SO_4/acetic acid/ethanol for the visualization of carbohydrates.

Preparative chromatographies were performed using Buchi Sepacore® chromatography system, (Buchi Labortechnik AG, Switzerland) using Buchi plastic chromatography cartridges or homemade glass columns manually packed with 60-200 mesh Premium Rf silica gel (Sorbent Technologies Inc., Atlanta, GA). All solvents used for preparative chromatography were HPLC grade obtained from Fisher Scientific Co (Pittsburgh, PA).

LC-MS data was obtained with an Agilent system, Agilent Technologies (Santa Clara, CA) with a time-of-flight (TOF) analyzer coupled to a Thermo Electron TSQ-LC/MS ESI mass spectrometer.

NMR spectra were recorded using 400MR Varian-400 Hz spectrometer in deuterated solvents, namely D_2O, d_4-MeOD, d_6-DMSO, $CDCl_3$, CD_2Cl_2. All deuterated solvents were purchased from Cambridge Isotope Laboratories, Inc. (Andover, MA). ^{1}H-NMR spectra were recorded at 399.7 MHz and ^{13}C-NMR spectra were recorded at 101 MHz. Spectra were analyzed using MNova software (version 7.0.1-8414, Mestrelab Research S.L. (Santiago de Compostela, Spain)).

SEC was conducted using 1.0 wt% acetic acid/0.1 M Na_2SO_4 as eluent at a flow rate 0.3 mL/min on size exclusion chromatography columns [CATSEC1000 (7μ, 50×4.6), CATSEC100 (5μ, 250×4.6), CATSEC300 (5μ, 250×4.6), and CATSEC1000 (7μ, 250×4.6)] obtained from Eprogen Inc. (Downers Grove, IL). Signals were acquired using Wyatt HELEOS II light scattering detector (λ = 662 nm), and an Optilab rEX refractometer (λ = 658 nm). SEC trace analysis was performed using Astra V software (version 5.3.4.18), Wyatt Technologies (Santa Barbara, CA)). Biological sample fluorescence was measured with GENios Pro luminometer (TECAN US, Research Triangle Park, NC). Quartz Crystal Microbalance (QCM) experiments were performed on Q-Sense E4 QCM (Q-sense; Vastra Frolunda, Sweden) instrument. Differential scanning calorimetery (DSC) was conducted on a TA Instruments Q100 under nitrogen.

Typical procedure for the synthesis of 6-iodo-6-deoxy-2,3,4,5,2',3',4',5',6'-O-acetyl trehalose (2)

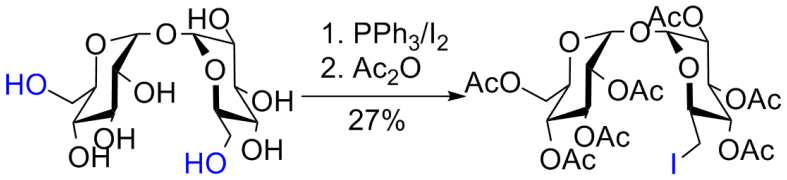

1 **2**

Iodine (47.50 g, 0.1871 mol) was placed in a flame-dried 1.5 L round-bottom flask and 800 mL of dry dimethylformamide (DMF) was added. Triphenylphosphine (51.55 g, 0.1965 mol) was dissolved in 150 mL of dry THF and added to the iodine suspension. *A*nhydrous trehalose (42.64 g, 0.1246 mol, used as received) was added quickly via a funnel. The reaction flask was closed with a septum, flushed with nitrogen, and placed in an oil bath. The reaction was allowed to proceed at 80 °C for 4 h. Solvents were removed under vacuum yielding a thick yellowish oil. The oil was poured into a 1 L solution of NaOMe in methanol. The solution pH was measured by placing a drop of the methanolic solution on a piece of wet indicator paper. The pH was adjusted to 9 using NaOMe and the reaction mixture was then allowed to stir for 1h at room temperature. Acidic resin DOWEX-2H (H^+ form) was added to neutralize the solution and subsequently filtered off. Methanol was removed on rotary evaporator yielding yellowish oil. The oil was poured into 600 mL of water causing PPh_3O precipitation. Importantly, a thin-tipped funnel was used to avoid the formation of large clumps of triphenylphosphine oxide. This solution was placed in a refrigerator at 4 °C for 12 h.

The aqueous solution was filtered to remove PPh_3O. The filtrate was extracted with 2x50 mL of dichloromethane (DCM) to remove any remaining organic impurities (PPh_3O and PPh_3). Water was removed on rotary evaporator, and obtained oil was dried for 20 h over P_2O_5 at 500 mTorr. The dry oil was dissolved in 800 mL of dry pyridine

(Py) and the solution was placed in an ice-bath. Acetic anhydride (190 mL, 205 g (d=1.08 g/mL), 2.01 mol) was added over ca. 15 min using an addition funnel. The reaction was allowed to stir at room temperature for 14 h. The reaction mixture was then poured on ice, forming a sticky precipite. The ice was allowed to melt and the reaction mixture was extracted with 4x200 mL of DCM. Organic extracts were combined, washed with a dilute sulfuric acid solution to remove Py and dried over Na_2SO_4 overnight. It should be noted that washing with NaCl(sat) solution leads to halogen exchange ($RCH_2I \rightarrow RCH_2Cl$) and has to be avoided. Na_2SO_4 was filtered off and DCM was removed on a rotary evaporator yielding a yellowish oil. The oil was loaded on a silica gel column (300 g of silica gel, DCM) and mixture of per-O-acetylated 6-iodo-6-deoxy and 6,6´-diiodo-6,6´-deoxy trehalose was separated from the rest of the mixture using DCM/Et_2O=5/1 eluent.

This mixture of two products was separated by column chromatography (ca. 2 gram portions of mixture, 100 g of silica gel) using eluent gradient DCM → DCM/Et_2O(5/1) to yield 22.3 g (24.0%) of **2**.

^{1}H-NMR (400 MHz, $CDCl_3$) δ ppm: 5.56 – 5.45 (overlapping doublets, J = 10.3 Hz, 2H), 5.38 (d, 3.9 Hz, 1H), 5.35 (d, 3.9 Hz, 1H), 5.19 (dd, J = 10.3, 3.9 Hz, 1H), 5.10 – 5.00 (m, 2H), 4.89 (dd, J = 10.0, 9.1 Hz, 1H), 4.27 – 4.19 (m, 1H), 4.08 – 3.98 (m, 2H), 3.93 (ddd, J = 10.0, 9.1, 2.5 Hz, 1H), 3.25 (dd, J = 11.0, 2.5 Hz, 1H), 3.13 – 2.99 (m, 1H), 2.15 (s, 3H), 2.09 – 2.07 (m, 9H), 2.05 (s, 3H), 2.03 (s, 3H), 2.02 (s, 3H). ^{13}C-NMR (101 MHz, $CDCl_3$) δ ppm: 170.67, 170.00, 169.94, 169.67, 169.58, 169.57, 92.21, 91.68, 72.46, 70.31, 70.11, 69.84, 69.56, 69.27, 68.70, 68.38, 68.05, 61.91, 25.70, 21.28, 20.79, 20.74, 20.68, 20.63, 2.61. ESI-MS positive ion mode: calculated m/z $[M+NH_4]^+$ 764.1257,

found m/z: 764.1297 (error 5 ppm); calculated m/z $[M+Na]^+$ 769.0811, found m/z: 769.0832 (error 3 ppm).

Typical procedure for the synthesis of 6-azido-6-deoxy-2,3,4,5,2',3',4',5',6'-O-acetyl trehalose (3)

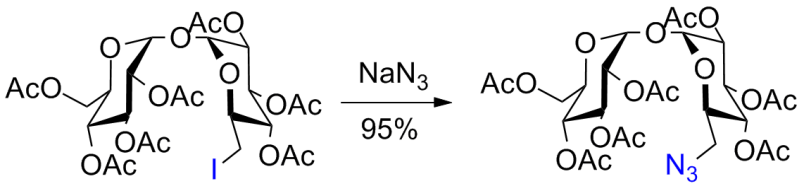

2 **3**

Compound **2** (16.56 g, 22.19 mmol) and NaN_3 (1.63 g, 25.1 mmol) were placed in a dry 500 mL flask equipped with a stir bar and capped with a septum. Next, 300 mL of dry DMF were added via cannula and nitrogen was bubbled through the solution for 20 min. The reaction mixture was brought to 60 °C and stirred for 4 h, cooled down and concentrated on a rotary evaporator to a final volume of ca. 150 mL. The resulting solution was poured into 700 mL of H_2O at 0 °C. It was extracted with 3x150 mL of ethyl acetate. Organic extracts were combined, washed with brine and dried over Na_2SO_4 overnight. The solids were filtered off and the solvent was removed on a rotary evaporator, yielding a white crystalline material. The product was recrystallized from ethylacetate/hexanes(1/3) to yield 11.94 g of **3** upon drying. The filtrate was placed in a freezer (-27 ^oC) resulting in precipitation of 1.62 g of **3**. Combined yield was 13.56 g (92.4%). ^{1}H-NMR (400 MHz, $CDCl_3$) δ ppm: 5.49 (ddd, J = 10.3, 9.3, 5.7 Hz, 2H), 5.35 – 5.30 (m, 2H), 5.04 (m, 4H), 4.25 (dd, J = 12.1, 5.7 Hz, 1H), 4.13 – 3.98 (m, 3H), 3.36 (dd, J = 13.3, 7.2 Hz, 1H), 3.17 (dd, J = 13.3, 2.5 Hz, 1H), 2.12 (s, 3H), 2.11 – 2.07 (2

overlapping singlets, 6H), 2.06 (s, 3H), 2.05 (s, 3H), 2.04 (2 overlapping singlets, 6H). ^{13}C-NMR (101 MHz, $CDCl_3$) δ ppm: 170.57, 169.97, 169.68, 169.53, 169.51, 92.82, 92.43, 70.03, 69.88, 69.86, 69.77, 69.70, 68.54, 68.26, 61.77, 50.94, 20.67, 20.65, 20.63, 20.61. ESI-MS positive ion mode: calculated m/z $[M+NH_4]^+$ 679.2318, found m/z: 679.2276 (error 6 ppm); calculated m/z $[M+Na]^+$ 684.1872, found m/z: 684.1825 (error 7 ppm).

Typical procedure for the synthesis of 6-amino-6-deoxy-trehalose (4)

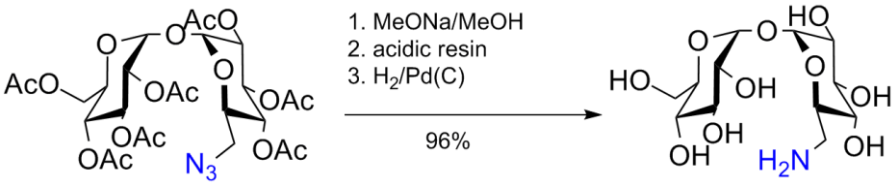

3 **4**

6-azido-6-deoxy-2,3,4,5,2',3',4',5',6'-O-acetyl trehalose (**3,** 11.81 g, 17.85 mmol) was dissolved in 450 mL of MeONa/MeOH (pH~9) and sonicated to assist dissolution. The reaction mixture was stirred at room temperature for 4h. The reaction progress was monitored by TLC/p-anisaldehyde stain (eluent: EtOAc/MeOH/H_2O=15/5/4). Ion exchange resin, DOWEX-50H, was added to reaction mixture; which was then stirred for 20 minutes (Note: DOWEX-50H might result in coloration of the reaction mixture, therefore, it is advisable to wash the resin with methanol prior to use). The resin was removed by filtration and the solvent evaporated to yield the crude produce, 6-azido-6-deoxy-trehalose as amorphous solid.

The crude 6-azido-6-deoxy-trehalose was dissolved in methanol. The reaction mixture was deoxygenated by bubbling nitrogen through the solution for 30 min.

Palladium on carbon (5% dispersion, 499 mg, 0.234 mmol) was added and hydrogen gas was bubbled through the solution for 20 h using a gas diffuser. After 20 h, nitrogen was bubbled through the solution to remove the remaining dissolved hydrogen. The Pd(C) was filtered off using Celite and the solvent was removed using a rotary evaporator to yield the title compound **4** (5.83 g, 95.8% yield). ^{1}H-NMR (400 MHz, D_2O) δ ppm: 5.10 – 4.97 (two doublets, J = 4.4 Hz, 2H), 3.73 – 3.54 (m, 6H), 3.49 (dd, J = 9.9, 3.8 Hz, 2H), 3.29 (t, J = 9.4 Hz, 1H), 3.16 (t, J= 9.4 Hz, 1H), 2.85 (dd, J = 13.8, 2.5 Hz, 1H), 2.59 (dd, J = 13.8, 7.8 Hz, 1H). ^{13}C-NMR (101 MHz, D_2O) δ ppm: 93.03, 92.91, 72.35, 72.30, 72.01, 71.26, 70.99, 70.89, 69.53, 60.35, 48.73, 41.32. ESI-MS positive ion mode: calculated m/z $[M+H]^+$ 342.14, found m/z: 342.10 (error 0.01%).

Synthesis of 6-methacrylamido-6-deoxy trehalose (5)

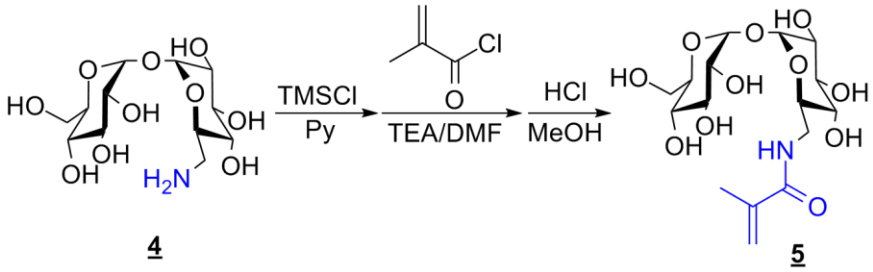

4 **5**

2-Deoxy-2-aminotrehalose (**4,** 3.74 g, 11.0 mmol) was suspended in 200 mL of dry pyridine. The reaction mixture was placed in an ice bath and trimethylsilyl chloride (TMSCl, 10.0 g, 92.0 mmol, 1.2 eq per -OH) was added using an addition funnel. The reaction mixture was allowed to slowly warm to room temperature, and the reaction was allowed to proceed overnight. The reaction mixture was cooled down to ca. 0 ºC and poured into 600 mL of ice-cold carbonate buffer (pH=9). The aqueous suspension was extracted with 3x150 mL of hexanes. The extracts were combined and washed with

water, followed by brine and finally dried over Na_2SO_4. The solid was filtered off and hexanes were removed under reduced pressure on a rotary evaporator. A white crystalline material was obtained upon evaporation and was then dried at 500 mTorr over P_2O_5 to yield 8.83 g (95.2%) of the 6-amino-6-deoxy-2,3,4,5,2′,3′,4′,5′,6′-nano-*O*-trimethylsilyl trehalose. ^{1}H-NMR (400 MHz, CD_2Cl_2) δ ppm: 4.87 – 4.74 (two overlapped doublets J = 3.2 Hz, 2H), 3.84 (td, J = 9.0, 3.2 Hz, 2H), 3.73 – 3.52 (m, 4H), 3.44 – 3.26 (m, 4H), 2.83 (dd, J = 13.2, 3.0 Hz, 1H), 2.73 (dd, J = 13.2, 5.4 Hz, 1H).

The TMS protected aminotrehalose (1.687 g, 1.993 mmol) was dissolved in 2 mL of DCM and 35 mL of DMF. This solution was cooled in an ice bath and triethylamine (0.55 mL, 0.40 g (d=0.726 g/mL), 3.9 mmol) was added. Freshly distilled methacryloyl chloride (0.22 mL, 0.24 g (d=1.07 g/mL) 2.3 mmol) dissolved in 5 mL of dry DCM was slowly (over ca. 10 min) added to the reaction mixture. The reaction was allowed to proceed at 0 ºC for 1H and, additionally, 3h at room temperature. The reaction mixture was then cooled in an ice bath and poured into 200 mL of the ice-cold carbonate buffer (pH~8) that contained ice. The resulting suspension was extracted with 3x30 mL of hexanes. The organic extracts were combined and washed with water, followed by brine and finally dried over Na_2SO_4 overnight. The solids were filtered off and the hexanes were removed under vacuum to yield a colorless oil. This oil was dissolved in 20 mL of dry methanol and placed in an ice bath. Next, 0.2 mL of a ~1.25M HCl solution in methanol was added and the reaction was allowed to warm to room temperature, and further stirred for additional 10 min. Methanol was removed under vacuum using a rotary evaporator (the rotovap water bath temperature was kept at 25 ^{o}C), yielding 0.765 g (93.3%) of the title compound (**5**) as a white solid foam. ^{1}H-NMR (400 MHz, CD_3OD) δ

ppm: 5.73 (s, 1H), 5.40-5.35 (m, J = 1.4 Hz, 1H), 5.09 (d, J = 3.8 Hz, 1H), 5.07 (d, J = 3.8 Hz, 1H), 3.94 (dt, J = 9.8, 4.8 Hz, 1H), 3.86 – 3.74 (m, 4H), 3.68 (dd, J = 11.9, 5.4 Hz, 1H), 3.55 (d, J = 4.8 Hz, 2H), 3.48 (td, J = 9.8, 3.8 Hz, 2H), 3.33 (dd, J = 9.8, 9.0 Hz, 1H), 3.17 (dd, J = 9.8, 9.0 Hz, 1H), 2.00 – 1.84 (m, 3H).

Synthesis of polytrehalose 6 (pMAT$_{51}$)

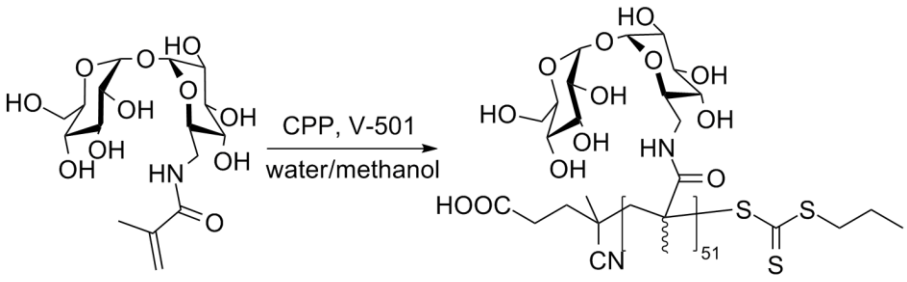

5 **6**, polytrehalose

6-Methacrylamido-6-deoxy trehalose (**5,** 0.765 g, 1.867 mmol, 65 eq) was dissolved in 7.000 mL of acetate buffer in D_2O. CPP (7.97 mg, $2.87x10^{-2}$ mmol, 1 eq) was dissolved in 645 µL of MeOD and added to the solution of **5**, followed by V-501 (0.805 mg, $2.87x10^{-3}$ mmol, 0.1 eq) in 244 µL of MeOD. Finally, 861 µL of MeOD was added to a final volume of 1.750 mL of MeOD in the mixture. The reaction flask was capped with a septum and connected to an NMR tube via cannula. The setup was deoxygenated by bubbling nitrogen through the solution for 45 min. At that time, 0.50 mL of reaction solution was transferred into the NMR tube. Polymerization was conducted in an NMR instrument at 70 °C while spinning the reaction tube at 20 Hz for 9 h. ^{1}H-NMR spectra were acquired at various time points. The rest of the reaction mixture was kept in the refrigerator overnight. Once the polymerization kinetics were established, the reaction mixture was removed from the refrigerator and deoxygenated by bubbling nitrogen through the solution for 45 min. The flask was placed in an oil bath pre-heated

to 70 ^{o}C. The reaction was allowed to proceed for 6 h to yield 77% monomer consumption (according to the established kinetics) and a targeted degree of polymerization of 50. The reaction was stopped by removing the septum and cooling the reaction mixture on ice. The reaction mixture was then transferred to a dialysis bag having a 3500 Da molecular weight cut-off. It was dialyzed against ultra-pure water acidified to pH 4-5 with HCl. Water changes were performed every 8-10 h. After 3 d of dialysis, the polymer solution was frozen and lyophilized to yield 490 mg of white, fluffy material. SEC (eluent: 1.0 wt% acetic acid/0.1 M Na_2SO_4, flow rate of 0.3 mL/min, light scattering detector (λ = 662 nm) and refractometer (λ = 658 nm)): M_n=21.0 kDa, dp_n=50.7~51, PDI=1.04. ^{1}H-NMR (400 MHz, D_2O) δ ppm: 5.76 – 5.28 (bs, 100H), 4.39 – 3.50 (m, 600H), 2.78 – 2.66 (bs, 2H), 2.53 – 0.68 (m, 264H).

Synthesis of diblock copolymers P1, P2 and P3

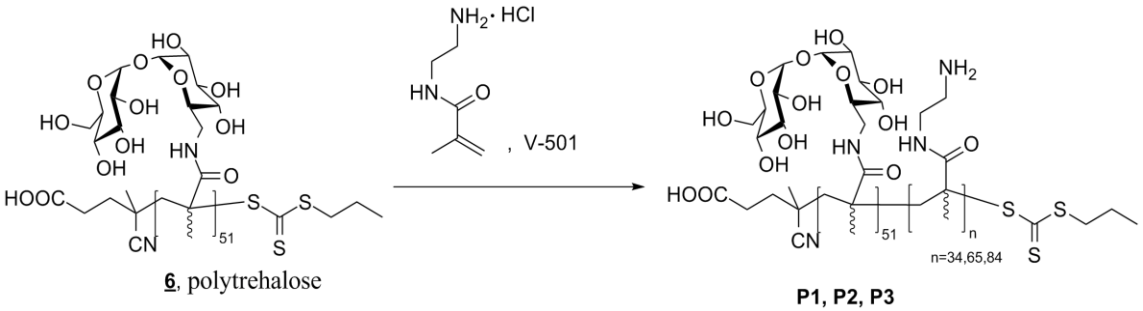

6, polytrehalose

P1, P2, P3

Polytrehalose (**6,** 327 mg, 1.56x10^{-2} mmol, 1.00 eq) was dissolved in 3.000 mL of acetate buffer and the resulting solution was placed in a flask that contained aminoethylmethacrylamide hydrochloride (AEMA·HCl, 311 mg, 1.89 mmol, 121 eq). To this, 0.780 mL of a solution containing V-501 radical initiator (0.44 mg, 1.56x10^{-3} mmol, 0.10 eq) was added and the flask was capped with a septum. The solution was

deoxygenated by bubbling nitrogen through the reaction solution for 45 minutes. The flask was then placed in an oil bath preheated to 70 ^{o}C for polymerization. Two 1.25 mL samples were taken with a syringe at 30 min (**P1**) and 60 min (**P2**) of reaction time. Each sample was sprayed into a vial which was immediately cooled on ice. After 90 min (**P3**), the reaction was stopped by removing the septum and placing the reaction flask on ice. All three samples were placed in dialysis bags having a 3500 Da molecular weight cut-off and dialyzed against 3x4L of 0.5 M NaCl solution, followed by 3x4L 0.1 M NaCl and finally 6x4L of ultra-pure water. All dialysis media were acidified with HCl to pH 4-5. Upon completion of dialysis, polymer solutions were lyophilized to yield white, fluffy powders.

MAT_{51}-*b*-$AEMA_{34}$(**P1**), 113 mg. SEC (eluent: 1.0 wt% acetic acid/0.1 M Na_2SO_4, flow rate of 0.3 mL/min, light scattering detector (λ = 662 nm) and refractometer (λ = 658 nm)): M_n=23.4 kDa, PDI=1.04.

MAT_{51}-*b*-$AEMA_{65}$(**P2**), 141 mg. SEC (eluent: 1.0 wt% acetic acid/0.1 M Na_2SO_4, flow rate of 0.3 mL/min, light scattering detector (λ = 662 nm) and refractometer (λ = 658 nm)): M_n=29.4 kDa, PDI=1.05.

MAT_{51}-*b*-$AEMA_{84}$(**P3**), 181 mg. SEC (eluent: 1.0 wt% acetic acid/0.1 M Na_2SO_4, flow rate of 0.3 mL/min, light scattering detector (λ = 662 nm) and refractometer (λ = 658 nm): M_n=31.8 kDa, PDI=1.06.

Synthesis of MAT_{51}-*b*-($AEMA_{33}$-*s*-AEMA-$fluorescein_1$) (P1-FITC)

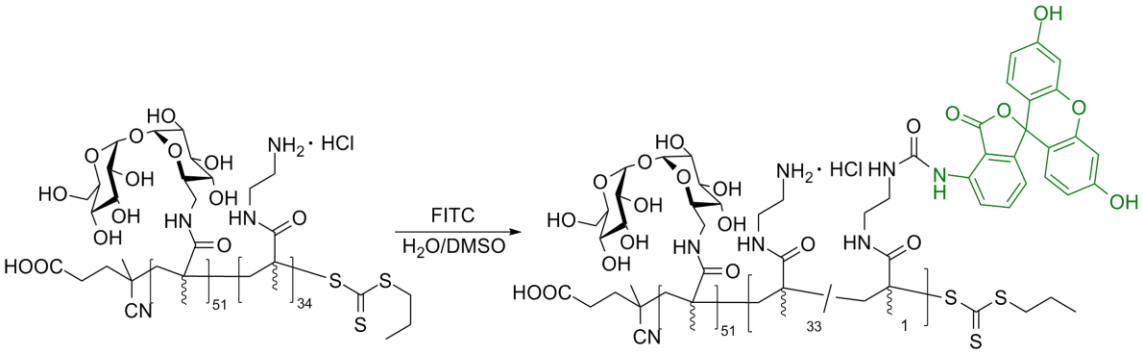

P1 (MAT_{51}-*b*-$AEMA_{34}$·34HCl, 12.0 mg, 34 eq) was dissolved in 850 µL of 0.1 M $NaHCO_3$ which was previously deoxygenated (bubbling N_2 though the solution for 30 min). The flask was placed in an ice bath and 20.0 µL of DMSO solution containing fluorescein isothiocyanate (FITC, 0.18 mg, 1 eq) was added with a pipette. Reaction mixture was allowed to slowly reach RT. After 12 h of stirring the reaction mixture was placed in a dialysis bag (3500 Da molecular weight cut-off) and dialyzed for 8 h against each of the following aqueous solutions: 0.1 M NaCl (4 L x 2), 0.07 M NaCl (4L), 0.03 M NaCl (4L), H_2O (4 x 3). The content of the dialysis bag was then transferred into a vial and lyophilized, yielding **P1-FITC** (11.1 mg (91.1%) as a bright yellow powder.

Synthesis and in situ analysis of the kinetics of polymerization of 2-methacrylamido-2-deoxy-trehalose

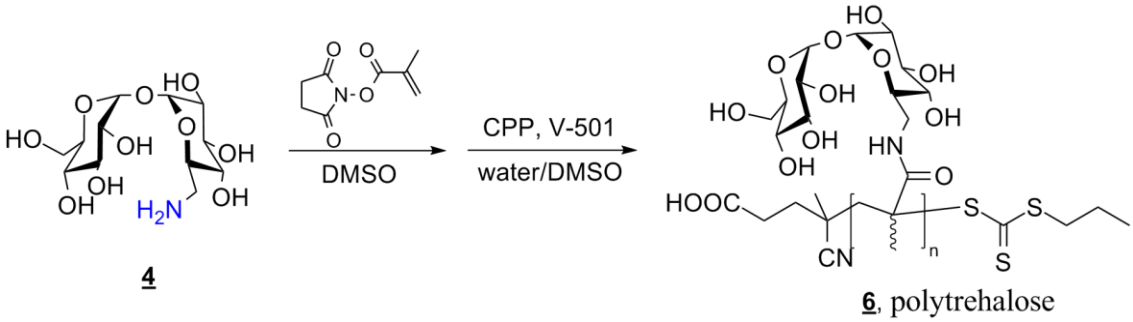

4 **6**, polytrehalose

2-amino-2-deoxytrehalose (**4,** 58.6 mg, 0.172 mmol, 1.20 eq) was dissolved in 326 μL of D_2O and N-(methacryloyloxy)succinimide (26.2 mg, 0.143 mmol, 1.00 eq) in 326 μL of d_6-DMSO was added. The reaction was allowed to proceed at room temperature for 18 h. Acetic acid (1.72 mg, 0.029 mmol) was added to neutralize the excess of **4**, followed by 77 μL of acetate buffer in D_2O and 28 μL of d_6-DMSO. Finally, CPP (0.580 mg, 2.09×10^{-3} mmol, 1/65 eq) in 29 μL of d_6-DMSO and V-501 (0.123 mg, 4.39×10^{-4} mmol, 1/325 eq) in 20 μL of d_6-DMSO were added. The reaction flask was capped with a septum and connected to an NMR tube with a cannula. The setup was deoxygenated by bubbling nitrogen through the reaction solution for 45 min. About 500 μL of the reaction mixture was transferred into an NMR tube via cannula, and polymerization was conducted in an NMR instrument at 70 °C. ^{1}H-NMR spectra were obtained at various time points. Monomer consumption rate was assessed by the integration of a signal corresponding to vinyl hydrogen at 5.58-5.50 ppm and normalizing that value against signal corresponding to anomeric hydrogens.

Evaluation of NHS involvement in RAFT polymerization of 6-methacrylamido-6-deoxy-trehalose 5

2-Amino-2-deoxytrehalose (**4,** 1.005 g, 2.945 mmol, 1.1 eq) was dissolved in 2.378 mL of D_2O and 1.000 mL of d_6-DMSO was added. N-(Methacryloyloxy)succinimide (0.490 g, 2.66 mmol, 1.0 eq) in 0.378 mL of d_6-DMSO was added to solution of **4** dropwise. Some precipitate formation was observed, which was soon dissolved. The reaction was allowed to proceed at room temperature for 17 h. The reaction appeared incomplete according to ^{1}H-NMR and additional 2-amino-2-

deoxytrehalose (**4,** 0.103 g, 0.302 mmol, 0.1 eq) was added. The reaction was allowed to proceed at room temperature for 15 h. Completion of the reaction was confirmed with ^{1}H-NMR. Acetic acid (32 μL, 34 mg, 0.56 mmol) was added to neutralize the excess of **4**, followed by 2.378 mL of D_2O, 0.500 mL of acetate buffer in D_2O and 2.676 μL of d_6-DMSO. Finally, CPP (10.9 mg, 3.93×10^{-2} mmol) in 206 μL of d_6-DMSO and V-501 (1.15mg, 4.10×10^{-3} mmol) in 92 μL of d_6-DMSO were added, and the reaction mixture was deoxygenated by bubbling nitrogen through it for 45 min. The reaction flask was placed in an oil bath pre-heated to 70 ºC and stirred for 6 h. The mixture was allowed to cool to room temperature and 0.5 mL of the reaction mixture was taken for NMR analysis. An additional portion of V-501 (1.15 mg, 4.10×10^{-3} mmol) was then added to the reaction mixture, deoxygenation was repeated and the reaction was allowed to proceed for an additional 6 h at 70 ºC. The reaction was stopped by removing the septum and cooling the reaction mixture in an ice-bath.

Comparison of the 2-methacrylamido-2-deoxyglucose polymerization via RAFT in the presence and absence of NHS

1. Polymerization of 2-methacrylamido-2-deoxyglucose in the absence of NHS.

A solution of 2-methacrylamido-2-deoxy-glucose in D_2O (696 μL at c=0.5747M, 0.400 mol) was placed in a 10 ml round bottom flask. Then solutions of CPP in d_4-MeOD (100 μL, c=6.55 mM, 0.655 mmol), V-501 in d_4-MeOD (100 μL, c=0.664 mM, 6.64×10^{-2} mmol) were added, followed by 12 μL of acetate buffer in D_2O and *92 μL of D_2O*. The reaction flask was capped with a septum and connected to an NMR tube via cannula. The setup was deoxygenated by bubbling nitrogen through the solution for 45 min. At that

time, 0.50 mL of reaction solution was transferred into the NMR tube. Polymerization was conducted in an NMR instrument at 70 °C while spinning the reaction tube at 20 Hz for 12 h. ^{1}H-NMR spectra were acquired at various time points.

2. Polymerization of 2-methacrylamido-2-deoxyglucose in the presence of 1 eq of NHS.

A solution of 2-methacrylamido-2-deoxy-glucose in D_2O (696 μL at c=0.5747M, 0.400 mol) was placed in a 10 ml round bottom flask. Then solutions of CPP in d_4-MeOD (100 μL, c=6.55 mM, 0.655 mmol), V-501 in d_4-MeOD (100 μL, c=0.664 mM, 6.64×10^{-2} mmol) were added, followed by 12 μL of acetate buffer in D_2O and finally *NHS solution* in D_2O (92 μL, c=4.339 M, 0.400 mol). The reaction flask was capped with a septum and connected to an NMR tube via cannula. The setup was deoxygenated by bubbling nitrogen through the solution for 45 min. At that time, 0.50 mL of reaction solution was transferred into the NMR tube. Polymerization was conducted in an NMR instrument at 70 °C while spinning the reaction tube at 20 Hz for 12 h. ^{1}H-NMR spectra were acquired at various time points.

Evaluation of the interaction between serum proteins and polytrehalose by quartz crystal microbalance

The sensors were cleaned prior to experiment with UV light under ozone, then washed first with a cleaning solution (water/30% H_2O_2/ammonia(conc.) 5/1/1) followed by ultrapure water and finally dried with air. The experiment was performed at a flow rate of 0.2 mL/min. The sensor was first equilibrated with ultrapure water and the experiment was started by applying the polytrehalose solution in water at concentration 20 μg/mL (time point 1, Fig. 3.11). A water wash (time point 2) was performed to

remove any unbound polymer. The change in frequency of -17 Hz indicates that polytrehalose was bound to the gold surface, likely by the trithiocarbonate end group.[16] FBS was applied as a solution in water in three steps with increasing concentration (0.1% - time point 3, 1.0% - time point 4, and 10% - time point 5). Finally, water was applied to remove any unbound proteins (time point 6). The difference of -15 Hz between time points 2 and 6 indicates that protein adsorption to polytrehalose takes place.

Polyplex formulation with P1, P2, P3 and siRNA

To a 2 μM solution of siRNA in RNase-free an equal volume of polymer solution at appropriate concentration was added via a pipette. The solution was mixed well by injecting/ejecting the solution with a pipette several times. Polyplexes were allowed to incubate undisturbed at room temperature for 1 h prior to transfection.

Polyplex lyophilization

Polyplexes were prepared in 1-mL microfuge tubes according to the procedure described above using 35μL of a 2 μM siRNA solution and 35 μL of the corresponding polymer solution. Once formed, polyplexes were allowed to incubate for 1h at room temperature. Microfuge tubes containing solutions of polyplexes were placed in a freezer at -27 $^{\circ}$C for ca. 2 h. Lyophilization was performed by placing the microfuge tubes in a 1L lyophilization jar at room temperature and 10-30 mTorr vacuum for 24 h. To re-dissolve polyplexes, 70 μL of RNase free water was added to lyophilized material and solution was allowed to incubate at room temperature for 1h.

Gel electrophoresis of polyplexes

A 0.6% w/w agarose gel was prepared by dissolving 0.3 g of agarose in 50 mL of TAE buffer while heating. The resulting agarose solution was allowed to cool to ca. 40-45 ^{o}C and 3 μL of ethidium bromide solution was added.

The polyplex solutions (20 μL) were prepared by following the protocol for polyplex formulation described above. Loading buffer (2 μL of Blue juice^{TM}) was added to each sample. The polyplex solutions (10 μL) were each loaded into the wells of the gel, and electrophoresis was performed at 60V for 45 min. Images of gels are obtained using 312 nm UV light to detect ethidium bromide.

Dynamic light scattering measurements

Polyplexes were prepared according to the standard protocol using 20 μL of 2 μM siRNA solution and 20 μL of polymer P1, P2 or P3 solution of appropriate concentration to yield polyplexes at N/P ratios 5, 10 and 20. After 1 h incubation at room temperature, polyplex solutions were diluted with water, OptiMEM, or DMEM with 10% serum to a final siRNA concentration of 400 nM. Solutions were transferred into cuvettes and particle sizes were measured at 25 ºC using 173º detection angle at various time points.

Evaluation of phase transitions of the polytrehalose and trehalose solutions with differential scanning calorimetry

Aqueous solutions of trehalose (0.58 mol%, 1.30 mol%, 2.21 mol%, 3.39 mol%, and 5.00 mol%) and polytrehalose (0.58 mol%, 1.30 mol%, 2.85 mol%, 3.39 mol%, 5.00 mol%, and 6.19 mol%) were prepared by weight using ultrapure water and trehalose

dihydrate (obtained from Fisher Scientific, used as received) and polytrehalose correspondingly. Solutions were incubated for 12 h at 40 ºC in closed containers to ensure the complete dissolution of the materials. Solutions were cooled to room temperature and 7-12 mg samples were immediately transferred into aluminum pans and hermetically sealed. An empty aluminum pan with a lid was used as a reference. Heating and cooling was done at a 5 ºC/min rate. Isothermal conditioning was applied for 10 min at both highest temperature (70 ºC) and lowest temperature (-65 ºC). The data recorded for the second heat/cool/heat cycle and analyzed using TA Instruments Universal Analysis 2000 software, version 4.5A (Waters Corporation, Milford, MA).

3.2.2 Cell culture experiments

Diethylpyrocarbonate (DEPC)-treated water for experiments involving the use of siRNA was obtained from Fisher Scientific (Pittsburgh, PA). Propidium iodide, Lipofectamine™2000, UltraPure™ Agarose-1000, trypsin, (3-(4,5-dimethylthiazol-2-yl)-2,5-diphenyl tetrazolium bromide (MTT), phosphate buffer saline (PBS), modified essential minimum eagle medium (Opti-MEM®) and Dulbecco's modified eagle medium (DMEM) were purchased from Invitrogen, Inc. (Carlsbad, CA). CellScrub™ Buffer was obtained from Genlantin, Inc. (San Diego, CA). Bovine albumin was purchased from Sigma-Aldrich (St. Louis, MO). The Luciferase Assay Kit and cell lysis buffer were obtained from Promega (Madison, WI). Bio-Rad DC Protein Assay Reagent A, Reagent B and Reagent S were obtained from Bio-Rad Laboratories, Inc. (Hercules, CA). Anti luc2 luciferase siRNA (sense strand sequence 5′-GGACGAGGACGAGCACUUCUU-3′;

antisense strand sequence 3′-UUCCUGCUCCUGCUCGUGAAG-5′) and Cy5-labeled anti Luc2 siRNA (sense strand sequence 5′-GGACGAGGACGAGCACUUCUU-Cy5-3′; antisense strand sequence 3′-UUCCUGCUCCUGCUCGUGAAG-5′) was purchased from Integrated DNA Technologies (Coralville, Iowa). Scrambled siRNA was obtained from Dharmacon, Inc (Lafayette, CO). Luciferase expressing human glioblastoma cells U-87 MG-luc2 (U-87_luc2) were obtained from Caliper LifeSciences, Inc. (Mountain View, CA). Luciferase-expressing glioblastoma cells (U-87_luc2) were used for target gene (luciferase) down-reulgation efficiency experiments, cellular uptake studies, and MTT assays for cell viability. The cells were grown in complete DMEM [supplemented with 10% (v:v) fetal bovine serum, 1% antibiotic-antimycotic solution (containing penicillin, streptomycin, and amphotericin B)] at 37 ºC and 5% CO_2.

Cellular uptake measurement by flow cytometry

Flow cytometry was performed to examine the cellular uptake of fluorescently-labeled siRNA within various formulations at 3 h post-transfection. In general, luciferase-expressing U-87_luc2 glioblastoma cells were seeded 300,000/well in 6-well plates 24 h prior to transfection. To transfect, 66 μL of polyplex solutions were prepared following the protocol described above. Each polyplex solution was pipetted into 1584 μL of pre-warmed Opti-MEM to yield the final transfection solution, of which 500 μL was added to each well. After 3 h, the medium was removed and cells were washed with 500 μL/well CellScrub™ Buffer for 15 min at room temperature. The CellScrub™ Buffer was then aspirated and cells were exposed to trypsin (0.05% (w/v), 500 μL/well) for 3 min to provide detachment from the plate, then complete DMEM (500 μL/well) was applied to inhibit trypsin. The cell suspension was collected and centrifuged at 1000 rpm for 10 min

at 4^{o}C. The supernatant was removed and cells were twice washed with 0.5 mL PBS and centrifuged to remove the extracellular polyplexes. Finally, 1 mL PBS was added and the suspensions were kept on ice prior to flow cytometry analysis. Propidium iodide (1.0 mg/mL, 2.5 μL) was added prior to the analysis. The flow cytometer (FACSCalibur, Becton Dickinson, San Jose, CA) equipped with a helium-neon laser to excite Cy5 at 633 nm was used to count twenty thousand events for each sample. The threshold fluorescence level was defined by manually adjusting the positive region such that <1% of negative control cells were positive for fluorescence. Each treatment was performed in triplicate.

Luciferase assay and protein assay

Luciferase-expressing glioblastoma cells (U-87_luc2) were seeded at 50,000 cells/well in 24-well plates 24 h prior to transfection. The anti-luciferase (Luc2) siRNA, control (siCon) siRNA, and polymer stock solutions were diluted with RNase-free water, and polyplexes were prepared following the protocol. The polyplex solution was diluted to a desired siRNA concentration (1 nM, 3 nM, 10 nM, 30 nM, 100 nM) with pre-warmed Opti-MEM or DMEM with 10% FBS to yield transfection solutions. Cells were washed with PBS before the addition of 200 μl of the transfection solution. The formation of siRNA-containing lipoplexes using Lipofectamine2000 was performed according to the manufacturer's protocol.

The cells were incubated with polyplex/lipoplex solutions for 4 h before complete DMEM was added. After 48 h, the cells were washed with 500 μL PBS and treated with 1x cell lysis buffer for 15 min at room temperature. Aliquots (5 μl) of cell lysate were examined on 96-well plates with a luminometer for luciferase activity over 10 s with 100

μL of luciferase substrate added in each well immediately prior to relative light unit (RLU) determination. The average of duplicate fluorescence measurements was utilized for calculation.

The amount of protein (mg) in cell lysates was calculated using a standard curve generated with bovine serum albumin by following the protocol included in Bio-Rad DC protein assay kit. The relative light unit (RLU)/mg protein was then calculated and averaged across replicate wells for comparison. The protein and luciferase levels of non-transfected cells were used for normalizing the data and calculating the extent of gene knockdown. Each treatment was tested in triplicate in 24-well plates.

Assessment of toxicity via MTT assay

MTT reagent (3-(4,5-dimethylthiazol-2-yl)-2,5-diphenyltetrazolium bromide) was used to estimate the cytotoxicty of the formulations. MTT can be reduced to purple formazan in living cells under the catalysis of mitochondrial reductase. Typically, U-87_luc2 glioblastoma cells were seeded at 50,000 cells/well in 24-well plates 24 h prior to transfection. The polyplexes were formed following the procedure described above. Transfection medium (200 μL) was added to each well; 4 h later, complete DMEM was added at a concentration of 1 mL/well. Twenty four hours later, the medium was aspirated and the cells were washed with PBS (500 μL/well). Serum-containing DMEM (1 mL) with 0.5 mg/mL of MTT was added to each well and the cells were incubated for 1 h. The medium was then replaced with 600 μL of DMSO for 15 min at room temperature. A 200 μL aliquot of the medium was transferred to a well of a 96-well plate for analysis by colorimeter with wavelength at 570 nm. Samples of non-transfected cells were used for the normalization.

Live cell confocal microscopy

Live cell imaging experiments were performed at 1, 3, 6, 12, 24, 36 and 48 h post transfection. The cells were plated in 35 mm glass bottom dishes with coverslip number 1.5 (MatTek Corporation, Ashland, MA). The cells were plated at a density of 80000 cells/dish at 24 hours prior to transfection in 4 mL DMEM supplemented with 10 % FBS and 1 % AB-AM and incubated at 37 ^{o}C and 5 % CO_2. Polyplexes were formulated by adding 15 µL of FITC-polymer P1 at 10 N/P ratio to 15 µL of Cy5-siRNA at 2 µM in DEPC treated water and then incubated for 1 h at room temperature. Prior to transfection the polyplex solution was diluted by adding 270 µL of OptiMEM® to make a final volume of 300 µL (final siRNA concentration of 100 nM). The cells were transfected by adding 300 µL/dish of diluted polyplex solution. The cells were allowed to transfect for 3 h at 37 ºC and 5 % CO_2. For the timepoints of 1 and 3 h, the cells were washed with PBS and 4 mL of phenol red free DMEM was added to each dish and imaged directly. For time points 6, 12, 24, 36 and 48 h, the cells were washed with PBS and 4 mL of 10 % FBS DMEM was added to the dish and further incubated for subsequent time points prior to imaging. In addition, for time points 36 and 48 h, the media was replaced with 4 mL of fresh 10 % FBS-containing DMEM at 24 hours post transfection. The controls were: (1) cells only where the cells were not transfected, (2) FITC only where the cells were transfected with polyplexes where the only the polymer was labeled with FITC, (3) Cy5 only control cells were transfected with polyplexes where only the siRNA was labeled with Cy5.

Olympus FluoView FV1000 inverted confocal microscope was used for imaging. The image size was 1024*1024 pixels (12 bits). Sampling speed was 2.0 µs/pixel. The oil

immersion objective used was PLAPON 60X O NA:1.42. The fluorophores used were FITC (fluorescein isothiocyanate) and Cy5 (Cyanine 5). The polymer was labeled with FITC in our laboratory as described above and the Cy5 labeled siRNA was ordered from Integrated DNA Technologies (Coralville, Iowa). The FITC fluorophore was excited by 488 nm laser and the Cy5 fluorophore was excited by 633 nm laser and all the images were acquired at the same laser settings and analyzed using Olympus FLUOVIEW software.

3.3 Discussion

To prepare polytrehalose, we employed reversible addition-fragmentation chain transfer (RAFT) polymerization because it yields polymers with low polydispersity index, provides precise control over molecular weight, tolerates the presence of many reactive functional groups, and allows for end-group functionalization and synthesis of multiblock polymers.[17-19] Moreover, this technique allows for polymerization from surfaces[20] and can potentially be used to grow polytrehalose directly from the surfaces of nanoparticles or macromolecules such as proteins.

Our development of a synthetic scheme to yield a functionalized, trehalose-containing monomer was guided by two criteria: the size of the linker connecting trehalose and a polymerizable functionality should be minimized, and the synthesis should avoid or minimize the use of lengthy and scale-limiting purification procedures. However, the C_2 symmetry of trehalose (**1**, Fig. 3.2) poses an inherent difficulty in yielding the desired asymmetrically-functionalized monomer. The most successful

attempt to date in breaking this symmetry was performed using kinetic control in acidic deprotection of 6,6´-bis(*tert*-butyldiphenyl)trehalose.[21] For our study, an approach similar to that previously published by Miura et al. (Fig. 3.2) was taken.[11] This route was found to be more practical in avoiding numerous protection/deprotection steps. Thus, triphenylphosphine-iodine was used to produce a mixture of di-iodo-, mono-iodo-, and unmodified trehalose. This mixture was then acetylated and the desired per-acetylated mono-iodo-trehalose **2** was obtained after column chromatography in 24% yield. However, the steps that followed were carried out in near quantitative yields; we substituted iodide for azide yielding **3** (95%), which was further deprotected and reduced affording 6-amino-6-deoxytrehalose (**4,** 96%). Conversion of **4** was performed via addition of methacryloyl chloride yielding the final monomer structure, 6-methacrylamido-6-deoxy trehalose (**5**) in 93% yield.

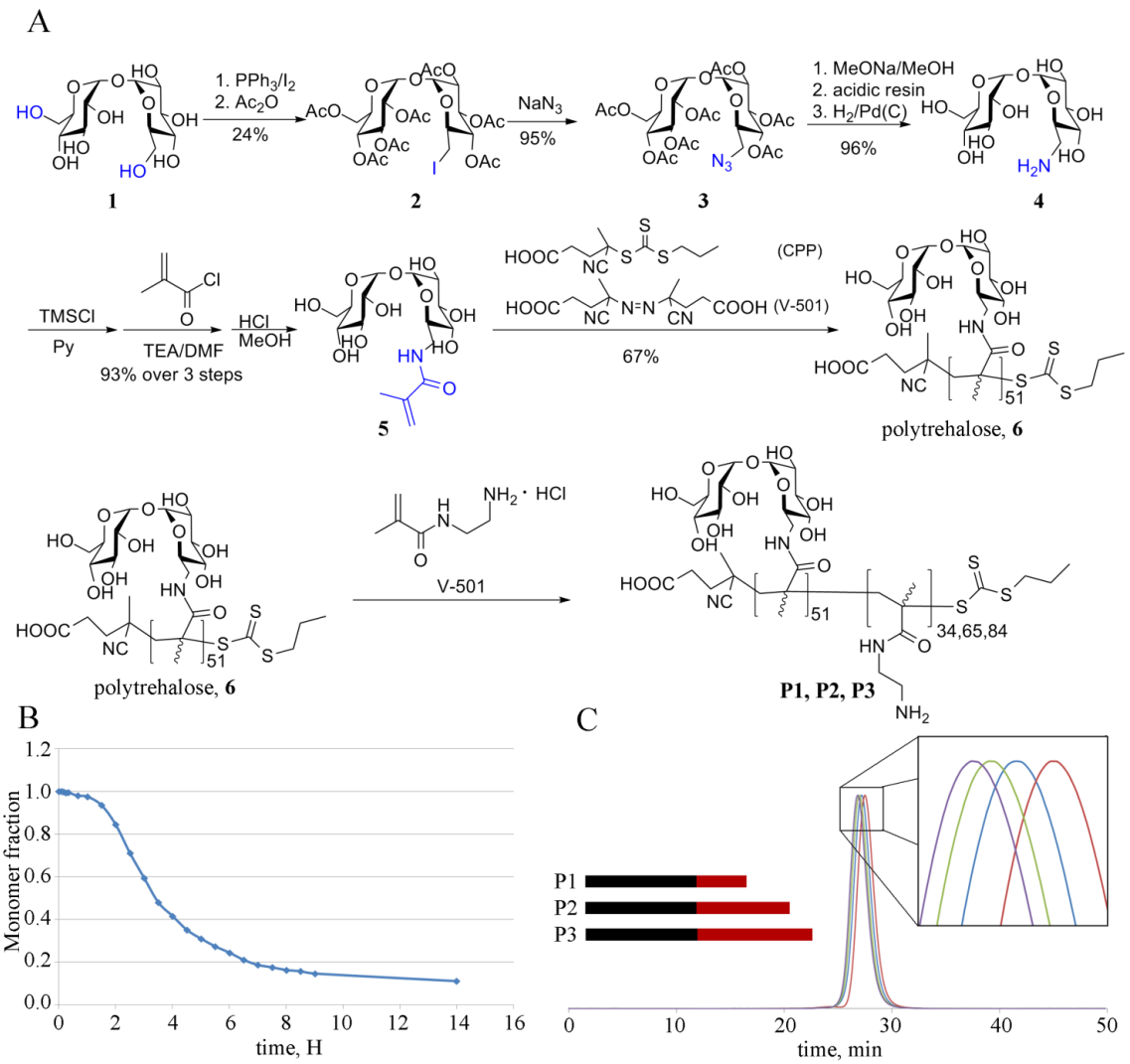

Figure 3.2. A. Synthesis of 2-methacrylamido-2-deoxy-trehalose (**5**), polytrehalose (**6**), and diblock polymers (**P1, P2, P3**). **B.** Monomer consumption based on the intensity decrease of the vinyl proton in ^{1}H-NMR experiment in the RAFT polymerization of **5**.**C.** SEC traces of polytrehalose (red), P1 (blue), P2 (green) and P3 (purple). Schematic blocks represent the relative trehalose- and amine- containing blocks in polymers P1, P2 and P3.

In our initial attempt in order to avoid additional purification steps, conversion of trehaloseamine to the corresponding methacrylamide was done *in situ* with the polymerization. Reaction with N-hydroxysuccinimide methacrylate proceeded smoothly at room temperature in the DMSO/water mixture (Fig. 3.3). Upon reaction completion,

the reaction mixture was diluted with acetate buffer, chain transfer agent (CPP) and the initiator (V-501) were added and the reaction mixture was deoxygenated. However, the attempted polymerization slowed down, reaching maximum conversion of ~35% (Fig. 3.4).

By carefully analyzing ^{1}H-NMR it was noted that the signal corresponding to N-hydroxysuccinimide (NHS) ethylene protons at 2.57 ppm was decreasing and new peaks at 2.11-2.31 ppm appeared (Fig. 3.5). It is also known that polymerization of NHS-methacrylate by RAFT results in the unusually high polydispersity index.[22] This and the results of NMR analysis suggest a role of NHS in a side reaction that interferes with polymerization and causes low conversion of monomer.

To confirm the influence of NHS on the RAFT process two control polymerizations were conducted using a more readily accessible carbohydrate monomer – 2-methacrylamido-2-deoxy-glucose (MAG). Polymerizations were conducted in identical conditions in the absence of NHS and in the presence of 1 eq of NHS (per monomer).

Drastic difference in monomer consumption was observed. Thus, 50% of MAG are consumed in 2 h in the absence of NHS; however, the monomer consumption did not reach 50% even after 12 h in the presence of NHS (Fig. 3.6). The difference in consumption rates can be numerically expressed by calculating reaction rate constants. Assuming pseudo first-order kinetics that are typical for RAFT polymerizations,[23] the constants based on 1-4 h reaction times are 0.5112 h^{-1} (without NHS) and 0.0638 h^{-1}(with NHS) which corresponds to $T_{½}$=1.4 h and $T_{½}$=10.9 h respectively. It is also important to

note that in the presence of NHS polymerization did not only proceed slowly but also slowed down.

On a large scale it may be possible to exploit the difference in solubility between NHS and the carbohydrate derivative, 6-methacrylamido-6-deoxy-trehalose **5**, in acetone to achieve the desired NHS removal prior to polymerization. However, on a small laboratory scale, NHS removal proved to be troublesome, and it was more convenient to follow an alternative route using TMS protecting groups as described above.

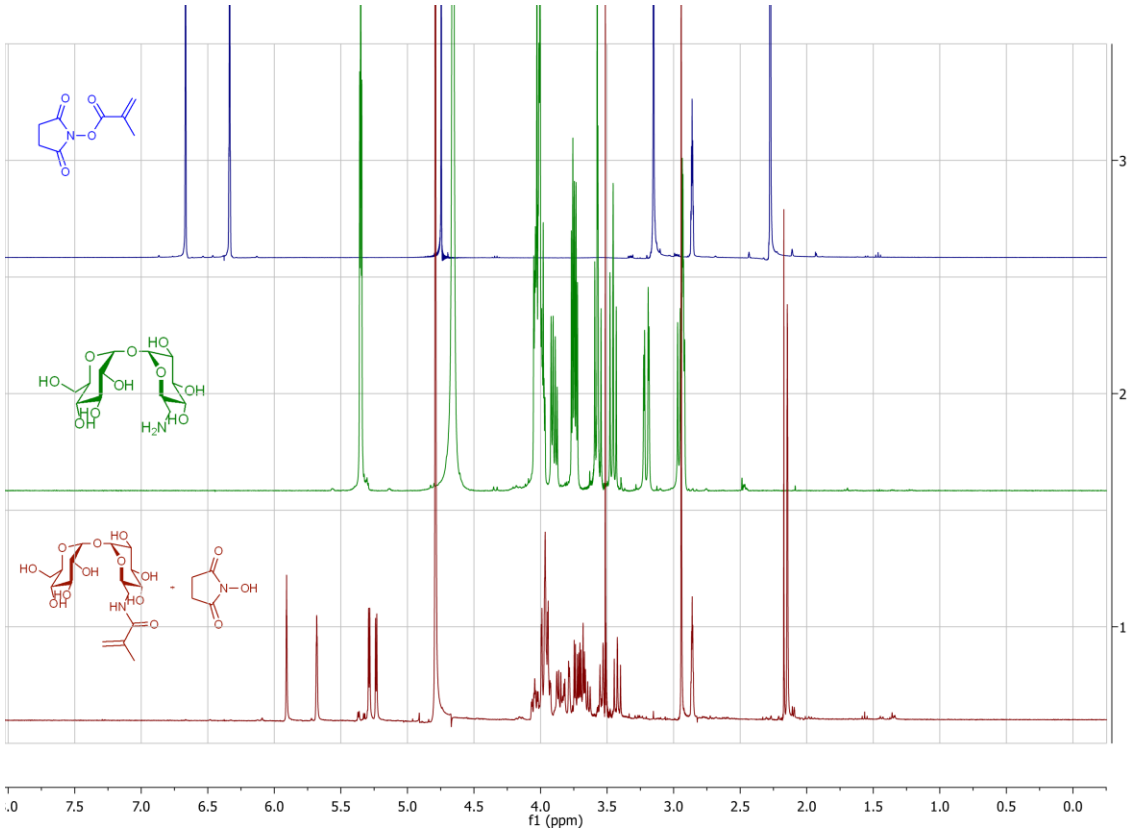

Figure 3.3 ^{1}H-NMR spectra of NHS methacrylate (top), trehaloseamine (middle), and reaction mixture between them at 12 h timepoint (bottom). All NMR were obtained in d_6-DMSO/D_2O (v/v=1/1) mixture.

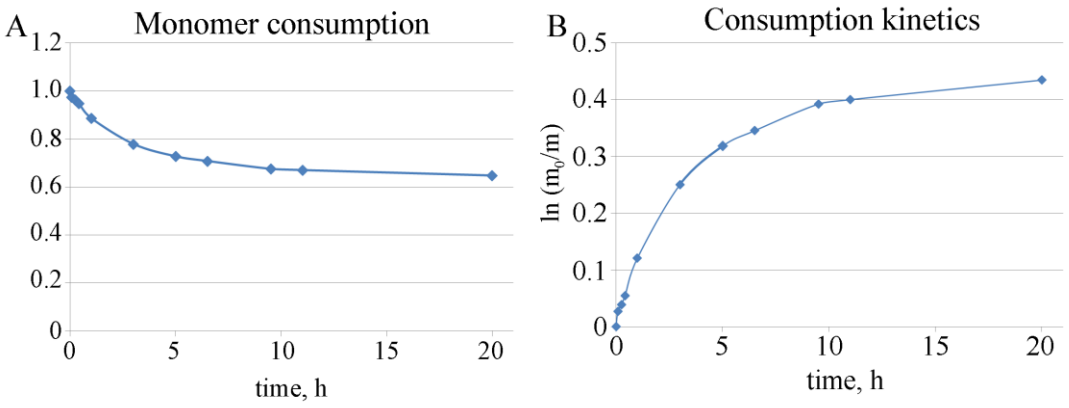

Figure 3.4. RAFT polymerization of methacrylamidotrehalose in the presence of NHS. **A.** Monomer consumption analyzed by ^{1}H-NMR. **B.** Consumption kinetics, assuming first order kinetics.

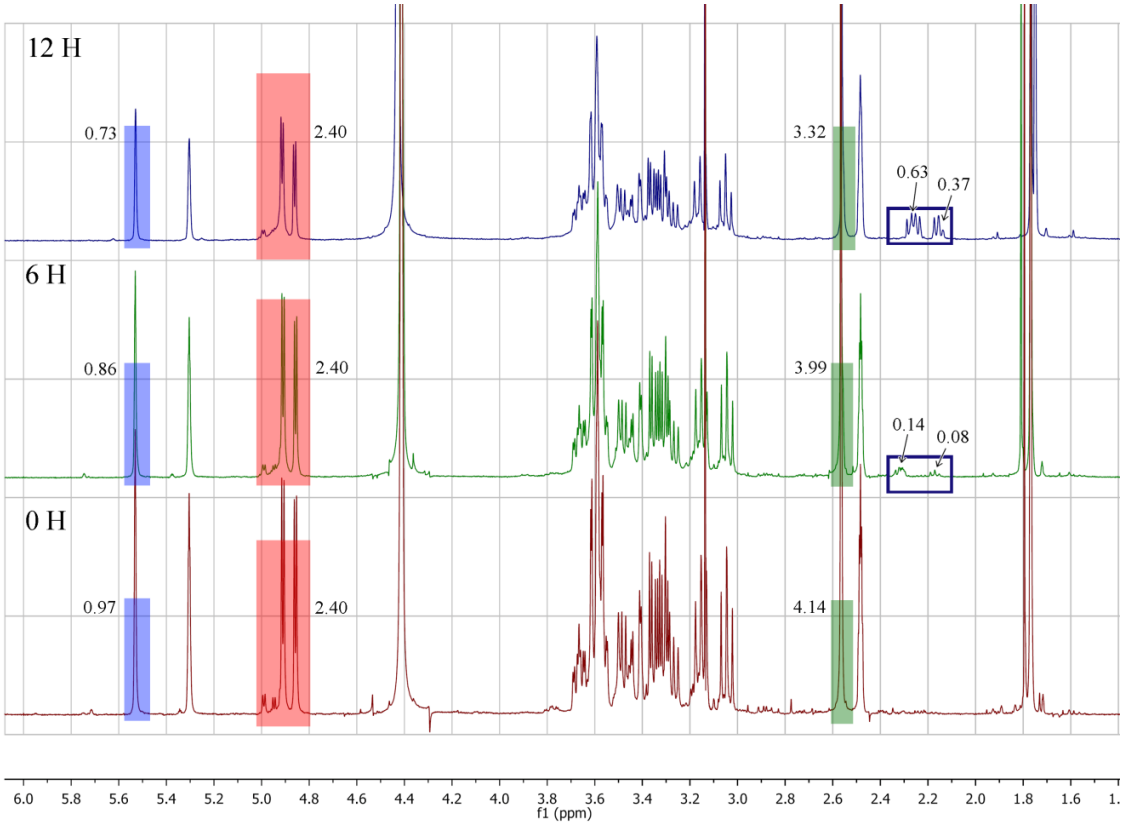

Figure 3.5. ^{1}H-NMR methacrylamidotrehalose polymerization in the presence of NHS.

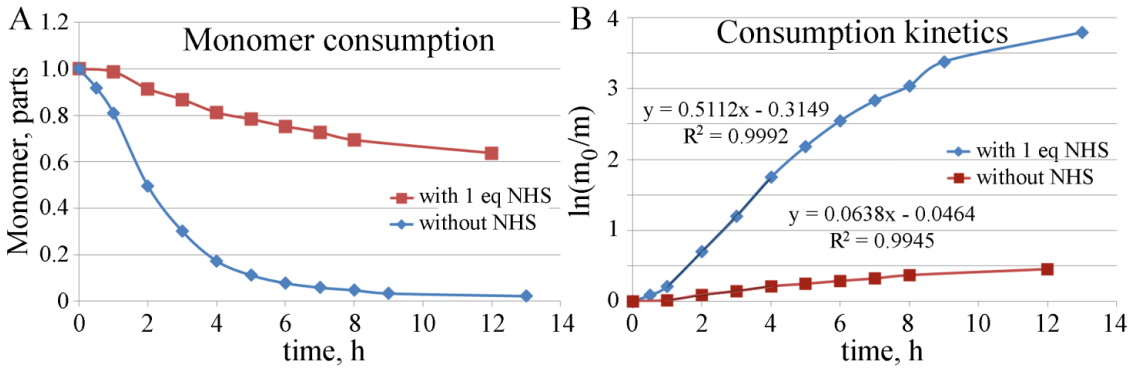

Figure 3.6. Comparison between MAG polymerization in the absence and presence of NHS. **A.** Monomer consumption rate and **B.** monomer kinetics. A significant influence of NHS on the RAFT polymerization was observed. Monomer consumption half-lives based on the rate constants between 1-4 h were calculated to be $T_{½}$=1.4 h in the absence and $T_{½}$=10.9 h in the presence of NHS.

Polymer syntheses were conducted via RAFT polymerization using 4-cyano-4-propyltrithiocarbonylpentanoic (CPP) or trithiocarbonyl-terminated polytrehalose as the chain transfer agent and 4,4'-azobis(4-cyanovaleric acid) (V-501) as the initiator. Kinetics were established in a water-methanol mixture buffered with AcOH/AcONa and used to create polytrehalose **6** and polytrehalose/polyamine-containing diblock polymers P1, P2, and P3.

The aforementioned lyoprotective properties of trehalose have been largely attributed to its ability to decrease water crystallization around biological membranes and proteins and to decrease the energy associated with phase transitions of H_2O (crystallization and melting).[24] To examine whether polytrehalose retained this property, we analyzed polytrehalose solutions of various concentrations via differential scanning calorimetry (DSC). Polytrehalose was similar to trehalose in depressing both the heat of ice melting (H_m) and the heat of water crystallization (H_{cr}), up to a concentration of 2.2

mol%, and was even more efficient at higher concentrations (Fig. 3.8). At 5 mole percent, polytrehalose lowers H_m by an additional 24 J/g and H_{cr} by an additional 35 J/g compared

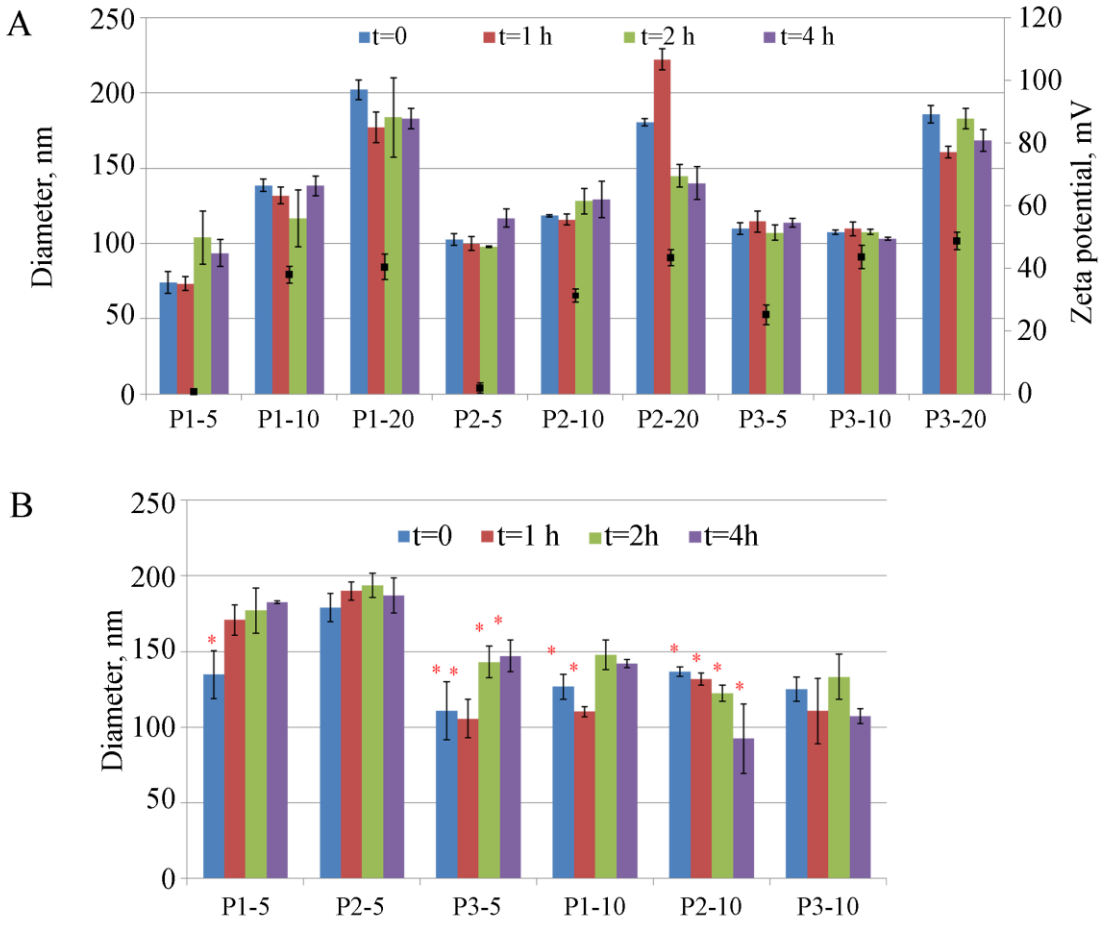

Figure 3.7. A. Hydrodynamic diameters based on the scattering intensity and ζ-potentials of polyplexes in water over the period of 4 h. Labels signify "polymer_name-N/P" **B.** Hydrodynamic diameters based on the scattering intensity of polyplexes after lyophilization and resuspension in water. A star (*) denotes cases in which second population of larger particles was present (500-1000 nm). Labels signify "polymer-N/P".

to trehalose; that concentration corresponds to about 23 water molecules per trehalose residue, which is nearly twice as many water molecules as are present in the hydration sphere of trehalose alone.[25] This enhanced efficiency is likely a result of the increased

viscosity of the polytrehalose solution compared to that of a solution of trehalose (small molecule).[26,27] Importantly, it was also discovered that, if the polytrehalose solution is cooled significantly below 0 ^{o}C, but at least 5 degrees above the temperature at which the onset of water crystallization is observed, no crystallization occurs even after prolonged storage (Fig. 3.9).

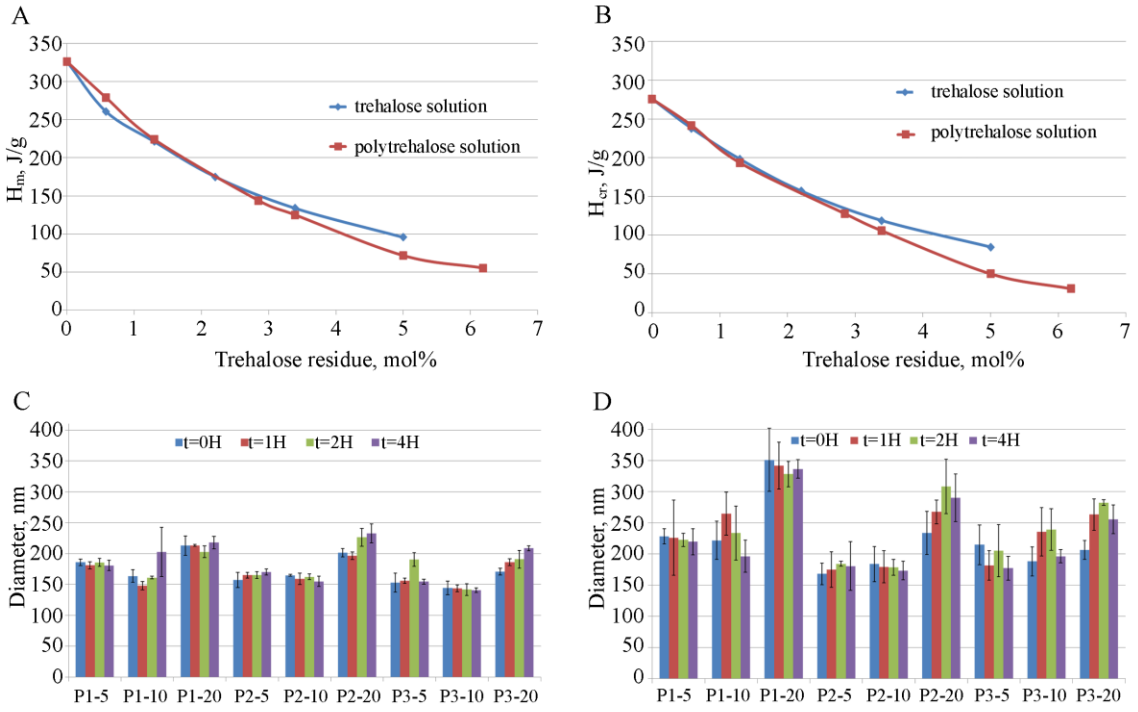

Figure 3.8. Depression in heats of ice melting, H_m, (**A**) and water crystallization, H_{cr}, (**B**) of trehalose and polytrehalose solutions at various concentrations. Hydrodynamic diameters based on the scattering intensity of polyplexes formed between siRNA and diblock polymers P1, P2 and P3 in OptiMEM (**C**), and DMEM containing 10% FBS (**D**). Labels signify "polymer–N/P ratio".

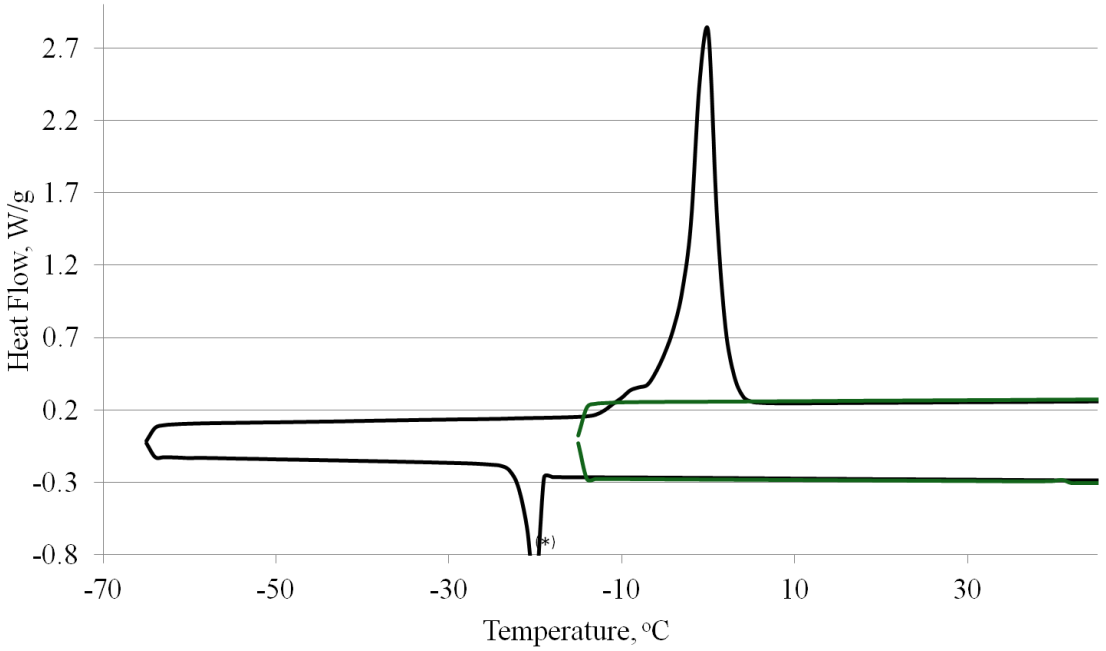

Figure 3.9. Differential scanning colorimetry of a 34 mol% aqueous solution of polytrehalose. Isothermal conditioning was applied for both cool-heat cycles at the lowest temperature for 30 min. The graphical representation of the exothermic peak does not display a 'loop' which results from overcooling (*).

To examine the properties that the polytrehalose motif imparts to nanoparticles, several interpolyelctrolyte (polyplex) formulations between siRNA and each diblock copolymer P1-P3 were prepared and investigated. All three polymers readily bind siRNA at low N/P ratios (molar formulation ratio between the number of amines on the diblock copolymer and the phosphate groups on the RNA), as evident from the gel electrophoresis assay (Fig. 3.10).

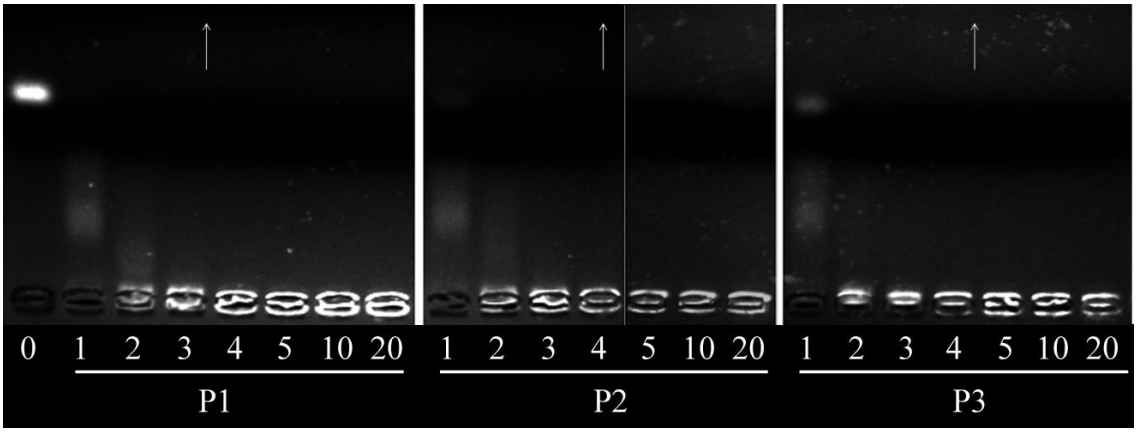

Figure 3.10. Gel electrophoresis assay. Numbers under each well correspond to polymer amine/siRNA phosphate (N/P) ratio. Arrows point towards anode(+).

The colloidal nanoparticles that are formed upon complexation demonstrated high stability from aggregation in culture media (both in the absence and presence of serum) containing physiological salt concentrations. Polyplex hydrodynamic diameters were between 150 to 200 nm in OptiMEM and somewhat larger in serum-containing DMEM (Fig. 3.8). The increased size in the presence of serum is suggestive of interactions between polyplexes and serum components, likely proteins. The possibility of protein adsorption to the polytrehalose corona was examined and confirmed using a quartz crystal microbalance (Fig. 3.11). The nature of interactions between polytrehalose and serum components is yet unknown and could potentially result from physical entrapment of proteins[28] or interactions with biological molecules via hydrogen bonding.[29] This could possibly be beneficial as it could help mask particles from potential actions of the immune system by 'hiding' the nanoparticle with a layer of innate proteins.[30] Interestingly, freezing of polyplex solutions, lyophilization to dryness, and subsequent

resuspension of the polyplex formulations yielded nanoparticles as determined via DLS that still retained their biological activity toward siRNA-mediated gene downregulation. At both N/P ratios, polymer P1 (with the greatest trehalose content among the three synthesized polymers) appeared to yield optimal results for facilitating stable resuspension of the polytrehalose-coated polyplexes within about an hour (Fig. 3.7 B).

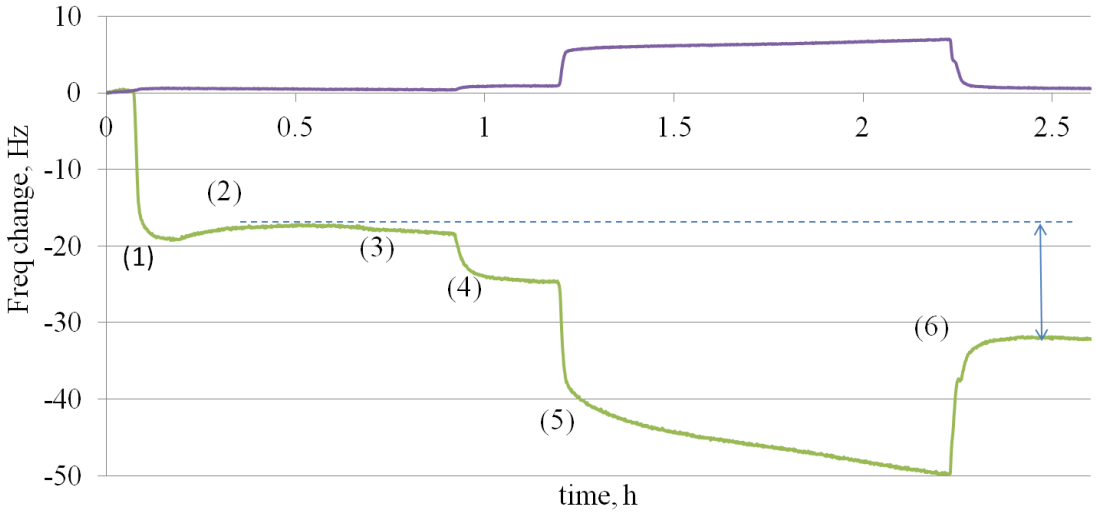

Figure 3.11. Changes in vibrational frequencies of the quartz crystal (green line) upon the adsorption of polytrehalose and serum components (proteins). The gold coated crystal was exposed to polytrehalose solution (1); water (2); 0.1% FBS in DMEM (3); 1% FBS in DMEM (4); 10% FBS in DMEM (5); water (6). The difference in frequency between time points (2) and (6) is 15 Hz and indicates that adsorption of proteins takes place. Purple line denotes impedance.

Upon administration and biodistribution, cellular internalization is the first barrier that polyplexes encounter during the delivery process and, to a large degree, is defined by the interactions between the nanoparticle surface and cell membranes. Thus, the ability of polytrehalose-coated polyplexes to undergo cellular internalization was studied in detail. Polyplexes were formulated with fluorescently-labeled siRNA, and the extent of their

internalization by U-87 glioblastoma cells was measured with flow cytometry. All three polymers yield efficient delivery of

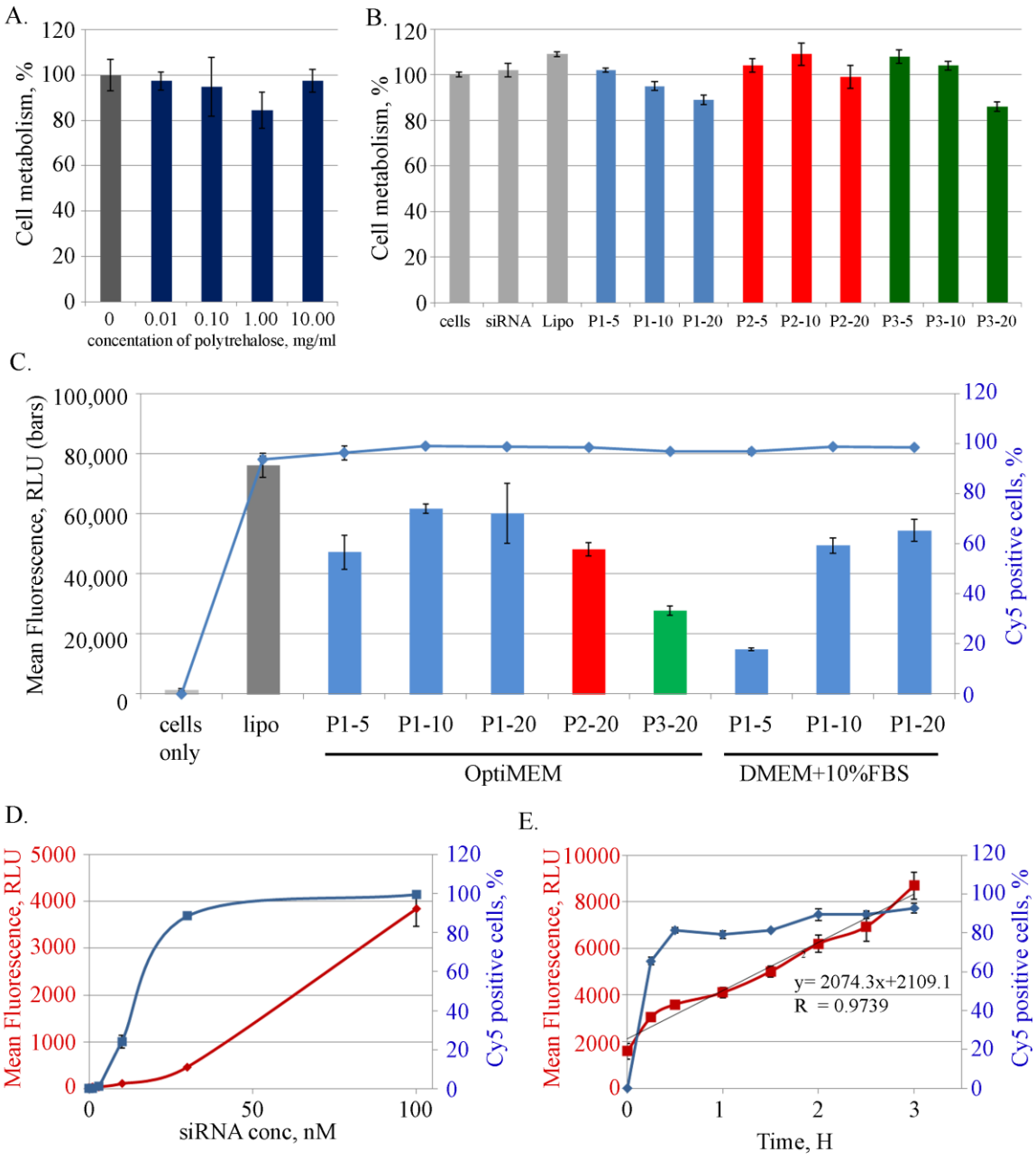

Figure 3.12. A. Cellular uptake by U-87 cells at siRNA concentration of 100 nM. Labels denote "polymer name-N/P ratio" **B.** Dependence of cellular uptake by U-87 cells on

siRNA concentration using polymer P1 at N/P of 10 in DMEM with 10% FBS. Red symbols indicate mean fluorescence (RLU) data; blue symbols denote Cy5-positive cells (%). **C.** Dynamics of cellular uptake by U-87 cells at 100 nM siRNA concentration, polymer P1 at N/P ratio 10 in DMEM with 10% FBS. Red symbols indicate mean fluorescence (RLU) data; blue symbols denote Cy5-positive cells (%).

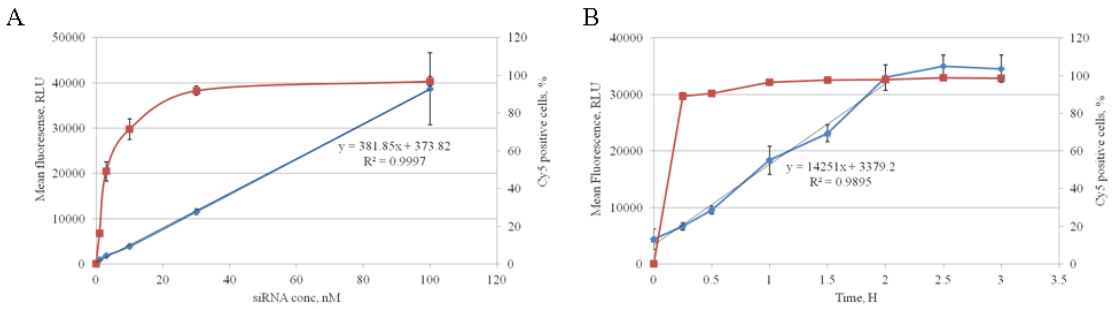

Figure 3.13. A. Dependence of cellular uptake by U-87 cells on siRNA concentration using polymer P1 at N/P of 10 in OptiMEM. **B**. Dynamics of cellular uptake by U-87 cells at 100 nM siRNA concentration, polymer P1 at N/P ratio 10 in OptiMEM.

siRNA to cells and do so homogeneously across the cell population; more than 90% of the cells tested positive for the presence of siRNA with all formulations studied. Polymer P1 was the most efficient among the three polymers tested, delivering the greatest number of siRNA copies per cell (as indicated by the greatest mean cellular fluorescence). It is important to note that polyplexes formed with each of the polymers at N/P of 20 have similar sizes and ζ-potentials (Fig. 3.7 A), the principle difference between them is the polytrehalose content (polymer P1 contains 83% of polytrehalose by mass, whereas P2 and P3 contain 71% and 66%, respectively). It can therefore be

concluded from these results that polytrehalose has a direct positive impact on the efficiency of U-87 uptake of these nanoparticles.

The N/P ratio at which the trehalose-coated polyplexes are formulated appears to have minimal influence on the uptake in serum-free media (Fig. 3.12). However, in the presence of serum, the impact of N/P ratio becomes more pronounced; in serum-supplemented DMEM, polymer P1 delivers 3 times more siRNA at N/P ratio 10 than at N/P ratio of 5. An even further increase in the amount of polymer (N/P ratio of 20) did not improve the uptake, suggesting that P1-10 is the close to optimal polyplex formulation for transfection of U-87 cells in the presence of serum. Additionally, there is a direct influence of siRNA concentration in the media on the uptake (Fig. 3.12 D). Greater than 90% of cells are transfected with siRNA when the concentration of siRNA in the medium reaches 30 nM, however, a further increase in concentration up to 100 nM results in a proportional increase in the siRNA copies per cell. It is interesting to note that uptake dependence on concentration is linear in serum-free OptiMEM (Fig. 3.13 A). These data indicate that the cellular internalization of polytrehalose-coated polyplexes is a very efficient process. After only 15 minutes of exposure, more than 70% of cells have detectable levels of fluorescently-labeled siRNA, in the presence of serum (Fig 3.12 E). In the absence of serum, this number is even higher, 90% of cells are positive for siRNA after only 15 minutes (Fig. 3.13 B). Interestingly, as shown in Figs. 3.12 C and 3.13 B, the average amount of delivered siRNA per cell is linearly dependent with time in both media types (in OptiMEM this was also found prior to eventual saturation after 2 hours, Fig. 3.13 B).

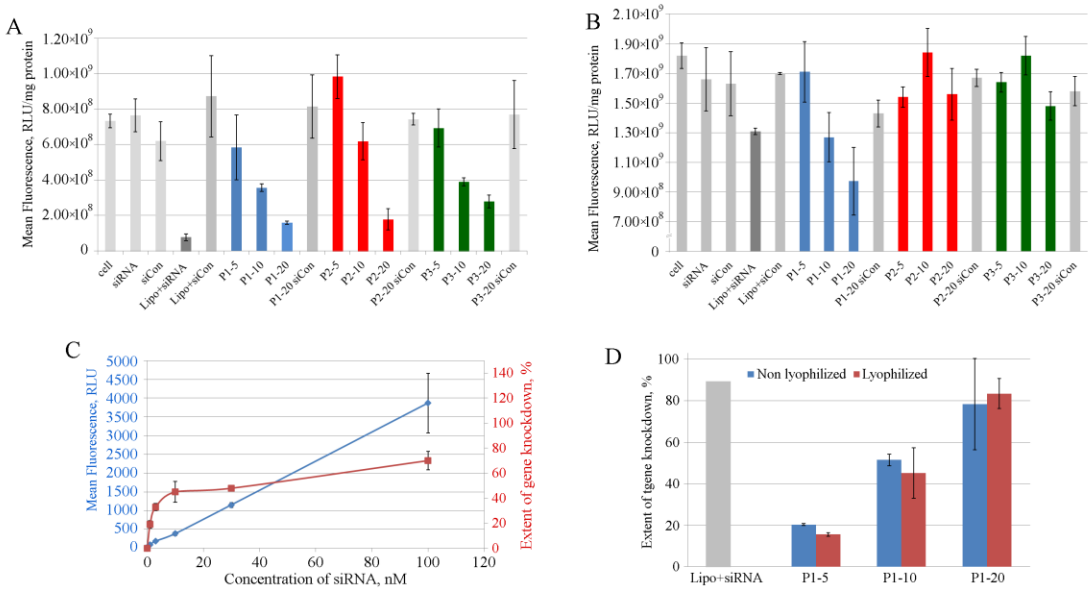

Figure 3.14. Luciferase gene knockdown in luciferase-expressing U-87 cells transfected in **A.** OptiMEM and **B.** serum-containing DMEM. **C.** Evaluation of the dependence upon siRNA concentration of cellular uptake and target gene down-regulation. Transfection performed at an siRNA concentration of 100 nM in OptiMEM. **D.** Comparison of target gene down-regulation in luciferase-expressing U-87 cells between freshly-prepared P1 polyplexes and previously-lyophilized P1 polyplexes. Transfections were performed at an siRNA concentration of 100 nM in OptiMEM. Labels signify "polymer name-N/P ratio", Lipo=Lipofectamine, siCon=siRNA with scrambled sequence (negative control).

The ability of polymer/siRNA nanoparticles to down-regulate a target gene was evaluated in U-87 glioblastoma cells that stably express luciferase. The extent of gene down-regulation is assessed by the decrease in light production via luciferase assay. All three polymers promoted significant gene knockdown in OptiMEM (Fig. 3.14 A). The efficiency increased with the increase in N/P ratio and, at an N/P ratio of 20, was similar

to that of Lipofectamine, our positive control. In serum-containing DMEM, only polymer P1, which contains the most trehalose by mass, was capable of promoting gene knockdown. Moreover, the observed dependence of gene siRNA-mediated knockdown on N/P ratio was found to be similar to that observed in serum-free conditions.

Interestingly, polyplex uptake increases linearly with siRNA concentration but the trend for luciferase gene knockdown increase was less profound at siRNA concentrations greater than 30 nM. A plausible explanation for this response saturation at higher siRNA concentrations is that possibly the cell can no longer process all the delivered siRNA into the RNA-induced silencing complex (RISC). However, the observed dependence of down-regulation on N/P ratio also suggests a role of the polymer in this phenomenon and using a different cationic block (responsible for binding, encapsulating and release of the nucleic acid) may have the potential to improve the knockdown efficiency even further. Studies on this phenomenon are in progress.

Polymer P1, containing the largest amount of polytrehalose among the three polymers tested, was found to promote the optimal polyplex resuspension after lyophilization, and also revealed to be the most effective at siRNA delivery. Therefore, it is expected to also impart the greatest ability to protect siRNA during the lyophilization of polyplexes possibly retaining its biological activity. To this end, lyophilized formulations of P1-siRNA polyplexes were lyophilized and the completely dry powder was resuspended in RNase-free water. Gene down-regulation with the resuspended P1 polyplexes was compared to freshly-prepared polyplexes made with the same polymer (Fig. 3.14 D). Amazingly, the extent of luciferase gene down-regulation induced by the lyophilized/resuspended polyplexes was identical that observed with the freshly-prepared

analogs. Importantly, the efficiency of gene down-regulation reached 80% for the lyophilized polyplexes at an N/P ratio of 20 (P1-20). This result shows that this *poly*trehalose motif displayed on the surface of the polyplexes, indeed retains the ability of trehalose to protect macromolecules and nanosystems during the freeze-drying proces.

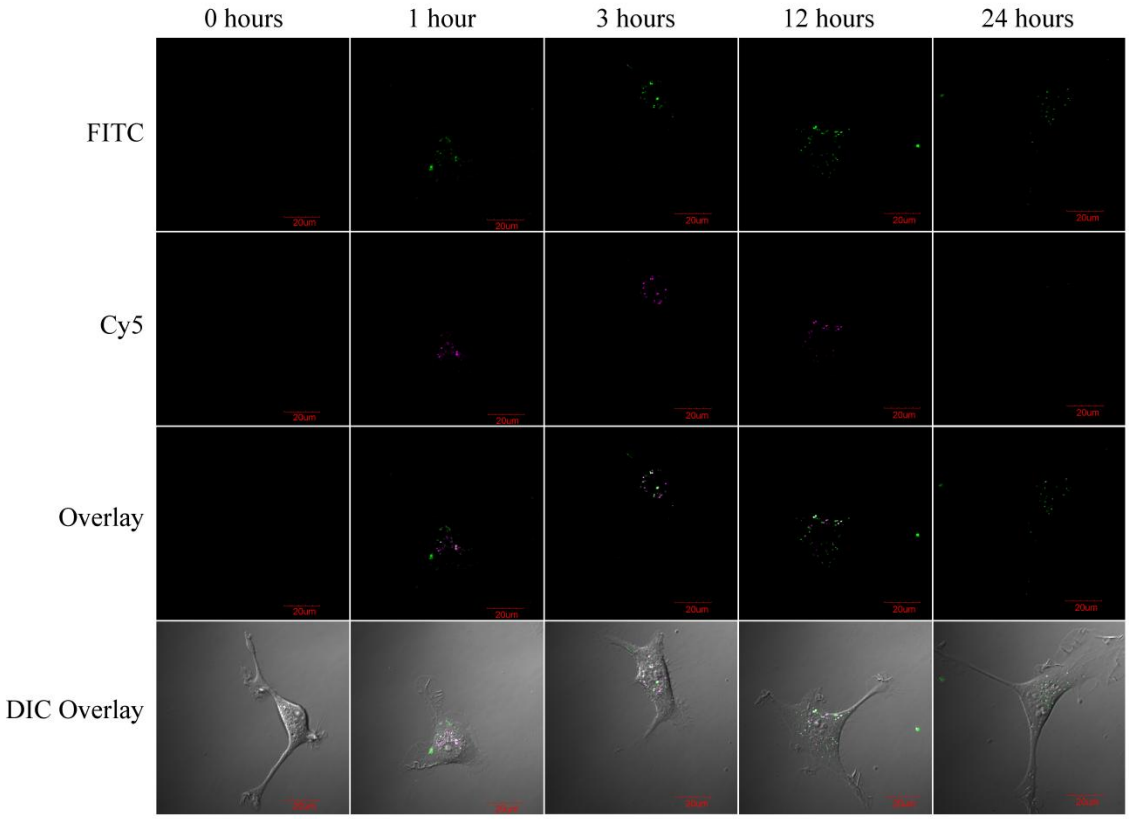

Figure 3.15. Confocal microscopy of U-87 cells transfected with Cy5-labeled siRNA (purple) and FITC-labeled polymer P1 at N/P ratio 10.

Live cell microscopy was performed using fluorescently-labeled polymer P1 (FITC-P1) and siRNA (Cy5-siRNA) to visualize polyplexes trafficking inside the cells (Fig. 3.15). The punctate nature of the fluorescence is clearly seen in both Cy5 and FITC.

Interestingly, there is a sharp drop in Cy5 fluorescence at 24 h time point, indicating that siRNA release takes place between 12 and 24 hours post transfection. At the same time FITC fluorescence that corresponds to the polymer FITC-P1 is maintained throughout the microscopy experiment (up to 48 h, Fig. 3.16) and remains punctate. This may suggest that while siRNA is capable of escaping the endosome/lysosome, the polymer may remain in those vesicles. The ultimate fate of the polymer inside the cell and kinetics of delivery are being further investigated.

3.4 Conclusions

The field of siRNA-based therapeutics has great potential, yet advanced materials-based delivery systems still need to be engineered to optimize efficacy. The polytrehalose motif presented in this report has many valuable properties that make it a great candidate for inclusion within the outer layer of many different macromolecules and nanosystems. The synthetic preparation of the monomer can be readily achieved and the polymer can be easily synthesized with a predefined length with low dispersity via the RAFT polymerization mechanism. Here, we have exploited it to stabilize inter-polyelectrolyte complexes with siRNA from salt and serum-mediated aggregation and lyophilization, while still retaining effective gene knockdown without toxicity *in vitro* (Fig. 3.12), and it promotes very efficient cellular internalization. Indeed, further studies *in vivo* are in progress to demonstrate the effectiveness of this novel motif for circulation stability, delivery efficacy, and its neuroprotective potential to prevent autophagy. None the less, polytrehalose has great promise to be a highly impactful component within

various types of macromolecule and nanoparticle formulations including micelles, liposomes, proteins, gold nanoparticles, quantum dots, and others relating to nanomedicine applications.

3.5 References

1 Teramoto, N., Sachinvala, N. D. & Shibata, M. Trehalose and trehalose-based polymers for environmentally benign, biocompatible and bioactive materials. *Molecules* **13**, 1773-1816 (2008).

2 Benaroudj, N. & Goldberg, A. L. Trehalose accumulation during cellular stress protects cells and cellular proteins from damage by oxygen radicals. *J. Biol. Chem.* **276**, 24261-24267 (2001).

3 Hagen, S. J., Hofrichter, J. & Eaton, W. A. Protein reaction kinetics in a room-temperature glass. *Science* **269**, 959 (1995).

4 Clegg, J. S., Seitz, P., Seitz, W. & Hazlewood, C. F. Cellular responses to extreme water loss: the water-replacement hypothesis. *Cryobiology* **19**, 306-316 (1982).

5 Adams, R. P., Kendall, E. & Kartha, K. Comparison of free sugars in growing and desiccated plants of Selaginella lepidophylla. *Biochem. Syst. Ecol.* **18**, 107-110 (1990).

6 Ramlov, H. & Westh, P. Survival of the cryptobiotic eutardigrade Adorybiotus coronifer during cooling to-196 C: effect of cooling rate, trehalose level, and short-term acclimation. *Cryobiology* **29**, 125-130 (1992).

7 Sømme, L. Anhydrobiosis and cold tolerance in tardigrades. *Eur. J. Entomol.* **93**, 349-358 (1996).

8 Crowe, J. H., Crowe, L. M., Oliver, A. E., Tsvetkova, N., Wolkers, W. & Tablin, F. The trehalose myth revisited: introduction to a symposium on stabilization of cells in the dry state. *Cryobiology* **43**, 89-105 (2001).

9 Sarkar, S., Davies, J. E., Huang, Z., Tunnacliffe, A. & Rubinsztein, D. C. Trehalose, a novel mTOR-independent autophagy enhancer, accelerates the clearance of mutant huntingtin and α-synuclein. *J. Biol. Chem.* **282**, 5641-5652 (2007).

10 Casarejos, M., Solano, R., Gómez, A., Perucho, J., de Yébenes, J. & Mena, M. The accumulation of neurotoxic proteins, induced by proteasome inhibition, is reverted by trehalose, an enhancer of autophagy, in human neuroblastoma cells. *Neurochem. Int.* (2011).

11 Wada, M., Miyazawa, Y. & Miura, Y. A specific inhibitory effect of multivalent trehalose toward Aβ (1-40) aggregation. *Polym. Chem.* (2011).

12 Tseng, W. C., Tang, C. H., Fang, T. Y. & Su, L. Y. Trehalose Enhances Transgene Expression Mediated by DNA-PEI Complexes. *Biotechnol. Prog.* **23**, 1297-1304 (2007).
13 Srinivasachari, S., Liu, Y., Zhang, G., Prevette, L. & Reineke, T. M. Trehalose click polymers inhibit nanoparticle aggregation and promote pDNA delivery in serum. *J. Am. Chem. Soc.* **128**, 8176-8184 (2006).
14 Crowe, J. H., Carpenter, J. F. & Crowe, L. M. The role of vitrification in anhydrobiosis. *Annu. Rev. Physiol.* **60**, 73-103 (1998).
15 Ishihara, T., Takeda, M., Sakamoto, H., Kimoto, A., Kobayashi, C., Takasaki, N., Yuki, K., Tanaka, K., Takenaga, M. & Igarashi, R. Accelerated blood clearance phenomenon upon repeated injection of PEG-modified PLA-nanoparticles. *Pharm. Res.* **26**, 2270-2279 (2009).
16 Fustin, C. A. & Duwez, A. S. Dithioesters and trithiocarbonates monolayers on gold. *J. Electron. Spectrosc. Relat. Phenom.* **172**, 104-106 (2009).
17 Moad, G., Rizzardo, E. & Thang, S. H. Living radical polymerization by the RAFT process. *Aust. J. Chem.* **58**, 379-410 (2005).
18 Moad, G., Rizzardo, E. & Thang, S. H. Living radical polymerization by the RAFT process—a first update. *Aust. J. Chem.* **59**, 669-692 (2006).
19 Moad, G., Rizzardo, E. & Thang, S. H. Living Radical polymerization by the RAFT process–a second update. *Aust. J. Chem.* **62**, 1402-1472 (2009).
20 Barbey, R., Lavanant, L., Paripovic, D., Schüwer, N., Sugnaux, C., Tugulu, S. & Klok, H. A. Polymer brushes via surface-initiated controlled radical polymerization: synthesis, characterization, properties, and applications. *Chem. Rev.* **109**, 5437-5527 (2009).
21 Patel, M. K. & Davis, B. G. Flow chemistry kinetic studies reveal reaction conditions for ready access to unsymmetrical trehalose analogues. *Org. Biomol. Chem.* **8**, 4232-4235 (2010).
22 Schilli Christine, M., Müller Axel, H. E., Rizzardo, E., Thang San, H. & Chong, Y. K. RAFT Polymers: Novel Precursors for Polymer?Protein Conjugates in *Advances in Controlled/Living Radical Polymerization* Vol. 854*ACS Symposium Series*Ch. 41, 603-618 pp. (American Chemical Society, 2003).
23 Moad, G., Mayadunne Roshan, T. A., Rizzardo, E., Skidmore, M. & Thang San, H. Kinetics and Mechanism of RAFT Polymerization in *Advances in Controlled/Living Radical Polymerization* Vol. 854*ACS Symposium Series*Ch. 36, 520-535 pp. (American Chemical Society, 2003).
24 Wang, G. & Haymet, A. Trehalose and other sugar solutions at low temperature: Modulated differential scanning calorimetry (MDSC). *J. Phys. Chem. B* **102**, 5341-5347 (1998).
25 Branca, C., Magazù, S., Maisano, G., Migliardo, F., Migliardo, P. & Romeo, G. α, α-Trehalose/water solutions. 5. Hydration and viscosity in dilute and semidilute disaccharide solutions. *J. Phys. Chem. B* **105**, 10140-10145 (2001).
26 Freed, K. F. & Edwards, S. Polymer viscosity in concentrated solutions. *J. Chem. Phys.* **61**, 3626 (1974).
27 Uhlmann, D. A kinetic treatment of glass formation. *J. Non-Cryst. Solids* **7**, 337-348 (1972).

28 Lins, R. D., Pereira, C. S. & Hünenberger, P. H. Trehalose–protein interaction in aqueous solution. *Proteins Struct. Funct. Bioinf.* **55**, 177-186 (2004).
29 Villarreal, M. A., Díaz, S. B., Disalvo, E. A. & Montich, G. G. Molecular dynamics simulation study of the interaction of trehalose with lipid membranes. *Langmuir* **20**, 7844-7851 (2004).
30 Walczyk, D., Bombelli, F. B., Monopoli, M. P., Lynch, I. & Dawson, K. A. What the cell "sees" in bionanoscience. *J. Am. Chem. Soc.* **132**, 5761-5768 (2010).

Chapter 4. Glucosamine-based Cationic Diblock Polymers for Nucleic Acid Delivery*

* Work described in this chapter is a result of collaborative efforts of the dissertation author, Dr. Adam E. Smith, Lian Xue and Giovanna Grandinetti. Glycopolymer chain extension with the cationic block and DLS measurements were performed by Dr. Adam E. Smith. Flow cytometry, cytotoxicity and transfection experiments were performed by Giovanna Grandinetti and Lian Xue. Microscopy images were acquired by Giovanna Grandinetti. Part of the work described in this chapter was published in Smith, A.E.; Sizovs, A.; Grandinetti, G.; Xue, L.; Reineke, T.M. *Biomacromolecules* **8**, 3015-3022 (2011).

Abstract

In this chapter the synthesis of the glucosamine-based cationic diblock polymers and their utility as pDNA delivery agents is investigated. An efficient and simple procedure for the synthesis of the carbohydrate monomer 2-methacrylamido-2-deoxy-D-glucose (MAG) was developed starting with commercially available glucosamine hydrochloride. The applicability of this procedure to other hexosamines was demonstrated using galactosamine. Glycopolymers (polyMAGs) of various lengths were synthesized using the reversible addition-fragmentation chain transfer (RAFT) polymerization. $pMAG_{46}$ was used to create three cationic diblock polymers with the second block comprised of aminoethylmethacrylamide (AEMA) repeating units (MAG_{46}-*b*-$AEMA_{21}$, MAG_{46}-*b*-$AEMA_{39}$ and MAG_{46}-*b*-$AEMA_{48}$). The gel electrophoresis assay was employed to demonstrate the efficient binding of pDNA by all three polymers. The strong nature of the nucleic acid binding was revealed using the competition assay with

negatively charged polysaccharide heparin. Enterpolyelectrolyte complexes that were formed between the diblock polymers and pDNA ('polyplexes') were examined by the dynamic light scattering (DLS) in two cell culture media, OptiMEM and serum containing DMEM, to reveal 55-115 nm sized particles that have demonstrated colloidal stability in both of these media over a period of 4 hours. Using fluorescently labeled plasmid we demonstrated the efficient cellular internalization of pDNA that is promoted by all three tested polymers, delivering pDNA to up 95% of the cells. FITC-labeled polymer P3 along with Cy-5 labeled pDNA was used to study the polyplexes by confocal microscopy inside HeLa cells. Using the pDNA that encodes a reporter gene luciferase it was revealed that the polymer with the shortest block of AEMA is the most efficient in promoting the gene expression among the three polymers tested. Overall it was concluded that pMAG is an easily accessible polymer with properties that make it a good candidate to be used as an outer layer for nanoparticles for biomedical applications.

4.1 Introduction

The trehalose-based research (Chapter 3) faced difficulties with the synthesis and that prompted the search for a simplified model with similar properties. Since the targeted trehalose-based monomer was an amine derivative of trehalose it was rational to choose a commercially available carbohydrate with amine functionality.

Glucosamine fits these properties well. This carbohydrate is inexpensive and easily available. It is the constituent of chitosan and is produced by hydrolysis of exoskeleton of arthropods (mostly crustaceans such as shrimp and crabs). Due to its availability glucosamine has been widely researched in the biopharmaceutical field. Despite some concerns regarding glucosamine interference with the glucose metabolism pathway,[1] it is generally regarded as a safe material[2] and it is available as a nutritional supplement across the world. Significant research effort has been devoted to the use of glucosamine for treatment of osteoarthritis,[3,4] although its effectiveness has been a subject of the debate.[5]

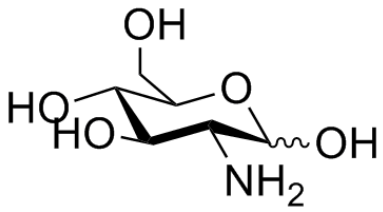

glucosamine

From a synthetic perspective glucosamine is a great monomer precursor because of its primary amine group which can be easily functionalized. Furthermore, opposite to another popular approach, namely the modification of the anomeric carbon, using the amino group of glucosamine for the introduction of a polymerizable moiety preserves the

ability of this molecule to form a pyranose ring – fundamental structural element of carbohydrates.

Glycopolymers, a class of polymers with pendant carbohydrate groups, have been a subject of high scientific interest. The ability of the glycopolymers to have multiple simultaneous interactions with a target is generally regarded as 'glycocluster effect'.[6] This property has been widely utilized in the field of lectin recognition[7,8] and lectin targeting with glycopolymers (reverse lectin targeting) has a potential in improving the site-specific nanoparticle drug delivery.[9,10]

Glycopolymers have been used for the stabilization and improvement of the biological compatibility of various nanomaterials including gold nanoparticles,[11-13] carbon nanotubes[14,15] and, importantly, as polymers for nucleic acid delivery.[16-18] In addition, 2-methacrylamido and 2-acrylamido derivatives of the glucosamine have been previously successfully polymerized via RAFT polymerization.[7,19,20]

In this chapter the synthesis of poly(2-methacrylamido-2-deoxy-glucose) (polyMAG) and its utilization for the nucleic acid delivery is researched. To make this glycopolymer an attractive polymer from the practical point of view we have developed a scalable and efficient method for the preparation of a methacrylamide monomer. Synthesis of polyMAG and the cationic diblock copolymers via RAFT and the evaluation of these materials is discussed in detail.

4.2. Materials and Methods

4.2.1. Materials and equipment.

All reagents were obtained at the highest possible purity from Fisher Scientific Co (Pitsburgh, PA) or Sigma-Aldrich Co (St. Louis, MO) and used as received unless noted otherwise. Aminoethylmethacrylamide hydrochloride (AEMA·HCl) was purchased from Polysciences (Warrington, PA). Dialysis membranes were obtained from Spectrum Laboratories, Inc. (Rancho Dominguez, CA). Dry methylene chloride, dimethyl formamide, methanol and tetrahydrofurane were purified with MBRAUN MB solvent purification system starting with HPLC grade solvents from Fischer Scientific Co (Pitsburgh, PA).

Thin layer chromatographies (TLC) were performed on aluminum-backed silica gel plates (silica gel 60, F_{254}) obtained from Merck (Darmstadt, Germany) and visualized with UV light (254 nm) or by using the staining agents: ninhydrin solution in ethanol for the visualization of amines, *p*-anisaldehyde solution in H_2SO_4/acetic acid/ethanol for the visualization of carbohydrates.

Preparative chromatographies were conducted using a Buchi Separcore® chromatography system (Buchi Labortechnik AG, Switzerland) on plastic chromatography cartridges packed with Buchi cartridge packing instrument or on homemade glass columns manually packed with a liquid packing method. All columns were packed with 60-200 mesh Premium Rf silica gel (Sorbent Technologies Inc., Atlanta, GA). All solvents used for the preparative chromatography were HPLC grade and were obtained from Fisher Scientific Co (Pittsburgh, PA).

LC-MS data was obtained with an Agilent system with a time-of-flight (TOF) analyzer coupled to a Thermo Electron TSQ-LC/MS ESI mass spectrometer. NMR spectra were recorded using 400MR Varian-400 Hz spectrometer in deuterated solvents. ^{1}H-NMR were recorded at 399.7 MHz and ^{13}C-NMR were recorded at 101 MHz. SEC was conducted using 1.0 wt% acetic acid/0.1 M Na_2SO_4 as eluent at a flow rate 0.3 mL/min on size exclusion chromatography columns [CATSEC1000 (7μ, 50×4.6), CATSEC100 (5μ, 250×4.6), CATSEC300 (5μ, 250×4.6), and CATSEC1000 (7μ, 250×4.6)] obtained from Eprogen Inc. (Downers Grove, IL). Signal acquisition was done using Wyatt HELEOS II light scattering detector (λ = 662 nm), and an Optilab rEX refractometer (λ = 658 nm). SEC trace analysis was done using Astra V (version 5.3.4.18, Wyatt Technologies (Santa Barbara, CA).

Human cervix adenocarcinoma (HeLa) cells were purchased from ATCC (Rockville, MD). The cells were grown in DMEM supplemented with 10% (v/v) fetal bovine serum, 1% antibiotic-antimycotic solution (containing penicillin, streptomycin, and amphotericin B) at 37 ºC and humidified atmosphere with 5% CO_2. JetPEI (PolyPlus Transfections, Illkirch, France), Lipofectamine 2000 (Invitrogen, Carlsbad, California), and Glycofect (Techulon, Blacksburg, VA) were used according to the manufacturers protocols. Propidium iodide, UltraPure™ Agarose-1000, trypsin, (3-(4,5-dimethylthiazol-2-yl)-2,5-diphenyltetrazolium bromide (MTT), phosphate buffer saline (PBS), modified essential minimum eagle medium (Opti-MEM®) and Dulbecco's modified eagle medium (DMEM) were purchased from Invitrogen, Inc. (Carlsbad, CA). CellScrub™ Buffer was obtained from Genlantin, Inc. (San Diego, CA). Bovine albumin was purchased from Sigma-Aldrich (St. Louis, MO). The Luciferase Assay Kit and cell lysis buffer were

obtained from Promega (Madison, WI). Bio-Rad DC Protein Assay Reagent A, Reagent B and Reagent S were obtained from Bio-Rad Laboratories, Inc. (Hercules, CA).

4.2.2. Experimental procedures

α-2-Amino-deoxy-1,3,4,6-tetra-(O-trimethylsilyl)glucopyranose (**15**)

A dry 500 mL flask was charged with glucosamine hydrochloride **12** (20.20 g, 93.68 mmol), flushed with nitrogen and 400 ml of dry pyridine were cannulated in. Bis(trimethylsilyl)acetamide (84g, 0.41mol, 1.1 eq per OH) was added using an additional funnel over ca. 10 min and the reaction was stirred at room temperature for 12 h.

The reaction mixture was cooled to 0 ^{o}C in an ice bath and then poured through a funnel into 1.5 L of 0.1M solution of K_2HPO_4 cooled to 0 ^{o}C. This caused the formation of a white solid. The precipitate was filtered and dissolved in 400mL of DCM. The DCM solution was washed with water and saturated sodium chloride solution (brine) and finally dried over Na_2SO_4 for 2 hours at room temperature. Na_2SO_4 was filtered and DCM was evaporated to yield 43.57 g of **15** as a colorless oil, which crystallizes upon standing. *(Product **15** obtained this way contained ca. 4.4% of DCM by mass, therefore the yield is 41.64 g, 95%).* A sample for analysis was dried under 500 mTorr vacuum and the rest of the material was taken to the next step.

^{1}H-NMR (400 MHz, $CDCl_3$) δ 5.12 (d, J = 3.3 Hz, 1H), 3.76 – 3.60 (m, 3H), 3.54 (t, J=8.9 Hz, 1H), 3.47 (t, J=8.9 Hz, 1H), 2.55 (dd, J = 9.2, 3.3 Hz, 1H), 0.20 (s, 9H), 0.18 (s,

9H), 0.16 (s, 9H), 0.10 (s, 9H). ^{13}C NMR (101 MHz, $CDCl_3$) δ 94.90, 77.88, 73.14, 72.33, 62.30, 57.74, 1.60, 1.10, 0.17, 0.00.

α-2-Methacrylamido-deoxy-1,3,4,6-tetra-(O-trimethylsilyl)glucopyranose (**16**)

Trimethylsilyl protected glucosamine **15** obtained after the DCM evaporation was dissolved in 400 mL of DMF. This solution was cooled in an ice-bath and TEA (20 ml, d=0.73 g/mL, 16 g, 0.16 mol) was added. Freshly distilled methacryloyl chloride (10.8 g, 0.103 mol) solution in 50 mL of dry DCM was slowly (over ca. 20 min) added to DMF solution of **15** and TEA. The reaction was stirred for 1 h in an ice-bath (0 ^{o}C) followed by 3 h at room temperature. DCM was evaporated under vacuum (water bath temperature 20 ^{o}C) and the remaining solution in DMF was down to 0 ^{o}C and poured through a funnel in 1.5 L of cold 0.1M solution of K_2HPO_4 which contained ca. 0.5 kg of ice. The aqueous mixture was allowed to warm to room temperature. It was extracted with 3×250 mL of hexanes. The hexane extracts were combined and washed first with water, followed by brine and finally dried over Na_2SO_4 overnight. Solids were filtered off, hexanes were evaporated and the product was dried under vacuum to yield 43.57g (86.78% over two steps) of off-white crystalline material. It can be further re-crystallized in cold hexane (m.p. = 102 ºC), however even without the re-crystallization this material contained no impurities according to ^{1}H-NMR. ^{1}H-NMR (400 MHz, CD_2Cl_2) δ 5.77 (d, *J* = 9.9 Hz, 1H, N*H*), 5.64 (s, 1H, C=C*H*H), 5.34 (s, 1H, C=CH*H*), 5.03 (d, *J* = 3.5 Hz, 1H, H^1), 3.99 (td, *J* = 9.9, 3.5 Hz, 1H, H^2), 3.76 – 3.55 (m, 5H, $H^{3,4,5,6,6'}$), 1.93 (s, 3H, C(O)CH_3), 0.16 (s, 9H, TMS), 0.14 (s, 9H, TMS), 0.09 (s, 9H, TMS), 0.08 (s, 9H, TMS). ^{13}C NMR (101 MHz, CD_2Cl_2) δ 167.95 (*C*=O), 140.94 (C–*C*(=C)–C), 119.91(H_2C=), 93.40 (C1), 74.84

(C3), 73.42(C4/C5), 72.66(C4/C5), 62.34(C6), 55.14(C2), 19.01(CH_3), 1.38((CH_3)$_3$Si), 1.17((CH_3)$_3$Si´), 0.18((CH_3)$_3$Si´´), 0.00((CH_3)$_3$Si´´´).

α-2-Methacrylamido-deoxy-glucose (MAG, **13**)

α-2-Methacrylamido-deoxy-1,3,4,6-tetra-(O-trimethylsilyl)-glucopyranose (**16**) (17.96 g, 33.51 mmol) was dissolved in 350 mL of dry methanol and cooled to 0 ^{o}C. HCl in methanol (0.5 mL, c~1M) was added with a syringe and the reaction was allowed to warm to room temperature (pH was checked by applying a drop of the solution to a wet pH indicator paper). Methanol was removed under reduced pressure on a rotary evaporator (water bath temperature was kept under 30 ^{o}C) to yield **13** as a white solid. The product was dissolved in 50 mL of water, producing a non-transparent solution that contained small solid particles. It was filtered through Celite® to yield a clear solution which was lyophilized to finally yield pure **13** (7.69 g, 93%) as a mixture of two anomers. ^{1}H-NMR (400 MHz, D_2O) δ 5.56 (bs, 1H), 5.38 (bs, 1H), 5.07 (d, J = 3.5 Hz, 0.5H, α anomer), 4.63 (d, overlapped with HOD, β anomer), 3.81 (dd, J=3.5, 10.7Hz, 0.5H, α anomer), 3.78 – 3.30 (m, 5.5H), 1.79 (s, 3H). ^{13}C-NMR (101 MHz, D_2O) δ 172.58, 172.46, 139.20, 138.96, 121.09, 120.96, 94.76, 90.74, 75.87, 73.64, 71.48, 70.43, 70.03, 69.84, 60.48, 56.76, 54.18, 17.67, 17.64.

2-Amino-deoxy-1,3,4,6-tetra-(O-trimethylsilyl)galactopyranose

Galactosamine hydrochloride (1.00 g, 4.64 mmol) was placed in a dry 50 mL round bottom flask and the flask was purged with nitrogen before 20 mL of dry pyridine were cannulated in. Bis(trimethylsilyl)acetamide (4.00 mL, d=0.832 g/ml, 3.33 g, 16.4

mmol) was added with a syringe and the reaction was allowed to stir at room temperature overnight. The reaction mixture was then cooled to 0 ºC and poured into 200 mL of 0.1M K_2HPO_4 solution (pH~8, cooled to 0 ºC) through a funnel. The aqueous mixture was extracted with 3×30 mL of hexanes. The organic extracts were combined, washed with water followed by the saturated NaCl solution and then dried over Na_2SO_4. The solids were filtered and hexanes were evaporated under the reduced pressure to yield 2.31 g (quantitative yield) of the product as colorless oil.

^{1}H-NMR (400 MHz, *d_2*-dichloromethane) δ 4.23 (d, J = 7.5 Hz, 1H), 3.66 (d, J = 2.6 Hz, 1H), 3.54 – 3.42 (m, 2H), 3.32 – 3.22 (m, 2H), 2.75 (dd, J = 9.9, 7.5 Hz, 1H), 1.32 – 1.16 (bs, 2H), 0.07 (s, 9H), 0.05 (s, 9H), 0.03 (s, 9H), 0.00 (s, 9H).^{13}C-NMR (101 MHz, CD_2Cl_2) δ 100.23, 76.62, 76.19, 71.17, 62.06, 55.76, 1.19, 1.02, 0.73, 0.00.

Typical procedure for the study of polymerization kinetics of MAG

MAG (1.0741 g, 4.3442 mmol, 125 eq) was dissolved in 6.951 mL of the acetate buffer in D_2O. 4-Cyano-4-(propylthiocarbonothioylthio)pentanoic acid (**CPP**, 9.64 mg, 3.47×10^{-2} mmol, 1 eq) and 4,4'-(diazene-1,2-diyl)bis(4-cyanopentanoic acid) (**V-501**, 0.974 mg, 3.47×10^{-3} mmol 0.1 eq) in 1.737 mL of ethanol were added. The reaction mixture was connected via cannula to an empty NMR tube capped with a septum and deoxygenated by bubbling N_2 through the reaction mixture for 45 minutes. 0.5 mL of the reaction mixture was transferred into NMR tube by the nitrogen pressure. For the monomer consumption study the reaction was carried out in the NMR instrument at 70 ^{o}C and ^{1}H-NMR spectra were acquired at various time points (see Fig. 4.3 A). The reaction flask was placed in an oil bath preheated to 70 ºC and the polymerization was carried out

while vigorously stirring with a magnetic stir bar. Small portions (ca. 0.2 mL) of the reaction mixture were taken at various time points and immediately cooled by spraying into a 2 ml glass vial that was placed in an ice-bath. These samples were diluted with SEC mobile phase (1.0 wt% acetic acid/0.1 M Na_2SO_4) and analyzed with SEC (Fig. 4.3 B).

Typical ^{1}H-NMR analysis procedure to obtain the monomer consumption vs. time plot

All proton NMR spectra were analyzed following the identical procedure: the spectra were phase corrected and base line corrected using MestReNova NMR analysis software. The peak at 6.13-5.89 ppm corresponding to a vinyl proton of MAG was integrated and normalized against the hexose protons at 4.34-3.64 ppm, which remain unchanged during the polymerization.

Synthesis of $pMAG_{46}$

MAG **13** (767.8 mg, 3.105 mmol, 50 eq) was dissolved in 4.696 mL of aqueous acetate buffer. 4-Cyano-4-(propylthiocarbonothioylthio)pentanoic acid (**CPP**, 17.2 mg, 62.0×10^{-3} mmol, 1 eq) and 4,4'-(diazene-1,2-diyl)bis(4-cyanopentanoic acid) (**V-501**, 3.48 mg, 1.24×10^{-2} mmol, 0.2 eq) in 1.2422 mL of ethanol was added. The reaction flask was capped with a septum and deoxygenated by running N_2 thorough the reaction mixture for 45 minutes while vigorously stirring. The reaction flask was placed in an oil bath which was pre-heated to 70 ^{o}C and stirred for 6 h. The reaction was stopped by removing the cap and placing the flask in an ice-bath. The cooled reaction mixture was placed in a dialysis membrane with 3500 Da molecular weight cut-off. It was dialyzed

against ultra-pure water acidified to pH 4-5 with HCl. Water changes were done every 4-10 h. After 2 days of dialysis the polymer solution was frozen and lyophilized to yield 260.4 mg (33%) of a fluffy material. ^{1}H-NMR (400 MHz, D_2O) δ ppm: 5.50-5.20 (bd, 36.3H), 5.10-4.90 (bs, 9.8H), 4.25-3.30 (m, 294.7H), 2.75-2.60 (bs, 2H), 2.25-0.50 (m, 251.4H). SEC M_n=11.7 kDa, PDI=1.24.

Synthesis of MAG_{46}-*b*-[$AEMA_{48}$/AEMAfluorescein$_1$]*

** procedure description adopted from Smith A.E., Sizovs A., Grandinetti G., Xue L., Reineke T.M. Biomacromolecules, 12, 3015–3022 (2011).*

MAG_{46}-*b*-$AEMA_{48}$·48HCl **P3** (14.19 mg, 48 eq) was dissolved in 1000 μL of 0.1 M $NaHCO_3$ which was previously deoxygenated (bubbling N_2 though the solution for 30 min). The polymer solution was cooled in an ice bath and 20.0 μL of DMSO solution containing fluorescein isothiocyanate (FITC, 0.20 mg, 5.1×10^{-4} mmol, 1 eq) were added with a pipette. The reaction mixture was allowed to slowly reach room temperature. After 12 h of stirring the reaction mixture was placed in a dialysis bag (MW cutoff 3500 Da) and dialyzed for 8 h against each of the following aqueous solutions: 0.1 M NaCl (4 L x 2), 0.07 M NaCl (4L), 0.03 M NaCl (4L), H_2O (4 x 3). The content of the dialysis bag was then transferred into a vial and lyophilized, yielding bright yellow powder.

Polymerization kinetics of MAG-*st*-AEMA

α-2-Methacrylamido-deoxy-glucose (MAG, 98.9 mg, 0.400 mmol, 60 eq) and aminoethylmethacrylamide hydrochloride (AEMA·HCl, 65.6 mg, 0.400

mmol, 65 eq) were dissolved in 1.600 mL of the acetate buffer in D_2O. MeOD (308.4 µL) was added followed by 54.9 µL of the MeOD solution containing 4-cyano-4-(propylthio-carbonothioylthio)pentanoic acid (CPP, 1.85 mg 6.67×10^{-3} mmol, 1 eq) and 36.7 µL of the MeOD solution containing radical initiator 4,4'-(diazene-1,2-diyl)bis(4-cyanopentanoic acid) (V-501, 0.187 mg, 6.67×10^{-4} mmol, 0.1 eq). The reaction flask was connected to an NMR tube with a cannula and the setup was deoxygenated by bubbling N_2 through the solution for 45 minutes. 0.5 mL of the reaction mixture was then transferred into NMR tube by the nitrogen pressure. For the monomer consumption study the reaction was carried out in the NMR instrument at 70 ^oC and spectra were acquired at various time points (Fig. 4.13). After 9 h the reaction mixture was exposed to air and cooled down on ice. It was placed in a dialysis bag (MW cutoff 3500 Da) and dialyzed for 8 h against the solutions of 0.1 M NaCl (4 L x 4) followed by the dialysis against ultrapure water (4L x 6). The polymer solution was then placed in a vial and lyophilized to yield white fluffy powder. The composition analysis of the obtained polymer was done using ^1H-NMR and D_2O as a solvent (see Fig. 4.13 C).

Heparin exclusion assay

The stock solutions of pDNA and polymer P3 (MAG_{46}-$AEMA_{48}$) were prepared in DNase/RNase-free water at a final concentrations of 0.1 mg/mL and 0.617 mg/mL respectively. The polyplexes were formulated at N/P=5 by pipetting 100 µL of the polymer solution into 100 µL of the pDNA solution and the resulting formulation was incubated for 1 h at room temperature. After 1 h 10 µL aliquots of the polyplex solution were pipetted into 10 µL of the heparin sulfate ammonium salt solutions of various

concentrations ranging from 300-900 μg/mL. These solutions were allowed to incubate for 15 minutes at room temperature.

For comparison polyethyleneimine (PEI) polyplexes were prepared using the same pDNA stock solution (c=0.1 mg/mL) and commercially available PEI solution (PolyPlus Transfections, Illkirch, France). The polyplexes were formulated at N/P=5 by pipetting 100 μL of PEI solution into the equal volume of pDNA solution. PEI polyplexes were allowed to incubate for 1 h. After 1 h, identical to P3 polyplexes, 10 μL aliquots of the PEI-polyplex solution were pipetted into 10 μL of the heparin sulfate ammonium salt solutions of various concentrations ranging 300-900 μg/mL. These solutions were allowed to incubate for 15 minutes at room temperature.

A loading buffer (1μL of Blue juice^{TM}) was added to each sample and 10 μL portions were transferred on the agarose gel, 0.6% w/w agarose gel was prepared by dissolving 0.3 g of agarose in 50 mL of TAE buffer at ca. 90 ºC. The resulting agarose solution was allowed to cool down to ca. 40-45 ^{o}C and 3 μL of ethidium bromide solution was added. Electrophoresis was conducted at 60 V for 45 min. Gels were visualized using 312 nm UV light to detect ethidium bromide.

Cellular uptake

(biological procedures were adapted from reference 16)

HeLa (human cervix adenocarcinoma) cells were cultured according to the established protocol (ATCC, Rockville, MD). Cells were seeded on six-well plates at 250 000 cells/well and allowed to incubate in supplemented DMEM at 37 ºC and humidified atmosphere that contained 5% CO_2 for 24 h. Fluorescently labeled (Cy5-labeled) pDNA

was prepared with a Label-IT Cy5 DNA labeling kit (Mirus, Madison, WI) according to the manufacturers protocol. The polyplexes were prepared by combining 250 μL of Cy5-labeled pDNA (5 μg) with 250 μL of P1, P2, or P3 at N/Ps of 2, 5, 10 or with 250 μL of JetPEI (N/P = 5) or Glycofect (N/P = 20). The cells were then transfected with 0.5 mL of the polyplex solutions in 1.0 mL of either Opti-MEM (serumfree media) or DMEM (10% FBS). The cells were incubated with each solution for 4 h to allow internalization of the polyplexes. After 4 h, supplemented DMEM was added, and the cells were incubated for an additional 20 h. The cell growth medium was replaced with supplemented DMEM 24 h after transfection. 48 h after initial transfection, the cells were incubated in CellScrub for 15 minutes at RT, trypsinized, pelleted, and resuspended in phosphate-buffered saline (PBS). A FACSCanto II (Becton Dickenson, San Jose, CA) equipped with a heliumneon laser to excite Cy5 (633 nm) was used. A total of 10 000 events were collected in triplicate for each sample. The positive fluorescence level was established by visual inspection of the histogram of negative control cells such that <1% appeared in the positive region.

Evaluation of the polyplex influence on cell viability via MTT assay

Cell viabilities after treatment with polyplexes of P1, P2, P3, and the positive controls were measured by an MTT assay. Cells were plated at a density of 50 000 cells/well in a 24-well plate. The cells were incubated for 24 h prior to transfection. Polyplexes were formulated in the same manner as described above using pCMV-luc plasmid and diluted with either OptiMEM or DMEM. Cells were transfected in triplicate with 1 μg of plasmid DNA added to each well. After 4 h, 800 μL of DMEM was added to

each well. The medium was replaced 24 h after the transfection with 1mL of DMEM. After 48 h, cells were washed with 0.5 mL of PBS per well, and 1 mL of DMEM containing 10% FBS and 0.5 mg/mL of MTT reagent was added to the cells. Cells were incubated with the MTT-containing media for 1 h at 37 ºC, the medium was aspirated off, cells were washed with PBS, and 600 μL of DMSO was added to each well. Cells were incubated on a shaker for 15 min to ensure even distribution of the purple formazan. Subsequently, 200 μL was pipetted out of each well and into a clear 96-well plate and analyzed for absorbance at 570 nm using a Tecan GENios Pro plate reader (TECAN US).

Gene expression promoted by P1, P2 and P3

To determine the transgene expression and cytotoxicity of the polyplexes, HeLa cells were cultured in 24-well plates (50 000 cells/well) in a manner similar to that described above and incubated for 24 h prior to polyplex exposure. Polyplexes were prepared immediately before transfection by combining solutions of each polymer (150 μL) with an equal volume of pDNA (3 μg) at N/P values of 2, 5, and 10. As positive controls, polyplexes formed with JetPEI (N/P = 5) and Glycofect (N/P = 20) were prepared. The polyplex mixtures were incubated for 1 h and diluted to 900 μL with either Opti-MEM or DMEM. The cells were transfected with 300 μL of polyplex solution or with naked pDNA in triplicate. After 4 h, 800 μL of DMEM was added to each well. The medium was replaced 24 h after the transfection with 1 mL of DMEM. After 48 h, the cells were washed with 500 μL of PBS and treated with lysis buffer (Promega, Madison, WI) for 15 min at room temperature. Aliquots (5 μL) of cell lysates were examined on 96-well plates with a luminometer (GENios Pro, TECAN US, Research Triangle Park,

NC) for luciferase activity. The amount of protein in the cell lysates was measured according a standard curve of bovine serum albumin by following the protocol provided by Bio-Rad (Hercules, CA) DC protein assay kit.

Confocal Microscopy

HeLa cells were seeded onto PLL-coated coverslips in a 12-well plate at 15 000 cells/well and incubated in DMEM containing 10% FBS at 37 C, 5%CO2 for 48 h to reach confluency. After incubation, polyplexes were formed by adding 50 μL of FITC-labeled P3 to 50 μL of a 0.02 mg/mL Cy5-labeled pDNA solution (1 μg) to give 100 μL of polyplex solution at an N/P ratio of 5. The DMEM was aspirated off the cells, cells were washed with 1 mL of PBS/well, and 1 mL of Opti-MEM was added to each well. The 100 μL of polyplex solution was added to each well, giving a total of 1 μg of pDNA/well. Four hours after transfection, 1 mL of supplemented DMEM was added to each well. Cells were fixed in 4% paraformaldehyde 4, 24, 48 h after transfection, stained with 4,6-diamidino-2-phenylindole (DAPI) (Molecular Probes) according to manufacturer's protocol and mounted on microscopy slides using ProLong Gold Antifade Reagent (Molecular Probes) according to the manufacturer's protocol. The slides were allowed to dry overnight in the dark before being sealed with clear nail polish and imaged on a Zeiss LSM 510 META confocal microscope (Carl Zeiss MicroImaging, LLC, Thornwood, NY). Images were taken using a slice thickness of 0.8 μm. Mander's coefficients were used to determine colocalization between P3 and plasmid DNA as previously described[21,22] and were obtained using the software NIH ImageJ.

4.3 Discussion

Similarly to the approach discussed in chapter 3 for the trehalose-based polymers, RAFT polymerization was used to create diblock copolymers with 2-methacrylamido-2-deoxy-glucose. These cationic diblock copolymers were evaluated as delivery vehicles for plasmid DNA (pDNA) in human cervical carcinoma cell line (HeLa) to reveal high delivering efficiency combined with low toxicity. In addition, polyMAG was demonstrated to stabilize polyplexes in the cell culture media even in the presence of serum proteins. These results are discussed in detail in this section.

For practical usability and extensive study of the polymer properties it is important to have straightforward access to the monomers. Synthesis of the carbohydrate containing molecules is often challenging due to their high polarity and insolubility in organic solvents. High polarity is an obvious obstacle for one of the traditional purification approaches – column chromatography with silica gel or alumina. The preferred purification way would be crystallization; however, crystallization, is not always possible.

The known methods for the synthesis of 2-deoxy-2-methacrylamido glucose (MAG) are based on the reaction of commercially available 2-deoxy-2-glucosamine hydrochloride with methacryloyl chloride in either water or methanol in the presence of a base (NaOMe, K_2CO_3, $NaHCO_3$) and KNO_2 as inhibitor.[23,24] The purification is done by first removing salts by filtration of the methanolic solution, followed by the addition of silica gel to the filtrate and removal of the solvent under the reduced pressure. The obtained crude mixture dispersed on the silica gel is loaded onto the silica gel column (solid load) and then separated using DCM/MeOH or EtOAc/MeOH solvent mixture as

an eluent. The best reported conversion using this procedure is 58%[24] and the isolated yield 32%.[23] Reproducing this procedure on the 10 g scale, 400 g of silica gel and 4 L of the eluent had to be used to wash all the product (MAG) off the silica gel column (2.7 g of MAG were collected in ca. 2.5 L of the eluent). Low yield, lengthy purification and the large amounts of solvents required for the purification prompted the improvement of the synthetic procedure.

The initial step was aimed at solving the problem of the incomplete conversion of the glucosamine. Since the obvious side reaction in water was the hydrolysis of methacryloyl chloride it was decided that methacryloylation should be carried out in methanol. Methylmethacrylate produced in this case as a side product can further react with amino group to give the desired MAG.

Scheme 4.1: Direct synthesis of MAG

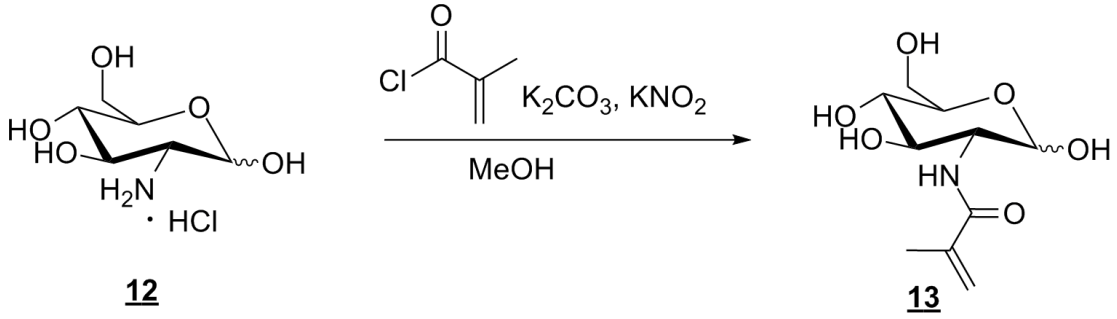

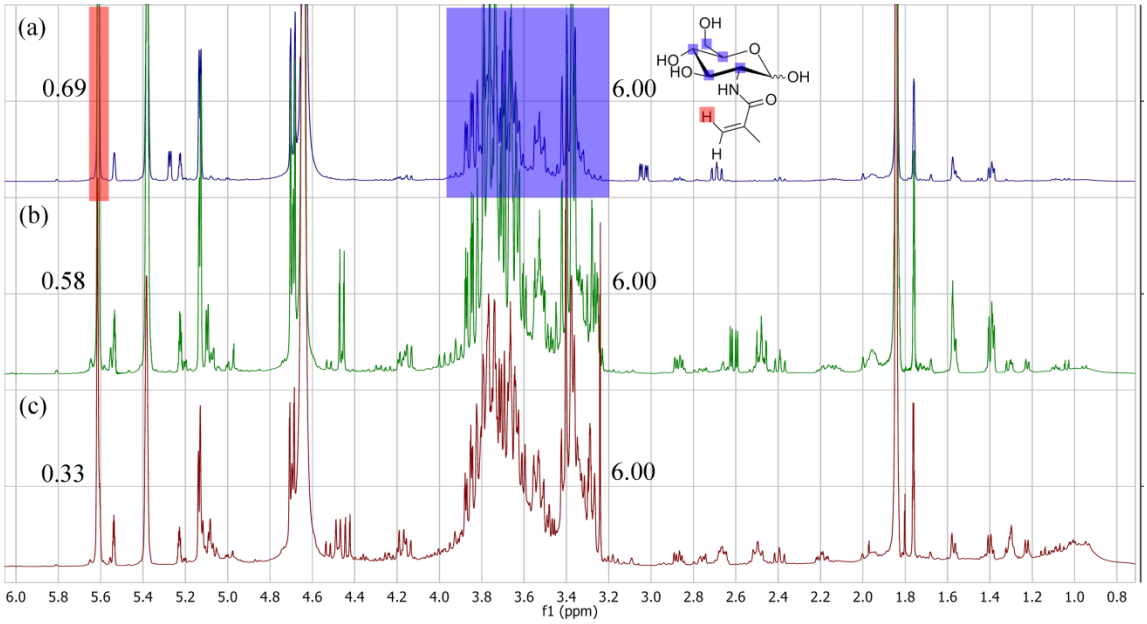

Figure 4.1 ^{1}H-NMR in D_2O obtained for the crude products of the reaction between glucosamine and 1 eq (a), 2 eq (b) and 4.6 eq (c) of methacryloyl chloride.

The reactions were carried out between 1 g of glucosamine hydrochloride and 1, 2 or 4.6 equivalents of methacryloyl chloride. The reactions were allowed to proceed for 12 h at room temperature. Methanol was evaporated; the crude product was re-dissolved in water and the aqueous solutions were washed with DCM to remove methyl methacrylate. The aqueous solutions were then frozen, lyophilized and subsequently analyzed with ^{1}H-NMR (**Fig 4.1**).

The region between 3.20-4.00 ppm corresponds to 6 hexose hydrogens and was used as a reference for the integration. The conversion was assessed by the integration of a vinyl peak at 5.61 ppm. It was observed that the number/amount of the side products

increased with an increase in equivalents of methacryloyl chloride (**Fig. 4.1a** and **Fig. 4.1c**).

A plausible route to the side products could be methacryloylation of the hydroxyls. Indeed, the side product that is visible on TLC with *p*-anisaldehyde stain (typically used to visualize carbohydrates) was less polar (R_f=0.42) than MAG (Rf=0.17, 0.23 for the two anomers) and it was suggested that this side product corresponds to the glucosamine derivative with two methacryl groups:

Scheme 4.2. Possible side reaction in the direct synthesis of MAG:

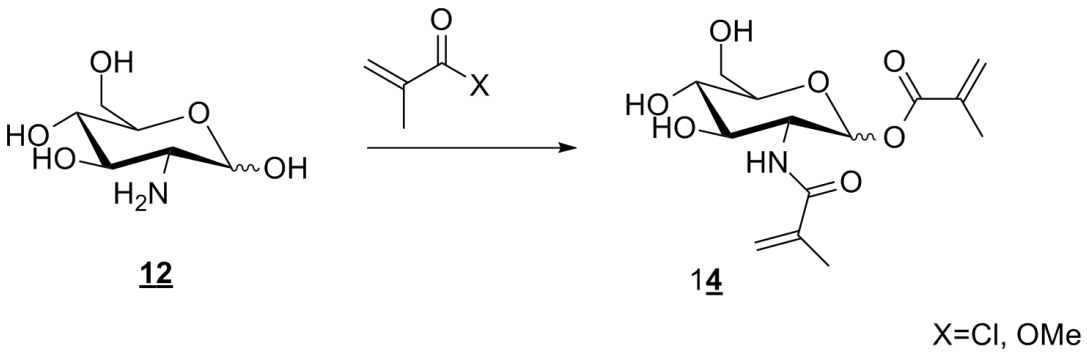

12 **14**

The non-polar impurity was collected during the chromatography, but ^{1}H-NMR analysis was not informative (**Fig 4.2b**)

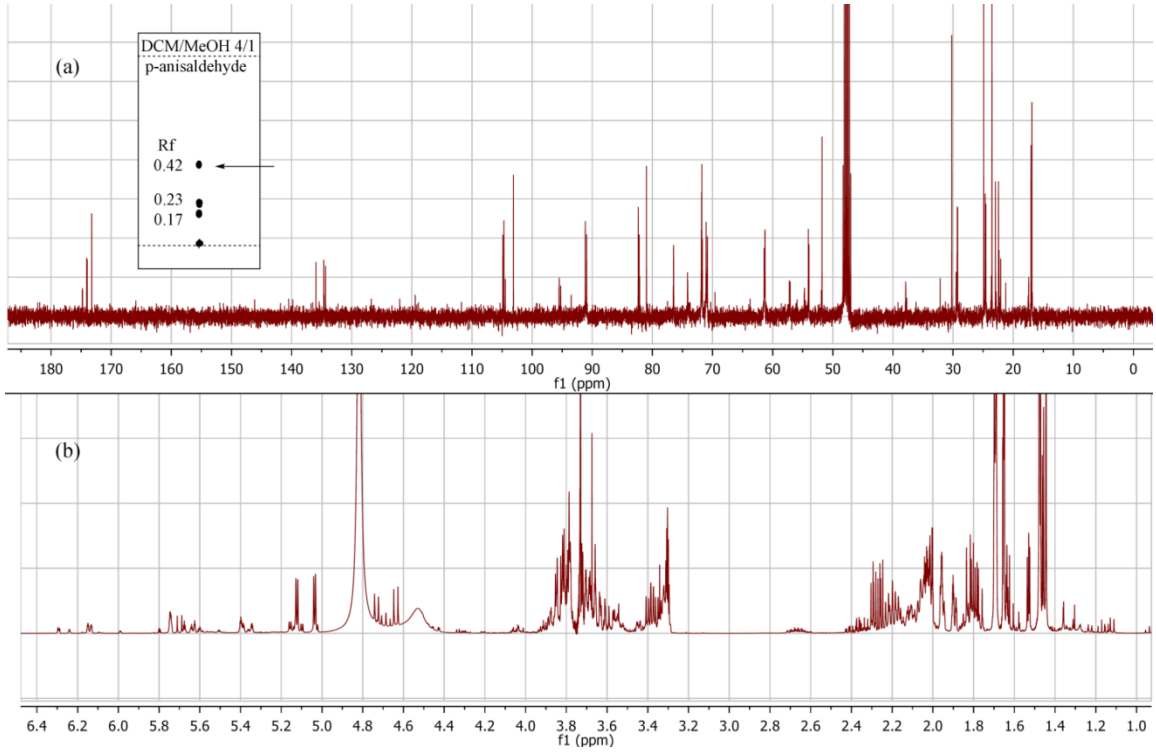

Figure 4.2. ^{13}C NMR (a) and ^{1}H-NMR (b) spectra of the non-polar impurity in a direct MAG synthesis

Both of the impurities (R_f=0.42, R_f~0) were generated regardless of the equivalents of methacryloyl chloride being used. It became clear that the column chromatography could not be avoided or simplified by varying the ratio between glucosamine and methacryloyl chloride.

In the next approach it was decided to introduce easily removable protecting groups for the hydroxyls. The major goal was not to protect hydroxyls from the side reactions, but to improve the solubility of the carbohydrate derivative in organic solvents. This would allow to remove chloride salts that are produced and to simplify the purification by chromatography. After thorough consideration, the trimethylsilyl (TMS) group was chosen for three reasons: (1) the protection of the hydroxyl group typically

relies on its nucleophilicity; however, amino group of glucosamine if a far better nucleophile and would be protected before the hydroxyls based on that principle. However, the Si-N bond is heterolytically weak and the TMS-amine functionality formation would not possess a problem; (2) four TMS groups would make the hexose very non-polar; (3) removal of the TMS group can be easily done in mildly acidic conditions producing volatile byproducts.

Scheme 4.3. Synthesis of MAG using TMS-protection strategy

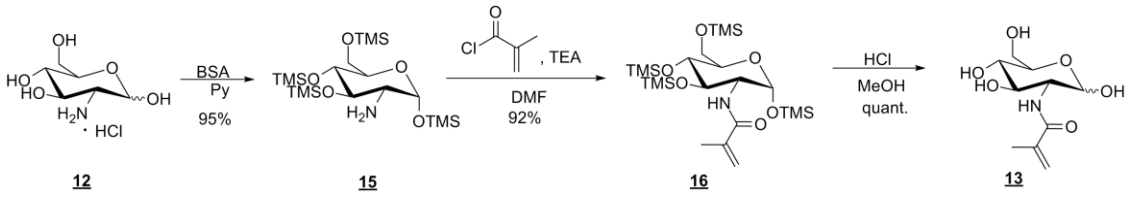

This strategy worked perfectly. The TMS protection was accomplished in pyridine using bis(trimethylsilyl)acetamide.[25] After the completion of the reaction, the reaction mixture was poured into phosphate buffer (pH=8) and extracted with hexanes to give the pure product – TMS protected glucosamine ($Glu(TMS)_4NH_2$). Moreover, when the reaction was carried out on the large scale (>1g of glucosamine hydrochloride) pouring the reaction mixture into aqueous phosphate solution results in the precipitation of the pure product as a white solid, which can be filtered off. The reaction is highly efficient giving the desired compound in 95% yield.

The methacryloylation of $Glu(TMS_4)NH_2$ can be done *in situ* with the protection; however, this caused the reaction mixture to become yellow-to dark orange. Additionally,

on the large scale formation of a side product which was not identified was observed using a one pot approach. Therefore all three steps starting with the glucosamine hydrochloride were performed as separate reactions.

The reaction of methacryloyl chloride with $Glu(TMS)_4NH_2$ was successfully carried out in DMF using triethylamine as a scavenger of HCl. The work-up was similar to the previous step; however the solid that is produced upon the aqueous work-up is not suitable for the filtration and the extraction is necessary regardless of the reaction scale. Evaporation of the dried hexane solution gave TMS-protected MAG ($MAG(TMS)_4$) in 92% yield as a pure white solid.

For the deprotection $MAG(TMS)_4$ was dissolved in dry MeOH and addition of the HCl solution in methanol at room temperature caused the instantaneous removal of TMS groups (TLC). The solvent was then removed to provide MAG as a white solid.

It is important to note here that dissolving the final product in water *sometimes* yields a milky solution. The composition of the dispersed particles was not determined as they are 'invisible' in the ^{1}H-NMR. They do dissolve when methanol is added, but no signals were observed in the ^{1}H-NMR performed in a mixture of d_4-methanol/D_2O.

In addition, due to the simplicity and the high yields, this approach has a great potential in glycopolymer field by allowing an easy access to some of the carbohydrate monomers. Indeed, the high yields are especially important in cases when the starting hexosamine is not readily available or is of a very high value. To test whether the described protocol can be extended to other carbohydrate amines 2-methacrylamido-2-deoxy-galactose was prepared starting from galactosamine hydrochloride. Similar to the

MAG synthesis, this procedure yielded the desired galactose derivative in high yield and without need for purification.

The polymer synthesis was performed following a typical reversible addition-fragmentation chain transfer(RAFT) polymerization procedure.[26] 4-Cyano-4-(propylthiocarbonothioylthio)pentanoic acid (CPP) was used as an easily accessible[27] chain transfer agent and 4,4'-azobis(4-cyanovaleric acid) (V-501) as a radical initiator.

The kinetics of the polymerization were established by means of ^{1}H-NMR (by monitoring the monomer consumption) and by means of SEC (by monitoring the molecular weight of the polymer). The results of the two methods were in a good agreement and the polymerization proceeded without any complications.

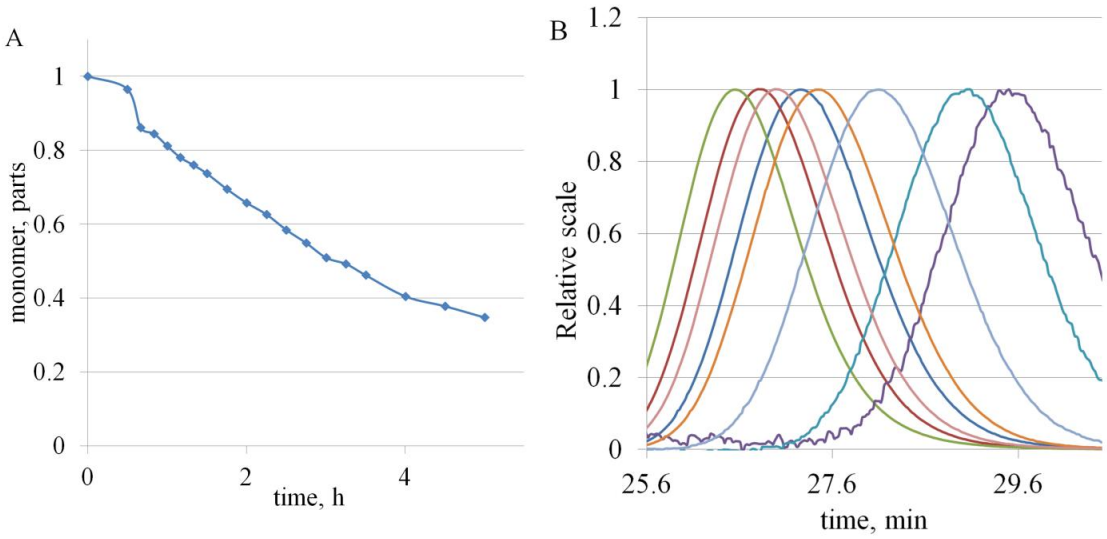

Figure 4.3. Monomer (MAG) consumption kinetics derived from ^{1}H-NMR experiments (A). SEC traces of the polymers obtained by varying the reaction time (B).

PolyMAGs (pMAGs) of various lengths were synthesized by varying the CTA to monomer ratio and the reaction time (Table 4.1).

Table 4.1. Results of SEC analysis of synthesized pMAG polymers.

M_w, kDa	M_n, kDa	PDI	dp_n
14.5	11.7	1.24	46
17.8	15.2	1.17	60
24.7	21.4	1.15	85
29.1	25.1	1.16	100
32.4	29.2	1.11	117
36.7	32.9	1.12	132
41.7	36.0	1.16	145

It was expected that pMAG polymers will not have acute cellular toxicity because these glycopolymers are neutral, well soluble in water and are grafted with natural saccharides. Indeed, as it can be seen from the MTT assay ((3-(4,5-dimethylthiazol-2-yl)-2,5-diphenyl**t**etrazolium bromide assay) the mitochondrial reductase activity was not affected by pMAG of different lengths even at concentrations as high as 10 mg/mL.

During the initial stages of this work the choice of the polymer length was arbitrary. Narain et al. have recently studied diblock polymers containing a block grafted with gluconamides and a block containing primary amines for nucleic acid complexation.[28] It was demonstrated that diblock polymers having 46 repeat units in a sugar containing block were capable of binding pDNA and forming nanoparticles. It

should be noted, however, that there is a significant difference in properties between gluconamide and glucosamide (namely, 2-deoxy-2-methacrylamidoglucose, MAG): gluconamide is not capable of closing in a pyranose ring (Scheme 4.4).

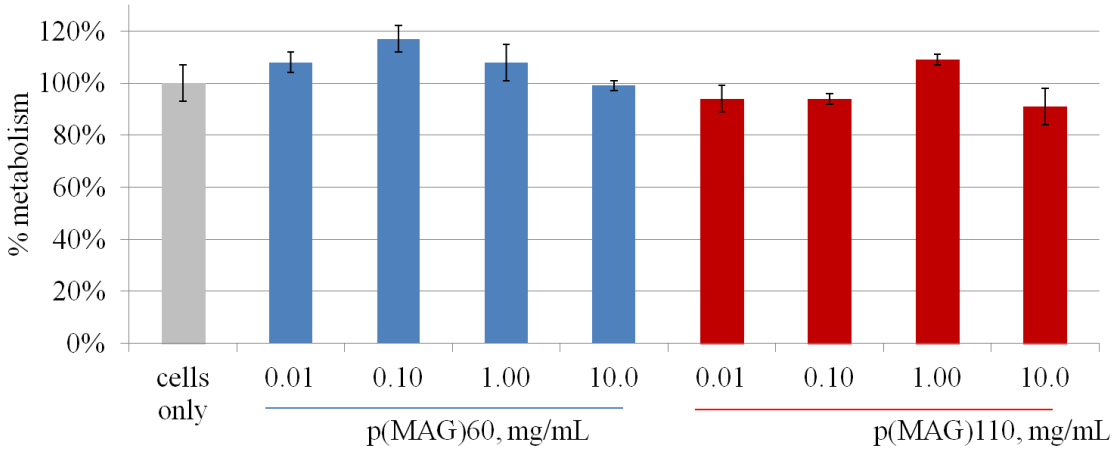

Figure 4.4. MTT assay performed with various concentrations of $p(MAG)_{60}$ and $p(MAG)_{110}$ in U-87 cells. Experiment performed by Lian Xue.

Scheme 4.4. Equilibria between open chain and pyranose forms of MAG and gluconamide.

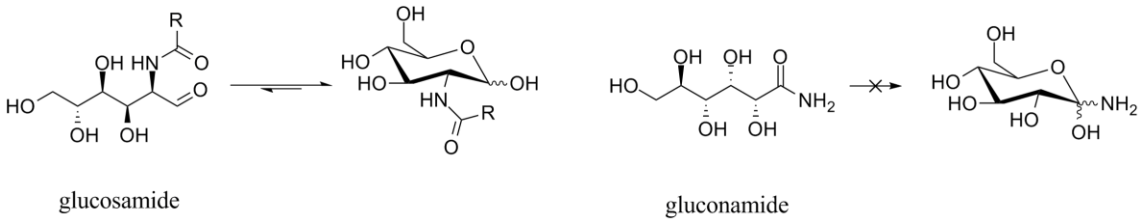

Nonetheless, there are obvious similarities between the gluconamides and MAG; therefore, a carbohydrate containing block with 46 repeat units was chosen for the initial biological evaluation. We expected good pDNA binding properties similar to those demonstrated in Narain's work, and also allow for direct comparison between the two

glycopolymers to shed some light on the influence of the pyranose ring on the properties of the material.

Second blocks of various lengths were synthesized using N-(2-aminoethyl)methacrylamide (AEMA) monomer, $p(MAG)_{46}$ as a chain transfer agent (macroCTA) and V-501 as an initiator. Lengths of the second block were chosen to be 21, 39 and 48 repeat units.

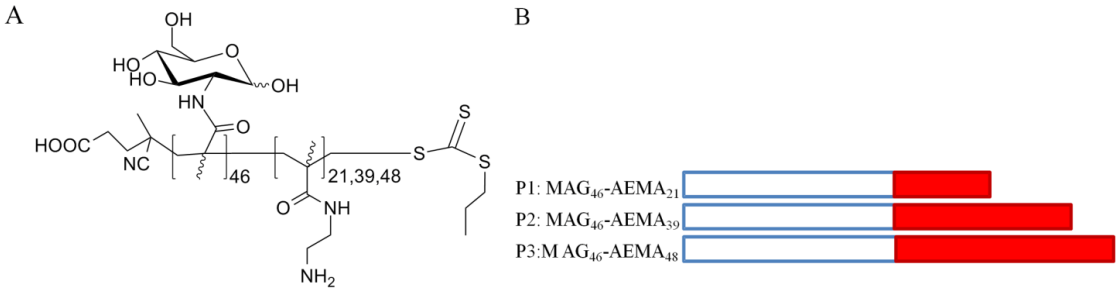

Figure 4.5. A. Polymer structures: P1(MAG_{46}-$AEMA_{21}$), P2(MAG_{46}-$AEMA_{39}$), P3(MAG_{46}-$AEMA_{48}$). **B.** Visual representation of the polymers. Relative ratios of the depicted block lengths are proportional to the relative ratios of block lengths. Cationic blocks were synthesized by Adam Smith.[18]

All three polymers were demonstrated to bind pDNA at low N/P ratios (Fig. 4.6). It is interesting to note here that although the difference between pDNA binding ability is insignificant but it is noticeable: polymer P1 retards the electrophoretic pDNA migration at a lower N/P ratio than P2 and P3. This phenomenon could be explained by a higher degree of freedom that the primary amine groups have in polymer P1: at the same N/P ratio the number of polymer P1 molecules is 48/21~2.3 times greater than the number of

P3 molecules. Hence, polymer P1 amino groups can more readily adopt a conformation favorable for pDNA binding, because the aminogroups on average are 2.3 times more independent from each other with respect to spatial orientation.

One of the most intriguing aspects of this research was the study of the colloidal stability of the polyplexes especially in the presence of serum proteins. Presumed such stability was based on the assumption that the dehydration of the well-hydrated carbohydrate residues will require a lot of energy, thus creating high a activation barrier for the non-specific interactions between glycopolymer-coated nanoparticles and proteins.

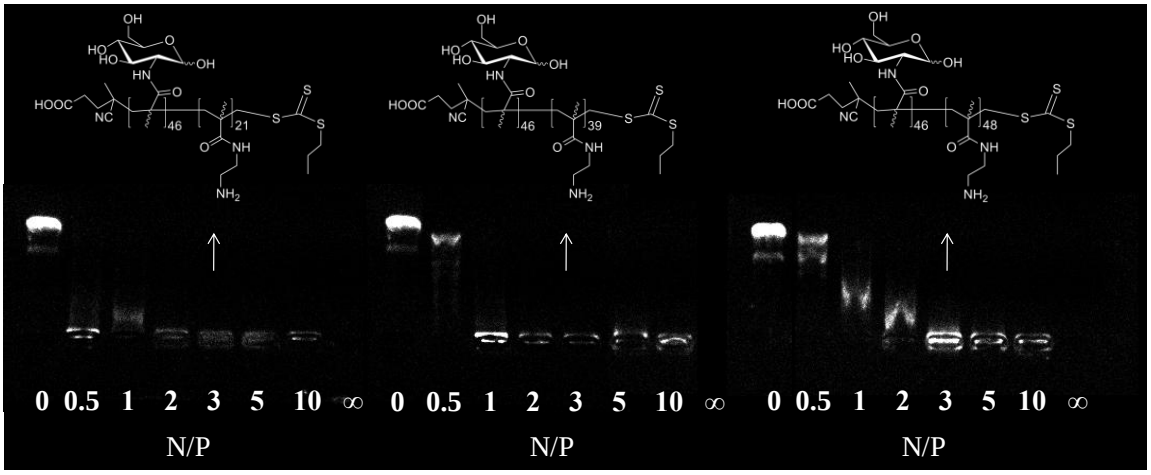

Figure 4.6. Photograph of agarose gel after electrophoresis. Arrows point towards anode(+) and indicate the direction of movement of free (unbound) pDNA.

Dynamic light scattering (DLS) was used to monitor the sizes of the polyplexes formed between pDNA and three diblock polymers P1, P2 and P3. This study was conducted in two cell culture media commonly used for *in vitro* assays, namely OptiMEM and DMEM with 10% fetal bovine serum (FBS). The time that is typically

used for the transfections is 3 h and 4 h; therefore, the stability of the polyplexes in solutions was monitored for 4 h (Fig. 4.7).

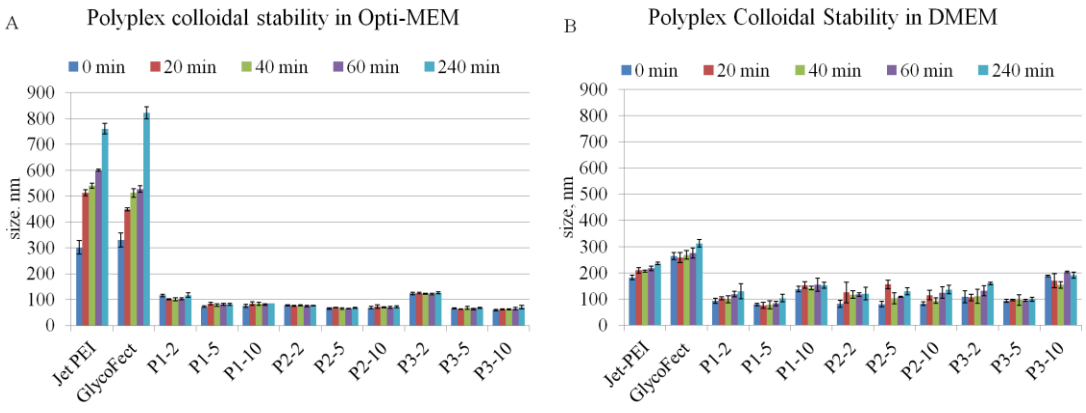

Figure 4.7. DLS measurements based on scattering intensity of polyplexes in OptiMEM(A) and DMEM containing 10% serum (B). JetPEI and GlycoFect correspond to the polyplexes formulated with commercially available transfection agents with the same names. Labels stand for "polymer–N/P ratio". Experiment was performed with Dr. Adam Smith.[18]

The results clearly demonstrate no increase in size over the tested period. Especially dramatic differences among polymers P1, P2, P3 and the commercially available gene delivery agents JetPEI® and GlycoFect® were observed in OptiMEM, while in serum containing DMEM controls did not increase in size significantly. Additionally, the sizes of the polyplexes of 70-100nm in OptiMEM and 120-190nm in DMEM are suitable for endocytosis.[29]

Endocytosis is a likely way of the polyplex entry into the cell, although multiple internalization routes have been previously observed.[30] To measure the efficiency of the internalization the fluorescently labeled plasmid (Cy5-labeled plasmid) was used in the formulation of polyplexes. HeLa cells were transfected with these polyplexes and the fluorescence was measured by the flow cytometry (Fig. 4.8).

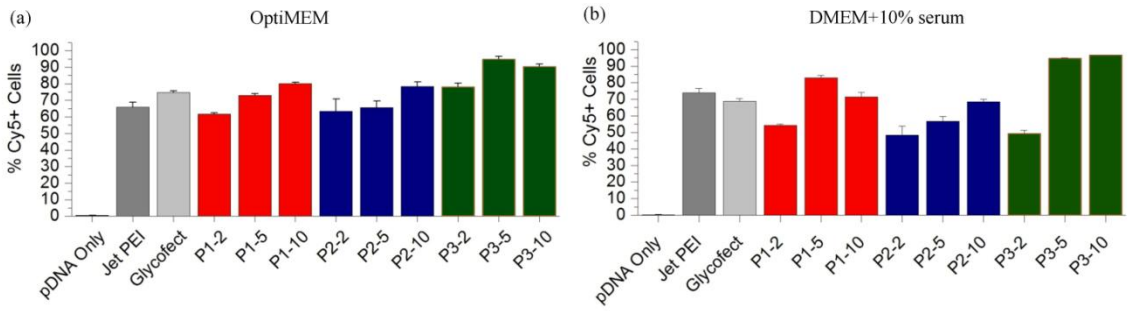

Figure 4.8. Flow cytometry results for HeLa cells transfected with polyplexes formulated with Cy5-labeled pDNA. pDNA only means that no transfection agent was used (negative control), JetPEI and GlycoFect correspond to polyplexes formulated with commercially available transfection agents with the same names. Labels stand for "polymer_name–N/P ratio". Experiment performed by Giovanna Grandinetti.

The internalization of P1, P2 and P3 derived polyplexes in OptiMEM was similar or more efficient than both of the positive controls (PEI and Glycofect polyplexes). Thus the polyplexes which were formulated with polymer P3 at NP=5 deliver Cy5-pDNA to 90% of the cells (Fig. 4.8 A). Furthermore, the presence of serum proteins did not impact the ability of diblock glycopolymers to deliver its cargo. Again, polymer P3

outperformed P1 and P2, delivering the fluorescently labeled pDNA to 95% of the cells at N/P ratios 5 and 10.

The efficiency of the cellular internalization is an important step in gene delivery. However once the polyplex is inside the cell it has other obstacles that must be overcome: endosomal/lysosomal escape, nuclear trafficking, nuclear internalization and finally gene expression. [31-34] Gene expression was measured to assess how well all these barriers are overcome by the delivery system. It is routinely done by using a reporter gene. In the case of P1, P2 and P3 a reporter gene that codes for luciferase was used.[35] If luciferase is expressed it will produce light (fluorescence) in the presence of the substrate – luciferin. By measuring the fluorescence the gene expression is assessed.

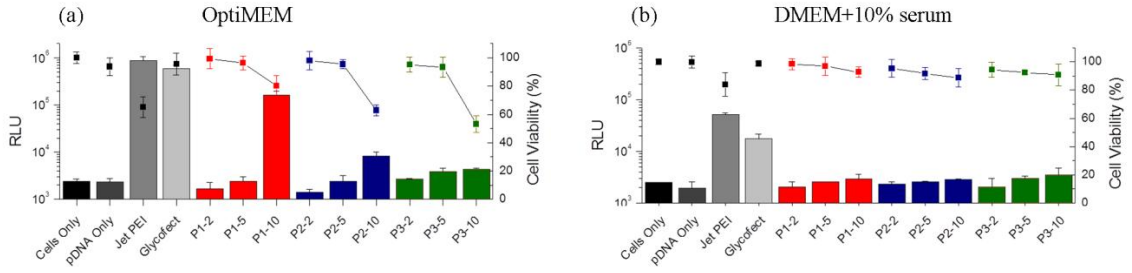

Figure 4.9. Luciferase gene expression by HeLa cells transfected with luciferase-pDNA containing polyplexes in OptiMEM (a) and serum containing DMEM (b). JetPEI and GlycoFect correspond to the polyplexes formulated with the commercially available transfection agents with the same names. Labels stand for "polymere–N/P ratio". Experiment performed by Giovanna Grandinetti.[18]

Despite the great cellular uptake that was demonstrated by all of the tested formulations, significant gene expression was observed only for the formulations that were prepared at high N/P ratios. It should also be noted that in OptiMEM the cell

viability decreases with the increase in N/P ratio from 5 to 10, which is more profound for P2 and P3-derived formulations (Fig 4.9 a).

Confocal microscopy was used to investigate the polyplex trafficking and the disassociation of the polyplex inside the cells. Having different fluorescent dyes on pDNA and a polymer that can be excited and observed independently allows studying the co-localization of the two formulation components. By monitoring the change in co-

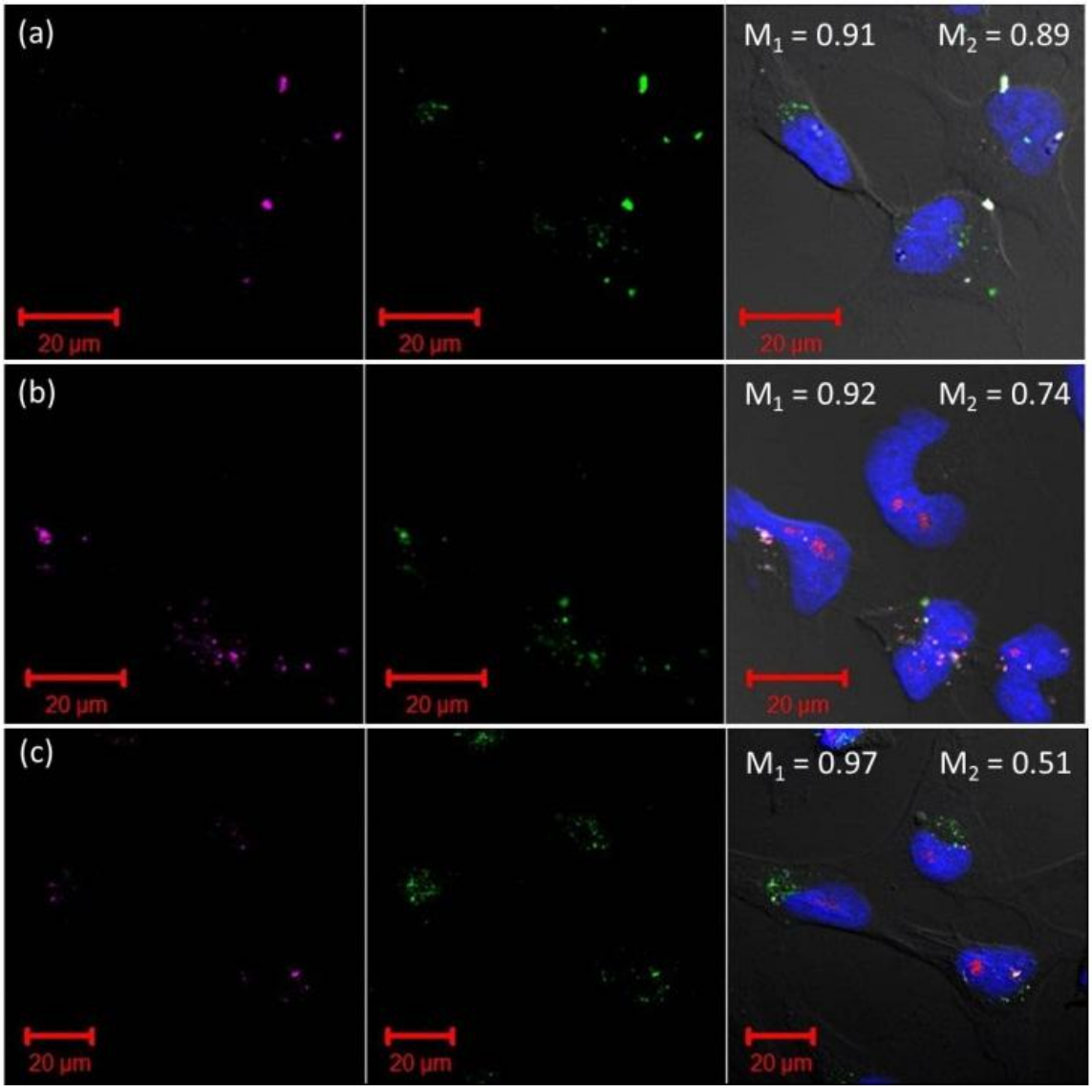

Figure 4.10. Confocal microscopy images of HeLa cells transfected with polyplexes with formulated with P3-FITC(green color) and Cy5-siRNA(magenta color). Nucleus was stained with DAPI (blue color).Experiment performed by Giovanna Grandinetti.[18]

localization over time it is possible to gain the information on pDNA release and the polyplex fate.[22] Polymer P3 was labeled with fluorescein isothiocyanate (FITC) in aqueous sodium bicarbonate solution, and it was subsequently used to formulate the polyplexes with commercially available Cy5-labeled pDNA at N/P ratio 5. HeLa cells were transfected with the obtained fluorescent polyplexes and micrographs were obtained using confocal microscopy at various time points (Fig. 4.10).

The signal overlap between the two dyes can be calculated to obtain Mander's coefficient *M*.[21,22] It can be calculated two ways: as the extent of overlap of Cy5 with FITC (M_1), and as the extent of overlap of FITC with Cy5 (M_2) [*For easy understanding imagine a pancake with an area of 100 cm^2 on a plate with an area of 1000 cm^2: in this case M_1 overlap of the pancake with the plate (M_1) is 100% and M_1=1.00, but the overlap of the plate with the pancake (M_2) is only 10%, therefore M_2=0.10*]. M_1 remained unchanged over a period of 48H ($M_1 \geq 0.9$), which means that during that time period most of the pDNA visible to the microscope is associated with the polymer. In contrast, M_2 decreases from 0.9 at 4H, to 0.7 at 24H, to 0.5 at 48H after the transfection. It can be reasoned that either the polyplexes become loose and the polymer is gradually 'unpeeling' from the polyplex, causing M_2 to decrease or alternatively pDNA is escaping

the polyplexes while the polymer still remains bound within the polyplex. Further investigation is required to understand the polyplex dissociation process.

There can be several reasons of why the gene expression is suboptimal and either of the barriers mentioned above could play a role. However it is evident from the microscopy results that the polyplex disassociation is slow. This observation coupled with the gel electrophoresis results points to strong polymer-pDNA binding preventing efficient cargo release.

To test this hypothesis the heparin exclusion assay was conducted. The heparin assay is a competition assay in which negatively charged heparin competes with negatively charged pDNA for the positively charged polymer.

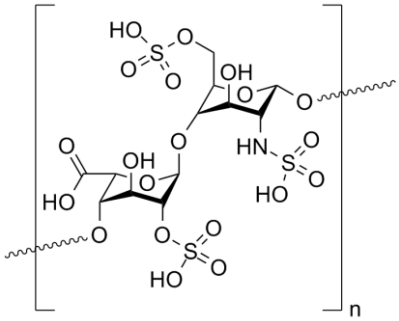

Figure 4.11. Structure of heparin. Heparin is a polysaccharide that belongs to glycosaminoglycan family and is highly negatively charged. It assumes a helical conformation in solution and is composed of various derivatives of disaccharides that are O- and N- sulfated. Iduronic acid and glycosamine derivatives are the most abundant and are depicted here.[36]

By incubating the polyplexes with heparin at various heparin concentrations it is possible to get an idea of the polyplex resistance to disassociation.[37] Keeping in mind the results of the gel electrophoresis assay performed on P1, P2 and P3-derived polyplexes (Fig. 4.6), polymer P3 was chosen as the least efficient pDNA binding polymer among the three diblock polymers. As can be seen from the heparin exclusion assay (Fig. 4.12) disassociation of Jet-PEI polyplexes happens at the heparin concentrations between 100 μg/mL and 150 μg/mL. However, to cause the pDNA release by the P3 polyplex that was formulated at the same N/P ratio of 5 the concentration of heparin must be nearly twice that value. This result indicates a significantly stronger association between the plasmid and P3 as compared to the plasmid-PEI complex. This strongly suggests that the release of pDNA in cell by pMAG-pAEMA polyplexes may be inefficient.

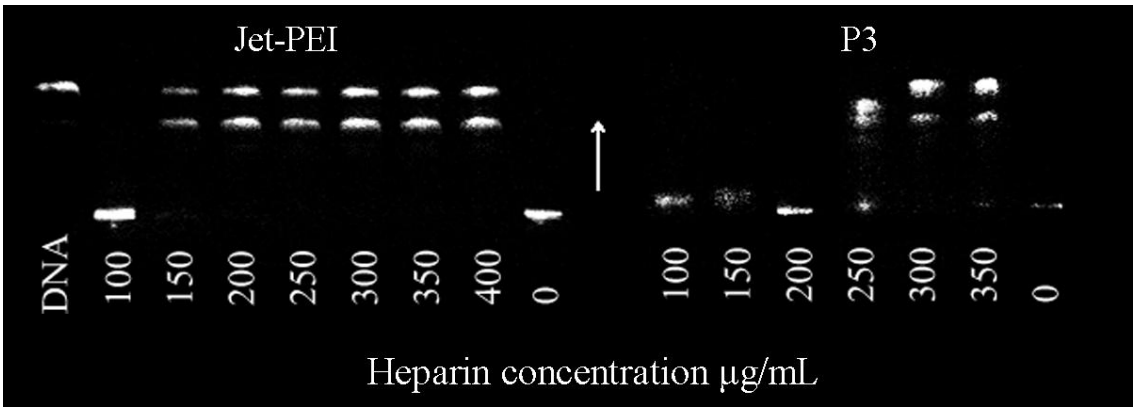

Figure 4.12. Photographs of the agarose gel after the heparin exclusion assay. Jet-PEI and P3 polyplexes were formulated with pDNA at N/P=5.

One possible way to overcome the problem of poor pDNA release is dilution of the positive charge centers (primary amines) along the backbone. This can be

accomplished by co-polymerizing both monomers MAG and AEMA is a statistical fashion and at different ratios to achieve the desirable composition. In this thesis the possibility of synthesizing the statistical polymers with MAG and AEMA has been explored.

There is a potential problem facing statistical radical polymerizations:

(1) $R_n\text{-}A\cdot + A \rightarrow R_n\text{-}A\text{-}A\cdot$
(2) $R_n\text{-}A\cdot + B \rightarrow R_n\text{-}A\text{-}B\cdot$
(3) $R_n\text{-}B\cdot + A \rightarrow R_n\text{-}B\text{-}A\cdot$
(4) $R_n\text{-}B\cdot + B \rightarrow R_n\text{-}B\text{-}B\cdot$

If the rates of the reactions in pairs (1) and (2) or (3) and (4) are significantly different, then the polymerization will result in the production of two different homopolymers (A_n and B_n) instead of the statistical polymer. In addition, if the reactivity of two monomers A and B is significantly different it will result in the polymer composition being different from the monomer feed ratio.

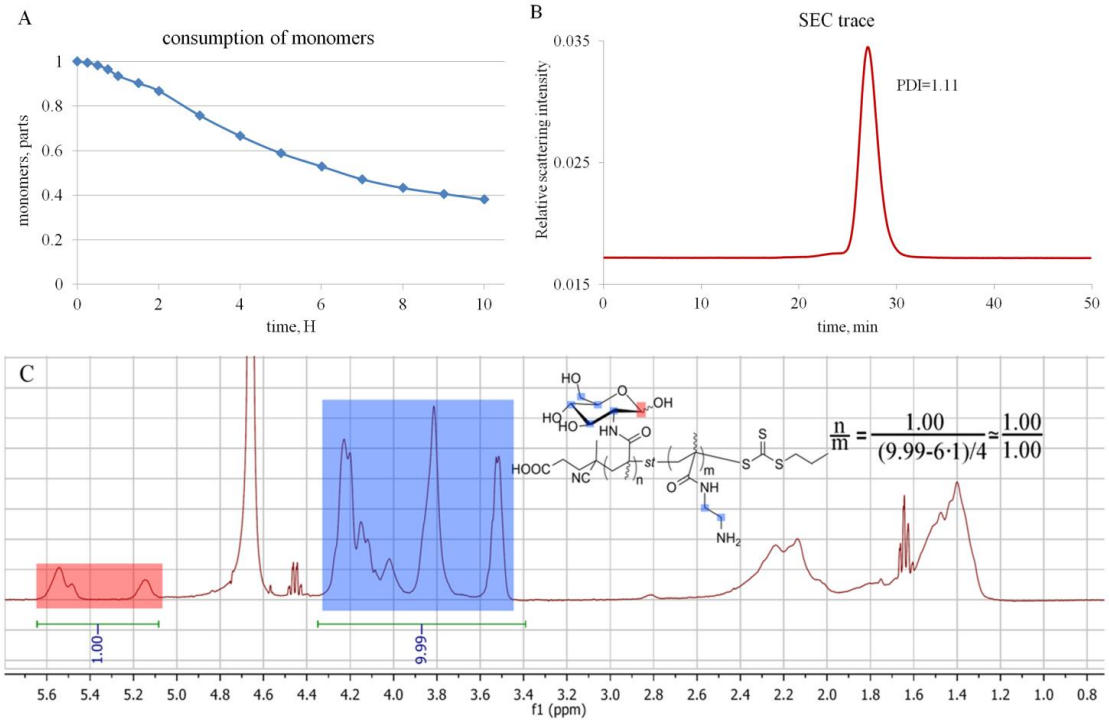

Figure 4.13. Synthesis of the statistical polymer MAG-st-AEMA with equimolar monomer feed ratio. A. Combined monomer consumption by ^{1}H-NMR. B. SEC trace of the MAG-st-AEMA polymer. C. ^{1}H-NMR of MAG-st-AEMA polymer.

None of the undesired situations described above was expected since both of the monomers had the same polymerizable moiety and similar statistical polymers have been previously synthesized;[17] however, the glucopyranose ring of MAG is significantly more bulky than the ethyleneamine moiety of AEMA. Therefore, it was important to demonstrate the absence of the difference in reactivity.

A steady monomer consumption is observed (Fig 4.13. A), suggesting no significant difference in the reactivity between the two monomers MAG and AEMA. Moreover, the SEC light scattering trace is monomodal without the presence of the

shoulders, confirming that only one polymer is generated and not a mixture of two homopolymers. Finally, it is possible to analyze the polymer composition by ^{1}H-NMR (Fig. 4.13. C). The molar ratio of monomers in a polymer is 1/1 and it proves that the synthesis of statistical polymer comprised of MAG and AEMA can be accomplished by means of RAFT polymerization with the possibility to control the polymer composition by adjusting the monomer feed ratio. Further investigation is required to establish whether statistical MAG-*st*-AEMA polymers can improve the pDNA release profile and be more efficient in promoting the gene expression as compared to MAG-*b*-AEMA polymers.

4.4. Conclusions

An efficient procedure for the synthesis of methacrylamidoglucose (MAG) was developed and the possibility of extending this procedure to other hexosamines was demonstrated with 2-amino-2-deoxy-galactose. The absence of a lengthy purification allows synthesizing these molecules on the large scale, which was accomplished with 2-amino-2-deoxy-glucose on the 20 g scale. The high yielding nature of this procedure should be especially beneficial for the modification of the hexosamines that are not readily accessible or are expensive. This protocol should be particularly useful in the field of glycopolymers.

A series of pMAG polymers was synthesized using RAFT polymerization. The polymerization was well controlled, yielding the macromolecules with low polydispersity indexes. Cationic diblock polymers $pMAG_{46}$-$AEMA_n$ were shown to efficiently bind pDNA forming the polyplexes at low amine to phosphate (N/P) ratios. These polyplexes

demonstrated great colloidal stability in two tested cell culture media, OptiMEM and DMEM, in the presence of 10% fetal bovine serum.

The polyplexes formulated with P1, P2 and P3 could enter HeLa cells well in OptiMEM and moderately well in serum containing DMEM without causing any apparent toxicity. The gene expression however was suboptimal, which could be attributed to inefficient polyplex disassociation. The dilution of the positive charges along the backbone, potentially via the synthesis of MAG-*st*-AEMA block, was suggested as a possible solution to this problem. It was demonstrated that synthesis of the statistical polymers can be accomplished using RAFT polymerization and the polymer composition can be controlled through the feed ratio.

Overall, a readily access to monomers, simple and scalable synthetic procedure, colloidal stability in the presence of serum proteins, and low cytotoxicity makes pMAG an attractive polymer to be used as an outer layer component for the nanoparticles in biomedical applications. Moreover, advances in controlled radical polymerization methods allow for polymer synthesis from the surfaces ('grafting from' approach)[38,39] which can be potentially used to grow pMAG polymers from the surfaces of pre-made nanosystems.

4.5 References

1 Tannis, A. J., Barban, J. & Conquer, J. A. Effect of glucosamine supplementation on fasting and non-fasting plasma glucose and serum insulin concentrations in healthy individuals. *Osteoarthr. Cartil.* **12**, 506-511 (2004).

2 Towheed, T., Maxwell, L., Anastassiades, T., Shea, B., Houpt, J., Robinson, V., Hochberg, M. & Wells, G. Glucosamine therapy for treating osteoarthritis. *Cochrane Database Syst. Rev.* **2** (2005).

3 Houpt, J., McMillan, R., Wein, C. & Paget-Dellio, S. Effect of glucosamine hydrochloride in the treatment of pain of osteoarthritis of the knee. *J. Rheumatol.* **26**, 2423 (1999).

4 McAlindon, T. E., LaValley, M. P., Gulin, J. P. & Felson, D. T. Glucosamine and chondroitin for treatment of osteoarthritis. *JAMA, J. Am. Med. Assoc.* **283**, 1469-1475 (2000).

5 Clegg, D. O., Reda, D. J., Harris, C. L., Klein, M. A., O'Dell, J. R., Hooper, M. M., Bradley, J. D., Bingham III, C. O., Weisman, M. H. & Jackson, C. G. Glucosamine, chondroitin sulfate, and the two in combination for painful knee osteoarthritis. *N. Engl. J. Med.* **354**, 795-808 (2006).

6 Lee, Y. Synthesis of some cluster glycosides suitable for attachment to proteins or solid matrices. *Carbohydr. Res* **67**, 509-514 (1978).

7 Stenzel, M. H., Zhang, L. & Huck, W. T. S. Temperature-Responsive Glycopolymer Brushes Synthesized via RAFT Polymerization Using the Z-group Approach. *Macromol. Rapid Commun.* **27**, 1121-1126 (2006).

8 Ting, S. R. S., Chen, G. & Stenzel, M. H. Synthesis of glycopolymers and their multivalent recognitions with lectins. *Polym. Chem.* **1**, 1392-1412 (2010).

9 Minko, T. Drug targeting to the colon with lectins and neoglycoconjugates. *Adv. Drug Del. Rev.* **56**, 491-509 (2004).

10 Seymour, L. W., Ferry, D. R., Anderson, D., Hesslewood, S., Julyan, P. J., Poyner, R., Doran, J., Young, A. M., Burtles, S. & Kerr, D. J. Hepatic drug targeting: phase I evaluation of polymer-bound doxorubicin. *J. Clin. Oncol.* **20**, 1668-1676 (2002).

11 Housni, A., Cai, H., Liu, S., Pun, S. H. & Narain, R. Facile preparation of glyconanoparticles and their bioconjugation to streptavidin. *Langmuir* **23**, 5056-5061 (2007).

12 Spain, S. G. & Cameron, N. R. Facile in situ preparation of biologically active multivalent glyconanoparticles. *Chem. Commun.*, 4198-4200 (2006).

13 Ahmed, M., Deng, Z., Liu, S., Lafrenie, R., Kumar, A. & Narain, R. Cationic glyconanoparticles: their complexation with DNA, cellular uptake, and transfection efficiencies. *Bioconj. Chem.* **20**, 2169-2176 (2009).

14 Ahmed, M., Jiang, X., Deng, Z. & Narain, R. Cationic glyco-functionalized single-walled carbon nanotubes as efficient gene delivery vehicles. *Bioconj. Chem.* **20**, 2017-2022 (2009).

15 Chen, X., Tam, U. C., Czlapinski, J. L., Lee, G. S., Rabuka, D., Zettl, A. & Bertozzi, C. R. Interfacing Carbon Nanotubes with Living Cells. *J. Am. Chem. Soc.* **128**, 6292-6293 (2006).

16 Zhou, D., Li, C., Hu, Y., Zhou, H., Chen, J., Zhang, Z. & Guo, T. Glycopolymer modification on physicochemical and biological properties of poly (l-lysine) for gene delivery. *Int. J. Biol. Macromol.* (2012).

17 Ahmed, M. & Narain, R. The effect of polymer architecture, composition, and molecular weight on the properties of glycopolymer-based non-viral gene delivery systems. *Biomaterials* (2011).
18 Smith, A. E., Sizovs, A., Grandinetti, G., Xue, L. & Reineke, T. M. Diblock Glycopolymers Promote Colloidal Stability of Polyplexes and Effective pDNA and siRNA Delivery in Physiological Salt and Serum Conditions. *Biomacromolecules* (2011).
19 Bernard, J., Hao, X., Davis, T. P., Barner-Kowollik, C. & Stenzel, M. H. Synthesis of various glycopolymer architectures via RAFT polymerization: From block copolymers to stars. *Biomacromolecules* **7**, 232-238 (2006).
20 Zhang, L. & Stenzel, M. H. Spherical Glycopolymer Architectures using RAFT: From Stars with a β-Cyclodextrin Core to Thermoresponsive Core–Shell Particles. *Aust. J. Chem.* **62**, 813-822 (2009).
21 Manders, E., Stap, J., Brakenhoff, G., Van Driel, R. & Aten, J. Dynamics of three-dimensional replication patterns during the S-phase, analysed by double labelling of DNA and confocal microscopy. *J. Cell Sci.* **103**, 857-862 (1992).
22 Manders, E., Verbeek, F. & Aten, J. Measurement of co-localization of objects in dual-colour confocal images. *J. Microsc.* **169**, 375-382 (1993).
23 Pearson, S., Allen, N. & Stenzel, M. H. Core-shell particles with glycopolymer shell and polynucleoside core via RAFT: From micelles to rods. *J. Polym. Sci. A.* **47**, 1706-1723 (2009).
24 Ting, S. R. S., Min, E. H., Zetterlund, P. B. & Stenzel, M. H. Controlled/Living ab Initio Emulsion Polymerization via a Glucose RAFT stab: Degradable Cross-Linked Glyco-Particles for Concanavalin A/Fim H Conjugations to Cluster E. coli Bacteria. *Macromolecules* **43**, 5211-5221 (2010).
25 Johnson, D. A. Simple procedure for the preparation of trimethylsilyl ethers of carbohydrates and alcohols. *Carbohydr. Res.* **237**, 313-318 (1992).
26 Moad, G., Rizzardo, E. & Thang, S. H. Living radical polymerization by the RAFT process. *Aust. J. Chem.* **58**, 379-410 (2005).
27 Xu, X., Smith, A. E., Kirkland, S. E. & McCormick, C. L. Aqueous RAFT Synthesis of pH-Responsive Triblock Copolymer mPEO− PAPMA− PDPAEMA and Formation of Shell Cross-Linked Micelles†. *Macromolecules* **41**, 8429-8435 (2008).
28 Deng, Z., Ahmed, M. & Narain, R. Novel well-defined glycopolymers synthesized via the reversible addition fragmentation chain transfer process in aqueous media. *J. Polym. Sci. A.* **47**, 614-627 (2009).
29 Rejman, J., Oberle, V., Zuhorn, I. S. & Hoekstra, D. Size-dependent internalization of particles via the pathways of clathrin-and caveolae-mediated endocytosis. *Biochem. J.* **377**, 159 (2004).
30 McLendon, P. M., Fichter, K. M. & Reineke, T. M. Poly (glycoamidoamine) vehicles promote pDNA uptake through multiple routes and efficient gene expression via caveolae-mediated endocytosis. *Mol. Pharm.* **7**, 738-750 (2010).
31 Cho, Y. W., Kim, J. D. & Park, K. Polycation gene delivery systems: escape from endosomes to cytosol. *J. Pharm. Pharmacol.* **55**, 721-734 (2003).

32 Khalil, I. A., Kogure, K., Akita, H. & Harashima, H. Uptake pathways and subsequent intracellular trafficking in nonviral gene delivery. *Pharmacol. Rev.* **58**, 32-45 (2006).
33 Schaffer, D. V., Fidelman, N. A., Dan, N. & Lauffenburger, D. A. Vector unpacking as a potential barrier for receptor-mediated polyplex gene delivery. *Biotechnol. Bioeng.* **67**, 598-606 (2000).
34 Cartier, R. & Reszka, R. Utilization of synthetic peptides containing nuclear localization signals for nonviral gene transfer systems. *Gene Ther.* **9**, 157 (2002).
35 Brasier, A., Tate, J. & Habener, J. Optimized use of the firefly luciferase assay as a reporter gene in mammalian cell lines. *BioTechniques* **7**, 1116 (1989).
36 Ehrlich, J. & Stivala, S. S. Chemistry and pharmacology of heparin. *J. Pharm. Sci.* **62**, 517-544 (1973).
37 Liu, Y. & Reineke, T. M. Hydroxyl stereochemistry and amine number within poly (glycoamidoamine) s affect intracellular DNA delivery. *J. Am. Chem. Soc.* **127**, 3004-3015 (2005).
38 Barbey, R., Lavanant, L., Paripovic, D., Schüwer, N., Sugnaux, C., Tugulu, S. & Klok, H. A. Polymer brushes via surface-initiated controlled radical polymerization: synthesis, characterization, properties, and applications. *Chem. Rev.* **109**, 5437-5527 (2009).
39 Edmondson, S., Osborne, V. L. & Huck, W. T. S. Polymer brushes via surface-initiated polymerizations. *Chem. Soc. Rev.* **33**, 14-22 (2004).

Chapter 5. Future Work

5.1 Suggested future research directions

Both glycopolymers investigated in this dissertation showed many characteristics that make them interesting and valuable materials for further research in the context of biomedical applications. Future research for both of these polymers should be conducted following the two general directions: applications and property investigations.

First, despite the valuable properties discussed in Chapters 3 and 4 it should be noted that only one length of the glycopolymers was investigated in detail. Therefore, future efforts should begin with the optimization of the glycopolymer length. It is impossible to give the definition of the optimal properties from molecular weight point of view, because many functions (e.g., antifouling, lyoprotection and cryoprotection, absence of toxicity, interactions with lectins and receptors on the cell surface) can show different dependence on the glycopolymer molecular weight. However, the optimization can be addressed in the context of a desired application.

The influence of the polymer length on the antifouling characteristics has been previously reported for a gluconamidoethylmethacrylate based glycopolymer.[1] Considering the protein adsorption that was observed with the quartz crystal microbalance technique (Chapter 3) for the polytrehalose polymer with dp=51, one can attempt to improve the antifouling characteristics of glycopolymers by increasing the polymer lengths. In addition to QCM other techniques such as ellipsometry,[2] surface plasmon resonance (SPR)[3] or back-scattering interferomentry[4] can be used to gain more

understanding on the nature and the strength of the glycopolymer interactions and the dependence of such interactions on the molecular weight.

The interactions with lectins must be investigated (sugar binding proteins).[5] Glycopolymer-lectin interactions is a widely investigated topic,[6] furthermore, polyMAG has been shown to bind to concanavalin A.[7] In animals lectins are known to participate in defense actions against the pathogens[8] and the possible interactions of polyMAG and polytrehalose with this type of lectins may lead to the undesirable accelerated clearance. On the other hand, recognition of the glycopolymers by lectins that are unique to certain cell types can be advantageous and the glycopolymers can be employed for targeting in such a case (reverse lectin targeting).[9]

Considering the excellent cellular internalization properties demonstrated by the polytrehalose-coated polyplexes in U-87 glioblastoma cells, it would be especially important to investigate the internalization mechanism and the potential interactions with receptors on the surface of U-87 cells. Brain tumors are known to be glucose-hungry and to overexpress glucose transporters; specifically Na^+ independent glucose transporter GLUT-1 is overexpressed in glioblastoma multiforme.[10] Trehalose is made of two glucose residues and the interaction of polytrehalose with GLUT-1 receptor that may facilitate the polyplex uptake cannot be excluded. Moreover, polytrehalose can be used for tumor-targeting in glioblastoma if such an interaction indeed takes place. A simple initial experiment to study this hypothesis can be comparison the polyplex uptake in the presence and absence of the large glucose in order to saturate glucose transporters.

The investigation of the possible immunogenicity of pMAG and polytrehalose must be the first animal-related experiment. If antibodies are generated against these

glycopolymers their further development for the delivery applications will be problematic. Additionally, the absence of the response from innate immune system through the complement activation must also be shown: it is known that complement component 3 (C3) produces C3b, which in turn can cause opsonization of invading pathogens and is reactive towards carbohydrates, preferentially reacting with hydroxyl in 6 position of the carbohydrate.[11] Both pMAG and polytrehalose have this hydroxyl available and therefore may potentially activate complement system.

Cryoprotective properties and the lyophilization protocols should be studied in detail. The suppression of water crystallization and lowering the energies associated with water to ice transitions should be investigated with a respect to molecular weight. It is well known that the polymer solution viscosity increases with the increase in polymer molecular weight[12] and it is also known that increase in viscosity favors glass formation over crystalline material.[13] It is therefore logical to assume that the higher molecular weight polytrehalose may have better cryoprotective properties. Additionally the rate of cooling plays a role in the formation of glass[13] and it should be investigated as well.

Beginning with the conceptual idea of using polytrehalose and later polyglucose (pMAG), their use was not thought of being limited to nucleic acid delivery only. In principle any nanoparticles for biomedical applications such as liposomes,[14] micelles,[15] gold particles,[16] magnetite (paramagnetic iron oxide) particles,[17] quantum dots,[18] silica particles[19] and others[20] can be coated with the glycopolymers presented in this dissertation. Employment of pMAG and polytrehalose in micelle research is already being investigated.[21]

With the development of pMAG and polytrehalose a new direction of research in the Reineke lab was started. The useful physical and biological properties that were demonstrated for these polymers make them appealing for further investigation while simple and scalable procedures that were developed for their synthesis allow for easy access to these materials. More investigation is needed in order for these glycopolymers to become practically useful; however, the exciting data presented in this dissertation indicates that these materials might become clinically relevant in the future.

5.2 References

1 Gu, J. S., Yu, H. Y., Huang, L., Tang, Z. Q., Li, W., Zhou, J., Yan, M. G. & Wei, X. W. Chain-length dependence of the antifouling characteristics of the glycopolymer-modified polypropylene membrane in an SMBR. *J. Membr. Sci.* **326**, 145-152 (2009).

2 Horisberger, M. An application of ellipsometry: Assessment of polysaccharide and glycoprotein interaction with lectin at a liquid/solid interface. *BBA - General Subjects* **632**, 298-309 (1980).

3 Mann, D. A., Kanai, M., Maly, D. J. & Kiessling, L. L. Probing low affinity and multivalent interactions with surface plasmon resonance: ligands for concanavalin A. *J. Am. Chem. Soc.* **120**, 10575-10582 (1998).

4 Kussrow, A., Kaltgrad, E., Wolfenden, M. L., Cloninger, M. J., Finn, M. & Bornhop, D. J. Measurement of Monovalent and Polyvalent Carbohydrate−Lectin Binding by Back-Scattering Interferometry. *Anal. Chem.* **81**, 4889-4897 (2009).

5 Kilpatrick, D. C. Animal lectins: a historical introduction and overview. *BBA - General Subjects* **1572**, 187-197 (2002).

6 Ting, S. R. S., Chen, G. & Stenzel, M. H. Synthesis of glycopolymers and their multivalent recognitions with lectins. *Polym. Chem.* **1**, 1392-1412 (2010).

7 Boyer, C. & Davis, T. P. One-pot synthesis and biofunctionalization of glycopolymers via RAFT polymerization and thiol–ene reactions. *Chem. Commun.*, 6029-6031 (2009).

8 Epstein, J., Eichbaum, Q., Sheriff, S. & Ezekowitz, R. A. B. The collectins in innate immunity. *Curr. Opin. Immunol.* **8**, 29-35 (1996).

9 Minko, T. Drug targeting to the colon with lectins and neoglycoconjugates. *Adv. Drug Del. Rev.* **56**, 491-509 (2004).

10 Jensen, R. L. & Chkheidze, R. The Role of Glucose Transporter-1 (GLUT-1) in Malignant Gliomas. *Tumors of the Central Nervous System* **1**, 99-108 (2011).
11 Sahu, A. & Lambris, J. D. Structure and biology of complement protein C3, a connecting link between innate and acquired immunity. *Immunol. Rev.* **180**, 35-48 (2001).
12 Freed, K. F. & Edwards, S. Polymer viscosity in concentrated solutions. *The Journal of Chemical Physics* **61**, 3626 (1974).
13 Uhlmann, D. A kinetic treatment of glass formation. *J. Non-Cryst. Solids* **7**, 337-348 (1972).
14 Samad, A., Sultana, Y. & Aqil, M. Liposomal drug delivery systems: an update review. *Curr. Drug Del.* **4**, 297-305 (2007).
15 Tyrrell, Z. L., Shen, Y. & Radosz, M. Fabrication of micellar nanoparticles for drug delivery through the self-assembly of block copolymers. *Prog. Polym. Sci.* **35**, 1128-1143 (2010).
16 Ghosh, P., Han, G., De, M., Kim, C. K. & Rotello, V. M. Gold nanoparticles in delivery applications. *Adv. Drug Del. Rev.* **60**, 1307-1315 (2008).
17 Chertok, B., Moffat, B. A., David, A. E., Yu, F., Bergemann, C., Ross, B. D. & Yang, V. C. Iron oxide nanoparticles as a drug delivery vehicle for MRI monitored magnetic targeting of brain tumors. *Biomaterials* **29**, 487-496 (2008).
18 Medintz, I. L., Uyeda, H. T., Goldman, E. R. & Mattoussi, H. Quantum dot bioconjugates for imaging, labelling and sensing. *Nat. Mater.* **4**, 435-446 (2005).
19 Anglin, E. J., Cheng, L., Freeman, W. R. & Sailor, M. J. Porous silicon in drug delivery devices and materials. *Adv. Drug Del. Rev.* **60**, 1266-1277 (2008).
20 Xu, Z. P., Zeng, Q. H., Lu, G. Q. & Yu, A. B. Inorganic nanoparticles as carriers for efficient cellular delivery. *Chem. Eng. Sci.* **61**, 1027-1040 (2006).
21 Yin, L., Dalsin, M.C., Sizovs, A., Reineke, T.M., Hillmyer, M.A. Glucose-functionalized, serum-stable polymeric micelles from the combination of anionic and RAFT polymerizations. *Macromolecules, DOI: 10.1021/ma300218n* (2012).

Apendix A: Important Spectra

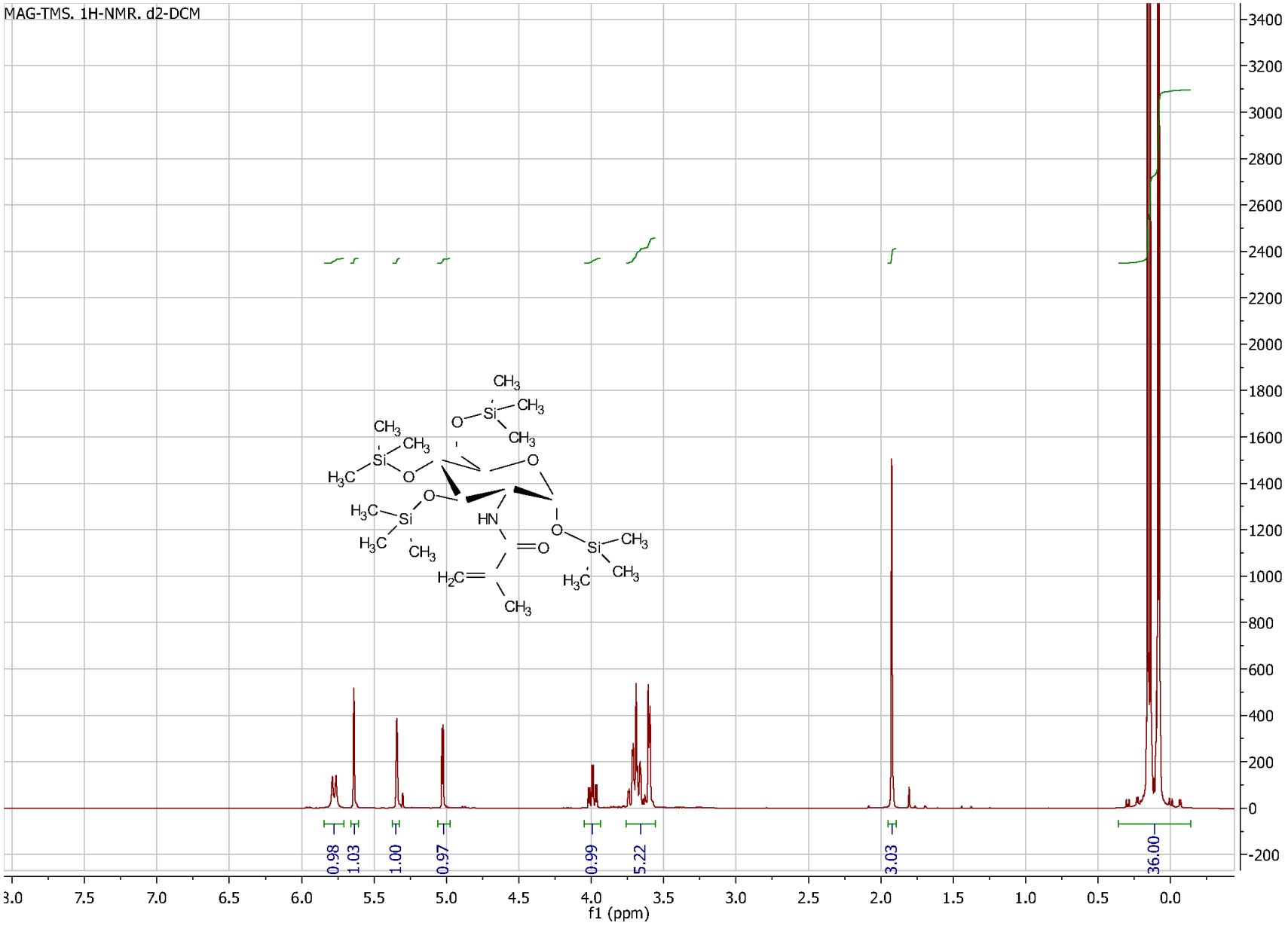
MAG-TMS. 1H-NMR. d2-DCM
0.98
1.03
1.00
0.97
0.99
5.22
3.03
36.00
f1 (ppm)

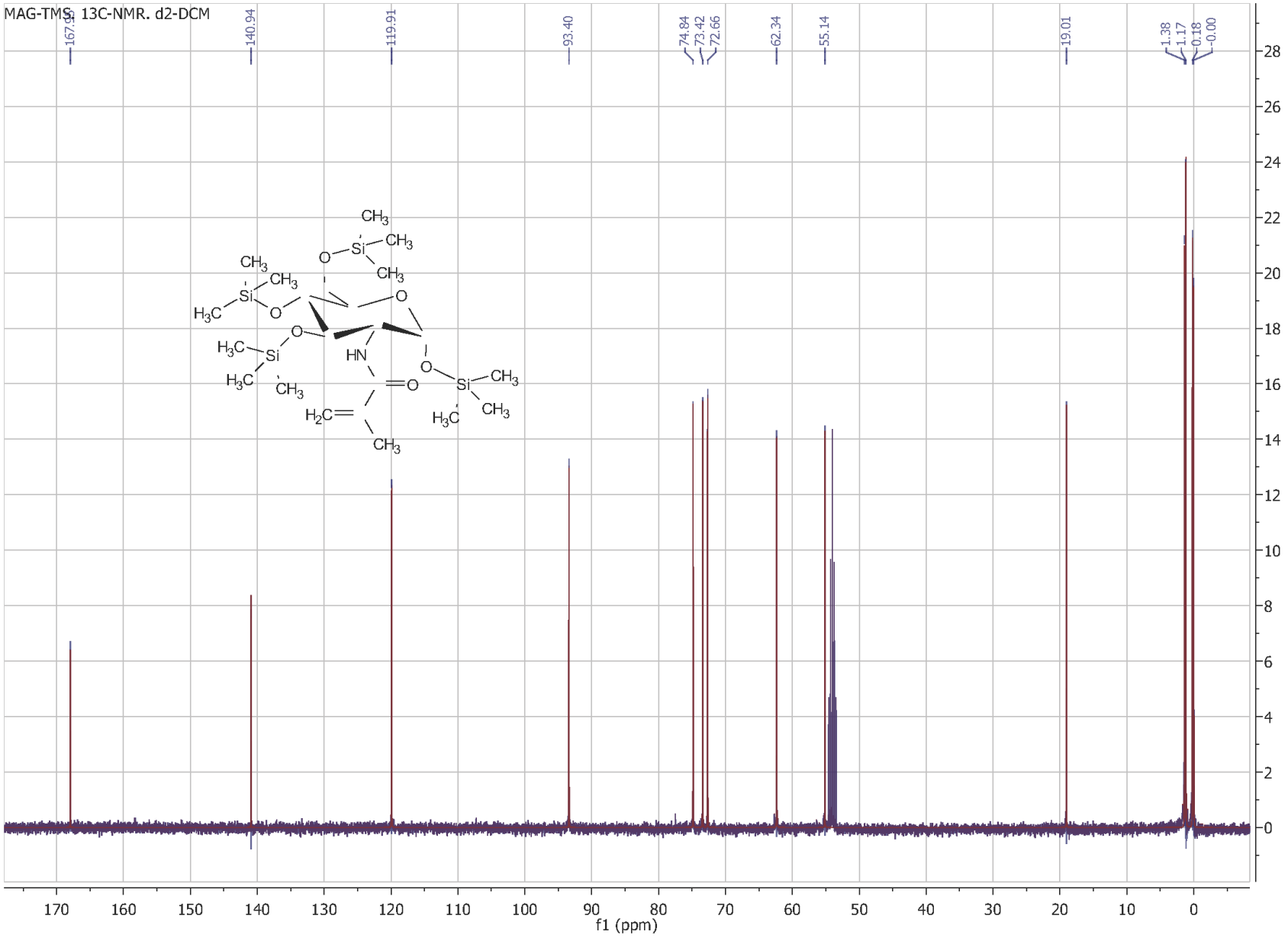
MAG-TMS, 13C-NMR. d2-DCM
167.31
140.94
119.91
93.40
74.84
73.42
72.66
62.34
55.14
19.01
1.38
1.17
0.18
-0.00
f1 (ppm)

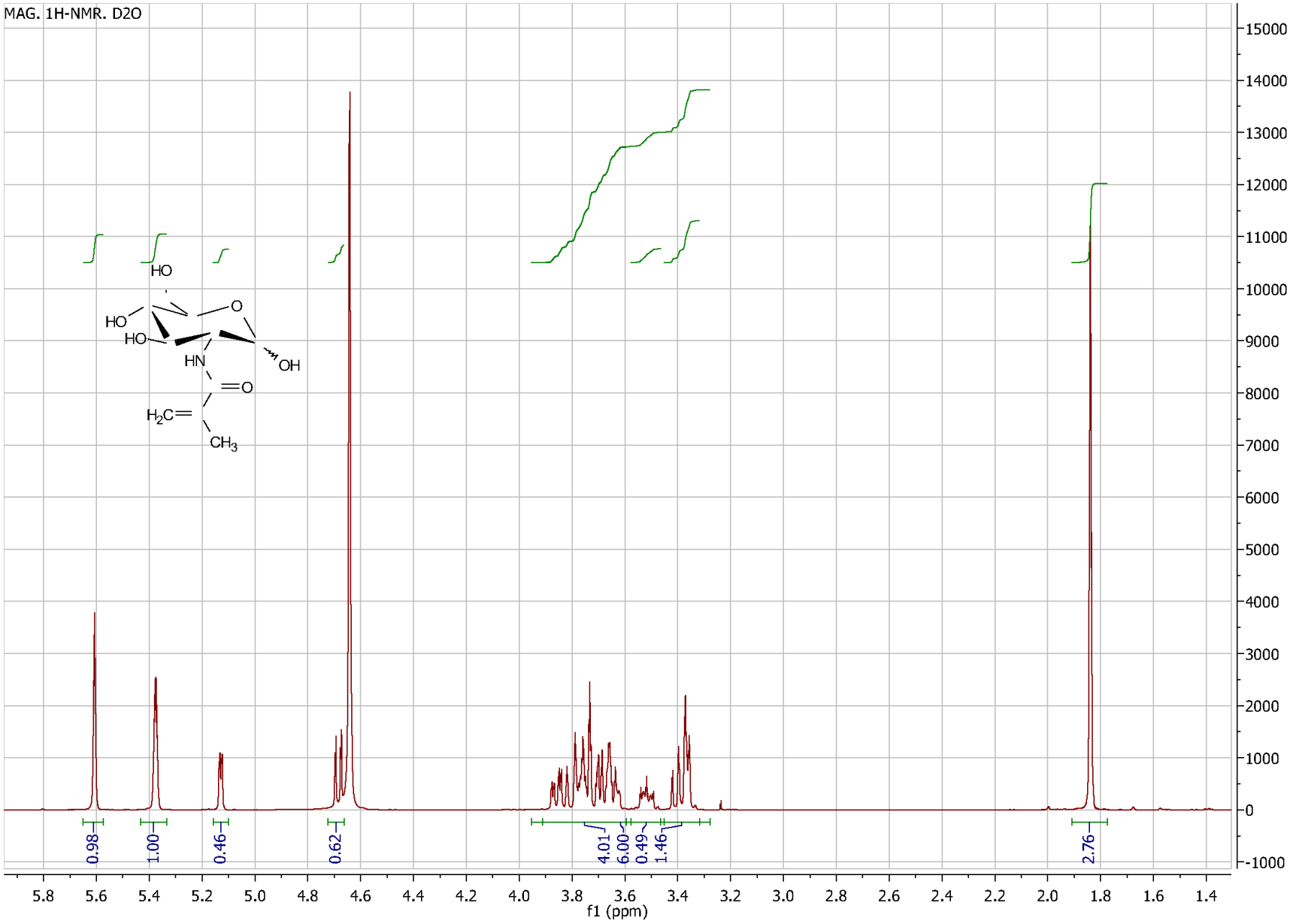
MAG. 1H-NMR. D2O
HO
HO
HO
O
HN
OH
=O
H2C=
CH3
0.98
1.00
0.46
0.62
4.01
6.00
0.49
1.46
2.76
f1 (ppm)

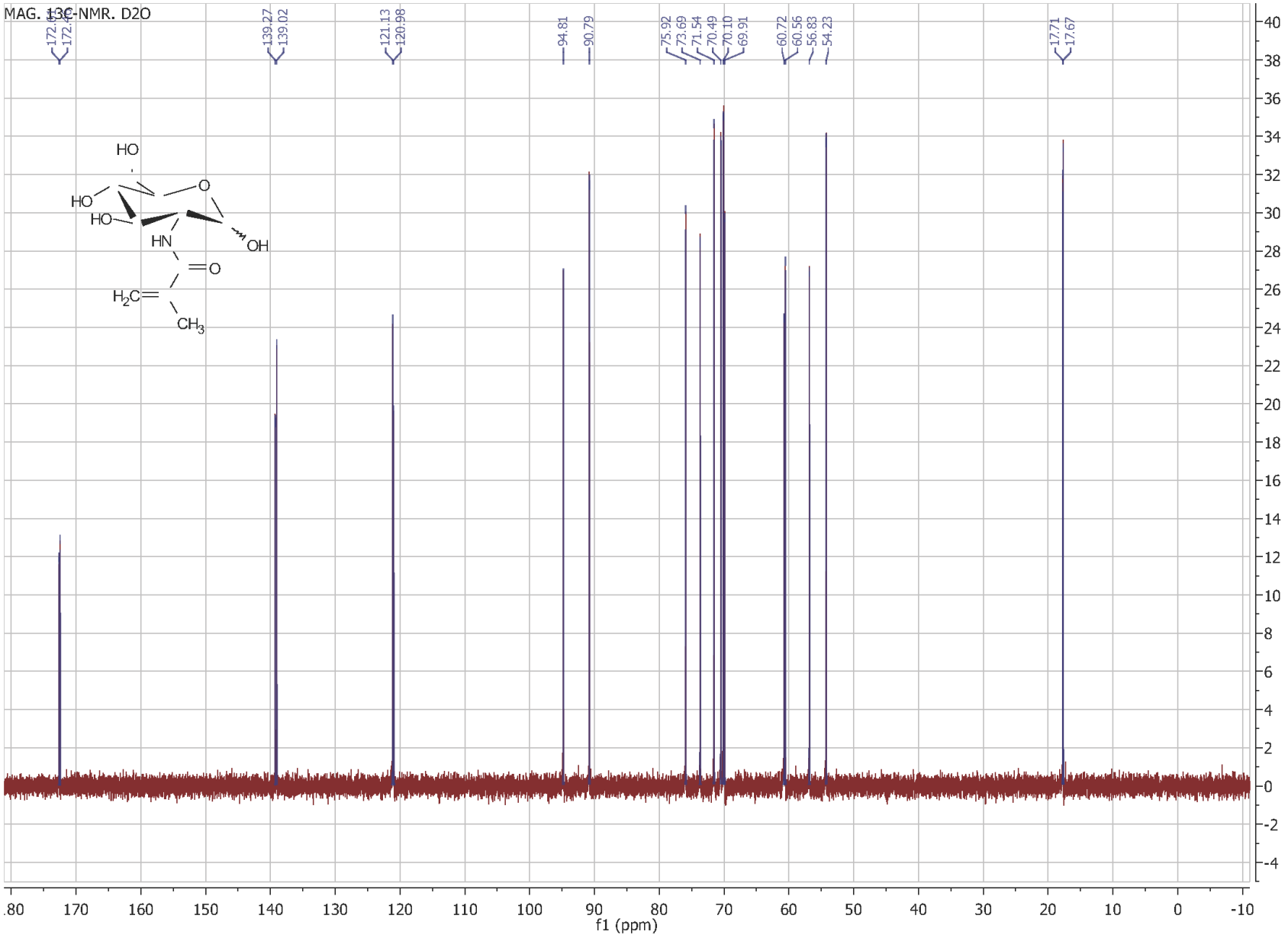
MAG. 13C-NMR. D2O
172.54
172.14
139.27
139.02
121.13
120.98
94.81
90.79
75.92
73.69
71.54
70.49
70.10
69.91
60.72
60.56
56.83
54.23
17.71
17.67
HO
HO
HO
O
HN
OH
O
H2C
CH3
f1 (ppm)

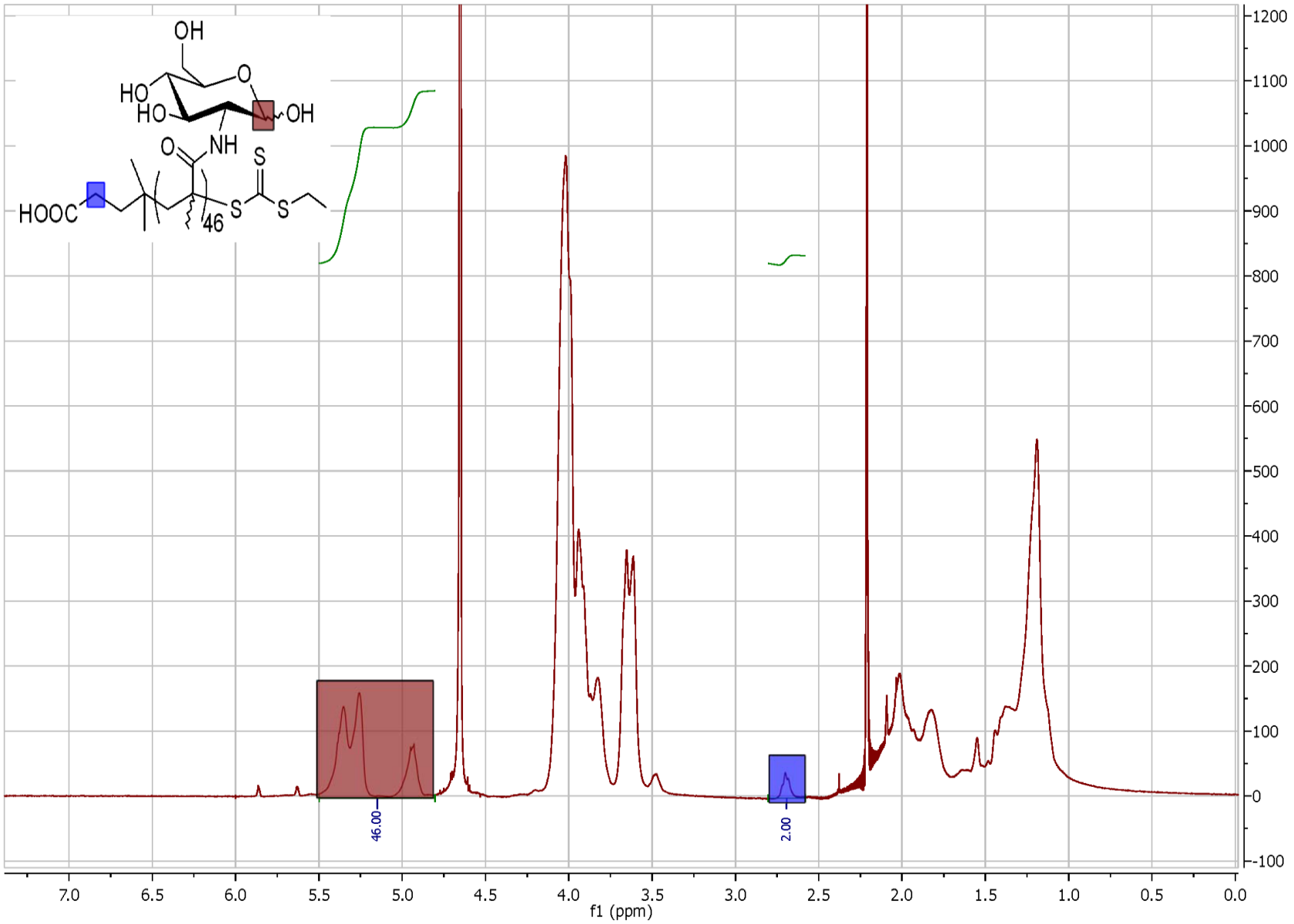
OH
HO
HO
O
OH
O
NH
S
HOOC
S
S
46
46.00
2.00
f1 (ppm)
7.0
6.5
6.0
5.5
5.0
4.5
4.0
3.5
3.0
2.5
2.0
1.5
1.0
0.5
0.0
1200
1100
1000
900
800
700
600
500
400
300
200
100
0
-100

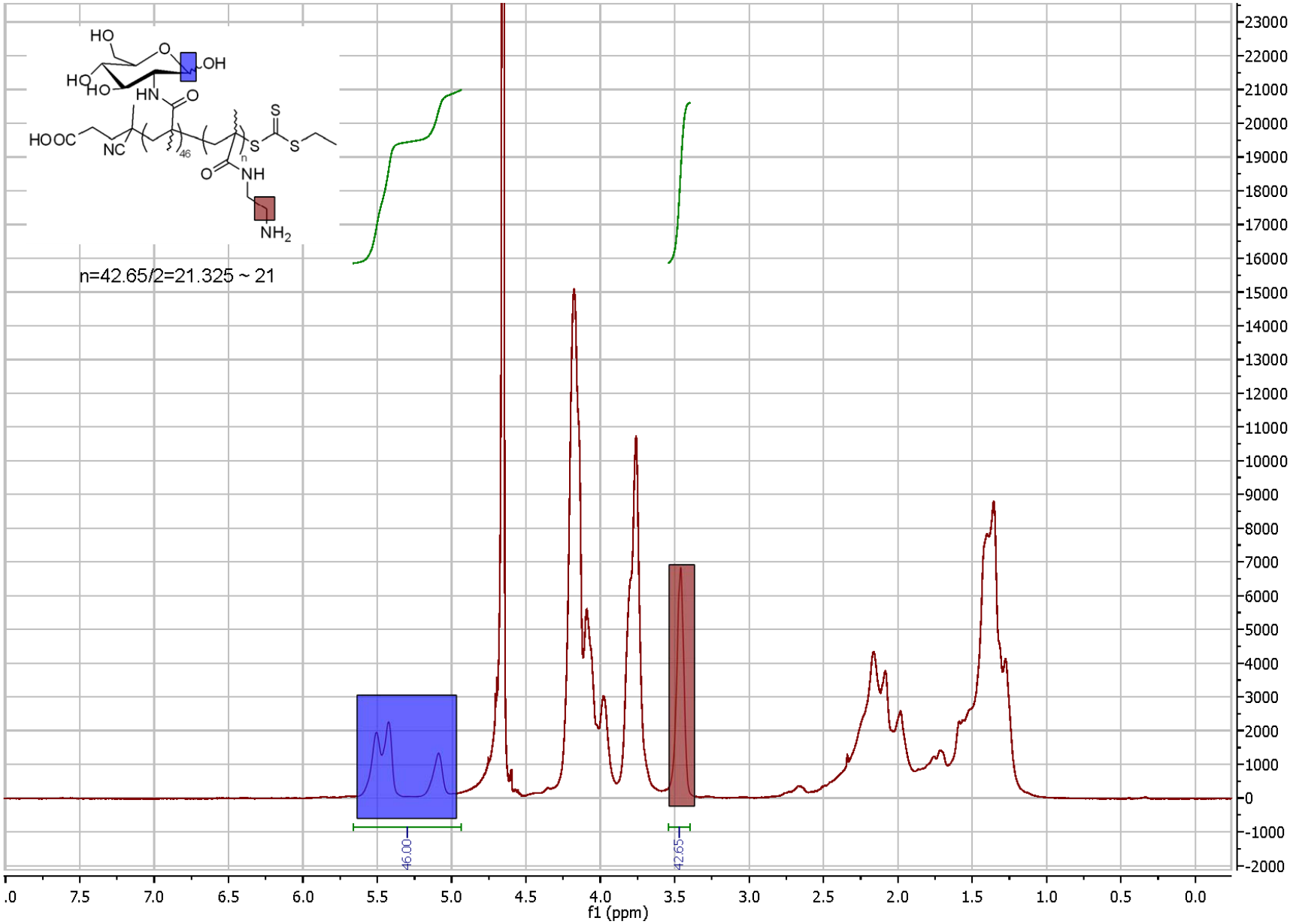
HO
O
OH
HO
HO
HN
O
HOOC
NC
46
S
S
S
n
O
NH
NH2
n=42.65/2=21.325 ~ 21
46.00
42.65
f1 (ppm)

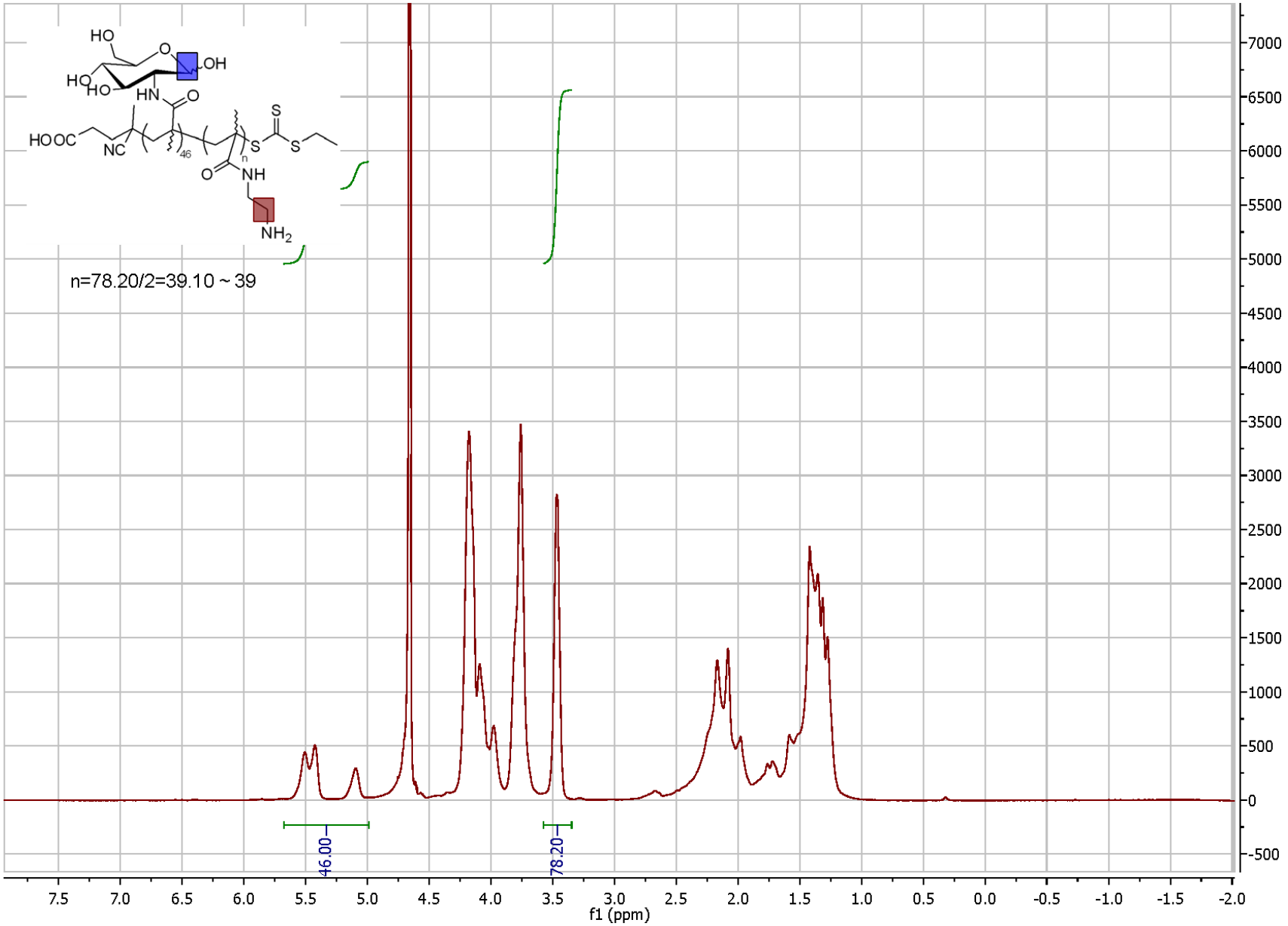
HO
O
OH
HO
HO
HN
O
HOOC
NC
46
n
S
S
S
O
NH
NH2
n=78.20/2=39.10 ~ 39
46.00
78.20
7.5
7.0
6.5
6.0
5.5
5.0
4.5
4.0
3.5
3.0
2.5
2.0
1.5
1.0
0.5
0.0
-0.5
-1.0
-1.5
-2.0
f1 (ppm)
7000
6500
6000
5500
5000
4500
4000
3500
3000
2500
2000
1500
1000
500
0
-500

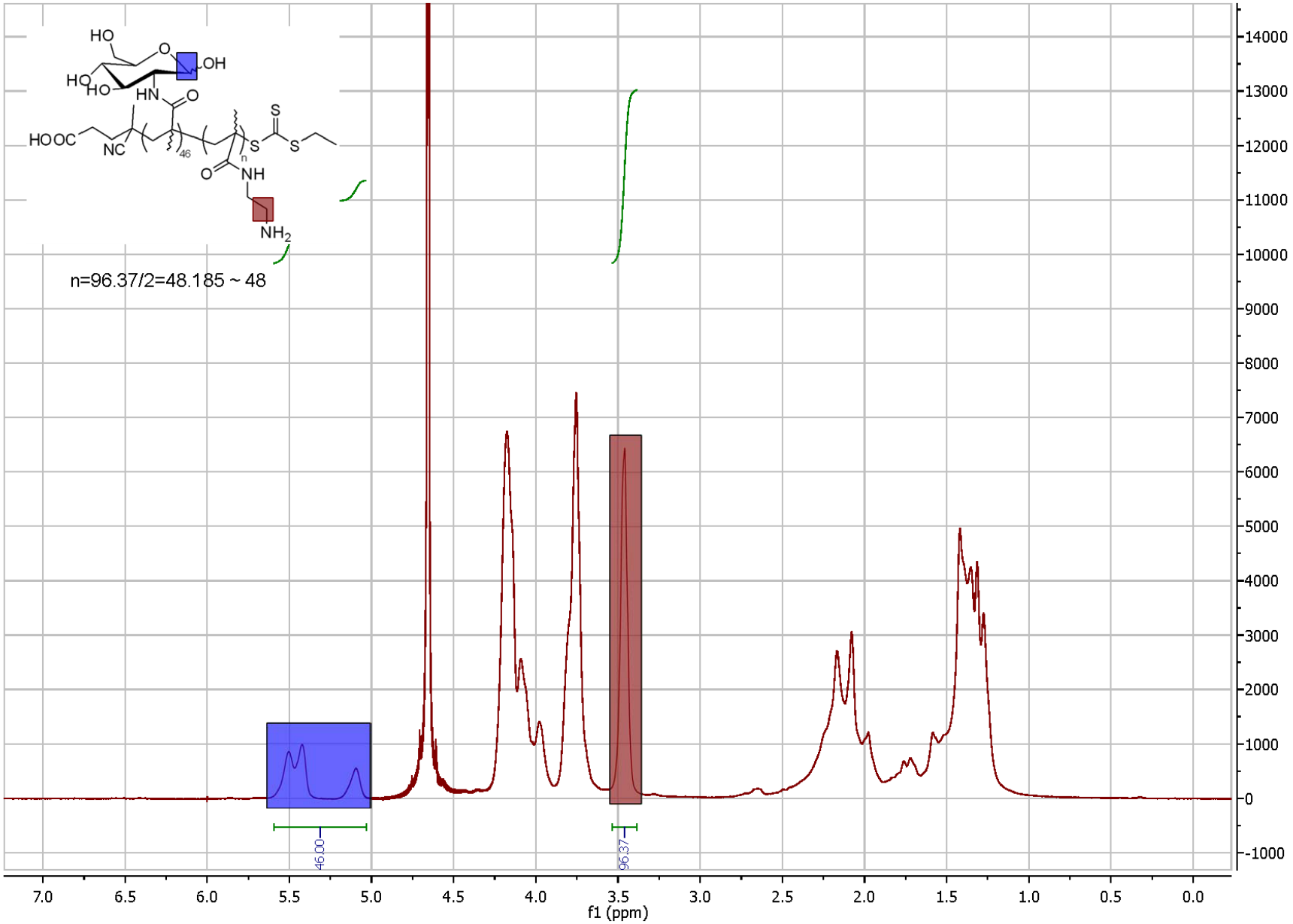
HO
O
OH
HO
HO
HN
O
HOOC
NC
46
S
S
S
n
O
NH
NH2
n=96.37/2=48.185 ~ 48
46.00
96.37
14000
13000
12000
11000
10000
9000
8000
7000
6000
5000
4000
3000
2000
1000
0
-1000
7.0
6.5
6.0
5.5
5.0
4.5
4.0
3.5
3.0
2.5
2.0
1.5
1.0
0.5
0.0
f1 (ppm)

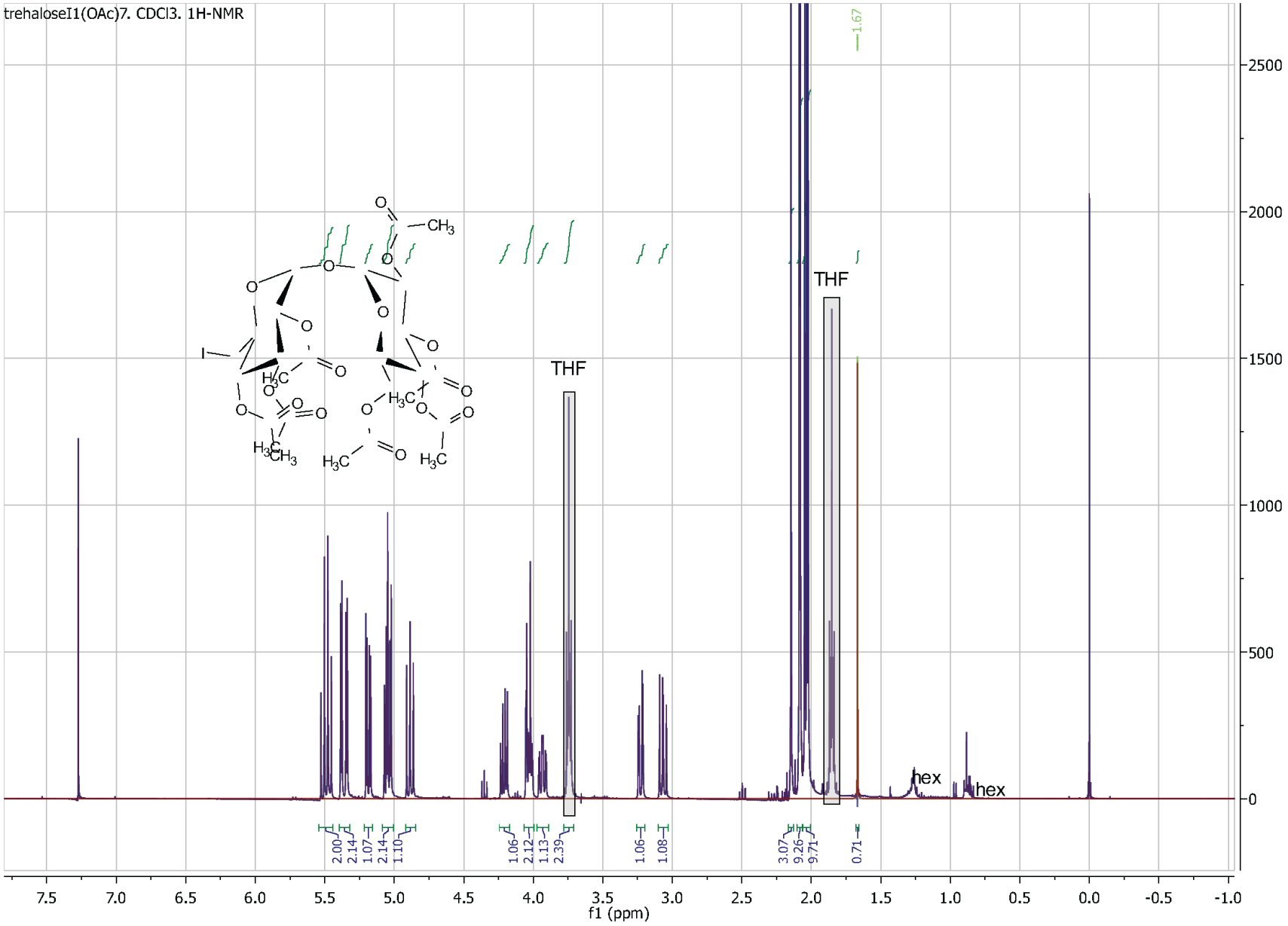
trehaloseI1(OAc)7. CDCl3. 1H-NMR
1.67
THF
THF
hex
hex
2.00
2.14
1.07
2.14
1.10
1.06
2.12
1.13
2.39
1.06
1.08
3.07
9.26
9.71
0.71
2500
2000
1500
1000
500
0
7.5
7.0
6.5
6.0
5.5
5.0
4.5
4.0
3.5
3.0
2.5
2.0
1.5
1.0
0.5
0.0
-0.5
-1.0
f1 (ppm)

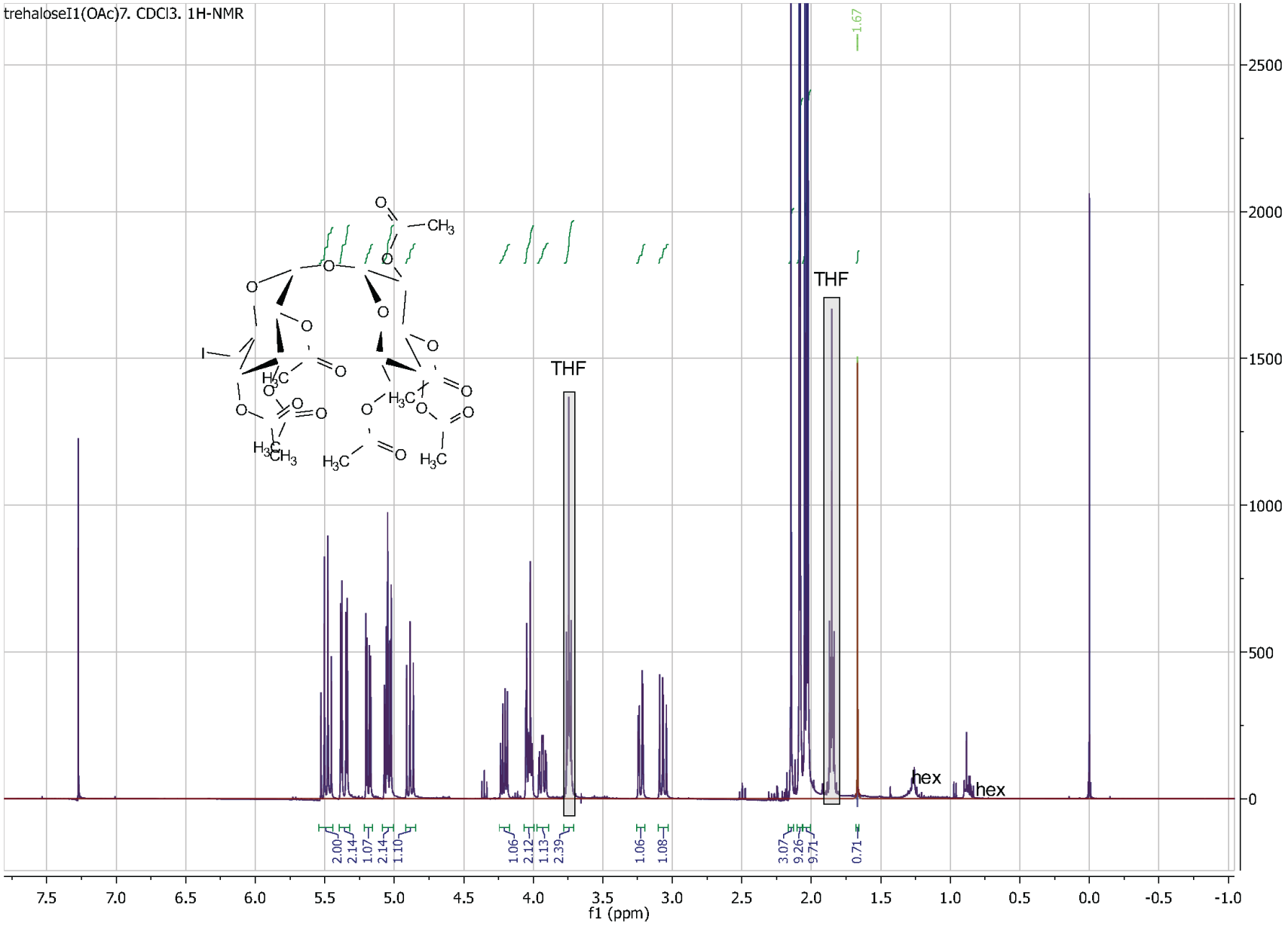
trehaloseI1(OAc)7. CDCl3. 1H-NMR
1.67
THF
THF
hex
hex
2.00
2.14
1.07
2.14
1.10
1.06
2.12
1.13
2.39
1.06
1.08
3.07
9.26
9.71
0.71
2500
2000
1500
1000
500
0
7.5
7.0
6.5
6.0
5.5
5.0
4.5
4.0
3.5
3.0
2.5
2.0
1.5
1.0
0.5
0.0
-0.5
-1.0
f1 (ppm)

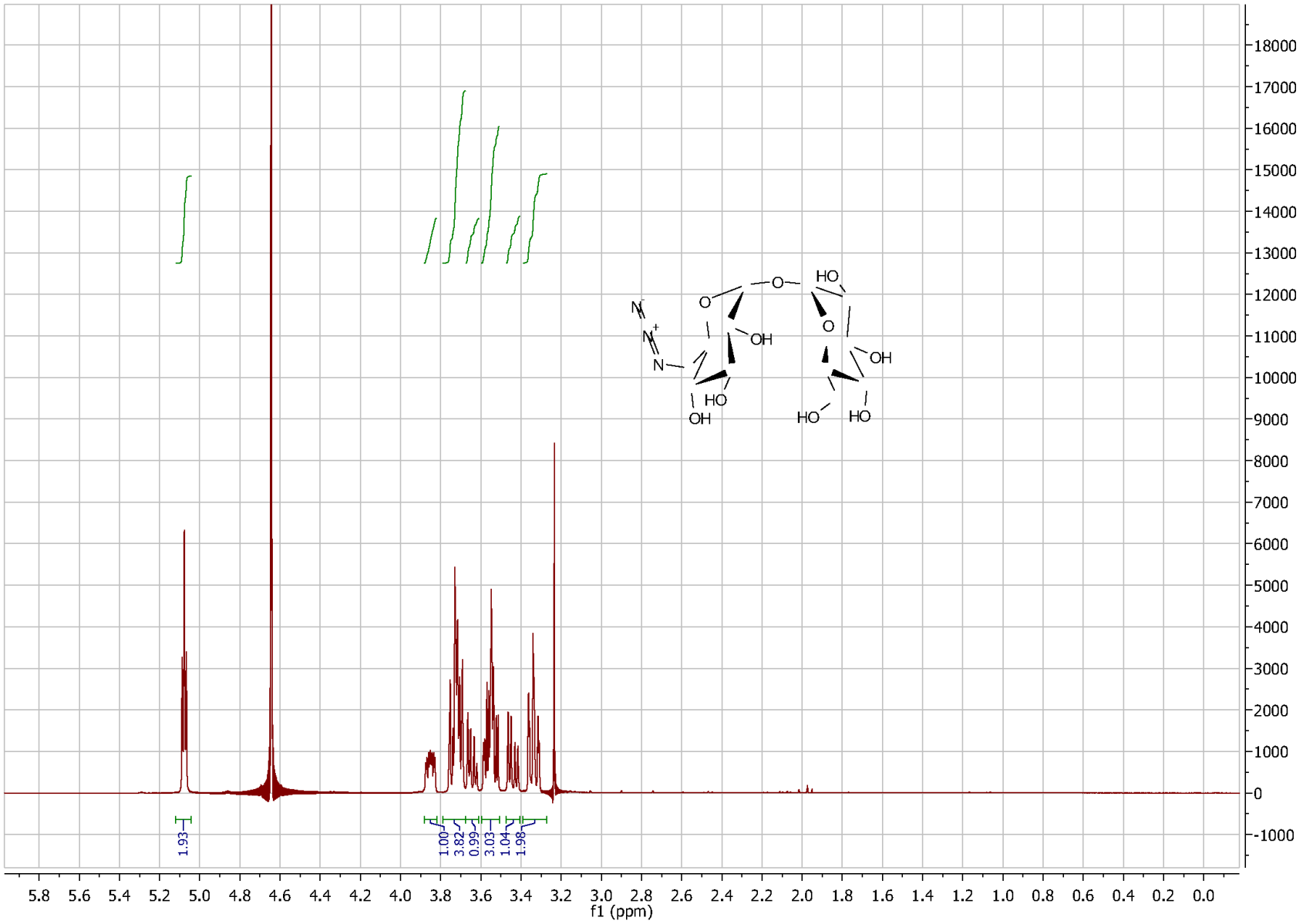
18000
17000
16000
15000
14000
13000
12000
11000
10000
9000
8000
7000
6000
5000
4000
3000
2000
1000
0
-1000
5.8 5.6 5.4 5.2 5.0 4.8 4.6 4.4 4.2 4.0 3.8 3.6 3.4 3.2 3.0 2.8 2.6 2.4 2.2 2.0 1.8 1.6 1.4 1.2 1.0 0.8 0.6 0.4 0.2 0.0
f1 (ppm)
1.93
1.00
3.82
0.99
3.03
1.04
1.98
N
N+
N
O
O
OH
HO
OH
HO
O
HO
OH
HO
HO

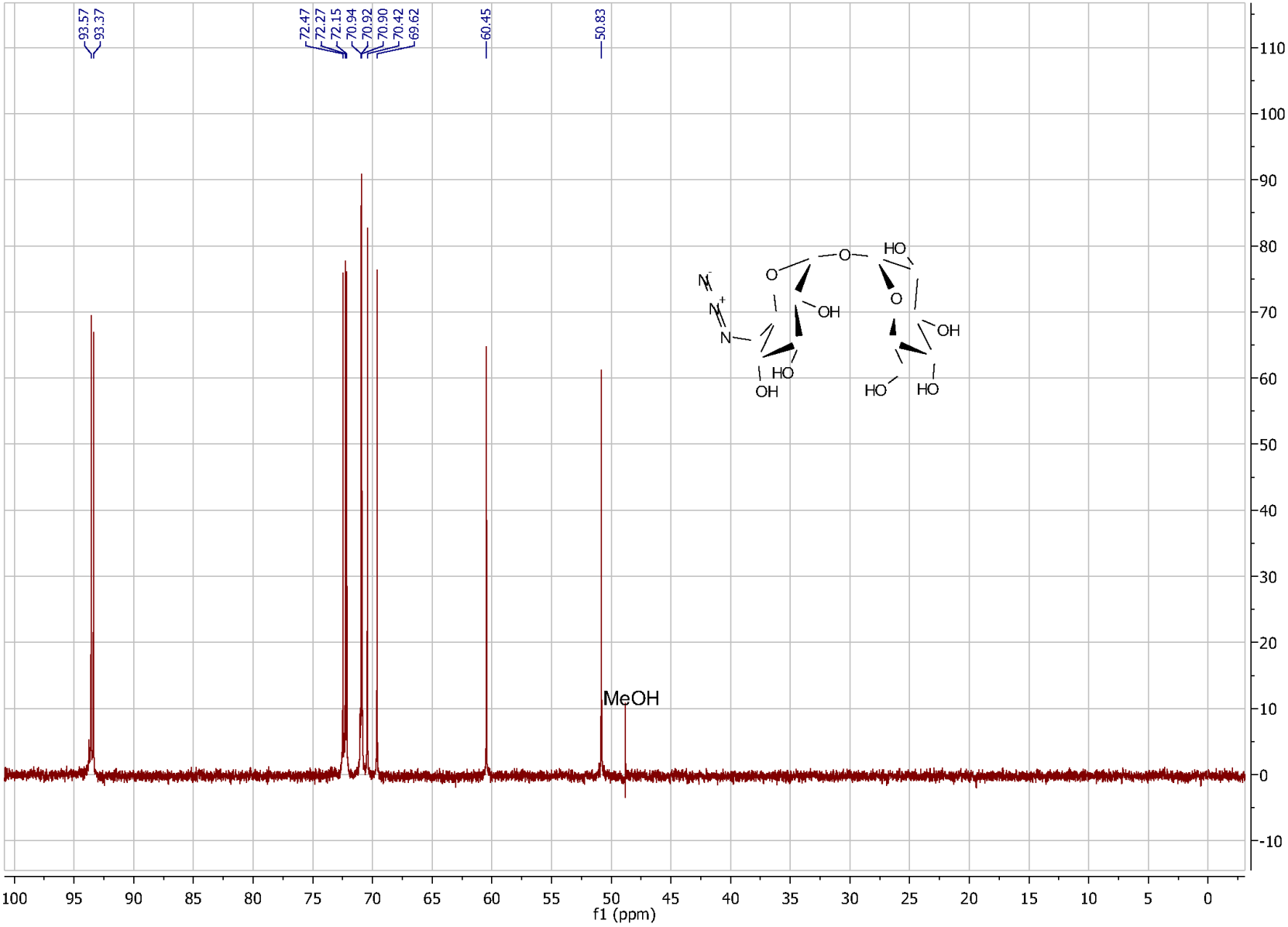
93.57
93.37
72.47
72.27
72.15
70.94
70.92
70.90
70.42
69.62
60.45
50.83
MeOH
f1 (ppm)

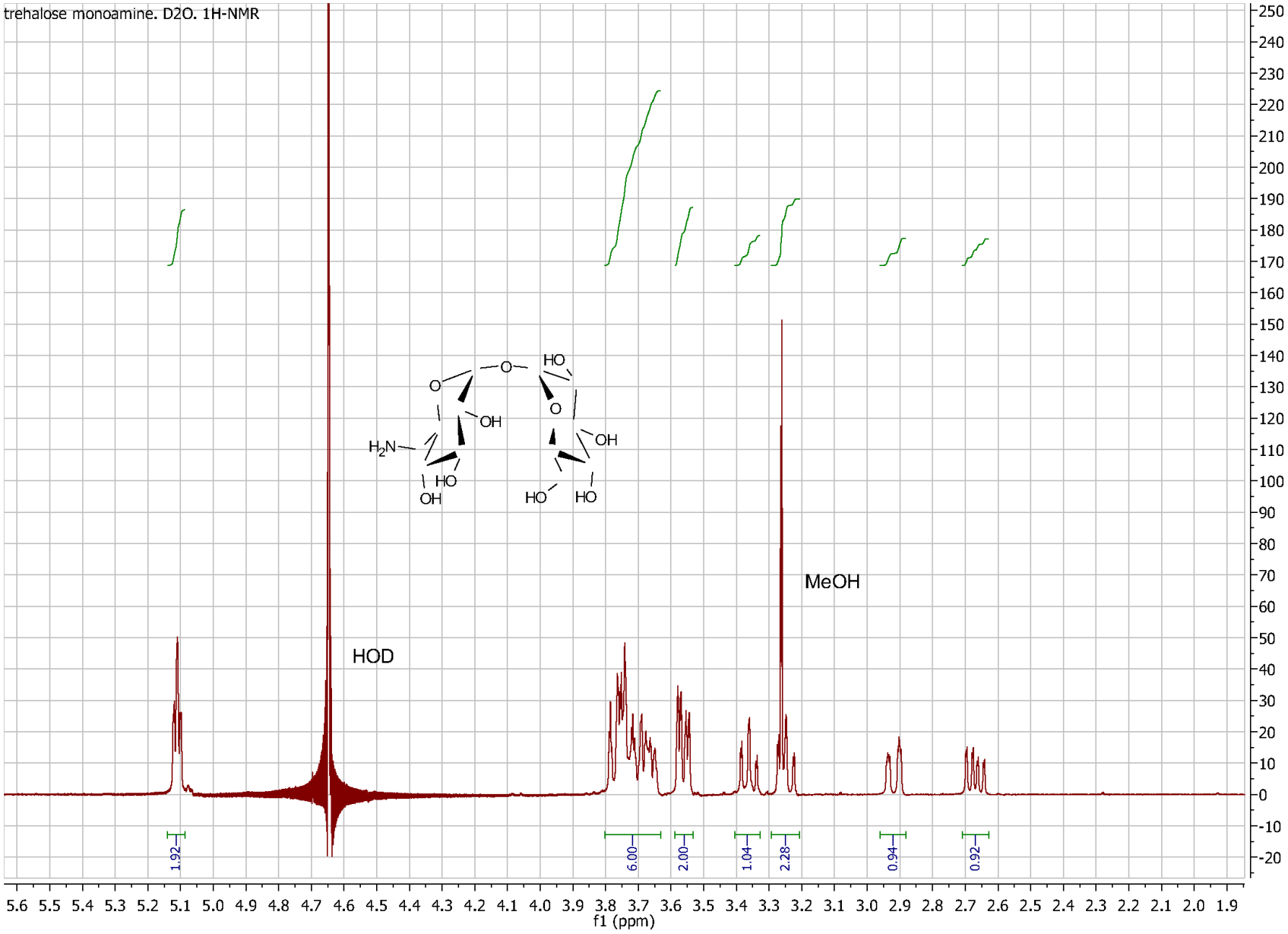
trehalose monoamine. D2O. 1H-NMR
HOD
MeOH
f1 (ppm)
1.92
6.00
2.00
1.04
2.28
0.94
0.92

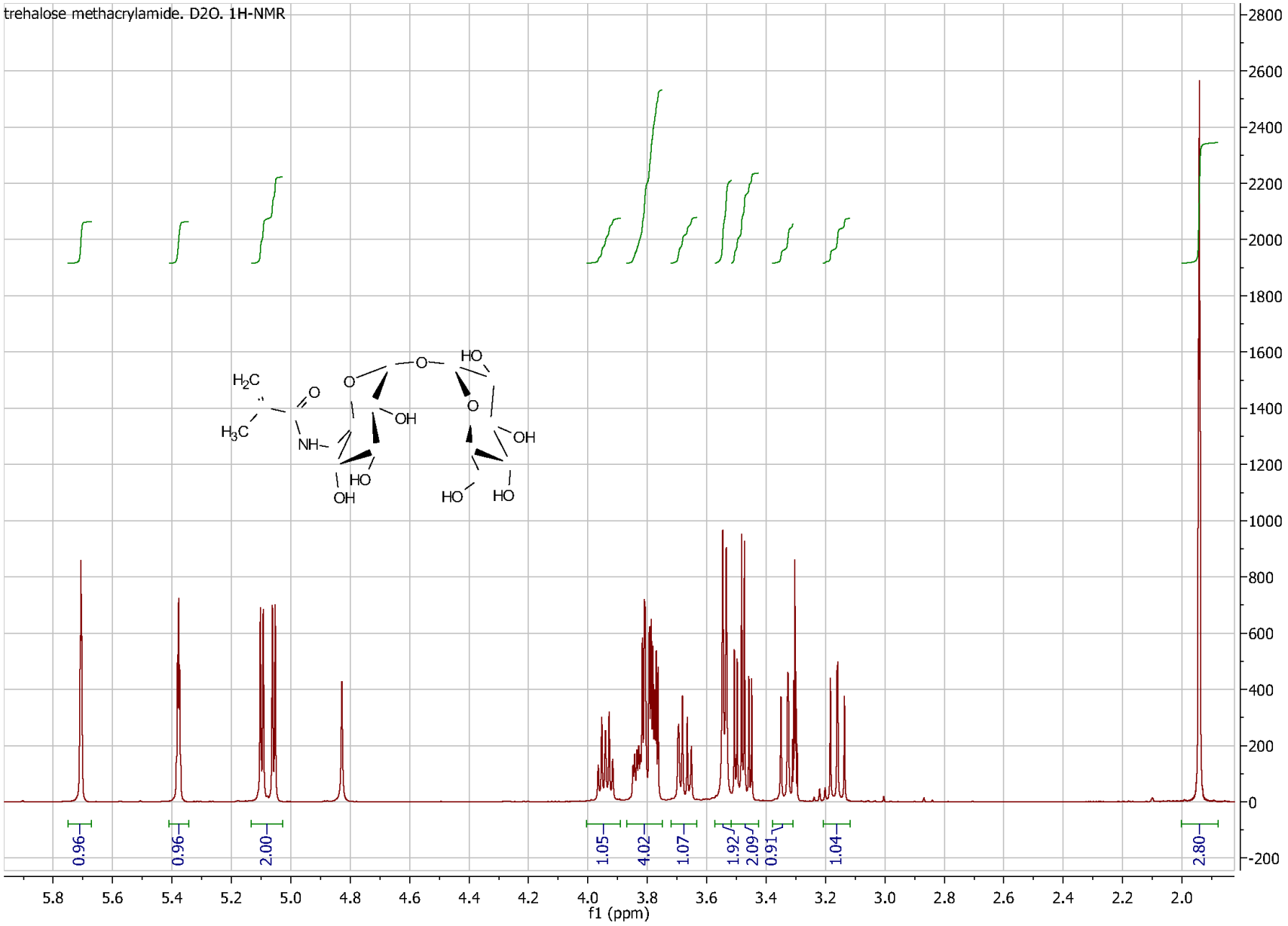
trehalose methacrylamide. D2O. 1H-NMR
f1 (ppm)
0.96
0.96
2.00
1.05
4.02
1.07
1.92
2.09
0.91
1.04
2.80

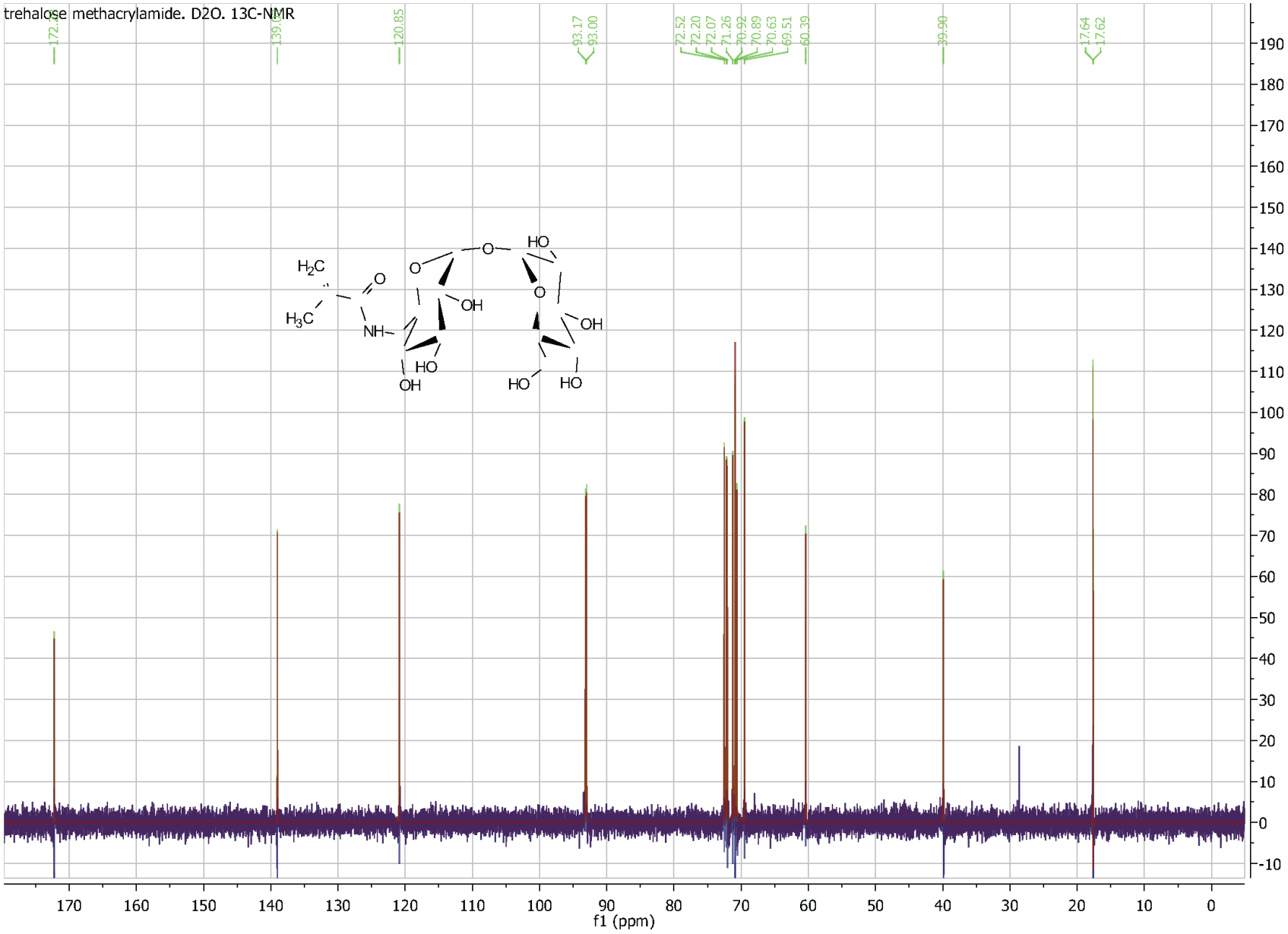
trehalose methacrylamide. D2O. 13C-NMR
172.49
139.78
120.85
93.17
93.00
72.52
72.20
72.07
71.26
70.92
70.89
70.63
69.51
60.39
39.90
17.64
17.62
H2C
H3C
O
NH
OH
HO
O
O
HO
OH
HO
HO
f1 (ppm)

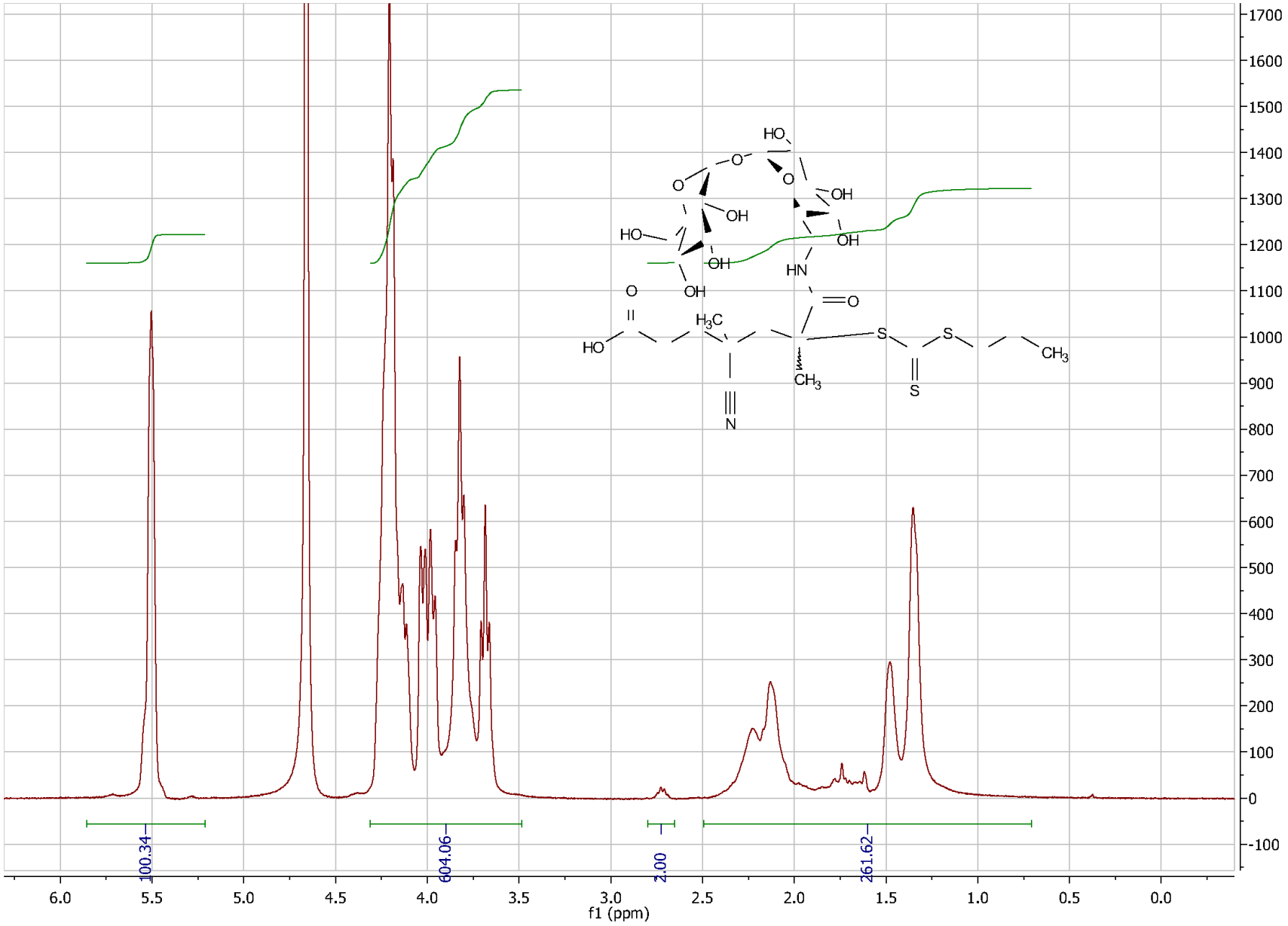
100.34
604.06
2.00
261.62
f1 (ppm)